The role of FoxO factors in maintaining intestinal homeostasis in *Drosophila melanogaster*

Dissertation

zur Erlangung des Doktorgrades

der Mathemathisch-Naturwissenschaftlichen Fakultät

der Christian-Albrechts-Universität zu Kiel

vorgelegt von

Mirjam Knop

Kiel, Dezember 2019

Erstgutachter: Prof. Dr. Thomas Roeder

Zweitgutachter: Prof. Dr. Holger Heine

Tag der Disputation: 27.02.2020

Table of contents

Summary

FoxO transcription factors are evolutionary conserved and involved in numerous molecular processes, such as DNA repair, apoptosis and cell death, life span, immune functions, cell cycle arrest, regulation of growth, metabolism and energy homeostasis. Therefore, FoxO presumably plays an important role in the maintenance of the intestinal tissue homeostasis and microbiota.

Intestinal epithelial integrity and an intact intestinal microbiota are important for maintaining a healthy organism. Thus, a dysbiosis and a deregulation of epithelial regeneration and proliferation may result in loss of intestinal integrity and chronic inflammatory diseases such as inflammatory bowel diseases (IBD). Both, a dysbiosis and a dysfunctional gut epithelium are also associated with aging. Moreover, the digestive tract with its microbiome has a significant influence on immunity, maintaining energy homeostasis, physiology and even the behavior.

The fruit fly *Drosophila melanogaster* was used as a model organism to investigate how FoxO activity affects the regulation of tissue homeostasis, the overall physiology and the intestinal microbial composition. Flies with an overall deficiency of dFoxO as well as flies with an overexpression of dFoxO in different cell types of the *Drosophila* intestine (ECs or ISCs and EBs) were used.

Surprisingly, the deficiency of dFoxO and the overexpression of dFoxO in ECs had the same negative effect on physiological features such as the survival, the gut functionality, locomotor activity, metabolic functions, starvation resistance and gut integrity. The overexpression in ISCs and EBs seems to have a rather positive effect on these physiological functions.

Moreover, the fecal microbiota in young dFoxO-deficient flies and those overexpressing dFoxO in ECs was not significant different compared to their controls. With aging, the microbial profiles of flies with a modified dFoxO expression showed increasing differences to their controls, which lead to a dysbiosis in older flies.

The treatment with DSS, a substance known to induce colitis in mammals, results in a reduced life span, an increased stem cell proliferation and a disorganized basement membrane structure in *Drosophila*. The deficiency of dFoxO as well as the overexpression in ISCs and EBs had a beneficial impact on the survival, possibly due to inhibition of

overproliferation and consequential dysplasia. In contrast, the overexpression of dFoxO in ECs appears not to influence the response to DSS.

Zusammenfassung

FoxO Transkriptionsfaktoren sind evolutionär konserviert und in zahlreiche molekulare Prozesse involviert, zu denen DNA Reparatur, Apoptose und Zelltod, Regulation der Lebensdauer, Immunfunktionen, Zellzykluskontrolle, Wachstumsregulierung, Steuerung von Metabolismus und Energiehomöostase gehören. Aus diesem Grund sollte FoxO auch eine bedeutende Rolle bei der Aufrechterhaltung der intestinalen Gewebehomöostase und der Zusammensetzung der Mikrobiota spielen.

Die Integrität des intestinalen Epithels und eine intakte intestinale Mikrobiota sind wichtig für die Gesundheit eines Organismus. Eine Dysbiose und die Deregulierung der epithelialen Regeneration und Proliferation könnte daher zum Verlust der intestinalen Integrität und zu chronischen Entzündungserkrankungen wie chronisch-entzündlichen Darmerkrankungen führen. Eine Dysbiose und ein funktionsgestörtes Darmepithel werden außerdem mit dem Altern in Verbindung gebracht. Darüber hinaus hat der Verdauungstrakt mit seinem Mikrobiom einen signifikanten Einfluss auf die Kontrolle der Immunreaktionen, die Aufrechterhaltung der Energiehomöostase, und er beeinflusst sogar die Physiologie und das Verhalten.

Die Fruchtfliege *Drosophila melanogaster* wurde als Modelorganismus verwendet um zu untersuchen, inwiefern die Aktivität von FoxO die Regulierung der Gewebehomöostase, die allgemeine Physiologie, sowie die Zusammensetzung der intestinalen Mikrobiota beeinflusst. Es wurden sowohl Fliegen mit einer genomischen dFoxO-Defizienz als auch Fliegen mit einer Überexpression von dFoxO in unterschiedlichen Zelltypen des Darmes (ECs oder ISCs und EBs) verwendet.

Überraschenderweise hatten dFoxO-Defizienz und Überexpression von dFoxO in Enterozyten den gleichen, eher negativen Effekt auf einige physiologische Aspekte wie zum Beispiel Lebensspanne, Darmfunktion, Aktivität, metabolische Funktionen, Resistenz gegen Verhungern und Integrität der Darmstruktur. Die Überexpression in intestinalen Stammzellen und Enteroblasten, scheint dem gegenüber eher einen positiven Effekt auf diese Funktionen zu haben.

Außerdem waren keine signifikanten Unterschiede in der fäkalen Mikrobiota von jungen dFoxO-defizienten Fliegen und Fliegen mit einer Überexpression in Enterozyten im Vergleich zu den jeweiligen Kontrollen festzustellen. Mit fortschreitendem Alter zeigten sich allerdings

zunehmend Unterschiede in den mikrobiellen Profilen von Fliegen mit veränderter dFoxO Expression, was letztendlich zu einer Dysbiose in älteren Fliegen führte.

Die Behandlung mit DSS, einer Substanz die in Säugetieren Kolitis verursacht, führt bei *Drosophila* zu einer Verkürzung der Lebensspanne, einer Zunahme der Stammzellproliferation und zu einer Zerstörung der Struktur der Basalmembran. Sowohl das Fehlen von dFoxO als auch die Überexpression in intestinalen Stammzellen und Enteroblasten hatten eine vorteilhafte Wirkung auf die Überlebensdauer, möglicherweise durch die Verhinderung einer Überproliferation und die daraus folgende Dysplasie. Im Gegensatz dazu schien die Überexpression von dFoxO in Enterozyten keinen wesentlichen Einfluss auf die mit DSS behandelten Fliegen zu haben.

List of abbreviations

AB	Antibody
AF488	α-rabbit Alexa Fluor® 488
Akt	protein kinase B
AMP	Antimicrobial peptide
AMPK	AMP-activated protein kinase
CD	Crohn's disease
cDNA	complementary DNA
CO_2	carbon dioxide
d	days
Da	Dalton
DABCO	1,4-diazabicyclo-[2,2,2]-octane
DAPI	4' ,6-Diamidino-2-phenylindole
Dlg1	Disc large 1
DNA	Desoxyribonucleic acid
DSS	Dextran Sulfate Sodium
EB	Enteroblast
EC	Enterocyte
EEC	Enteroendocrine cell
EGFR	epidermal growth factor receptor
ERK	extracellular signal-regulated kinase
Fkh	Forkhead
FoxO	Forkhead box class O
gDNA	genomic desoxyribonucleic acid
GFP	green fluorescent protein
h	hours
H_2O	water
Imd	inflammatory bowel disease
IGF	insulin-like growth factor
IMD	Immune deficiency
InR	insulin-like receptor
ISC	Intestinal stem cell
JAK	Janus kinase
JNK	c-Jun N-terminal kinase
kDA	Kilodalton
MAPK	mitogen-activated protein kinase
min	minutes
ml	milliliter
mm	millimeter
MST1	mammalian Ste20-like kinase
µl	microliter
µm	micrometer
nm	nanometer
NM	normal medium
NaClO	Sodium hypochloride
PBS	Phosphate buffered saline
PBT	Phosphate buffered saline with Triton-X-100

PFA	Paraformaldehyde
PI3K	Phosphoinositid 3 kinase
RNA	Ribonucleic acid
s	seconds
SD	standard deviation
SEM	standard error of the mean
SGK	serum and glucocorticoid-inducible kinase
STAT	signal transducer and activator of transcription protein
TOR	target of rapamycin
UAS	Upstream activating factor
UC	ulcerative colitis
v	volume
w	weight
wnt	wingless
wt	wildtype

1. Introduction

1.1. The digestive tract of *Drosophila melanogaster*

In recent years, the intestine received much interest as it plays an important role in immunity as well as in maintaining energy homeostasis by modulation of food intake, insulin secretion and exchange of information with other organs. Additionally, the behavior and physiology not only of the gut, can be influenced by the intestinal microbiota (Lemaitre & Miguel-Aliaga 2013; Miguel-Aliaga et al. 2018). Organismal health is strongly depending on a well-maintained epithelial integrity and microbiome. Thus, damages or deregulations can result in chronic diseases such as inflammatory bowel disease (IBD).

The *Drosophila* intestine shares great similarities with mammalian intestines regarding overall physiology, structure and cellular turnover (Fig. 1.1 C+D) (Casali & Batlle 2009; Pitsouli et al. 2009). The adult intestine consists of a tube lined with an epithelial monolayer surrounded by visceral muscles, nerves and trachea. It can be divided into three regions based on function, morphology and origin (Fig. 1.1 B). The midgut is of endodermal origin, whereas the foregut and the hindgut are ectodermally derived. The foregut is the most anterior part of the digestive tract. It is subdivided into esophagus, crop and proventriculus. The crop is assumed to be involved in early digestion, food storage, microbial control, and detoxification (Stoffolano & Haselton 2013). The proventriculus produces the peritrophic matrix, a protective chitinous layer facing the lumen of the gut (Hegedus et al. 2008), as well as antimicrobial peptides (AMPs) (King 1988; Tzou et al. 2000). The midgut comprises most parts of the digestive tract of *Drosophila* and is the major site of digestion and absorption (Demerec 1950). Based on distinct digestive and metabolic functions, the adult midgut can be subdivided into six major anatomical regions (R0 to R5), which are separated by narrow epithelial boundaries (Buchon et al. 2013a). These regions are further subcategorized based on histological and genetic features (Buchon et al. 2013; Marianes & Spradling 2013). At the junction between the midgut and the hindgut, excretory organs called malpighian tubules are located. The hindgut can be subdivided into four regions: the hindgut proliferation zone (HPZ), the pylorus, the ileum and the rectum (Guo et al. 2016; Miguel-Aliaga et al. 2018). Each region of the gut has specific physiological characteristics such as the luminal pH. The R1 and R2 regions of the anterior midgut have a neutral pH. The R3 region of the middle

midgut contains the acidic copper cell region, which functionally resembles the mammalian stomach. The acidic pH of 2 provides optimal conditions for the activity of peptidases, fighting ingested microorganisms and the uptake of metals and lipids. In the posterior midgut, nutrients are absorbed at a mildly alkaline pH. Finally, in the hindgut with a mildly acidic pH, water is resorbed and fecal waste is excreted (Buchon et al. 2013; Lemaitre & Miguel-Aliaga 2013; Overend et al. 2016).

The *Drosophila* midgut epithelium consists of only four cell types: intestinal stem cells (ISCs), absorptive enterocytes (ECs), the major cell type of the intestine, secretory enteroendocrine cells (EECs) and postmitotic progenitor cells called enteroblasts (EBs). The different cell lineages can be identified with specific markers. Delta (Dl), a ligand of the Notch pathway marks ISCs, while Escargot (Esg) labels both ISCs and EBs. Nubbin (Pdm1) and Brush Border Myosin (Myo1a) mark ECs and Prospero (Pros) marks EECs (Ohlstein & Spradling 2006; Micchelli & Perrimon 2006; Jiang et al. 2009). ISCs reside at the basement membrane and show a scattered distribution within the midgut epithelium. They usually divide asymmetrically, giving rise to an ISC and an EB. The EB then differentiates to either an EC or an EEC depending on Delta-Notch signaling. Daughter-EBs of ISCs with high Delta levels and thus strong Delta-Notch signaling, become ECs, whereas daughter-EBs from ISCs with little or no Delta receive only a weak Notch signal directing development into EECs (Ohlstein & Spradling 2007). Similarly to *Drosophila*, the mammalian digestive epithelium is also continuously regenerated by ISCs that are residing in the crypts (Fig. 1.1 D). ISCs divide and generate progenitor cells called transient amplifying cells, which further proliferate and differentiate into ECs or secretory cells such as EECs, Goblet cells or Tuft cells (Liu et al. 2017).

Under normal physiological conditions, the complete midgut epithelium is renewed every one to three weeks (Micchelli & Perrimon 2006; Ohlstein & Spradling 2006; Antonello et al. 2015). However, tissue defects caused for example by chemical feeding or bacterial infection, speed up the proliferation to ensure fast regeneration of damaged intestinal regions (Apidianakis et al. 2009; Amcheslavsky et al. 2009; Biteau et al. 2008; Buchon et al. 2009a; Buchon et al. 2009b; Jiang et al. 2009). The turnover rate is dependent on environmental factors, the metabolic state and the overall health conditions (Jiang & Edgar 2011; Liang et al. 2017). The ISC homeostasis in *Drosophila* as well as in the mammalian model is generally sustained by conserved pathways such as JAK-STAT-, Hippo-,

Wingless/Wnt- and epidermal growth factor receptor (EGFR)-pathways (Buchon et al. 2013; Karin & Clevers 2016).

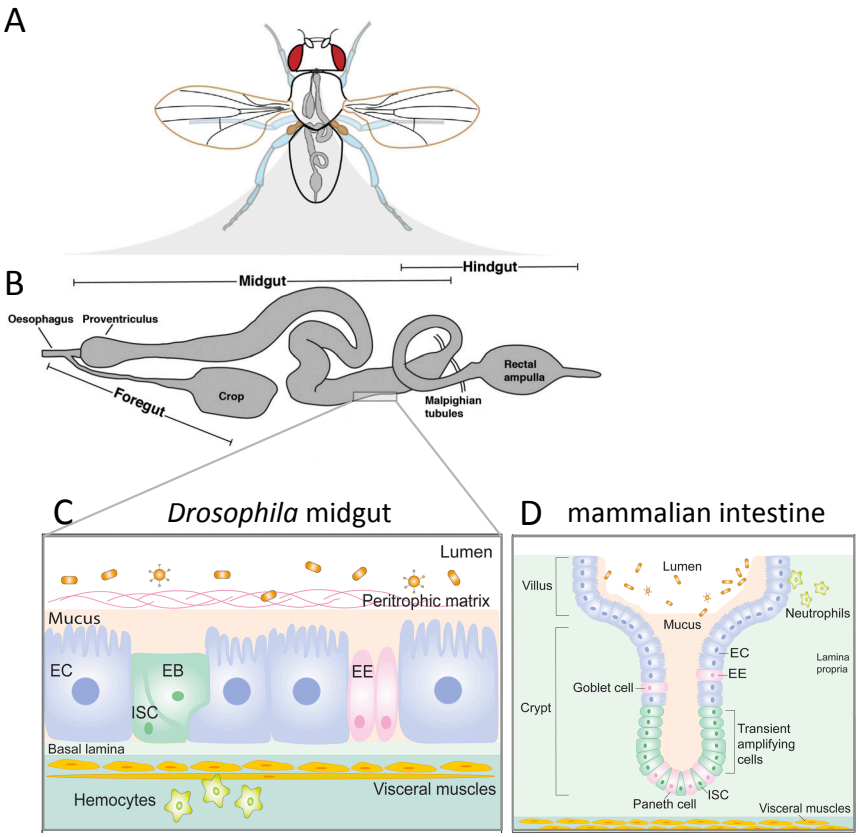

Fig. 1.1: Intestinal tract of *Drosophila* and comparison of *Drosophila* midgut epithelium and the mammalian intestinal epithelium. (A) Orientation of the intestine inside the fly. (B) Anatomical regions of the *Drosophila* intestine (modified from Miguel-Aliaga et al. 2018). (C) The *Drosophila* midgut epithelium comprises mainly of absorptive enterocytes (EC) and fewer secretory enteroendocrine cells (EE). Intestinal stem cells are scattered along the basement membrane. They mostly divide asymmetrically giving rise to an ISC and an enteroblast (EB), which further differentiate into an EC or an EE. The peritrophic membrane and a thin mucus layer protect the epithelium. (D) The mammalian intestine comprises of progenitor and Paneth cells which reside at the base of crypts and differentiate into transient amplifying cells, which proliferate and differentiate into absorptive cells (ECs) or secretory cells (goblet cells and EEs). A mucus layer protects the epithelium. Secreted signals are transmitted by (C) Hemocytes and (D) Neutrophils (modified from Liu et al. 2017).

The gastrointestinal tract is an active barrier that functions as the first layer of defense against pathogens, but it is also in direct contact gut microbes, which populate the intestine (Buchon et al. 2014). The epithelial immune response must be precisely regulated in order to eliminate potential pathogens while tolerating beneficial or benign microbes (Lemaitre & Hoffmann 2007; (Royet 2011; Davis & Engström 2012). In the *Drosophila* intestine, the immune response is facilitated by the production of antimicrobial peptides (AMPs) by the Imd-pathway (Tzou et al. 2000; Zaidman-Rémy et al. 2006) and FoxO (Fink et al. 2016), the production of microcidial reactive oxygen species (ROS) by the NADPH-oxidase Duox (Ha et

al. 2005) and pore forming toxins of the peritrophic membrane (Kuraishi et al. 2011). Additionally, several lysozyme genes are expressed in the gut upon infection with bacteria (Roxström-Lindquist et al. 2004).

1.2. The microbial composition of the *Drosophila* intestine

The microbial diversity in *Drosophila* is lower than in mammals. Approx. 30 bacterial species have been identified in wild-caught and laboratory-reared *Drosophila*, with *Lactobacillus* and *Acetobacter* being most dominant and abundant (Cox & Gilmore 2007; Chandler et al. 2011; Broderick & Lemaitre 2012; Broderick et al. 2014; Wong et al. 2011, 2013). Interestingly, the microbial composition of *Drosophila* populations often show great differences between laboratories and sometimes even populations from the same laboratory (Chandler et al. 2011). Bacteria are transferred to the next generation by contamination of the eggshell, which is ingested by larvae after hatching (Bakula 1969).

The microbiota is shaped by several environmental and host factors such as diet (Chandler et al. 2011; Sharon et al. 2010) and immunity (Ryu et al. 2008; Buchon et al. 2009b). Additionally, aged flies often show an increase in load and diversity of intestinal microbes. This dysbiosis, which impairs gut function, might be due to immune dysregulation (Buchon et al. 2009b; Guo et al. 2014; Li et al. 2016; Clark et al. 2015).

1.3. The process of aging

Almost all species are affected by the universal phenomenon of aging. It is broadly defined as the time-dependent functional deterioration of organisms, which increases the susceptibility to death. The major characteristic of aging is the decline in tissue regeneration due to stem cell exhaustion (López-Otín et al. 2013). Although the biological processes causing aging are not fully understood, a major cause of aging is thought to be the time-dependent accumulation of cellular damages (Kirkwood 2005; Vijg & Campisi 2008). However, several studies show that only 20 to 30 % of the variations in life span are due to genetic factors. One major influence on the process of aging are environmental factors such as diet, exercise or stress (Christensen et al. 2006; Herskind et al. 1996; Hjelmborg et al. 2006; Ljungquist et al. 1998; Skytthe et al. 2003; Dato et al. 2017). Unlike being assumed for many years, age-related tissue decline is not a passive process, but regulated by classical

signaling pathways and transcription factors. Stress response genes and nutritional sensors are often involved in age-related mutations (Kenyon 2010).

In many different species, dietary restriction is known to extend life span by regulating several nutrient-sensing pathways such as insulin/ insulin-like growth factor (IGF-1) signaling (Arum et al. 2009; Honjoh et al. 2008) and the kinase target of rapamycin (TOR) (Hansen et al. 2007; Kaeberlein et al. 2005; Kapahi et al. 2004).

In mammals, aging is known to result in a decline of innate as well as adaptive immunity described as “immune-senescence” and a low pro-inflammatory status referred to as “inflammaging” caused by accumulation of pro-inflammatory tissue damages (Salminen et al. 2008; 2012).

1.4. FoxO transcription factors

FoxO transcription factors belong to a large group of Forkhead proteins. They are characterized by a conserved DNA binding domain consisting of 100 amino acids referred to as the ‘forkhead box or FOX’. Forkhead proteins are conserved and present in all eukaryotes (Kaestner et al. 2000). In humans, at least 50 FOX genes have been identified (Jackson et al. 2010) and are divided into 19 subgroups (FOX A to S) (Greer & Brunet 2005). The first discovered FOX gene was *forkhead* (*fkh*) in *Drosophila.* It is essential for the development of terminal structures in the embryo. Mutations in the *forkhead* gene cause the formation of ectopic head structures in the gut, resembling a fork-like structure (Weigel et al. 1989), hence the name Forkhead.

FoxO genes are evolutionary conserved and ubiquitously expressed key regulators of insulin/ IGF-1 signaling (Kenyon 2005; Ziv & Hu 2011). They are involved in many molecular processes such as DNA repair and protection from DNA damage (Tran et al. 2002; Huang et al. 2006), regulation of growth (Jünger et al. 2003; Kramer et al. 2003) cell cycle arrest (Kops et al. 1999; Medema et al. 2000), metabolism and energy homeostasis (Zhang et al. 2006; Varma et al. 2014), apoptosis and cell death (Brunet et al. 1999; Luo et al. 2007), life span (Giannakou et al. 2004; Hwangbo et al. 2004) and immune functions (Varma et al. 2014; Fink et al. 2016).

While in mammals, four different FoxO proteins could be identified (FOXO1, FOXO3a, FOXO4 and FOXO6) (Anderson et al. 1998; Furuyama et al. 2000), invertebrates only have one FoxO

protein, named Daf-16 in *Caenorhabditis elegans* (Kenyon et al. 1993) and dFoxO in *Drosophila* (Kramer et al. 2003).

Because of their function in regulation of growth arrest and apoptosis in response to DNA damage and oxidative stress responses, FoxO factors are thought to play a key role in inflammatory processes (Greer & Brunet 2005). In *Drosophila*, it was shown that dFoxO could induce the release of antimicrobial peptides (AMPs). Since dFoxO is activated by reduced insulin signaling, the immune status of metabolic tissues, such as the fat body or the intestine, can be regulated by the organismal energy condition (Becker et al. 2010; Varma et al. 2014). Additionally, dFoxO is activated in enterocytes, the major cell population of the intestine, by oral infection and thus playing a role in the innate immune response (Fink et al. 2016). AMPs not only fight infection as part of the immune system but can also regulate the commensal microbiota (Varma et al. 2014). Therefore, dFoxO may influence and shape the microbiome.

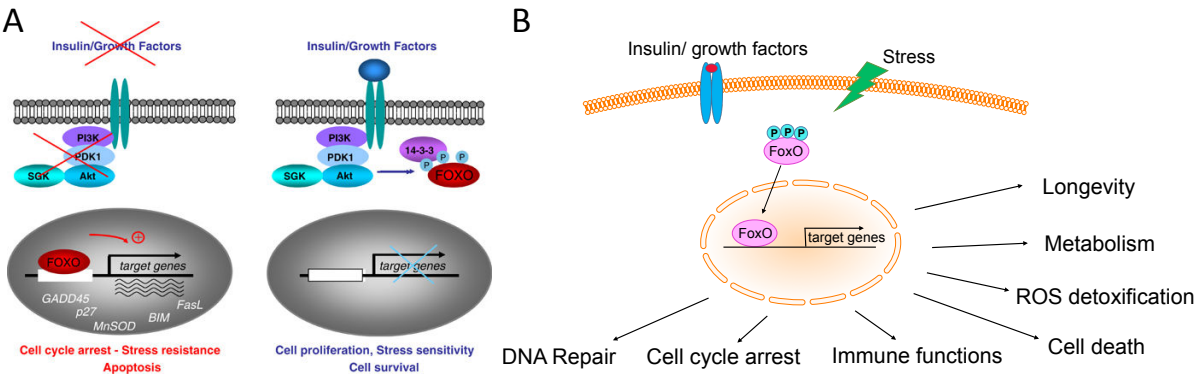

Fig. 1.2: Regulation of FoxO by Insulin/ growth factors or stress. (A) In the absence of insulin or growth factors, FoxO transcription factors are dephosphorylated, activated and translocated to the nucleus where they upregulate several target genes and cause for example cell cycle arrest, stress resistance and apoptosis. In the presence of insulin or growth factors, the PI3K-Akt/SGK pathway is activated. Akt and SGK migrate to the nucleus where they phosphorylate FoxO on three conserved residues. Phosphorylated FoxO binds to 14-3-3 proteins, which causes the translocation of FoxO to the cytoplasm. Inhibited FoxO-dependent transcription results in cell proliferation, stress sensitivity and cell survival. p27, cyclin-dependent kinase inhibitor (p27KIP1); MnSOD, manganese superoxide dismutase; FasL, Fas ligand; GADD45, growth arrest and DNA damage-inducible protein 45 (Greer & Brunet, 2005). (B) Absence of insulin or growth factors or presence of stress factors causes a dephosphorylation and translocation of FoxO to the nucleus, which causes numerous processes (modified from (Carter & Brunet 2007).

It was shown that the activation of Daf-16 in *C. elegans* (Kenyon et al. 1993; Lin et al. 1997) as well as the overexpression of dFoxO in the *Drosophila* fat body (Giannakou et al. 2004; Hwangbo et al. 2004) extended the life span in these organisms. In humans, FOXO3a is associated with longevity (Willcox et al. 2008; Flachsbart et al. 2009) while the other three FOXO genes could not be linked to human life span (Kleindorp 2011).

1.5. Regulation of FoxO transcriptional factors

FoxO transcription factors are regulated by a variety of external stimuli such as growth factors, neurotrophins, cytokines, nutrients and stress stimuli (Calnan & Brunet 2008).

1.5.1. Regulation in response to insulin and growth factors

Growth factors such as insulin-like growth factor 1 (IGF-1) (Brunet et al. 1999; Rena et al. 1999), insulin (Kops & Burgering 1999; Nakae et al. 1999), interleukin 3 (Dijkers et al. 2000), erythropoietin (Kashii et al. 2000), epidermal growth factor (Jackson et al. 2000) and nerve growth factor (Zheng et al. 2002) are able to regulate FoxO factors *via* the conserved PI3K-Akt/SGK pathway. In the presence of growth factors, the phosphoinositide kinase (PI3K) is activated, which then activates protein kinases Akt and serum and glucocorticoid-inducible kinase (SGK). Akt and SGK phosphorylate FoxO at three conserved sites, which causes the translocation into the cytoplasm and inhibition of transcription of target genes (Biggs et al. 1999; Brunet et al. 1999; 2002; Kops & Burgering 1999; Nakae et al. 1999). Once FoxO is phosphorylated, 14-3-3 proteins bind to the first two phosphosites. 14-3-3 proteins are located in both, the cytoplasm and the nucleus (Brunet et al. 1999; Obsil et al. 2003). Interactions of FoxO with 14-3-3 proteins in the nucleus lead to the export into the cytoplasm, whereas the binding of both in the cytoplasm prevents FoxO from translocating to the nucleus (Brunet et al. 2002; Obsilova et al. 2005).

1.5.2. Regulation in response to stress stimuli

Although FoxO is negatively regulated in response to insulin and growth factors, the activation and translocation of FoxO proteins into the nucleus can be caused by stress stimuli even in the presence of growth factors (Brunet et al. 2004; Kitamura et al. 2005, Frescas et al. 2005). Stress stimuli that can regulate FoxO include oxidative stress, heat shock, UV radiation (Brunet et al. 2004) and metabolic stress (Brunet & Webb 2014). Apart from being phosphorylated by Akt and SGK, FoxO can also be modified post-translationally at several other residues. These modifications may compose a ‘molecular FoxO code’ that can be recognized by selective protein partners to regulate programs of gene expression (Calnan & Brunet 2008). Phosphorylation of FoxO at different residues can be caused by several different stress-inducible protein kinases such as JNK (Essers et al. 2004; Oh et al.

2005), AMPK (Greer et al. 2007), MST1 (Lehtinen et al. 2006) and ERK and p28 MAPK (Asada et al. 2006; Yang et al. 2008) . Post-translational modification of FoxO include acetylation/ deacetylation, arginine and lysine methylation and ubiquitination in response to stress stimuli (Brunet et al. 2004; Calnan et al. 2012; Van Der Horst et al. 2004; Yamagata et al. 2008).

1.6. Research model *Drosophila*

Drosophila melanogaster has been used as a model for scientific and medical research for over 100 years. The advantages include the short life cycle, easy husbandry, high number of offspring, the easiness of genetic manipulation and the completely sequenced genome (Adams et al. 2000).

The complete life cycle of *Drosophila* from the embryo to the eclosing of the adult fly takes approx. 10 days at 25°C. After fertilized eggs are laid onto the medium, it takes one day for the embryos to develop and hatch as 1^{st} instar larvae. Two more moltings result in 2^{nd} and 3^{rd} instar larvae at day three after egg deposition. Within two to three days, 3^{rd} instar larvae crawl out of the medium and pupate. Approx. four days later, adult flies eclose from the pupae (Fig. 1.3 A).

One of several possibilities to genetically modify *Drosophila* is the bipartite Gal4-UAS expression system that derived from yeast. It allows temporally and spatially regulated expression of target genes. One parental line is required to contain the transcriptional activator Gal4 fused to a specific promotor or enhancer region (driver line). In the other parental line, referred to as responder line, the gene of interest is fused to UAS (Upstream Activation Sequence). Upon crossing a driver line carrying the desired Gal4 construct to the responder line carrying the gene of interest fused to UAS, target genes are tissue specific activated in the F1-generation (Brand & Perrimon 1993) (Fig. 1.3 B). An extension of the Gal4-UAS system is the TARGET (temporal and regional gene expression targeting) system. Gal80, a temperature sensitive repressor of Gal4, is co-expressed in the driver line. At low temperatures (< 19°C), $Gal80^{ts}$ binds to Gal4, which inhibits the binding of Gal4 to UAS und thus preventing the expression of the target gene. A shift to a higher temperature (29°C) $Gal80^{ts}$ is degraded and thus stops the repression of Gal4 and target genes can be expressed (McGuire et al. 2003).

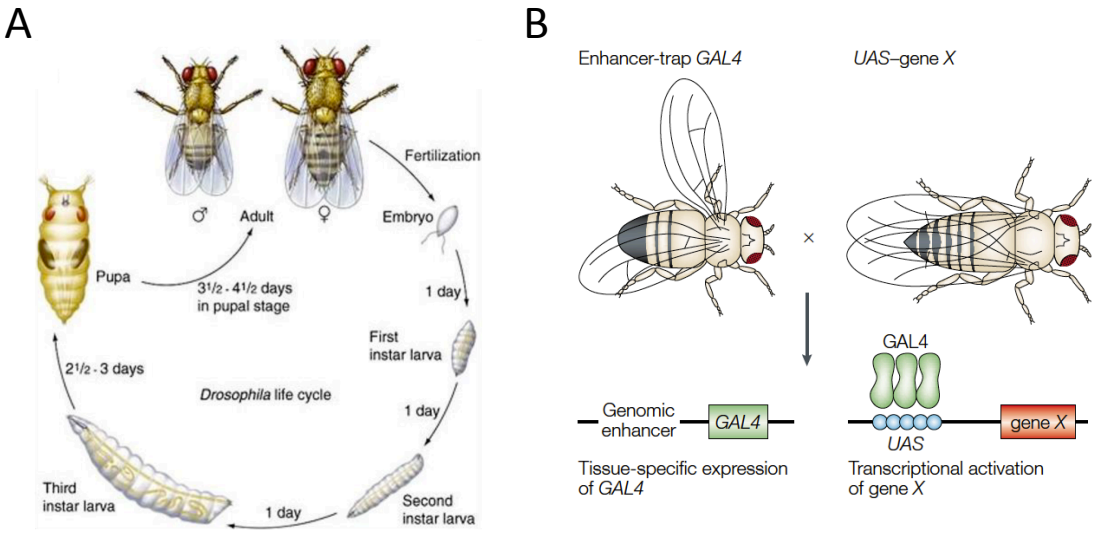

Fig. 1.3: Life cycle of *Drosophila melanogaster* at 25°C and bipartite Gal4-UAS expression system. (A) The life cycle of *Drosophila* is temperature-dependent and takes approx. 10 days at 25°C from egg deposition to eclosion of the adult fly (from https://www.creative-diagnostics.com/Drosophila.htm). (B) The two-component Gal4-UAS expression system comprises of a Gal4-driver line carrying a tissue specific enhancer/promotor and a UAS-responder line carrying a UAS fused to the gene of interest. By crossing both lines, both constructs are expressed in the F1 generation allowing a tissue-specific expression of genes (St Johnston 2002).

1.7. Dextran Sulfate Sodium or Bleomycin induced tissue damage

Crohn's disease (CD) and ulcerative colitis (UC) are the most important inflammatory bowel diseases (IBD). In Europe and North America, approx. 2.2 and 1.4 million people suffer from UC and CD, respectively (Loftus 2004; Hanauer 2006), with the incidence and prevalence increasing worldwide (Molodecky et al. 2012).

The most common model to study colitis in mice is the exposure to Dextran Sulfate Sodium (DSS). This chemical colitogen is water-soluble, negatively charged and has anticoagulant properties. The molecular weight of DSS varies between 5 kDa and 1400 kDa, with 40 to 50 kDa being the most effective in inducing colitis in mice which resembles human UC (Okayasu et al. 1990; Kitajima et al. 2000). Due to its highly negative charge, DSS causes impaired barrier integrity. The consequential epithelial permeability allows bacteria to invade the colon and cause inflammation (Fig. 1.4 A). The ability to induce acute, chronic or relapsing conditions of IBD makes the DSS mouse model very suitable for research. Additionally, it has the advantage of being simple, rapid, reproducible and controllable (Chassaing et al. 2014).

In *Drosophila*, the DSS model was introduced by Amcheslavsky et al. in 2009. They revealed that DSS shortens the life span in a dose-dependent manner. Additionally, they showed the

disruption of basement membrane organization (Fig. 1.5 A-D), an increase in stem cell division and in number of enteroblasts after ingestion of DSS (Fig. 1.5 E), but no enteroblast differentiation.

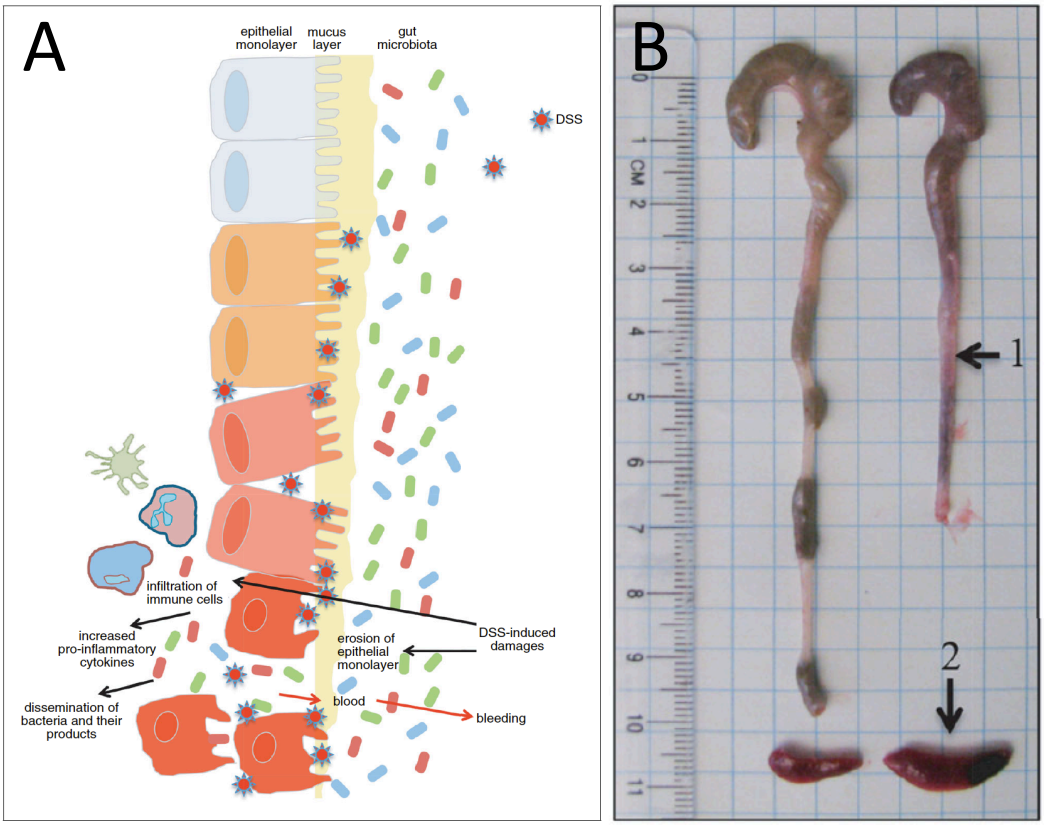

Fig. 1.4: Effects of DSS on the intestinal morphology of mice. (A) Schematic illustration of DSS-induced colitis. (B) Colons of 8-week-old mice treated with 2.5 % DSS in drinking water (right) or drinking water only (left). DSS-treated mice showed shortened and bleeding colons (1) and enlarged spleens (2) (modified from Chassaing et al. 2014).

Bleomycin is an antibiotic cytostatic anticancer drug. It causes the fragmentation of DNA and is used in cancer therapy and for experimental purposes (Takada et al. 2003; Morel et al. 2008). It is produced by the bacterium *Streptomyces verticillus* and was first described by Umezawa et al. in 1966. Because of its toxicity and severe side effects, Bleomycin is not used as an antibiotic drug although it is effective in fighting bacterial infections. In *Drosophila*, oral application of Bleomycin causes a reduction of life span, a disorganization of the intestinal epithelial layer (Fig. 1.5 F-I) and an increase in proliferation (Fig. 1.5 J) (Amcheslavsky et al. 2009).

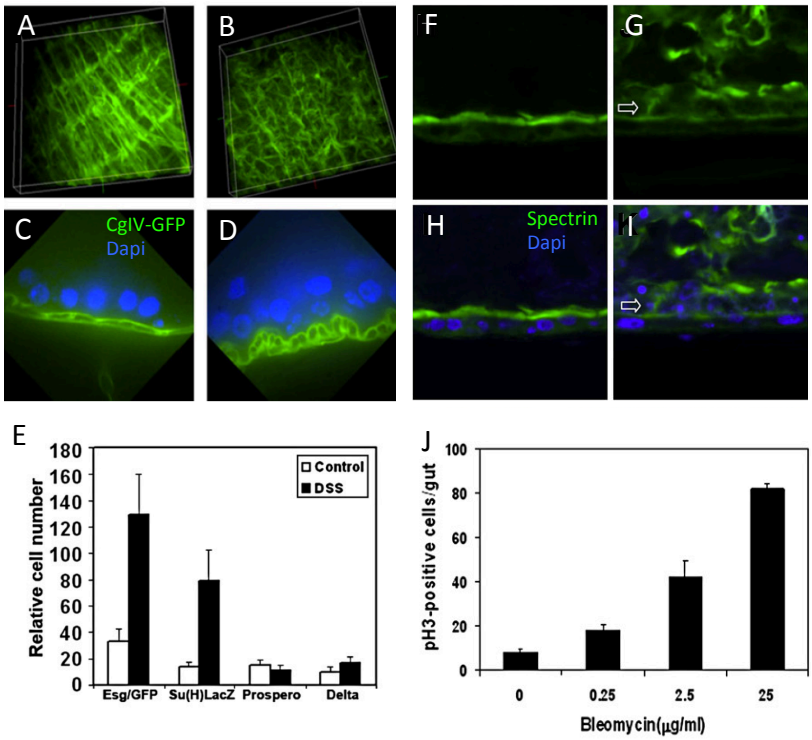

Fig. 1.5: Effects of DSS and Bleomycin on the intestinal morphology of *Drosophila*. (A+B) Surface views of 3D reconstructed confocal images of dissected guts from a collagen IV-GFP reporter fly line. In control flies, the longitudinal and transverse filaments are connected and present probably the basement membrane structure (A). Upon DSS-treatment, the structure is disrupted (B). (C+D) confocal sagittal views of dissected guts from a collagen IV-GFP reporter fly line. In DSS-treated flies (D), both layers of the longitudinal filaments are thicker and more rounded compared to controls (C). (E) Quantification of relative cell numbers of cells according to expressed cell markers upon DSS-treatment. The number of esg$^+$ cells (ISCs and EBs) and Su(H)LacZ$^+$ cells (EBs) are strongly increased after treatment with DSS. In prospero- (EECs) and delta-marked cells (ISCs), DSS induced only minor changes in cell number. (F-I) confocal sagittal view of dissected guts labeled with spectrin antibody. (G+I) After treatment with Bleomycin, ECs were shed off the epithelial layer (arrows), (F+H) untreated controls. (J) Dose-dependent increase of pH3$^+$-cells upon Bleomycin treatment (modified from Amcheslavsky et al. 2009); ICSs = intestinal stem cells; EBs = enteroblastes; EECs = enteroendocrine cells; esg = escargot; cgIV-GFP = collagen IV-GFP.

1.8. Aims of this study

A well-maintained tissue homeostasis and microbiome are essential for the individual health of an organism. Thus, a deregulation of tissue turnover or a dysbiosis may result in impaired gut integrity and chronic inflammatory diseases such as IBD. Both, bacterial dysbiosis and dysplasia due to an imbalance of epithelial regeneration and proliferation is associated with aging.

The transcription factor FoxO has been linked to the maintenance of the intestinal microbiome and epithelial homeostasis. In non-senescent *Hydra* for example, it can regulate stem cell division as well as the release of antimicrobial peptides. FoxO activity also affects the life span in several organisms including humans.

To understand how FoxO activity is involved in regulating tissue homeostasis, the overall physiology and the intestinal microbial composition, dFoxO overexpression was induced in different cell types of the *Drosophila* intestine (ECs or ISCs and EBs). Additionally, flies with an overall deficiency of dFoxO were used for experiments.
The major questions addressed in this thesis were:

1. How does a manipulation of dFoxO influence physiological functions?
2. Does dFoxO expression have an effect on the response to stress such as DSS, Bleomycin or starvation?
3. Do different dFoxO expression levels result in tissue specific transcriptomic changes?
4. Does dFoxO have an influence on the intestinal microbiota?
5. Is the function of dFoxO cell specific?

2. Material and Methods

2.1. Devices

Analytical balance (ABS)	Kern & Sohn GmbH(Balingen, Germany)
AxioImager	Zeiss (Oberkochen, Germany)
Balance (MXX-412)	Denver Instrument GmbH (New York, USA)
Bead ruptor 24	Omni International (Kennesaw, USA)
Centrifuge (5415 D)	Eppendorf (Hamburg, Germany)
Centrifuge (5417 R)	Eppendorf (Hamburg, Germany)
Electrophoresis chambers	Biometra GmbH (Göttingen, Germany)
Geldocumentation (Transilluminator)	Heinrich Eimecke GmbH (Kiel, Germany)
Incubators (WB250K, WB120K)	Heinrich Eimecke GmbH (Kiel, Germany)
LabGard (IBS)	INTEGRA biosciences GmbH (Biebertal, Germany)
LEDetect 96	Labexim Products (Lengau, Austria)
Light source (U-RFL-T)	Olympus (Hamburg, Germany)
Magnetic stirrer (RET)	IKA®(Staufen, Germany)
Magnetic stirrer (MR3001)	Heidolph (Schwabach, Germany)
pH 340/ION	WTW (Weilheim, Germany)
Power supply (EV245)	ConsortNT (Nürnberg, Germany)
StepOne Real-Time PCR System	Applied Biosystems (Foster City, USA)
Stereo microscope (MZ10F)	Leica Microsystems (Wetzlar, Germany)
Stereo microscope (S6E)	Leica (Wetzlar, Germany)
Stereo microscope (Stemi 506)	Zeiss (Oberkochen, Germany)
Stereo microscope, fluorescence (SZX12)	Olympus (Hamburg, Germany)
Spectrophotometer (DS-11)	DeNovix® (Wilmington, USA)
Tecan plate reader (Infinite M200 Pro).	Tecan (Männedorf, Switzerland)
Thermocycler (Labcycler)	SensoQuest GmbH (Göttingen, Germany)
Thermomixer comfort	Eppendorf (Hamburg, Germany)

2.2. General materials

Ceapren stopper (Ø 50 mm)	Greiner Bio-One (Kremsmünster, Austria)
Cellulose stopper (Ø 29 mm)	nerbe plus GmbH (Winsen, Germany)
Cover slips (24 x 50 mm)	Carl Roth (Karlsruhe, Germany)
Drosophila food vial (50 ml)	nerbe plus GmbH (Winsen, Germany)
Drosophila food vial (175 ml)	Greiner Bio-One (Kremsmünster, Austria)
Falcon tubes (15 ml, 50 ml)	nerbe plus GmbH (Winsen, Germany)
Filter tips (10, 100, 1000 µl)	nerbe plus GmbH (Winsen, Germany)
Forceps	neoLab® (Heidelberg, Germany)
MicroAmp® Fast Optical 48-Well Reaction Plate (0.1 ml)	Applied Biosystems (Foster City, USA)
Petri dishes, plastic	nerbe plus GmbH (Winsen, Germany)
Reaction tubes, low binding (0.2, 0.5, 1.5, 2 ml)	nerbe plus GmbH (Winsen, Germany)
Reaction tube, screw, 2 ml	Sarstedt (Nümbrecht, Germany)
Serological pipettes (5 ml, 10 ml, 25 ml)	nerbe plus GmbH (Winsen, Germany)
Slides	Carl Roth (Karlsruhe, Germany)

Tips, low-binding (10, 100, 1000 µl)	nerbe plus GmbH (Winsen, Germany)
Well plates (12-well, 96-well)	Sarstedt (Nümbrecht, Germany)

2.3. General chemicals

Bleomycin (sulfate)	Cayman Chemicals (Ann Arbor, USA)
Brewer`s yeast	Leiber (Bramsche, Germany)
Brilliant Blue FCF food dye; E133	Ruth GmbH & Co.KG)
Bromcresol Purple	Sigma Aldrich (Munich, Germany)
Cornmeal	Mühle Schlingemann (Waltrop, Germany)
Dithiotheitol (DTT)	Thermo Fisher Scientific (Waltham, USA)
dNTPs	Promega (Madison, USA)
Dextran Sulfate Sodium (DSS, MW= 36.000 -50000 Da)	MP Biomedicals (Solon, USA)
Ethidiumhomodimer III	Biotium (Fremont, USA)
m-cresol Purple	Sigma Aldrich (Munich, Germany)
Micrococcus lysodeikticus ATCC	Sigma Aldrich (Munich, Germany)
Molasses	Biohof Heidelicht (Gerdau, Germany)
Methyl 4-Hydroxybenzoate reagentplus® (nipagin)	Sigma Aldrich (Munich, Germany)
Normal goat serum	Sigma-Aldrich (Munich, Germany)
PFA	Polysciences Inc. (Warrington, USA)
Schneider's *Drosophila* Medium	Genaxxon bioscience (Ulm, Germany)
Sugar beet syrup	Kanne Brottrunk (Selm-Bork, Germany)
triglycerides	Thermo Fisher Scientific (Waltham, USA)
trioleate standard	Sigma Aldrich (Munich, Germany)

All other chemicals were purchased from Carl Roth (Karlsruhe, Germany).

2.4. Enzymes and kits

DNeasy Blood and Tissue DNA Extraction Kit	Quiagen (Venlo, Netherlands)
PureLink™ RNA Mini Kit	Life Technologies (Carlsbad, CA, USA)
One Glo Luciferase Assay System	Promega (Mannheim, Germany)
Phusion Hot Start II DNA Polymerase (F-549L)	Thermo Fisher Scientific (Waltham, USA)
5x Phusion HF Buffer (F-518)	Thermo Fisher Scientific (Waltham, USA)
Pierce™ BCA Protein Assay Kit	Thermo Fisher Scientific (Waltham, USA)
qPCRBIO SyGreen Mix Hi-Rox	PCR Biosystems Ltd (London, UK)
SuperScript IV Reverse Transcriptase	Thermo Fisher Scientific (Waltham, USA)
5x SuperScript IV reaction buffer	Thermo Fisher Scientific (Waltham, USA)

2.5. Oligonucleotides

Table 2-1: Primer and primer sequences used for polymerase chain reaction.

Primer	sequence (5' → 3')
kune_F	AGGTTGTGGGCTCTGTTTTC
kune_R	ATCCCGAGAATCTCCTTTGG
dlg1_F	AGAGTCGCGATGAGAAGAATG
dlg1_R	GCTGGTGCTGCTCACAACT
socs36e_F	GAGATCCTCACAGAGGCCACT
socs36e_R	GCGAAACTTTCCACCTGACC
decad_F	GACGAATCCATGTCGGAAAA
decad_R	TCACTGGCGCTGATAGTCAT
prospero_F	AGGAGGCGCTATCAACAACC
prospero_R	TCTCTCCATTCACCAGAAGGC
foxo_F	GCCTCGTTATTGAGCACCTC
foxo_R	CTCCCTGAACACGTACAGCA
upd3_F	GAGAACACCTGCAATCTGAA
upd3_R	AGAGTCTTGGTGCTCACTGT
upd2_F	AGCAGAAGAGCCTCAACGAG
upd2_R	CTGGCGTGTGAAAGTTGAGA
V2_27_F	AGAGTTTGATCCTGGCTCAG
V2_338_R	TGCTGCCTCCGGTAGGAGT
OligodT T7	GAGAGAGGATCCAAGTACTAATACGACTCA CTATAGGGAGATTTTTTTTTTTTTTTTTTTTTTTTV

2.6. Bacteria

Lactobacillus plantarum^{WJL}*, Lactobacillus brevis*^{EW}*, Acetobacter pomorum, Commensalibacter intestini*^{A9111T} *and Enterococcus faecalis* were all received as a kind gift from Carlos Ribeiro.

2.7. Fly husbandry

Fly lines were cultivated on normal medium (NM) in *Drosophila* food vials at RT and transferred to fresh vials once a week. For crossings, virgin females were mated with males of the desired genotype. Temperature sensitive crossings were raised at 18°C, all others at 25°C.

If not stated otherwise, five to seven day old female flies were used for experiments. The F1 progeny containing temperature-inducible genetic modules and their corresponding controls were kept at 18°C for five days before the induction of the expression of the gene of interest at 29°C for five days.

Normal Medium (NM), 500ml:

31.25 g	brewer's yeast
31.25 g	cornmeal
10 g	D-glucose, monohydrate
5 g	agar agar
15 g	sugar beet syrup
15 g	molasses

500 ml H_2O were added, mixed well, boiled in water bath and cooked for approx. 15 min until the mixture thickened. It was autoclaved for 20 min and cooled down to 60°C. 5 ml of propionic acid (10 % in ddH_2O) and 15 ml of nipagin (10 % in 70 % EtOH) were added. The medium was poured into *Drosophila* food vials or petri dishes, dried at RT and stored at 4°C.

2.8. *Drosophila* fly lines

Table 2-2: *Drosophila* fly lines

Name	Genotype	Source
foxo$^{21/21}$	*yw;*;dfoxo21/dfoxo21*	M. Tatar, R. Yamamoto, Brown University, USA
w^{1118}	*w[1118]*	Bloomington #5905
yw	*y[1]w[1118]*	Bloomington #6598
NP1-Gal4	*NP1-Gal4;tubPGal80ts*	D. Ferrandon, Straßburg
esg-Gal4	*esg-Gal4,UAS-GFP;tub-Gal80ts*	
EGT;Luc2	*+; p{Esg-Gal4}, p{UAS-GFP}, p{tubulin-Gal80ts}; p{UAS Luciferase at attp2}*	M. Markstein, University of Massachusetts, USA
esg-GS	Mifepristone-inducible gene switch	
UAS-foxo	*y[1] w[*]; P{w[+mC]=UAS-foxo.P}2*	Bloomington (9575)
UAS-foxoTM	yw; UASdFoxoTM/Cyo	(Hwangbo et al. 2004)
UAS-foxo GFP	*pUAST foxo-GFP*	Christina Wagner Kiel University, Germany

2.9. Survival

The life span experiment of flies was performed in modified cell culture flasks. Five replicates with 40 to 50 mated female flies each were used. Normal medium (NM) was poured into 5 cm petri dishes and fixed to the flasks. The medium was changed every three to four days. Dead and escaped flies were monitored three times a week until all flies had died.

2.9.1. Survival under DSS or Bleomycin treatment

The influence of DSS and Bleomycin on the life span of *Drosophila* was tested in standard *Drosophila* vials filled with approx. 10 ml of 1.5 % agar-agar. Five to ten biological replicates with 10 to 20 mated female flies were tested for each treatment. The substances (5 % DSS (w/v) or 25 µl/ml Bleomycin in 5 % sucrose (w/v)) were applied on stripes of filter paper. The filter paper was exchanged three times per week, the vials once a week. Dead and escaped flies were counted every day (sucrose controls every second day).

2.9.2. Survival under starvation condition

The life span of flies under starvation condition was performed in standard *Drosophila* vials filled with approx. 10 ml of 1.5 % agar-agar to prevent a dying of thirst. Dead flies were counted every two hours during the day until all flies had deceased.

2.10. Food consumption

The consumption of food was assessed with the previously described consumption-excretion method (Shell et al. 2018) with minor adjustments. This method allows measuring the ingested food as well as the excretion of flies. NM or blue dyed NM (0.5 % (w/v) Brilliant Blue FCF food dye; E133) was pipetted into caps of 2 ml screw cap vials. Individual flies were transferred into 2 ml screw cap vials with regular NM. Vials were loosely closed to ensure air supply. After several hours of adaptation, caps were replaced with blue NM. After 24 hours caps containing blue NM were replaced with clean empty ones. Flies in tubes were anesthetized on ice. 500 µl H_2O and three ceramic beads were added and samples were homogenized using a bead ruptor (OMNI International, OMNI Bead Ruptor 24) for 90 sec at 3.25 m/s. The homogenate was centrifuged at 3000 rpm for 3 min to pellet the tissue debris. 200 µl of the clear blue supernatant was transferred to clear 96-well-plates. The absorbance at 630 nm was quantified using a SYNERGY H1 microplate reader (BioTek). Two technical replicates of each biological replicate were measured. A standard curve of a dilution series of the blue food was used to calculate the amount of ingested food.

2.11. Measurement of fecal output

Standard *Drosophila* vials were placed tilted and filled with approx. 3 ml of blue dyed NM (0.5 % (w/v) Brilliant Blue FCF food dye and a cover slip (24 x 50 mm). Several hours before the experiment, flies were placed onto blue dyed medium to ensure that all excreted fecal spots were labeled blue and easy to recognize. Three female flies were placed in each experimental vial. The cover slip was fixed with the plug and served as the bottom. After 24 hours, all fecal spots were counted and calculated per fly.

2.12. Transit time assay

To measure the transit time of ingested food through the intestine, flies were monitored from ingestion of food until defecation. Yeast paste was liquefied with apple vinegar and dyed with blue food dye (Brilliant Blue FCF food dye; E133). Lids of 0.2 ml PCR tubes were removed, filled with the food up to the top and placed in 24-well plates. One female fly was placed in each well and the plate was sealed with the lid. Because flies showed differences in beginning to feed, they were checked every 15 min for blue abdomen, indicating the ingestion of food and after that for the presence of fecal spots and thus a complete gut transit. The transit time was determined for every fly.

2.13. Body composition

The body fat of *Drosophila* was measured in the coupled colorimetric assay (CCA) as previously described (Hildebrandt et al. 2011). The protein content was determined using the Pierce™ BCA Protein Assay Kit according to the manufacturer's protocol.

Groups of five flies were weighed using a microbalance (ABS 80-4, Kern & Sohn GmbH), transferred to 2 ml screw cap vials and frozen until further use. 1 ml of 0.05 % Triton-X 100 in PBS and 3 ceramic beads were added before homogenization using the bead ruptor (OMNI International, OMNI Bead Ruptor 24) for 2 min at 3.25 m/s. The homogenate was incubated at 70°C for 5 min und then centrifuged at 3000 rpm for 3 min to pellet the debris. 500 µl of the clear supernatant was transferred into a fresh 1.5 ml reaction tube and centrifuged at 2500 rpm for 3 min. For the CCA assay, 50 µl of the samples were transferred into clear 96-well-plates. For each biological replicate, three technical replicates were measured. The absorbance at 540 nm (t_0) was measured using a standard plate reader

(LEDetect 96, Labexim products). 200 µl of pre-warmed (37°C) triglycerides (Thermo Fisher Scientific) were added to each well. After an incubation at 37°C with mild shaking (120 rpm) for 30 min, the absorbance at 540 nm was measured again (t_1). Concentrations were calculated using a standard curve of a dilution series with triolate standard. For the BCA, two technical replicates of each biological replicate were measured. 25 µl of each sample were transferred into clear 96-well-plates. 200 µl of the working reagent of the kit were added and mixed with the samples. After an incubation at 30°C with slight shaking (120 rpm), the absorbance at 562 nm was measured using a SYNERGY H1 microplate reader (BioTek). Concentrations were calculated using a standard curve according to the manufacturer's protocol.

2.14. Activity monitoring

The activity of flies was measured using the *Drosophila* Activity Monitor System (DAM, TriKinetics) as previously described with minor modifications (Pfeiffenberger et al. 2010). Individual flies were transferred into glass tubes filled with NM. Tubes were sealed with cotton wool and placed horizontally into the DAM device. To avoid any disturbances that might affect the behavior of the flies, the monitor was set up in climate chamber with a 12 h light/ 12h dark cycle and 65 % humidity. After adaptation to the conditions for one day, the activity was monitored for three additionally days. Activity was detected by flies crossing the light beam of the DAM system. The data was analyzed using the DAMFileScan software (DAMFileScan 110 Libs).

2.15. Metabolic rate

The metabolic rate was measured according to the protocol published by Yatsenko et al. in 2014 with slight adjustments. The fly respirometers were assembled from a 1 ml pipette tip air tightly attached to a 50 µl capillary. A small piece of foam was placed deep into the pipette tip. Three pieces of soda lime were soaked in water, placed on top of the foam and covered by a second piece of foam. After three flies were transferred into the respirometer, it was sealed with plasticine. Two respirometers without flies served as atmospheric controls. Several fly respirometers were placed in a chamber with blue colored water (Brilliant Blue FCF food dye; E133) with the tip of the capillary submerging into the water.

After 15 min of equilibration, a picture was taken (t_0). Two hours later, another picture was taken (t_1). The produced CO_2 was absorbed by the soda lime. Due to capillary pressure, the liquid in the capillary ascended proportionally to the production of CO_2. The amount of CO_2 produced per fly and hour was calculated with the following formula:

$$\frac{(\pi * R2) * (\Delta d - \Delta c) * 1000}{n * h}$$

R: radius of microcapillary
Δd: upper water level of sample
Δc: mean upper water level of atmospheric controls
n: number of flies in respirometer
h: duration in hours

2.16. Gut integrity

Age matched female flies were transferred from NM to vials filled with approx. 10 ml of 1.5 % agar-agar for 24 hours. 5 % sucrose solution dyed with Brilliant Blue FCF food dye (E133, Ruth GmbH & Co.KG) was applied onto filter paper to serve as food source. The loss of gut integrity leads to the leaking of blue food into the body, which causes a blue staining of the whole fly. Flies displaying this blue phenotype are referred to as “smurf” (Rera et al. 2011). After 24 hours, flies were checked for smurf phenotypes (smurf or dead smurf) as a result of leakiness of the gut. Flies were then transferred back to NM. Populations were checked once a week for five (at 25°C) or three to four (at 29°C) weeks.

2.17. pH staining

7 days old female flies were transferred to vials filled with approx. 5 ml of 5 % sucrose in 1.5 % agar agar and 0.05 % each of pH-indicators Bromcresol Purple (pH 5.2 – 6.8 yellow to purple; sigma # B5880-5G) and m-cresol Purple (pH 1.2 – 2.8, red to yellow; 7.4 – 9.0 yellow to violet; sigma 857890-5G) for 24 h. Guts were dissected in PBS. Immediately, pictures were taken because the pH only stays stable for a couple of minutes after dissection. Depending on the pH condition, regions of the gut were labeled yellow, orange, red or purple (Overend et al. 2016).

2.18. Gut length

Guts were dissected and collected in PBS. For fixation, the PBS was replaced by 4 % PFA for 30 to 45 min. Subsequently, the guts were washed with PBS and then embedded in Mowiol. Microscopic pictures were taken using the Axio Imager.Z1 (Zeiss) in the lowest magnification. Pictures were assembled with Image Composite Editor if possible, or PowerPoint. The length of the midgut was measured with ImageJ.

2.19. Fecundity

Ten virgin females of each fly line were transferred to individual vials on NM. Each female was mated with three males of the respective line for 2 days. Then males were removed, laid eggs were counted and females were transferred to new vials for 24 hours. This was repeated for 13 days. The vials containing the eggs were kept at 25°C. The formation of pupae and eclosion of adults was monitored.

2.20. Lysozyme assay

To measure the lysozyme activity, homogenates of *Drosophila* intestines were pipetted onto agarose plates containing cell walls of *Micrococcus lysodeikticus.* For plates, 0.05 M NaAC was mixed with 0.9 % agarose and boiled. 0.6 mg/ml *Micrococcus lysodeikticus* ATCC No. 4698 (sigma Aldrich, M3770-5g) was solved in 1 ml NaAc at 37°C and shaking. After the agarose cooled down to under 50°C, the *Micrococcus* solution was added. 10 ml were poured into petri dishes (9 cm). Eight holes of 4 mm were punched into each plate.

15 intestines were dissected and homogenized in 50 µl PBS with 3 ceramic beads using a bead ruptor (OMNI International, OMNI Bead Ruptor 24) for 2 min at 3.25 m/s. 10 µl of the homogenate was added into the holes on plates. Five biological replicates with four technical replicates each were used. Plates were incubated at 37°C. After 24h, the diameter of the lysis zone was measured.

2.21. Quantification of eggs in ovaries

After treatment with DSS or Bleomycin, ovaries were dissected in PBS and eggs were counted manually.

2.22. Luciferase assay

The luciferase assay was performed as described by Markstein et al. (2008) with slight modifications. After 1, 3, 5 and 7 days of the respective treatment (DSS, Bleomycin, sucrose or NM), intestines of three female flies per replicate were dissected and transferred to 150 µl Glo Lysis buffer (Promega). After homogenization in the bead ruptor (OMNI Bead Ruptor 24) for 2 min at 3.25 m/s, samples were transferred into new reaction tubes and centrifuged at 12,000 g for 3 min. The supernatant was transferred into new reaction tubes and stored at -20°C until quantifying. For measuring, samples were thawed on ice. 50 µl were transferred into white 96-well plates with white flat bottom. To avoid signals of different treatment groups interfering with each other, one row of wells was left empty between them. Directly before signal detection, samples were mixed with 50 µl of the substrate from the One Glo Luciferase Assay System (Promega). A Tecan plate reader (Tecan, Infinite M200 Pro) was used to measure the luciferase signal. All samples were normalized to a standard that was used on every plate.

2.23. Immunohistochemistry

Table 2-3: Antibodies and dyes used for Immunohistochemistry.

Primary antibodies	**Dilution**	**Vendor**
α-prospero (mouse)	1:50	DSHB
α-phospho-Histone H3 (S10) (rabbit)	1:50	Cell Signaling Technology
α-GFP (rabbit)	1:150	Sigma Aldrich
Secondary antibodies		
α-mouse-AlexaFluor 488, goat	1:300	Jackson ImmunoResearch Laboratories
α-rabbit-AlexaFluor 488, goat	1:500	Life Technologies
α-mouse Cy3, goat	1:1000	Jackson ImmunoResearch Laboratories
Fluorescent dyes		
DAPI (4,6-diamidino-2-phenylindole)	1:2000	Carl Roth
Flash Phalloidin Red594	1:50	BioLegend

All antibodies were stored at -20 °C in 50 % glycerol. Phalloidin was dissolved in Methanol according manufacturer's instructions.

Intestines were dissected in PBS and fixed in 4 % PFA for 45 min. Subsequently, intestines were washed three times for 20 min with 0.1 % PBT (0.1 % Triton X in PBS). After blocking with 5 % NGS in 0.1 % PBT, the first antibody (in blocking buffer) was added and incubated

over night at 4°C. The tissue was washed three times for 20 min with 0.1 % PBT before the second antibody (in blocking buffer) was added and incubated again over night at 4°C. Afterwards, the tissue was washed with PBT and nuclei were labeled with DAPI (1:2000 in PBS). After incubation for 20 min in the dark, DAPI was replaced by PBS and intestines were mounted into Mowiol (with 25 mg DABCO/ ml) analyzed microscopically.

Phosphate buffered saline (PBS):

136 mM NaCl

2.7 mM KCl

1.5 mM KH_2PO_4

7 nM Na_2HPO_4

ad with H_2O, pH adjusted to 7.3 with HCl and autoclaved.

Mowiol mounting medium:

2.4 g Mowiol 4-88

6 g Glycerol

6 ml H_2O

were mixed well and incubated at RT for several hours.

12 ml Tris-Cl (pH 8.5) was added and incubated for approx. 2 hours at 50°C with occasionally mixing. Mowiol was stored in aliquots of 1 ml at -20°C. Addition of 2.5 % DABCO (optional) reduces fading of embedded samples.

2.24. Vibratome sectioning

After removal of the head, wings and legs, the abdomen was carefully opened with forceps at least at three different positions. Prepared flies were fixed in 4 % PFA overnight, washed with PBS and embedded in 5 % agarose. Boiling agarose was poured into wells of a 12-well plate. Fixed flies were immediately placed carefully into the hot agarose, one per well. After cooling and hardening, the agarose blocks were stored in PBS at 4°C until sectioning. Flies were cut into 100 µm thick sections using a vibratome (Freq = 80 Hz, amplitude= 0.5, V= 20). Sections were collected in PBS and subsequently labeled with Phalloidin (1:50 in PBS) and DAPI (1:2000 in PBS). After incubation for 20 min in the dark, sections were washed with PBS, mounted into Mowiol (25 mg DABCO/ ml) analyzed microscopically.

2.25. Microscopy

Microscopic analyses were performed with dissected intestines and vibratome sections using the Axio Imager.Z1 (Zeiss) and the AxioVision software (AxioVision SE64 Rel. 4.9).

2.26. Dechorionation and recolonisation

Parental flies of desired lines or crossings were placed in large *Drosophila* vials (315 ml). The vials were closed with a petri dish containing apple juice agar and several chunks of fresh yeast mixed with few drops of apple vinegar. The containers were placed upside down and incubated overnight (maximum 18 h) at 20°C. The petri dish was then removed. The eggs were loosened using water and a Drigalski spatula und poured through a small sieve to collect the eggs. The sieve was placed in a glass beaker containing 6 % NaClO for 5 min for dechorionation. Subsequently, the eggs were sprayed with 70 % EtOH and then rinsed with 500 ml sterile water. The gaze of the sieve was cut with sterile scissors and transferred to sterile *Drosophila* vials with NM.

The germfree embryos were recolonized with a mix of five bacteria species: *Lactobacillus plantarum*^{WJL}, *Lactobacillus brevis*^{EW}, *Acetobacter pomorum, Commensalibacter intestini*^{A9111T} *and Enterococcus faecalis* which were all received as a kind gift from Carlos Ribeiro. The culturing and the adjustment of specific optic densities were performed as described by Santos et al. (2017). After adding the same volume of sterile glycerol, the bacteria mix was stored at 80°C. Each *Drosophila* vial was inoculated with 50 µl of the bacterial suspension.

2.27. 16S analysis of fecal samples

Recolonized flies (2.26) were kept in sterile vials on NM. They were transferred into fresh vials every four to five days. After 24 h, 5 days, 10 days, 20 days and 30 days, feces were collected with a swab soaked in PBS under sterile conditions. Swabs were transferred into 2 ml screw cap tubes und stored at -20°C until DNA was extracted.

The bacterial variable regions 1 and 2 of 16S rRNA genes were amplified as previously described (Rausch et al. 2016) and sequenced with the Illumina MiSeq with 2x300 bp paired-end sequencing. The sequences were analyzed using QIIME 1.9.0 (Caporaso et al. 2011) and the SILVAngs analysis platform (arb-silva.de). Multidimensional scaling- plots and p-values

were calculated based on percentage of the respective group. Distances (euklidian) were calculated using R-function “dist”. MDS-scaling was based on R-function “cmdscale. For p-values, distances from the same group were compared to distances of all groups.

2.27.1. Extraction of genomic DNA

Genomic DNA (gDNA) from *Drosophila* feces for 16S analysis was extracted with the DNeasy Blood and Tissue Kit (Quiagen, #69504). The manufacturer’s protocols “Pretreatment for Gram-Positive Bacteria” and subsequently “Purification of Total DNA from Animal Tissues” were followed. The extracted DNA was eluded in 100 µl sterile AE buffer. To check for bacterial DNA, a standard PCR (2.30.1) with bacteria specific primers was performed. Until sequencing, the DNA was stored at -20°C.

2.28. Total RNA extraction

Total RNA was extracted using RNA Magic and the Ambion PureLink™ RNA Mini Kit. Eight to ten dissected *Drosophila* intestines were transferred to 2 ml screw cap tubes containing 1 ml RNA Magic and 3 ceramic beads and homogenized using the bead ruptor (OMNI International, OMNI Bead Ruptor 24) for 3 min at 3,25 m/s. At this point, the homogenate could be stored at -20°C. After incubation at RT for 5 min, 200 µl of chloroform was added. Samples were shaken for 10 s, incubated on ice for 5 min and centrifuged at 4°C and 12,000 x g for 15 min for phase separation. 400 µl of the upper phase containing the RNA was transferred into a 1.5 ml reaction tube. The RNA was purified according to the manufacturer’s protocol (Purifying RNA from Animal Tissue; steps Binding, Washing; and Elution). Samples were eluted in 30 µl RNase-free water and sored at -80°C. The extracted RNA was measured using a spectrophotometer. The quality was checked by 260/280 and 260/230 ratios and visualization of RNA bands by agarose gel electrophoresis.

2.29. First strand DNA synthesis

Reverse transcription of mRNA was performed to generate cDNA using SuperScriptIV reverse transcriptase (ThermoFisher).

Table 2-4: Components and temperatures for first strand cDNA synthesis

Component	Volume
RNA	5.75 µl
Oligo(dT)$_{18}$ Primer	0.5 µl
dNTPs (10 mM)	0.5 µl
Incubation 5 min at 65°C 2 min on ice	
5 x Buffer	2 µl
Ribolock RNase Inhibitor	0.5 µl
DTT (0.1 M)	0.5 µl
SuperScriptIV Reverse Transcriptase	0.25 µl
Incubation 10 min at RT Incubation 20 min at 50°C Stop 10 min at 80°C Store at -20°C	

2.30. Polymerase chain reaction

The polymerase chain reaction (PCR) was performed to amplify specific DNA sequences through DNA replication with target-specific primers.

2.30.1. Standard PCR

Standard PCR was used to check for bacterial DNA in gDNA extracted from *Drosophila* fecal samples before 16S sequencing.

Table 2-5: Components for standard PCR

Component	Volume	Final concentration
5x Phusion Reaction buffer	2 µl	1 x
dNTP-Mix (10 mM)	0.2 µl	0.2 mM
Forward-Primer (2 µM)	4 µl	1 µM
Reverse-Primer (2 µM)	4 µl	1 µM
Phusion DNA-Polymerase (5 U / µl)	0.05 µl	0.25 U
DNA template	x µl	100 ng
Millipore H_2O	5.75 – x µl	
Total volume	10 µl	

Table 2-6: Standard PCR program

Step	Temperature	Time
Initial denaturation	98°C	30 s
Amplification (up to 40 cycles)		
1. Denaturation	98°C	9 s
2. Annealing	55°C	60 s
3. Elongation	72°C	90 s
Terminal elongation	72°C	10 min

2.30.2. Quantitative real time PCR

Quantitative real time polymerase chain reaction (qRT-PCR) allows the relative quantitative monitoring of newly synthesized PCR-products in real time. The quantification is based on the intercalation of a fluorescent dye into dsDNA. The fluorescence increases proportionally to the amount of PCR product. Quantitative real time PCR was performed using the qPCRBIO SyGreen Mix Hi-Rox, MicroAmp fast Optical 48-well Reaction plates (0.1 ml) and the StepOne Real-Time PCR System. The expression levels, relative to the reference gene *rpl32*, were calculated using comparative ΔΔCT-Method.

Table 2-7 : qRT-PCR reaction mix for one reaction

Component	Volume [µl]
Master mix	5
Forward primer	0.5
Reverse primer	0.5
cDNA	4 [5 ng/µl]
Total volume	10

Table 2-8: qRT-PCR program

Step	Temperature [°C]	Time
Initial denaturation	95	10 min
Amplification (40 cycles)		
1. Denaturation	95	15 sec
2. Annealing	60	20 sec
3. Elongation	72	35 sec
Melt curve stage	95	15 sec
	60	60 sec
	95	15 sec

2.31. Agarose gel electrophoresis

A horizontal gel electrophoresis was performed to check the quality of extracted RNA or to separate PCR products. Within an electric field, the negatively charged nucleic acids migrate distinct distances through the agarose matrix based on their size. 1 % agarose (w/v) was dissolved in 1x TBE buffer, boiled and stored at 60°C in a water bath. For visualization RNA or DNA fragments, Ethidium bromide (1 %; 4 µl per 100 ml agarose) was added. Ethidium bromide intercalates with DNA or RNA strands and is visible under UV light. The electrophoresis was performed with 100 V for 30 min. To determine the size of PCR products, the GeneRuler™ DNA Ladder Mix (Thermo Scientific) was used. Gels were imaged using Geldocumentation (Transilluminator).

2.32. Transcriptomic profiling

For RNA profiling, flies were kept on NM at 25°C for 7 days after hatching (dFoxO-deficient flies and controls) or at 18°C for 5 days and subsequently at 30°C or 18°C for 5 days (dFoxO overexpression in ECs induced or not induced). 15 intestines per replicate were dissected in PBS. RNA was extracted as described in 2.28. The samples were sequenced by the Institute of Clinical Molecular Biology (IKMB) of Kiel University using HiSeq4000. Sequences were analyzed using CLC Genomics Workbench software (version 9.5.2). The genome references were downloaded from the National Center for Biotechnology Information (NCBI, www.ncbi.nlm.nih.gov).

2.33. Statistical analysis

GraphPad Prism 7 was used for statistical analysis and figure creation. For survival and transit time assay, Log-rank (Mantel-Cox) test was used. Other data sets were tested for normal Gaussian distribution by Shapiro Wilk normality test. Normal distributed data were further analyzed with Unpaired t-test for statistical significance, other by nonparametric Mann-Whitney test.

3. Results

Numerous studies show that FoxO plays a role in many physiological aspects such as life span (Giannakou et al. 2004; Hwangbo et al. 2004), cell cycle arrest (Kops et al. 1999; Medema et al. 2000), metabolism and energy homeostasis (Zhang et al. 2006; Varma et al. 2014) and immune functions (Varma et al. 2014; Fink et al. 2016). In order to reveal the effect of dFoxO levels on molecular processes and the physiology of *Drosophila*, various experiments were performed with four different lines or crossings. Besides a fly line with a dFoxO-deficiency in the whole fly, three crossings with overexpression of dFoxO in different cell types of the intestine were used: flies overexpressing native dFoxo or a constitutive active form of dFoxO in enterocytes (ECs) and flies with an overexpression of native dFoxO in intestinal stem cells (ISCs) and enteroblasts (EBs). Among others, the survival, digestion, body weight and fat content, metabolism, activity and gut integrity were investigated. Additionally, since FoxO is also activated by stress stimuli (Brunet et al. 2004), the effect of substances known to damage the intestine was examined.

Because the overexpression of dFoxO is lethal during the development, inducible crossings had to be used for all overexpression experiments.

3.1. Effects of a dFoxo-deficiency

3.1.1. Influence of a dFoxO-deficiency on survival

Previous studies showed that FoxO is associated with lifespan. In *Drosophila* for example, the overexpression of dFoxO in the fat body prolongs the life span (Giannakou et al. 2004; Hwangbo et al. 2004). To reveal the effect of a reduced expression level of dFoxO in the entire fly on the lifespan of *Drosophila*, the survival rate of dFoxo-deficient flies was measured. Five populations of 50 flies each were monitored until all flies had deceased. A dFoxO-deficiency strongly decreased the median as well as the maximum life span. In dFoxo-deficient flies, the medium lifespan was reduced by approx. 50 % from 49 days in controls to 25 days (Fig. 3.1).

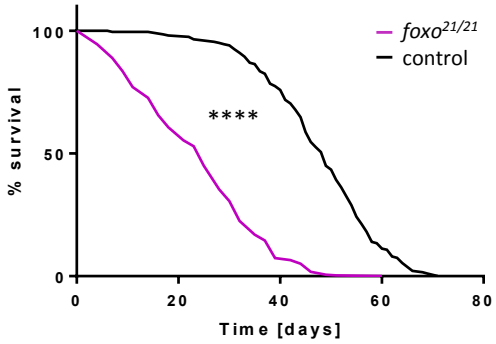

Fig. 3.1: Effect of a dFoxO-deficiency on survival. Flies were monitored until all individuals had died (n = 5; 50 flies each). control = w^{1118}; ****p < 0.0001.

3.1.2. Effect of a dFoxO-deficiency on digestion

FoxO factors are known to play a role in energy homeostasis. In order to investigate the impact of a reduction of dFoxO on the gut functionality of *Drosophila*, food intake, fecal output and transit time through the gut were analyzed.

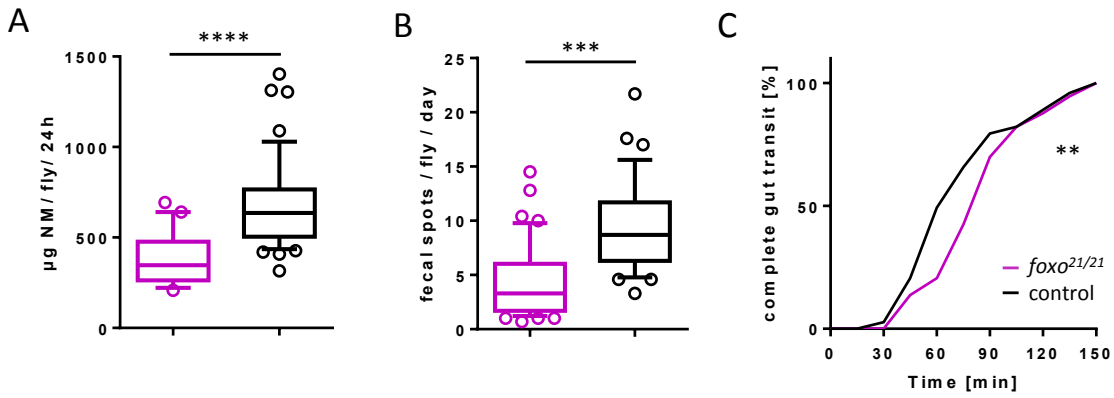

Fig. 3.2: Influence of a dFoxO-deficiency on digestion. (A) The amount of ingested food (n = 19-49) and (B) the fecal output (n = 35-46) was measured for 24 h. (C) The transit time of ingested food was monitored for 150 min (n = 73). control = w^{1118}, **P < 0.01, ***p < 0.001. ****p < 0.0001. Box and whiskers represent mean and 10 – 90 percentile (A+B).

The amount of ingested food was quantified for 24 hours. Individual flies were fed with blue dyed NM. After 24 hours, flies and all fecal output were homogenized and photometrical quantified. It showed that dFoxO-deficient flies ingested significantly less food than control flies (Fig. 3.2 A). Further, counting the number of fecal spots in 24 hours assessed the fecal output. The fecal output of dFoxO-deficient *Drosophila* was significantly reduced compared to the control (Fig. 3.2 B). Additionally, the transit time of ingested food through the fly's intestine was measured. Blue dyed NM was given to individual flies in 24-well plates. Flies

were monitored until blue fecal spots appeared. Since flies showed a high variability in starting the food intake, the transit time was defined from the moment the abdomen of the fly showed a blue staining from ingested food until the first blue fecal spot was excreted. Not only was the number of fecal spots reduced, also the transit time of the food though the fly's intestine was prolonged (Fig. 3.2 C).

3.1.3. Body fat and protein content of dFoxO-deficient flies

Since the amount of ingested food was highly reduced in dFoxO-deficient flies (Fig. 3.2 A), it was tested whether this results in a change of weight and body composition. The weight, body fat and protein content were measured in young individuals (7 days old) and older individuals (21 days old) of the same population. The later time point was chosen based on the median life span of dFoxO-deficient flies.

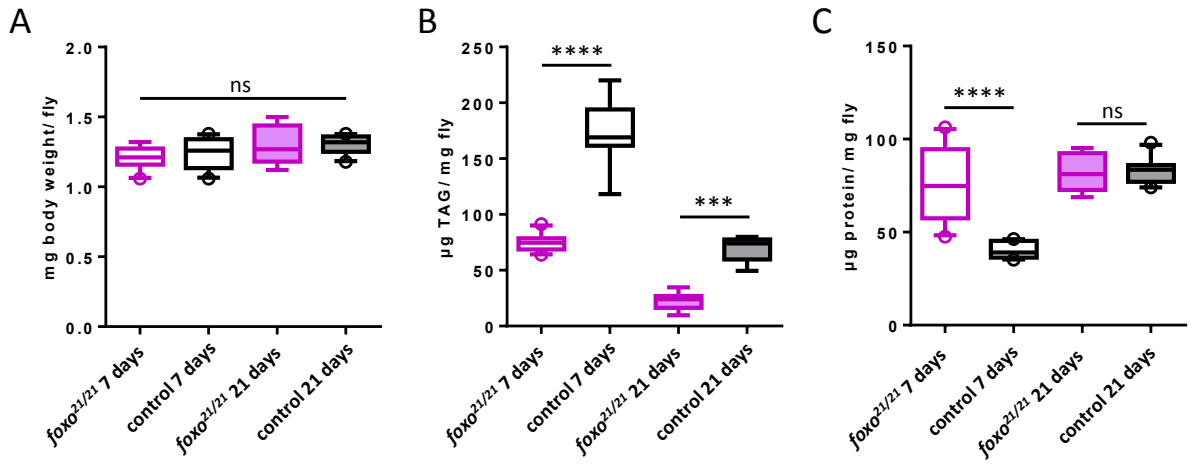

Fig. 3.3: Analysis of the body fat content in young and older dFoxO-deficient flies. (A) Weight, (B) body fat content, (C) prptein content of dFoxO-deficient flies and controls at age 7 days and 21 days (n = 10). control = w^{1118}, ****p < 0.0001, ns = not significant. Box and whiskers represent mean and 10 – 90 percentile.

The weight was neither influenced by the treatment nor by the age of the flies (Fig. 3.3 A). However, in young flies, the amount of body fat was decreased by more than 50 percent in dFoxO-deficient flies. The same pattern of loss of body fat was observed in older flies (Fig 3.3 B). Furthermore, the body fat content in both treatment and control groups was drastically reduced in older flies (Fig. 3.3 B). Interestingly, in young flies, the protein content was opposed to the fat content. DFoxO-deficient flies had significantly more protein than

control flies (Fig. 3.3 C). In older flies, the protein content was of dFoxO-deficient flies was similar to control flies and also to young dFoxO-deficient flies (Fig. 3.3 C).

3.1.4. Activity and metabolism

The downregulation of dFoxO led to significant changes in food ingestion, fat storage, digestion and excretion (Fig. 3.2 and 3.3). Therefore, it was tested if there is also an effect on the activity and the metabolic rate. The circadian rhythm as well as the total activity was measured in the *Drosophila* Activity Monitor system (DAM) with a 12 hour dark/ 12 hour light cycle for three consecutive days after adaptation to the condition for one day. The circadian rhythm showed the usual morning and evening peak in the control. The dFoxO-deficient flies in contrast displayed only a smaller evening peak and hardly any morning peak (Fig. 3.4 A). The total activity was decreased by approx. 40% in dFoxO-deficient flies (Fig. 3.4 B).

The metabolic rate was measured for two hours during the resting phase in the afternoon. It was significantly reduced in dFoxO-deficient flies compared to the control (Fig. 3.4 C).

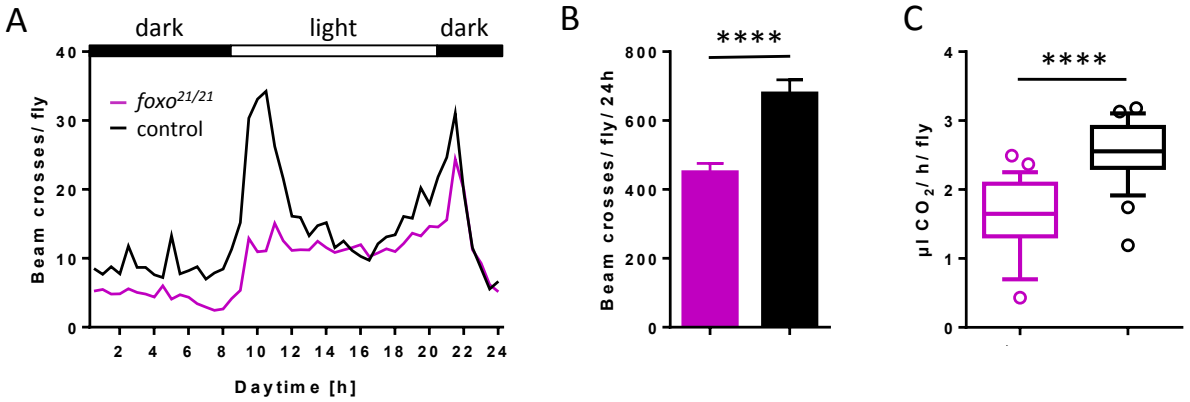

Fig. 3.4: Activity, circadian rhythm and metabolic rate upon deficiency of dFoxO. (A) The circadian rhythm was averaged from recordings of three consecutive days with the DAM system and (B) the total activity was calculated (n = 56-60) (C) the metabolic rate was measured for 2 h (n = 24-28). control = w^{1118}, ****p < 0.0001. Represented are means ± SEM (B). Box and whiskers represent mean and 10 – 90 percentile (C)

3.1.5. Gut integrity and morphology upon reduction of dFoxO

FoxO is known to play a major role in inflammatory processes by regulating for example DNA-repair, growth arrest, apoptosis and general responses to oxidative stress (Greer & Brunet 2005). Because these processes might affect the morphology of the intestine, 7-day-

old flies were embedded in agarose, cross-sectioned and labeled with phalloidin to visualize F-actin structures. Control as well as dFoxO-deficient flies did not show any differences or damages in the structure of the intestinal villi or the brush border (Fig. 3.5 A-B').

The pH of the gut was measured using pH indicators. The labeling showed no differences in dFoxO-deficient flies compared with the control. In both groups, the anterior and posterior midgut regions had an alkaline pH. The crop and the hindgut had a neutral pH. Only the copper cell region in the middle midgut is acidic (Fig. 3.5 C-D).

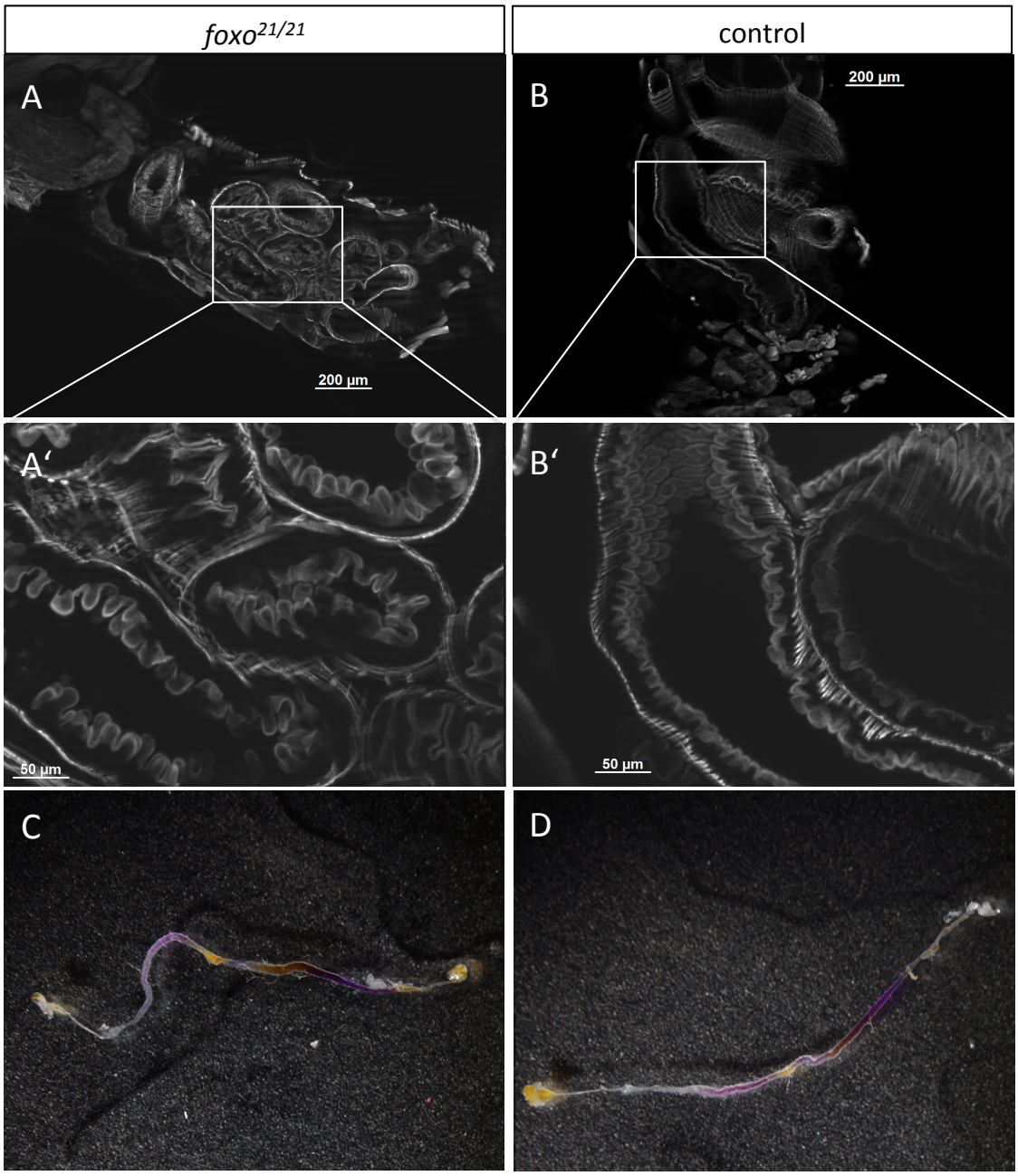

Fig. 3.5 Morphology of intestines upon dFoxO-deficiency. (A-B') Longitudinal sections through the abdomen of 7 days old flies. Sections were labeled with Phalloidin to visualize brush borders. (C-D) *Drosophila* intestines labeled with pH indicators Bromcresol purple and m-cresol purple. control = w^{1118}.

Furthermore, the gut length of 8-day-old flies was measured (Dustin Hanke, Bachelor thesis 2018). Significant differences were not observable (Fig. 3.6 A).

The loss of integrity of the gut was tested with a smurf-assay (Rera et al. 2011) to recognize any other damages in the epithelial layer, not visible by the F-actin staining. Once a week, flies were transferred from NM to agarose medium and fed with a sucrose solution dyed with blue food dye. In healthy flies, the blue dye is limited to the digestive tract. An impairment of the intestinal epithelium caused the leaking of food into the whole body and thereby blue stained flies, described as smurfs (Fig. 3.6 C). Over the course of five weeks, both control and dFoxO-deficient flies showed an increase of smurf individuals (dead and alive) over time. However, in dFoxO-deficient animals, the proportion of flies displaying a smurf phenotype was significantly higher at every time point (Fig. 3.6 B, Table 3-1).

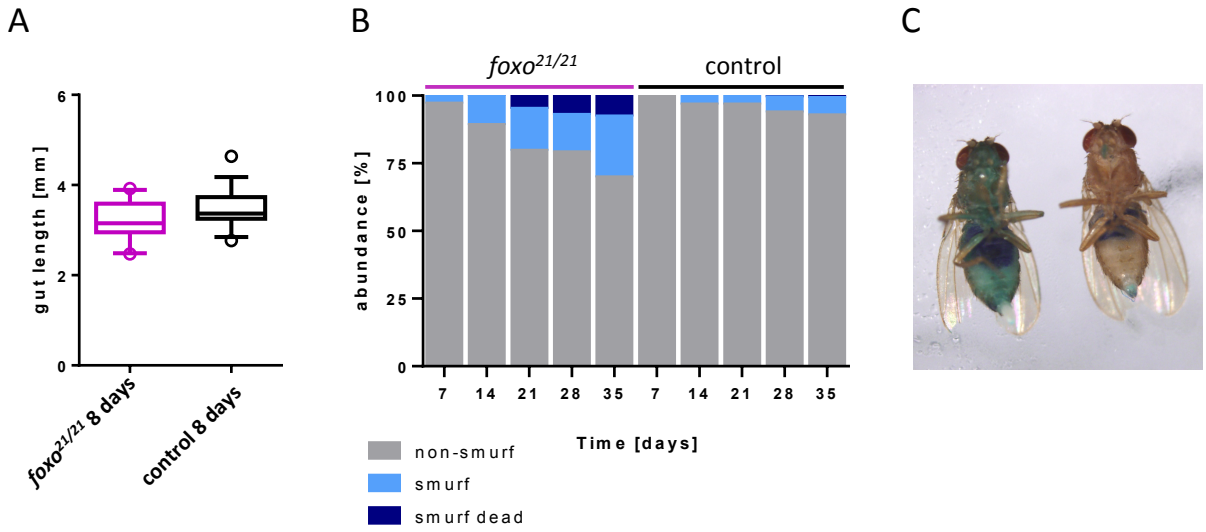

Fig. 3.6: Effects of a dFoxO deficiency on gut length and integrity. (A) Length of the guts of eight-day-old flies fed with 5 % sucrose. Significant differences were not measurable (n = 11-15). (B) The deficiency of dFoxO resulted in an impaired gut integrity that aggravated over time (n = 5). (C) Image of smurf (left) and non-smurf (right) phenotypes of dFoxO-deficient flies. control = w^{1118}. Box and whiskers represent mean and 10 – 90 percentile (A).

Table 3-1: Significance of total number of smurf individuals.

Age of flies	p-value (comparison with control)	significance
7 days	0.1071	ns
14 days	0.0130	*
21 days	0.0043	**
28 days	0.0159	*

3.1.6. Transcriptome analysis of intestines of dFoxO-deficient flies

The deficiency of dFoxO expression has a massive influence on numerous molecular and physiological aspects in *Drosophila* such as survival (Fig. 3.1), food consumption and digestion (Fig. 3.2 A-C), body fat content (Fig. 3.3 B), metabolic rate and activity (Fig. 3.4 A-C). In order to identify genes or gene clusters specifically regulated in dFoxO-deficient flies, a transcriptome analysis was conducted with seven-day old flies (Appendix, Table 9.1). Fig. 3.7 displays the heat map of all transcripts of dFoxO-deficient and control flies with an FDR-p-value < 0.05 and a fold change > 1.5. It shows only minor variation of all four replicates of the respective experimental group.

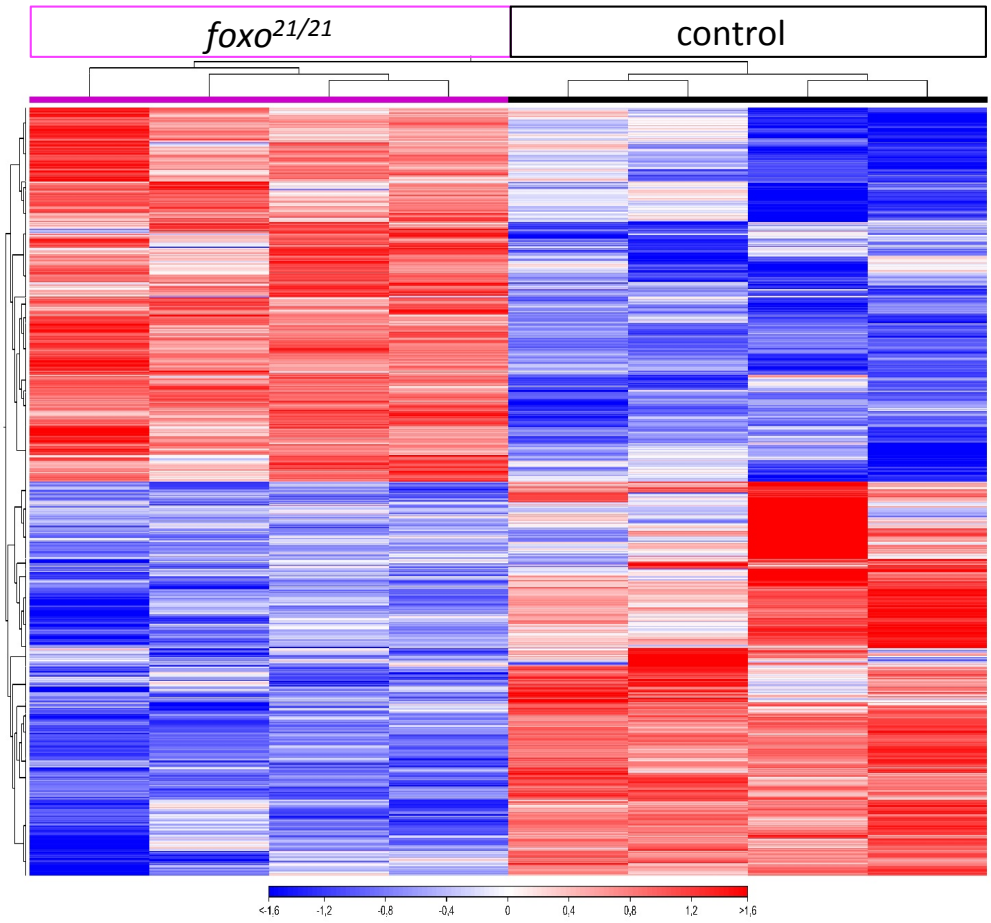

Fig. 3.7: Heatmap of mRNA expression profiles of intestines of dFoxO-deficient and control flies. All transcripts with FDR p-value < 0.05 and fold change > 1.5 were used for analysis, n = 4**,** control = *yw.*

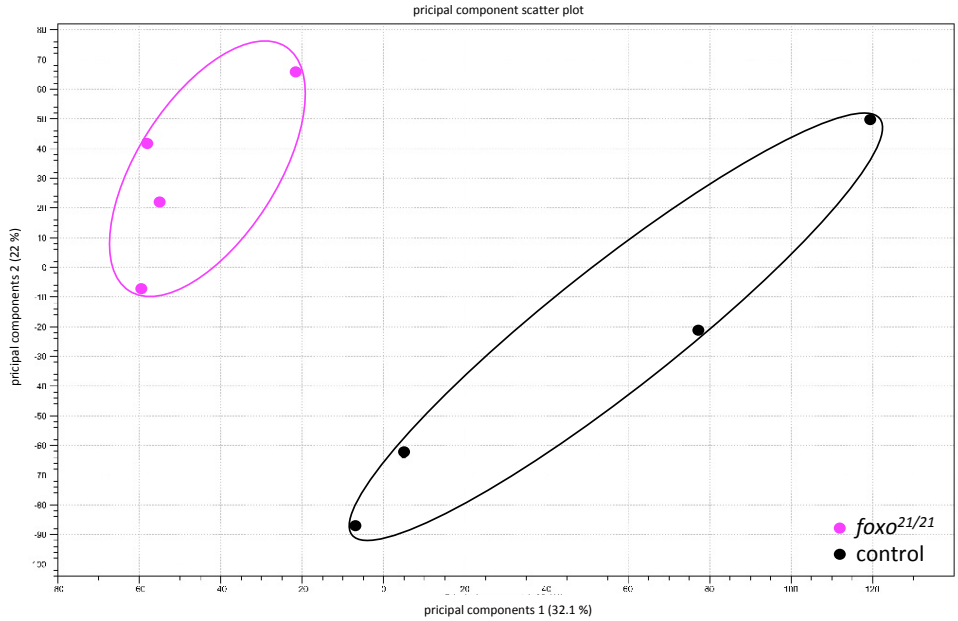

Fig. 3.8: Multidimensional Scaling (MDS) revealed a distinct clustering of both groups. All transcripts with FDR p-value < 0.05 and fold change > 1.5 were used for analysis Ellipses were added manually. n = 4, control = *yw*.

A principal coordinate analysis based on all transcripts with a FDR p-value < 0.05 and a fold change > 1.5 showed a distinct clustering for flies overexpressing dFoxO in ECs and controls (Fig. 3.8).

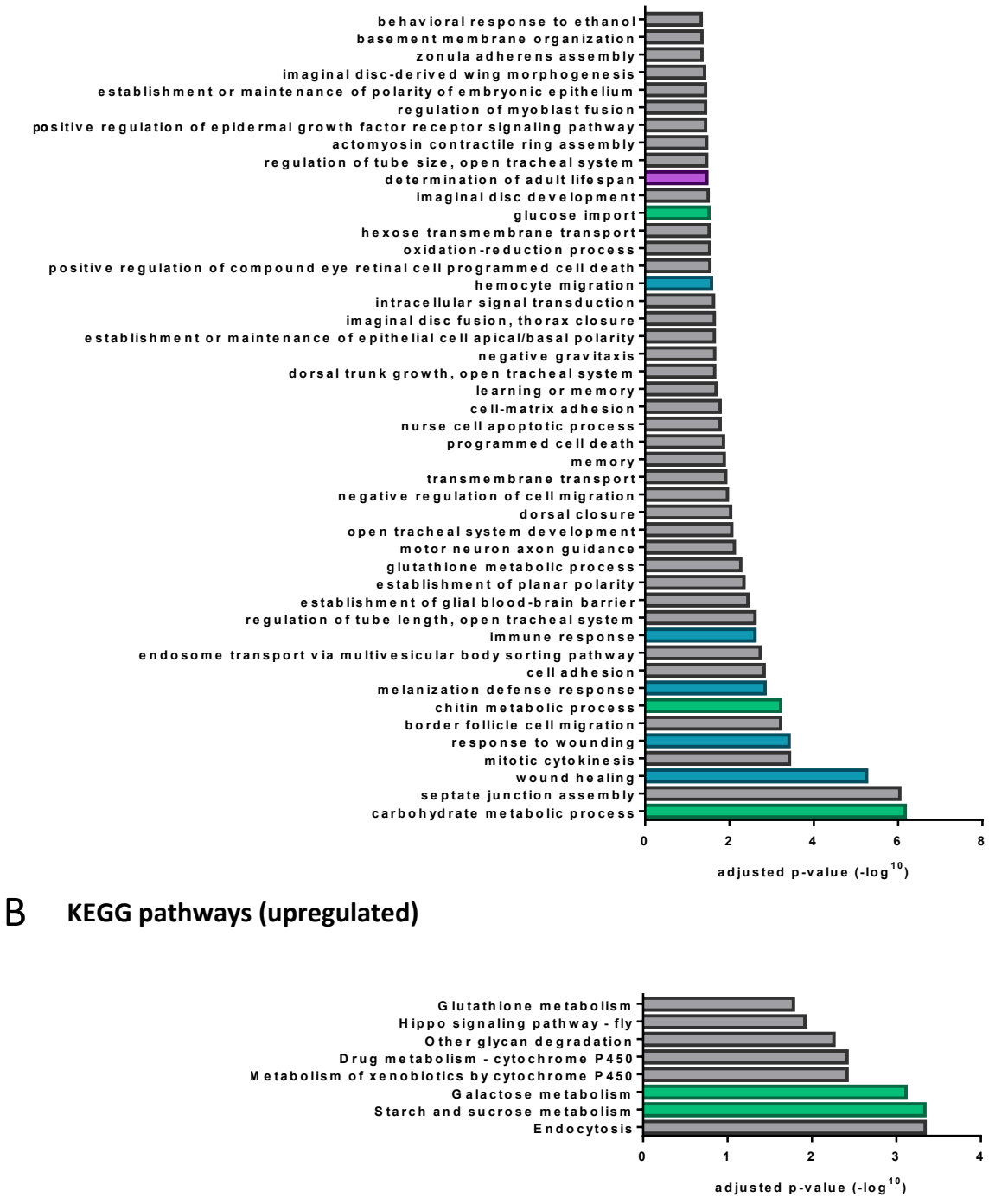

Fig. 3.9: GO-analysis identified upregulated biological processes and KEGG pathways in intestines of dFoxO-deficient flies. All transcripts with FDR p-value < 0.05 and fold change > 1.5 were used for analysis. Colored bars highlight GOs associated with life span (purple), metabolism (green) and immunity (blue).

The gene ontology (GO) analysis using the DAVID bioinformatics database with all transcripts with an FDR-p-value < 0.05 and a fold change > 1.5 identified numerous significantly up- and

downregulated biological processes, KEGG pathways (Fig. 3.9 A+B and Fig. 3.10 A+B) and molecular functions (Fig. 3.11 and appendix).

From 47 upregulated biological processes, one is associated with life span, three with metabolism and five with immunity (Fig. 3.9 A). Eight KEGG pathways were also significantly upregulated, including two associated with metabolism (Fig. 3.9 B).

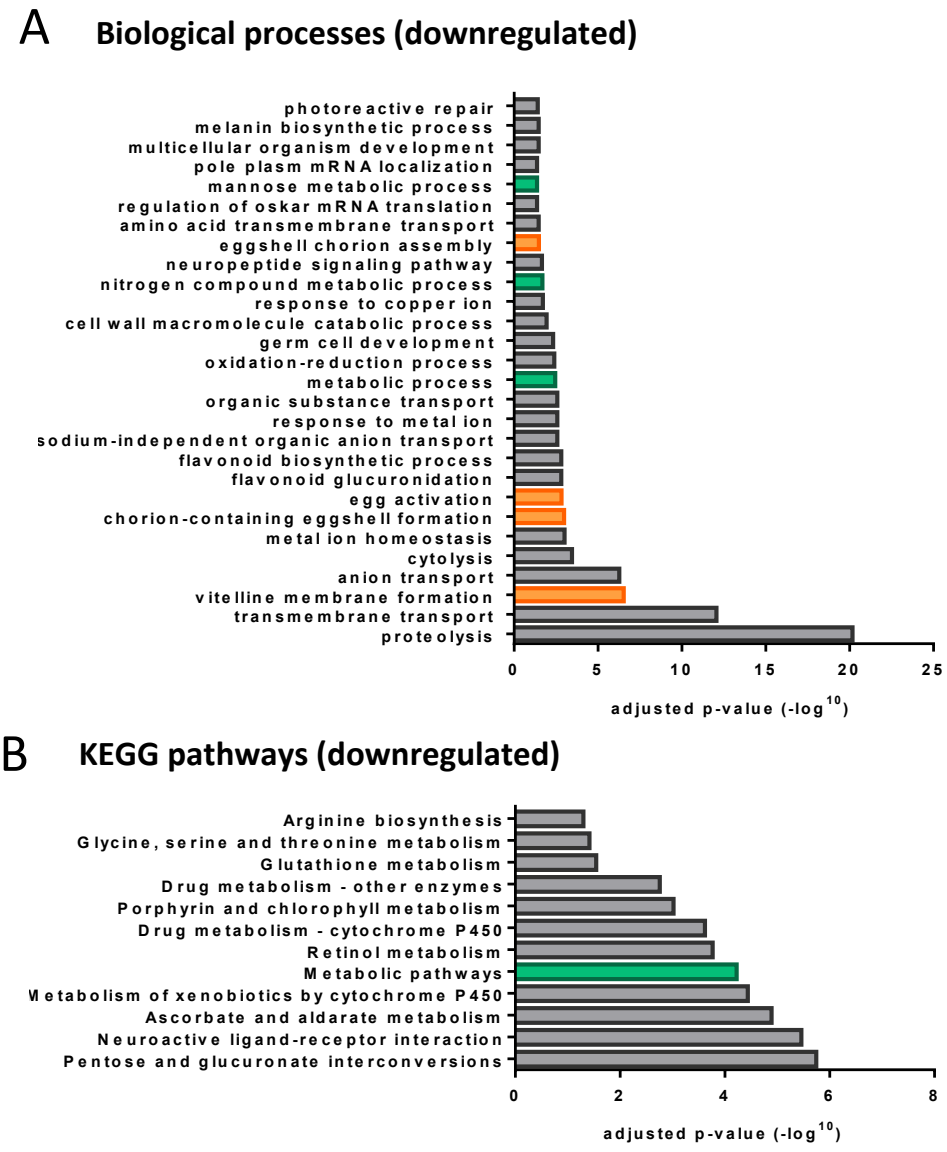

Fig. 3.10: GO-analysis identified downregulated biological processes and KEGG pathways pathways in intestines of dFoxO-deficient flies. All transcripts with FDR p-value < 0.05 and fold change > 1.5 were used for analysis. Colored bars highlight GOs associated with eggshell and chorion formation that might be associated with fecundity (orange) and metabolism (green).

The GO analysis identified 28 significantly downregulated biological processes with four being associated with chorion and egg formation (Fig. 3.10, orange bars) and three involved

in metabolism (Fig. 3.10 green bars). Since many genes involved in chorion and egg formation were downregulated, a fecundity assay was performed (3.1.7).

Additionally, 24 downregulated molecular functions were identified, among other lysozyme activity (Fig. 3.11, blue bar).

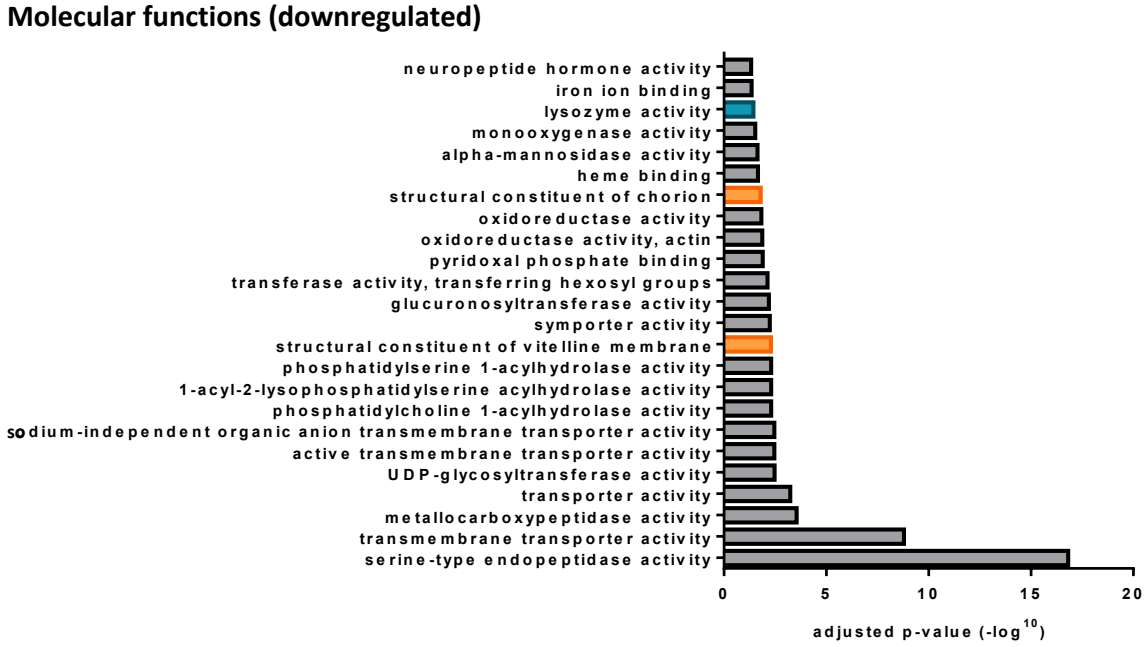

Fig. 3.11: GO-analysis identified downregulated molecular functions pathways in intestines of dFoxO-deficient flies. All transcripts with FDR p-value < 0.05 and fold change > 1.5 were used for analysis. Colored bars highlight GOs associated with eggshell and chorion formation that might be associated with fecundity (orange) and lysozyme activity (blue).

Four lysozyme genes were significantly downregulated (Table 3-2). To confirm a reduced lysozyme activity in the fly, a lysis assay was performed (3.1.8).

Table 3-2: Downregulated lysozyme genes in dFoxO-deficient flies.

gene	fold change
lys e	-2.9
lys d	-5.2
lys s	-5.5
lys b	-6.3

3.1.7. Reduced fecundity of dFoxO-deficient flies

The transcriptome analysis showed a downregulation of several biological processes and molecular functions related to eggshell chorion and egg (Fig. 3.10 A+B). In order to investigate a possible effect on the fecundity, laid eggs as well as pupae and adults that

develop from these eggs were counted every 24 hours for 13 days. dFoxo-deficient females laid less eggs than control flies. In both groups, most eggs were laid at day 3 (Fig. 3.12, solid line). Remarkably, the majority of eggs of controls developed to pupae (dashed line) and then to adults (dotted line), whereas from dFoxO-deficient eggs only a small proportion developed further.

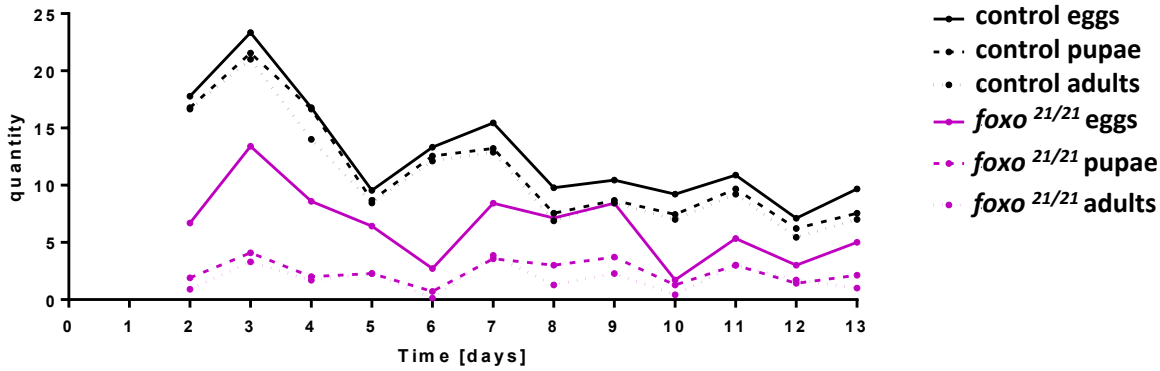

Fig. 3.12 Fecundity of dFoxO-deficient *Drosophila*. The number of laid eggs is drastically reduced in dFoxO-deficient flies (solid line). From these eggs, the majority develops further to pupae (dashed line) and adults (dotted line) in controls. In dFoxO-deficient flies, only a small proportion of eggs develops further. n = 9-10, control = w^{1118}.

3.1.8. Reduced lysozyme activity upon deficiency of dFoxO

The RNASeq analysis of dissected intestines of dFoxo-deficient flies revealed a downregulation of four different lysozymes genes (*lysB*, l*ysD*, *lysE* and *lysS*; Table 3-2). Therefore, a lysozyme lysis assay was conducted. The homogenate of dissected intestines was pipetted into petri dishes containing agarose mixed with cell walls of *Micrococcus lysodeikticus.* Due to lysozyme activity, a clear zone of lysis can be observed. Interestingly, two distinct zones were visible, a clear inner zone of inhibition and a more opaque outer zone (Fig. 3.13 B). Both were significantly smaller in dFoxO-deficient flies compared to controls (Fig. 3.13 A+B), which confirms the results from the RNASeq analysis. When compared to a standard curve, the differences between dFoxO-deficient and control flies were even larger than the measured diameter (Fig. 3.13 C+D). Most likely, these two zones are the result of the activity of different lysozymes.

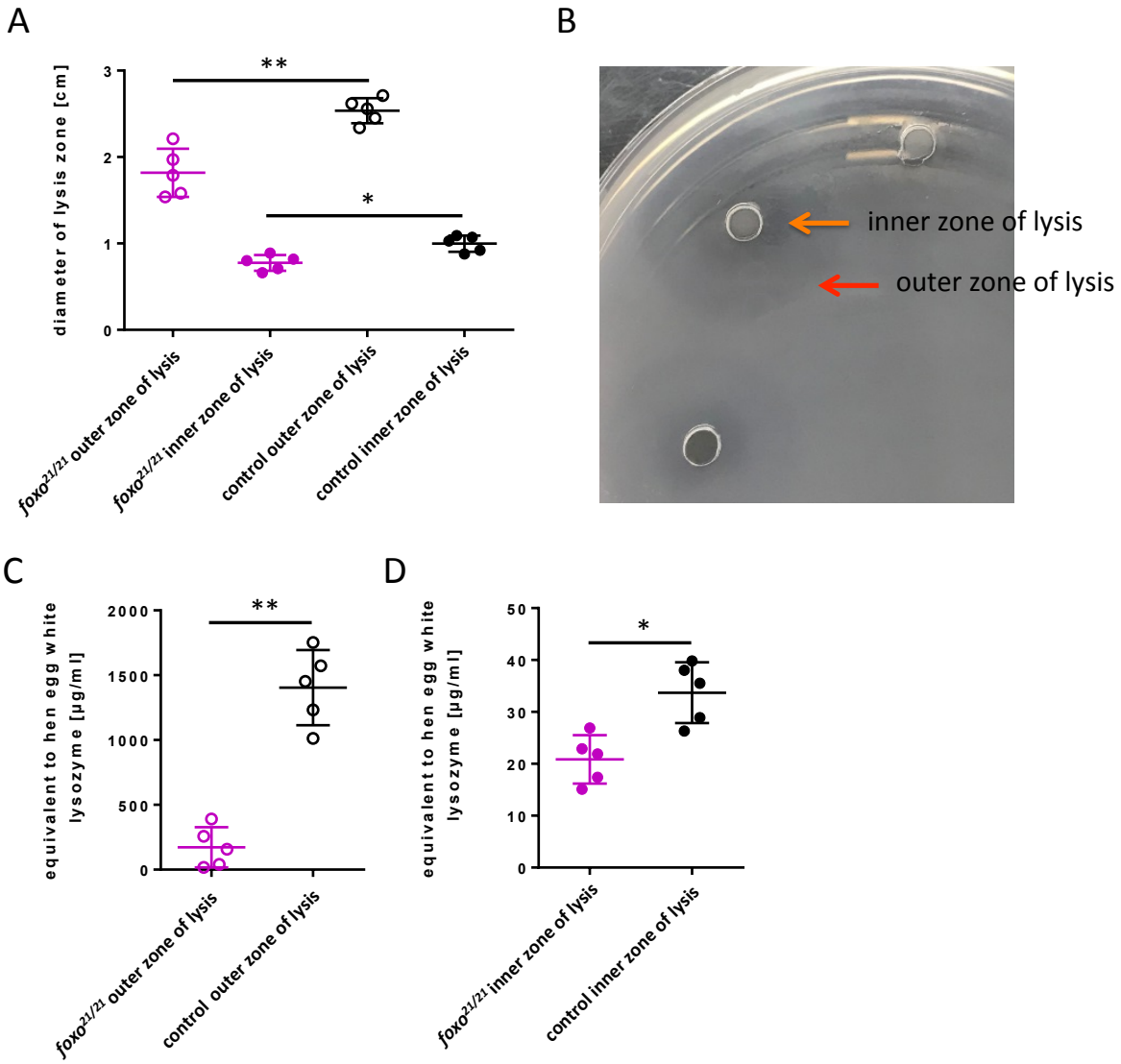

Fig. 3.13: Lysozyme lysis assay of intestines dissected from dFoxO-deficient flies. (A) (B) Image of lysis plate with inner zone of inhibition (orange arrows) and outer zone of inhibition (red arrows). control = *yw*; ****p < 0.0001, ***p < 0.001, n = 5. Represented are means ± SD.

3.1.9. Survival under starvation condition

FoxO factors can be activated by various stress stimuli. For this reason, the survival of dFoxO-deficient flies under starvation stress was examined. Age-matched flies (7 days old) where transferred to vials containing only 1.5 % agar agar for moisture. Populations of 10 flies each were monitored every 2 hours during the day until all flies had died.

In dFoxO-deficient flies, the survival was significantly reduced when deprived of food. The median life span of 47 hours was reduced by 50 % compared to 94 hours in control flies (Fig. 3.14)

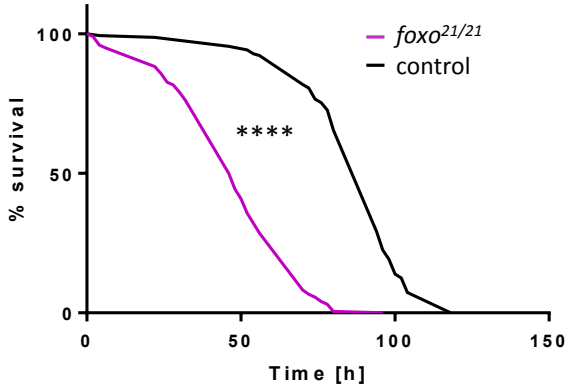

Fig. 3.14: Effect of a dFoxO-deficiency on survival under starvation condition. Flies were monitored every 2 hours during the days until all individuals had died (n = 7-10; 10 flies each). control = w^{1118}; ****p < 0.0001

3.1.10. Changes of the microbial composition

FoxO factors are known to play an important role in immunity by controlling the release of antimicrobial peptides (AMPs) (Varma et al. 2014; Fink et al. 2016). Therefore, dFoxO is likely to influence the microbial composition of the *Drosophila* gut.

Germfree *Drosophila* embryos were generated by dechorionation and recolonized with a defined mix of five *Drosophila* gut bacteria (Santos et al. 2017). After hatching, four replicates of 70 to 100 female flies each were transferred into sterile vials on NM. Since several flies died over the course of the experiment, populations got smaller over time. After 24 hours, 5 days, 10 days, 20 days and 30 days fecal swab samples were collected. Genomic DNA was extracted and amplified with specific primers for bacterial variable regions 1 and 2 of 16S rRNA genes. The amplificates were sequenced using Illumina MiSeq. The bacteria mix used for recolonization was analyzed as well (Sarah Frömbling, Master thesis 2019). Besides the desired bacteria *Lactobacillus*, *Acetobacter*, *Enterococcus* and *Commensalibacter*, a contamination of 2 percent of other, not specifiable bacteria were found (Fig. 3.15 A). Consequently, the analyzed fecal samples were contaminated as well. The contaminations include Alpha-Proteobacteria, Gamma-Proteobacteria, Bacilli, Bacteroidia, Actinobacteria and other with Gamma-Proteobacteria being most abundant. In general, the results show a high variance between individual replicates. The results at day 5 and 30 were chosen to represent changes in the microbiota from early life to in old flies (Fig. 3.15 B+C). The results for every single time point are shown in the appendix (Fig. 9.1).

All four replicates of dFoxO-deficient flies at day 5 show great differences between each other. While the sample from replicate 1 contained 52 percent of *Acetobacter*, replicate 2 contained only 13 percent and replicate 3 and 4 no measurable amounts. Replicates 3 and 4 showed contaminations of 74 and 75 percent, with *Rhodanobacter* being the most dominant. Interestingly, *Commensalibacter* could only be found in one of the replicates and *Enterococcus* was missing in all samples although both were added with the bacteria mix (Fig. 3.15 B). Control flies at day 5 also had a high variability among each other, but fecal samples from replicates 1 and 4 showed a very similar microbial composition. Both contained mainly *Acetobacter* and *Lactobacillus* with 17 and 27 percent contamination. The microbiota of replicate 3 consisted mainly of *Acetobacter* while replicate 2 was almost completely contaminated (86 percent) (Fig. 3.15 C). Older dFoxo-deficient flies at age 30 showed fewer differences. Replicate 2 to 4 contained mainly *Acetobacter* and *Lactobacilli* with 21 to 37 percent contamination (Fig. 3.15 B). Control samples of the same age were mainly colonized with *Acetobacter* and smaller amounts of *Lactobacilli*. Samples 2 and 4 were contaminated by approx. 20 percent, but sample 1 and 3 only showed contaminations of 4 and 7 percent. *Commensalibacter* and *Enterococcus* were not measured in any of the samples (Fig. 3.15 C). Altogether, samples from dFoxO-deficient flies showed much higher contaminations than control samples.

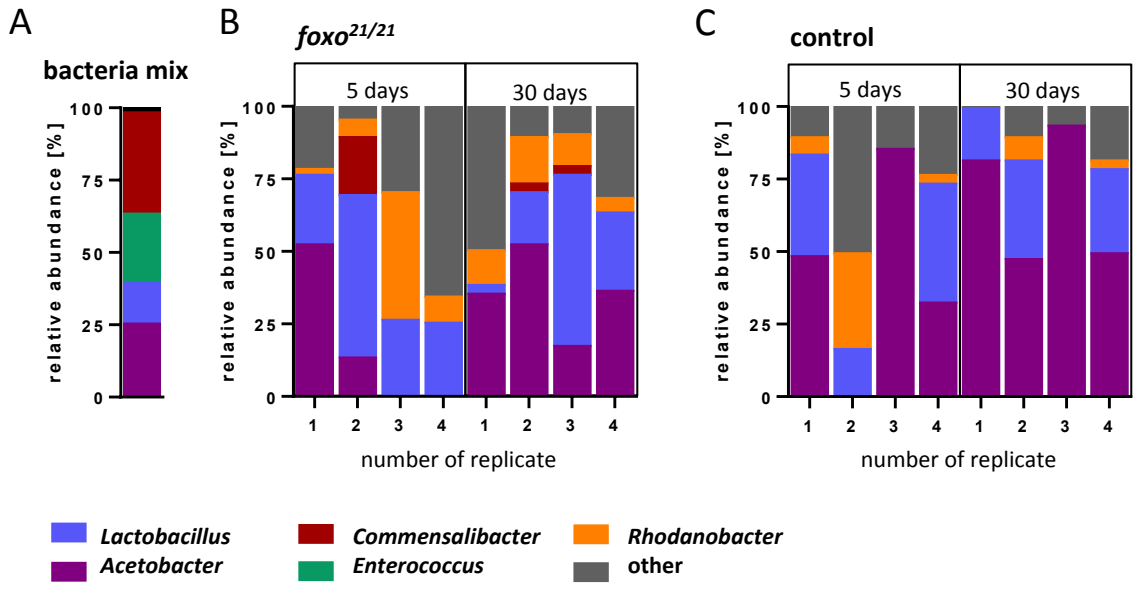

Fig. 3.15: Microbial composition of the bacteria mix used for recolonization and of feces collected from dFoxo-deficient and control flies. (A) The bacteria mix consisted of 25 % *Acetobacter*, 14 % *Lactobacilli*, 24 % *Enterococcus*, 35 % *Commensalibacter* and 2 % of contamination with not specifiable other bacteria (Sarah Frömbling, Master thesis 2019). (B) Microbial composition of individual replicates of dFoxO-deficient and (C) control flies at age 5 and 30 days. *Rhodanobacter* and other bacteria were undesirable contaminations, control = *yw*, n = 4-5.

A Principal Coordinates Analysis (PCoA) visualized the level of similarity of the microbial profiles of fecal samples dFoxO-deficient flies compared to control flies. The analysis showed that in young flies (age 5 days), microbial compositions of dFoxO-deficient and control flies are mainly overlapping, while at old age (30 days), a separation into two distinct profiles are conjecturable. Although the result at day 30 is just not significant (p = 0.0502), a trend is clearly recognizable (Fig 3.16). The PCoA plots for all time points are shown in the appendix (Fig. 9.2).

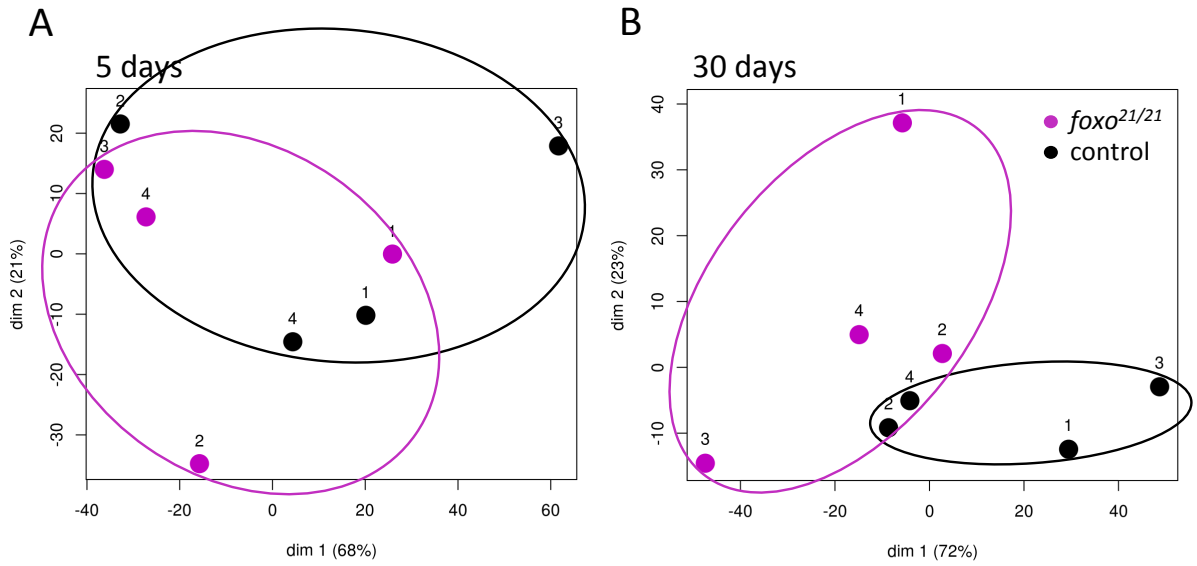

Fig. 3.16: PCoA plots were calculated to identify clusters of microbial compositions. (A) At age 5, the microbial profiles of feces from dFoxO-deficient flies and controls are mainly overlapping. (B) After 30 days, the microbiota of both groups clusters not significantly (p = 0.0502), but a trend is clearly visible. Ellipses were added manually. control = *yw*.

Age-related changes in the intestinal microbiota can result in a dysbiosis with detrimental effect for the host. Therefore, the microbial compositions of young and old flies of both fly lines were compared to each other to detect age-induced changes (Fig. 3.17). No significant differences could be detected in bacterial of either dFoxO-deficient flies (p = 1.00) or controls (p = 0.79).

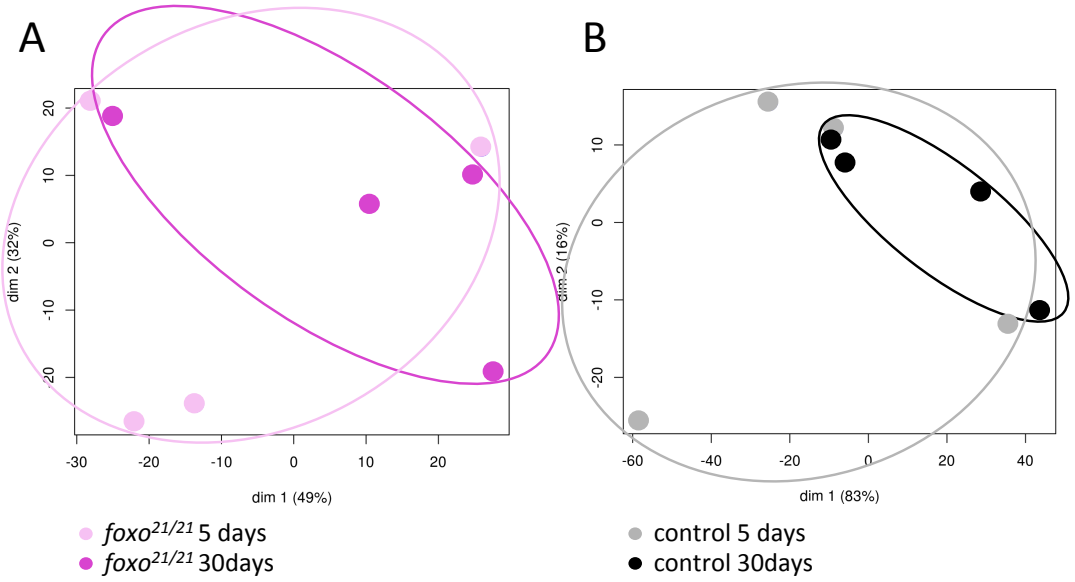

Fig. 3.17: PCoA plots show clusters of microbial compositions of young and old flies. (A) Microbial profiles of feces from 5 and 30 days dFoxO-deficient flies are mostly overlapping. (B) In control flies at age 5 and 30 days, the microbiota of both groups seem to be diverting into two clusters, but not significantly different to each other. Ellipses were added manually. control = *yw.*

3.2. Effects of an overexpression of dFoxo in Enterocytes

A dFoxO-deficiency had drastic effects on various molecular functions of *Drosophila* (3.1). Therefore, it was examined whether an overexpression of dFoxO in enterocytes, the main cell type in the *Drosophila* gut, also influences these functions. A Gal4-line that drives expression specifically in enterocytes was crossed to a *UAS-foxo* line. The offspring was used in experiments. The Gal4- and UAS-line crossed to wildtype flies served as controls.

3.2.1. Survival upon overexpression of dFoxo in enterocytes

Five populations with 50 female flies each were monitored every two to three days until all individuals had deceased. Surprisingly, the overexpression of dFoxO in enterocytes of the *Drosophila* gut also led to a severe decrease in life span compared to both controls (Fig. 3.18). The medium life span of both controls (31 and 32 days) was reduced by approx. 25 % to 23 days in the treatment group.

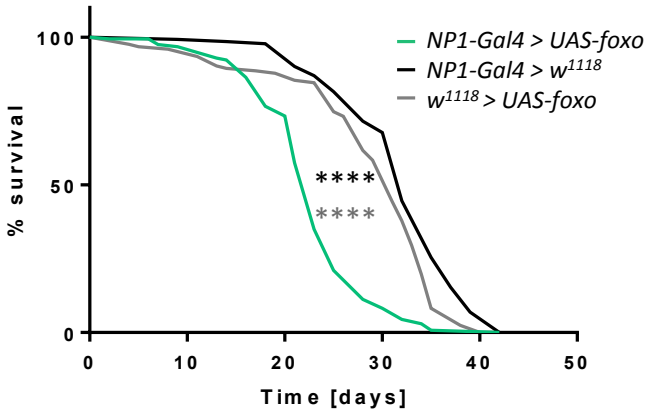

Fig. 3.18: Influence of an overexpression of dFoxO in enterocytes on survival. Flies were monitored until all individuals had died (n = 5; 50 flies each). Color of asterisks indicates the corresponding control. *NP1-Gal4 = NP1-Gal4;tubPGal80ts*; ****p < 0.0001.

3.2.2. Influence of an overexpression of dFoxO on digestion

The deficiency of dFoxO led to a significant reduction in the amount of ingested food and the number of excreted fecal spots as well as an increase in the gut transit time (3.1.2). The effect of an overexpression of dFoxO in enterocytes on these digestive functions was also tested. Remarkably, the effect on the food consumption and the fecal output was very similar to the dFoxO deficient flies. The amount of ingested food as well as fecal output was quantified for 24 hours. The transit time through the gut was measured from ingestion until defecation. Overexpression flies fed significantly less than their genetic control (Fig. 3.19 A). Furthermore, the number of excreted fecal spots was drastically reduced while the transit time of ingested food was significantly prolonged (Fig. 3.19 B+C).

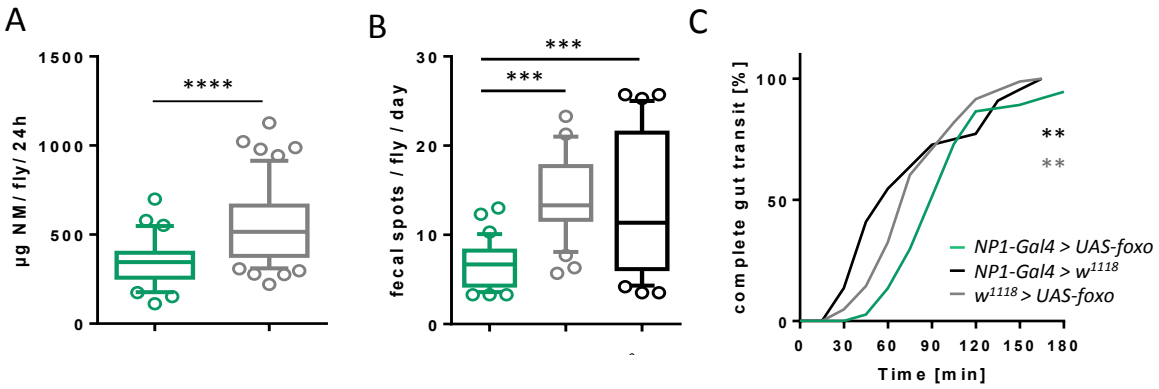

Fig. 3.19: Effect of an overexpression of dFoxO in enterocytes on digestion. (A) The amount of ingested food (n = 30-52) and (B) the fecal output (n = 32-42) was measured for 24 hours. (C) The transit time after ingestion of food was monitored for 180 min (n = 23-84). Color of asterisks indicates the corresponding control. *NP1-Gal4 = NP1-Gal4;tubPGal80ts*, **p < 0.01, ***p < 0.001. ****p < 0.0001. Box and whiskers represent mean and 10 – 90 percentile (A+B).

3.2.3. Effect of an overexpression of dFoxO in ECs on the body composition

The deficiency of dFoxO massively reduced the body fat and the fat to protein ratio of *Drosophila*, while the body weight was constant (Fig. 3.3 A+B). In flies overexpressing dFoxO in ECs, the body fat is also drastically reduced in young flies (6 days post induction) and older flies (14 days post induction) (Fig. 3.20 B). The protein content showed high variability among samples, but no significant differences between flies expressing dFoxO in ECs and controls. Interestingly, the protein content was higher in older flies (Fig. 3.20 C). However, the body weight was constant except in older dFoxO-overexpression flies where the weight was significantly higher compared to younger flies and to controls of the same age (Fig. 3.20 A).

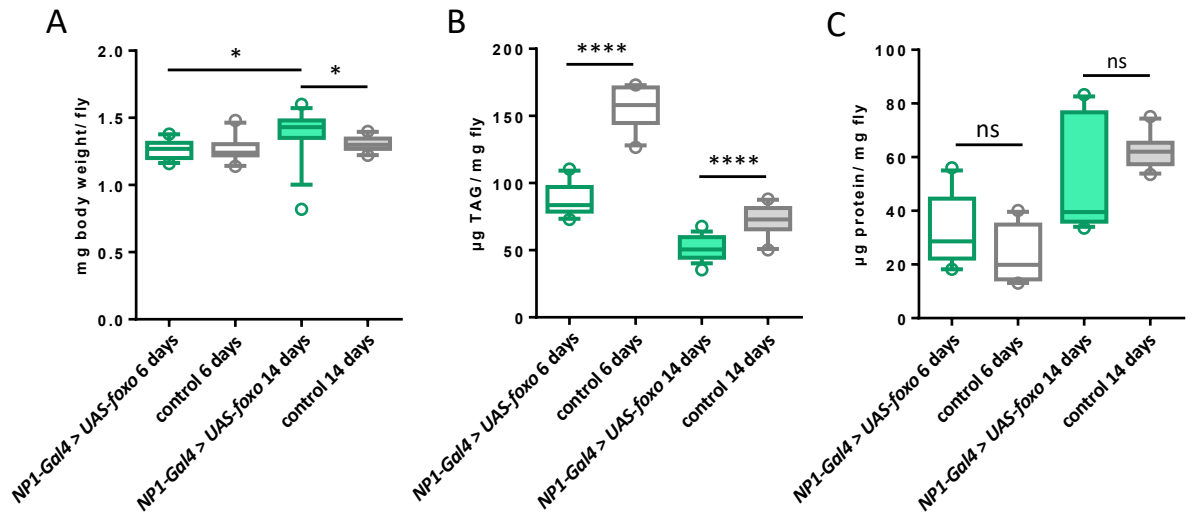

Fig. 3.20: Analysis of the body composition in young and older flies overexpressing dFoxO on ECs. (A) Weight, (B) body fat content, (C) protein content of flies overexpressing dFoxO in ECs and controls at age 6 days and 14 days (n = 10-16). control = w^{1118} > *UAS-foxo*, *NP1-Gal4 = NP1-Gal4;tubPGal80ts*, ns = not significant, *p < 0.05, ****p < 0.0001. Box and whiskers represent mean and 10 – 90 percentile.

3.2.4. Activity and metabolic rate

The circadian rhythm and the total activity, which was measured in the *Drosophila* Activity Monitor system (DAM) with a 12 hour dark/ 12 hour light cycle for three consecutive days after adaptation to the condition for one day, showed a lower activity in dFoxO-deficient flies. The circadian rhythm was affected as well. The usual morning peak was almost not measurable, and the evening peak was slightly weaker (Fig. 3.4 A+B).

In flies overexpressing dFoxO in enterocytes, the circadian rhythm and total activity are also impaired. Compared with the genetic controls, the morning and evening peak is considerably

smaller. The activity during the resting phase at daytime was slightly elevated in comparison to both controls. The total activity is significantly reduced compared with the UAS-control, but not the Gal4-control (Fig 3.21 A+B). Interestingly, in contrast to dFoxO-deficient flies (Fig 3.4 C), the metabolic rate is not affected by the overexpression of dFoxO (Fig 3.21 C).

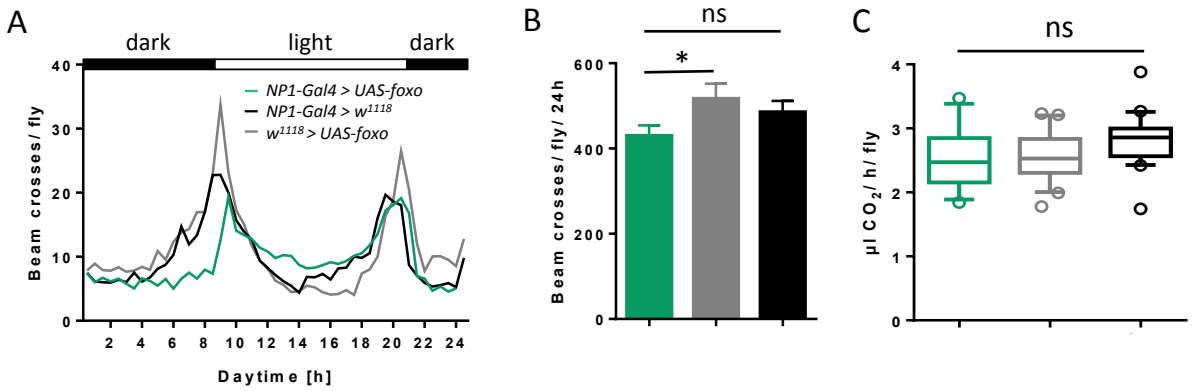

Fig. 3.21: Activity, circadian rhythm and metabolic rate in flies overexpressing dFoxO in enterocytes. (A) The circadian rhythm was recorded for three consecutive days with the DAM system and (B) the total activity was calculated (n = 35-86). (C) the metabolic rate was measured for 2 hours (n = 16-21). Color of asterisks indicates the corresponding control. *NP1-Gal4 = NP1-Gal4;tubPGal80ts*, **p < 0.01, *p < 0.05, ns = not significant. Represented are means ± SEM. Box and whiskers represent mean and 10 – 90 percentile (C.)

3.2.5. Gut integrity

A 'smurf' assay revealed that the integrity of the guts of dFoxO-deficient flies is severely impaired compared to control flies (Fig 3.6 B). Once a week, flies were transferred from NM to agar-agar medium and fed with blue dyed sucrose solution for 24 hours. Due to disruptions in the intestinal epithelium, the food is not restricted to the intestine but leaking into the fly's body resulting in blue flies referred to as 'smurf' individuals (Fig. 3.6 C). Compared to both genetic controls, flies overexpressing dFoxO in enterocytes displayed a strongly increased number of alive and dead smurfs at every time point (Fig. 3.22, Table 3-3). At age 21 days, 25 percent of all tested flies showed the smurf phenotype (Fig 3.22).

Table 3-3: Significance of total number of smurf individuals upon overexpression of dFoxO in ECs.

Age of flies	p-value (comparison with UAS-control)	p-value (comparison with Gal4-control)	significance
7 days	0.0238	0.0038	*
14 days	0.0079	0.0159	*
21 days	0.0079	0.0079	**

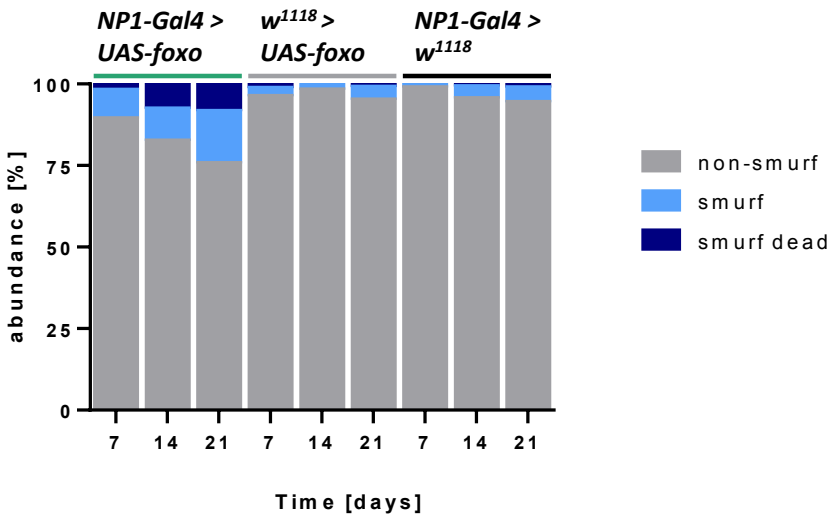

Fig. 3.22: Effects of an overexpression of dFoxO in enterocytes on gut integrity. (A) Compared to both genetic controls, an overexpression of dFoxO resulted in impaired gut integrity. With advancing age, the damage increased (n = 5). *NP1-Gal4 = NP1-Gal4;tubPGal80ts.*

3.2.6. Transcriptome analysis of intestines upon overexpression of dFoxO in enterocytes

The overexpression of dFoxO in ECs has a strong effect on many physiological functions in *Drosophila* as for instance survival (Fig 3.18), food consumption (Fig. 3.19 A), digestion (Fig. 3.19 B+C), body fat content (Fig. 3.20 B), activity Fig. 3.21 A+B), metabolic rate (Fig. 3.21 C). A transcriptome analysis was carried out after 7 days of induction at 30°C. As control, flies from the same crossing were kept at 18°C to prevent induction.

All transcripts with an FDR-p-value < 0.05 and a fold change > 1.5 were used for further analysis (Appendix, Table 9.2). 462 significantly upregulated and 398 downregulated genes were identified. A heat map of all significantly regulated transcripts revealed only slight variations among of all four replicates of the respective experimental group (Fig. 3.23).

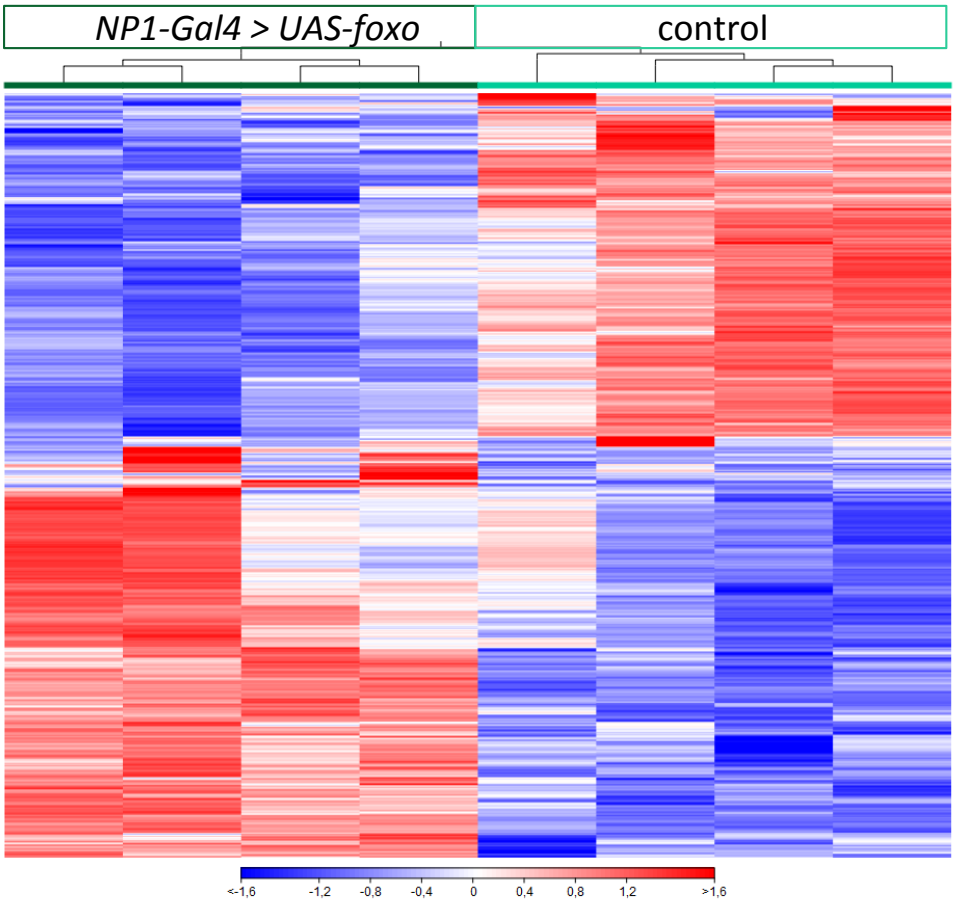

Fig. 3.23: Heatmap of mRNA expression profiles of intestines of flies overexpressing dFoxO in ECs and controls. All transcripts with FDR p-value < 0.05 and fold change > 1.5 were used for analysis, n = 4**,** *NP1-Gal4 = NP1-Gal4;tubPGal80ts* control = *NP1-Gal4 > UAS-foxo uninduced at 18°C.*

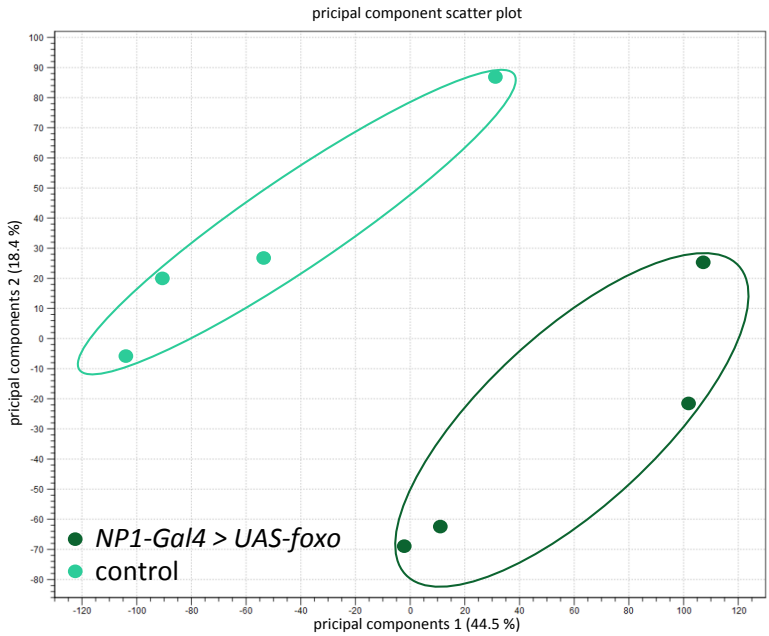

Fig. 3.24: A principal coordinate analysis including all transcripts revealed distinct clustering of both groups. Ellipses were added manually**.** control = *NP1-Gal4 > UAS-foxo at 18°C* not induced)*, NP1-Gal4 = NP1-Gal4;tubPGal80ts.*

A principal coordinate analysis based on all transcripts showed a distinct clustering for flies overexpressing dFoxO in ECs and controls (Fig. 3.24).

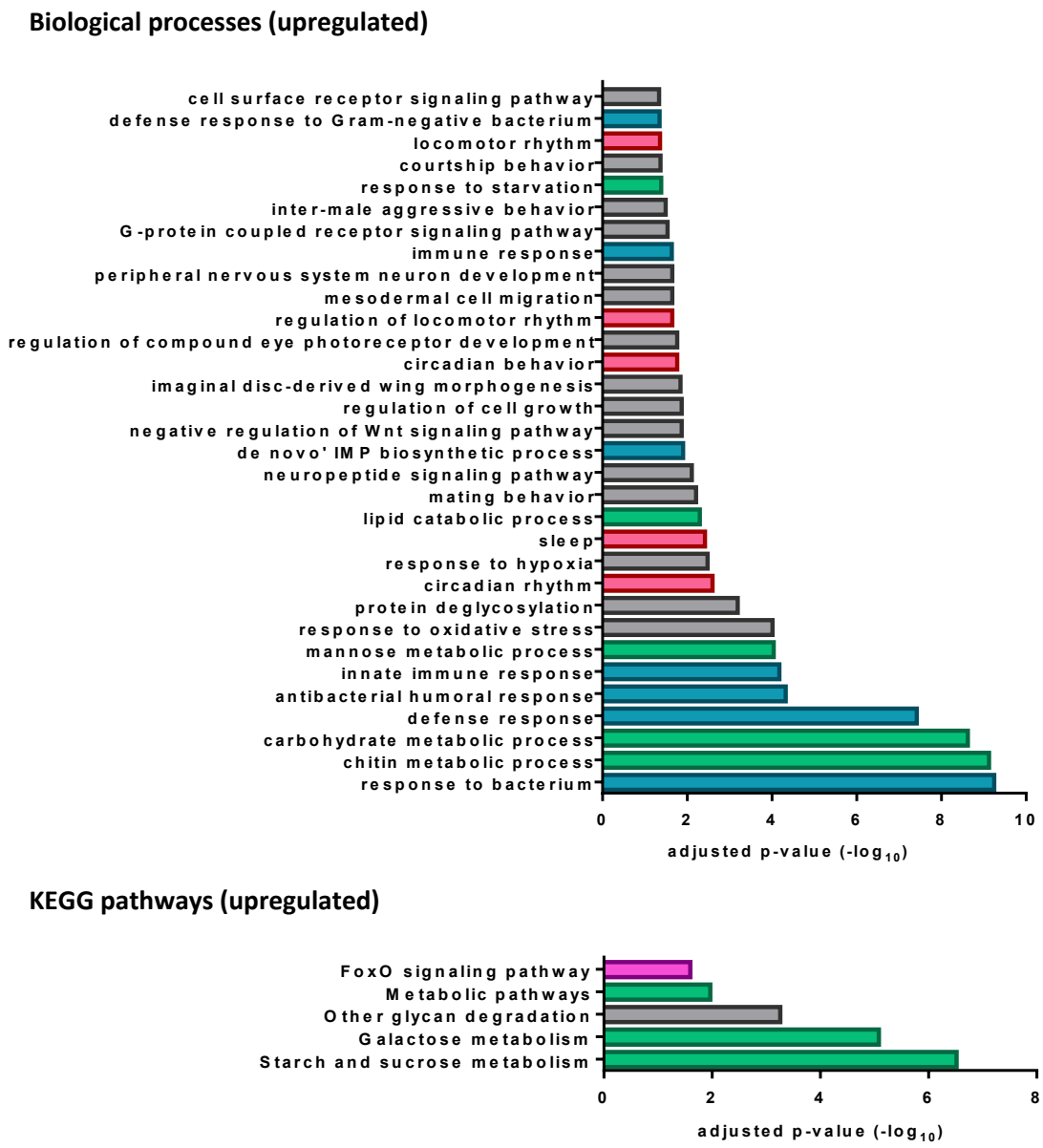

Fig. 3.25: GO-analysis identified upregulated biological processes and KEGG pathways in intestines of flies overexpressing dFoxO in ECs. All transcripts with FDR p-value < 0.05 and fold change > 1.5 were used for analysis. Colored bars highlight GOs associated with immunity (blue), metabolism (green), locomotor activity (rot) and FoxO signaling (pink), ECs = enterocytes.

The DAVID bioinformatics database was used for GO-analysis with all transcripts with an FDR-p-value < 0.05 and a fold change > 1.5. 32 significantly upregulated biological processes were identified, with seven being involved in immunity, four with metabolic functions and five with locomotor activity and circadian rhythm (Fig. 3.25 A). Additionally three

significantly upregulated KEGG pathways involved in metabolism and one associated with FoxO signaling were identified (Fig. 3.25 B).

Furthermore, nine downregulated biological processes and 11 downregulated KEGG pathways were detected (Fig. 3.26 A+B).

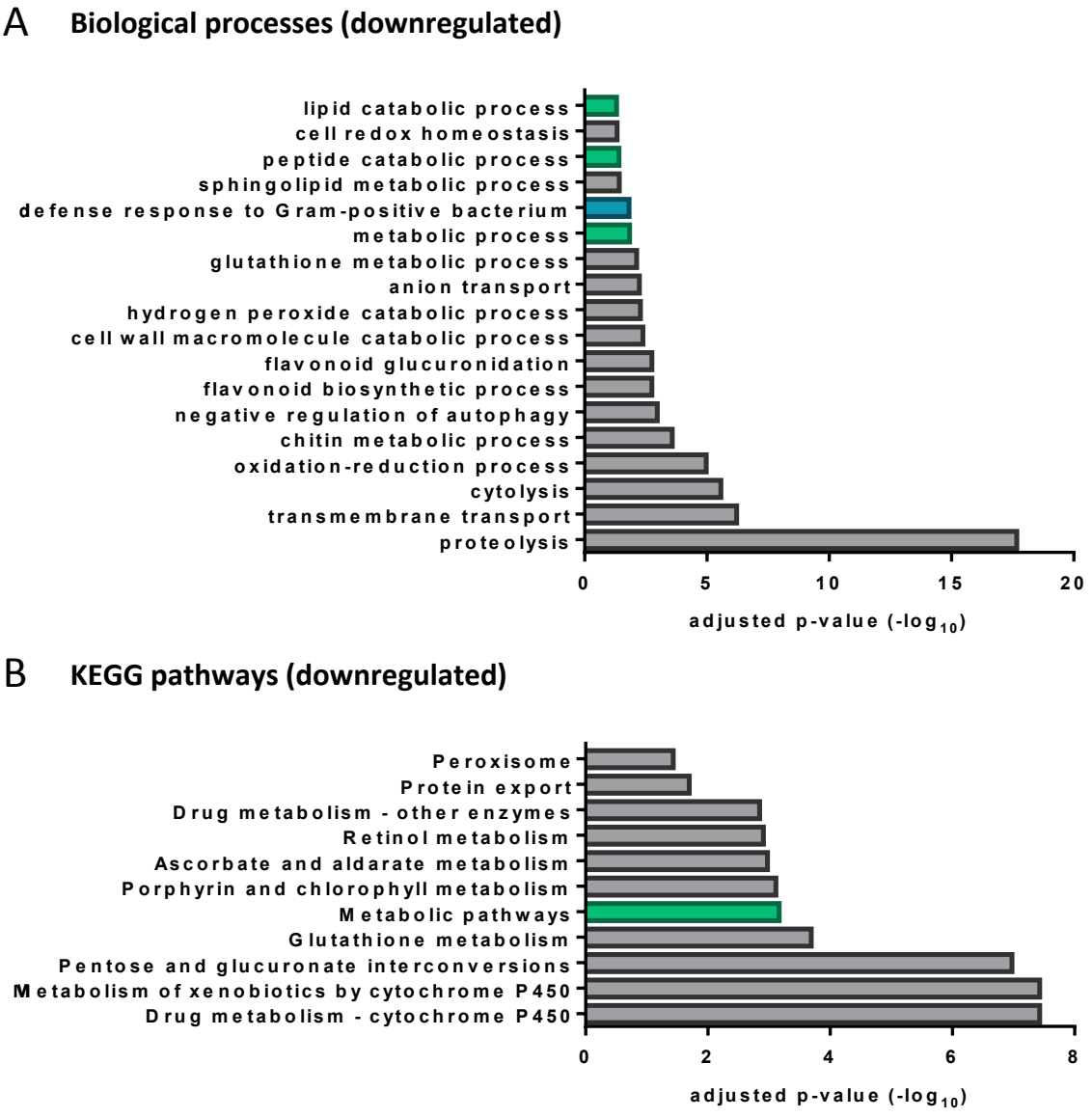

Fig. 3.26: Downregulated biological processes and KEGG pathways in intestines of flies overexpressing dFoxO in ECs were identified by GO-analysis. All transcripts with FDR p-value < 0.05 and fold change > 1.5 were used for analysis. Colored bars highlight GOs associated with immunity (blue) and metabolism (green). ECs = enterocytes.

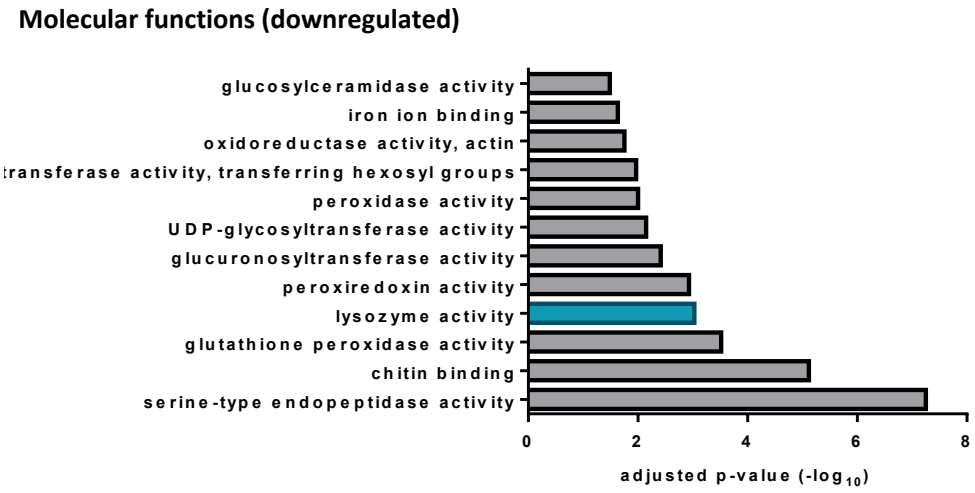

Fig. 3.27: Downregulated molecular functions in intestines of flies overexpressing dFoxO in ECs were detected by GO-analysis. All transcripts with FDR p-value < 0.05 and fold change > 1.5 were used for analysis. Colored bar highlights lysozyme activity (blue). ECs = enterocytes.

Four lysozyme genes were significantly downregulated (Table 3-4). To confirm a reduced activity in the fly, a lysis assay was performed (3.2.8).

Table 3-4: Downregulated lysozyme genes in flies overexpressing dFoxO in ECs:

gene	fold change
lys d	-2.9
lys b	-4
lys e	-7.5
lys x	-10.2

3.2.7. Differentially expressed genes in dFoxO-deficient and flies overexpressing dFoxo in ECs

Interestingly, many genes were similarly regulated in both, dFoxO-deficient flies and those overexpressing dFoxO in ECs. In order to identify genes that are differentially expressed in intestines of both data sets, a Venn diagram was generated from all significantly regulated genes (fold change > 1.5). 47 genes were significantly upregulated and 101 genes significantly downregulated in both groups (Fig. 3.28). 35 genes were upregulated in dFoxO-deficient flies, but downregulated in flies overexpressing dFoxO in ECs, while 31 genes were downregulated in dFoxO-deficient flies, but upregulated in flies overexpressing dFoxO in ECs (Fig. 3.28). However, these overlaps were not significant.

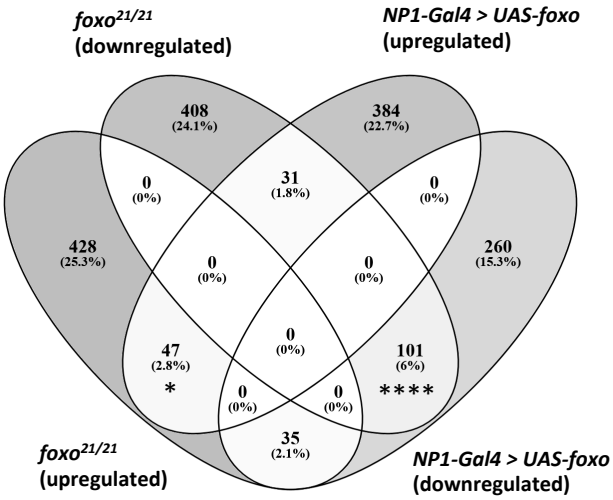

Fig. 3.28: Venn diagram of differentially expressed genes in dFoxO-deficient and flies overexpressing dFoxo in ECs. Overlaps represent all genes differentially expressed in respective groups. Fisher's exact test shows a significant overlap of 47 genes that were upregulated in dFoxO-deficient and dFoxO-overexpression flies and a significant overlap of 101 genes downregulated in dFoxO-deficient and dFoxO-overexpression flies. Overlaps of upregulated genes in dFoxO-deficient and downregulated genes in dFoxO-overexpression flies and vice versa are not significant. *NP1-Gal4 = NP1-Gal4;tubPGal80ts.* *p < 0.05, ****p < 0.0001, ECs = enterocytes.

Functional annotation analysis was conducted to identify gene ontologies of all up- and downregulated genes of both groups. The analysis detected two biological processes (Fig 3.29 A), four molecular functions (Fig. 3.29 B) and two KEGG pathways (Fig. 3.29 C) that were significantly upregulated.

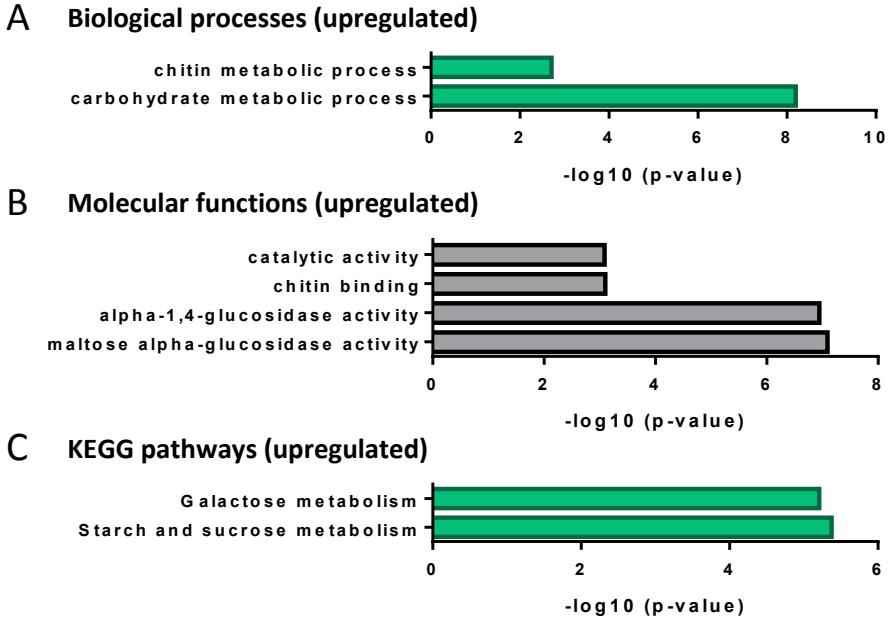

Fig. 3.29: Upregulated biological processes, molecular functions and KEGG pathways were detected by GO-analysis of genes regulated in dFoxO-deficient flies and flies with an overexpression of dFoxO in ECs. All transcripts with FDR p-value < 0.05 and fold change > 1.5 were used for analysis. Colored bar highlights metabolic processes (green). ECs = enterocytes

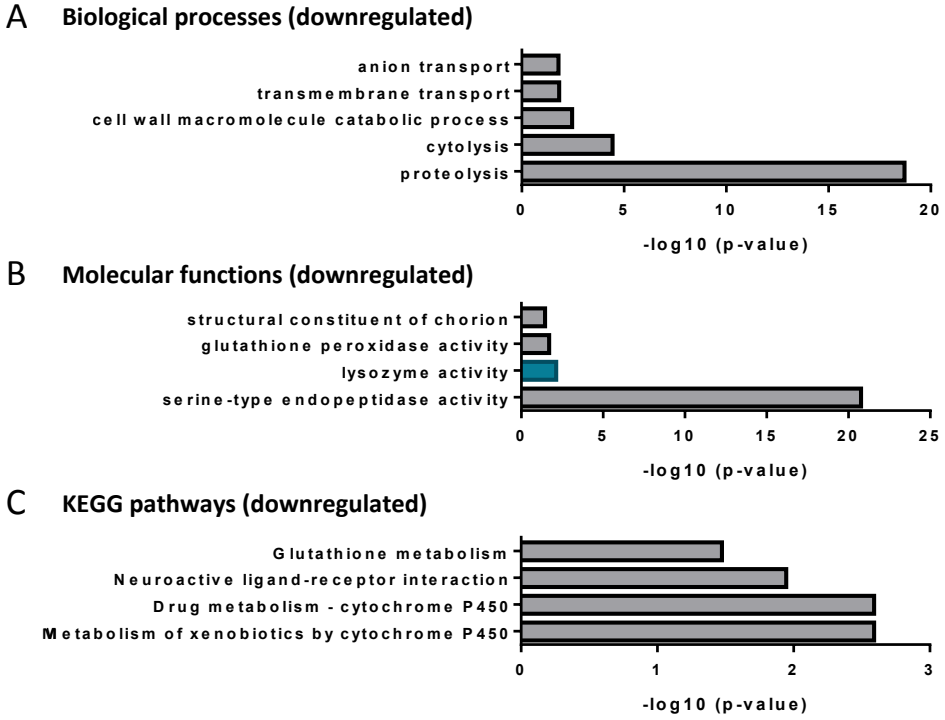

Fig. 3.30: Downregulated biological processes, molecular functions and KEGG pathways were detected by GO-analysis of genes regulated in dFoxO-deficient flies and flies with an overexpression of dFoxO in ECs. All transcripts with FDR p-value < 0.05 and fold change > 1.5 were used for analysis. Colored bar highlights lysozyme activity (blue). ECs = enterocytes.

The transcriptomic data of the intestines of dFoxO-deficient flies and those overexpressing dFoxO in ECs was compared to the transcriptome of trachea of dFoxO-deficient larvae and larvae overexpressing dFoxO in the trachea (Judith Bossen, unpublished data).

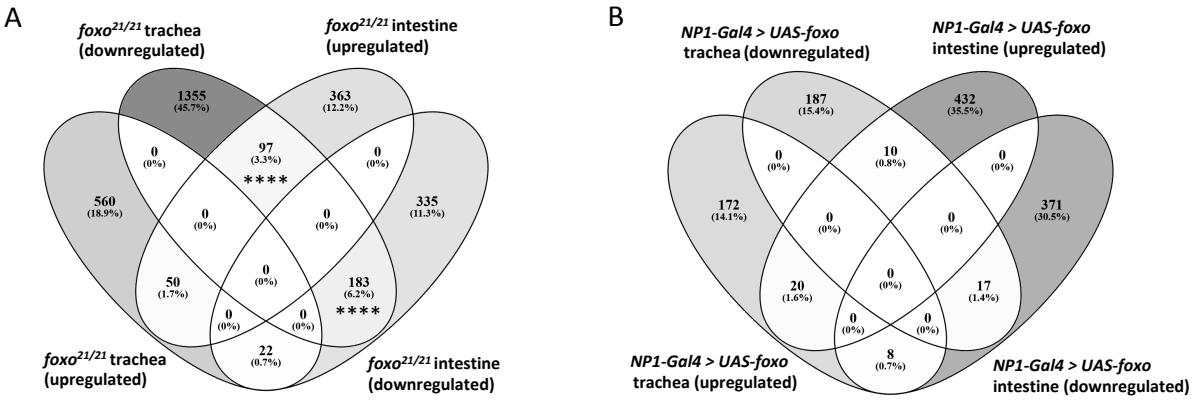

Fig. 3.31: Venn diagram of differentially expressed genes in trachea and intestines of dFoxO-deficient and flies overexpressing dFoxo in ECs. Overlaps represent all genes differentially expressed in respective groups. (A) Regulated genes in dFoxO-deficient flies. Fisher's exact test shows a significant overlap of 183 genes that were downregulated in the intestine and trachea and a significant overlap of 97 genes downregulated in the intestine but upregulated in trachea. Overlap of genes upregulated in both investigated tissue and overlap of genes upregulated in the intestine but downregulated in trachea was not significant. (B) Regulated genes in flies overexpressing dFoxo in ECs. Only few genes were similarly regulated in both tissues, so overlaps are not significant. *NP1-Gal4 = NP1-Gal4;tubPGal80ts.* ****p < 0.0001.

The overlaps of the Venn diagrams illustrate genes that were regulated in both tissues. Although in all comparisons some genes were regulated, only those downregulated in both trachea and intestine of dFoxO deficient flies and those downregulated in trachea but upregulated in the intestine were significant (Fig. 3.31 A).

3.2.8. Reduced Lysozyme activity upon overexpression of dFoxO in enterocytes

In dFoxO-deficient flies, the RNASeq analysis identified a downregulation of four different lysozymes genes (*lysB*, l*ysD*, *lysE*, *lysS*) (Table 3-2) and a lysis assay confirmed these findings (3.1.8). Interestingly, in flies with an overexpression of dFoxO in enterocytes, several lysozyme genes were also downregulated (*lysB*, l*ysD*, *lysE*, *lysX*) (Table 3.4). To confirm this result, the lysozyme lysis assay performed with the homogenate of dissected intestines. Based on lysozyme activity, cell walls of *Micrococcus lysodeikticus* mixed with agarose were lysed resulting in a clear zone of lysis. As the RNASeq result suggested, intestines of flies overexpressing dFoxO in enterocytes create smaller zones of lysis compared to control flies indicating a lower lysozyme activity (Fig. 3.32 A-C).

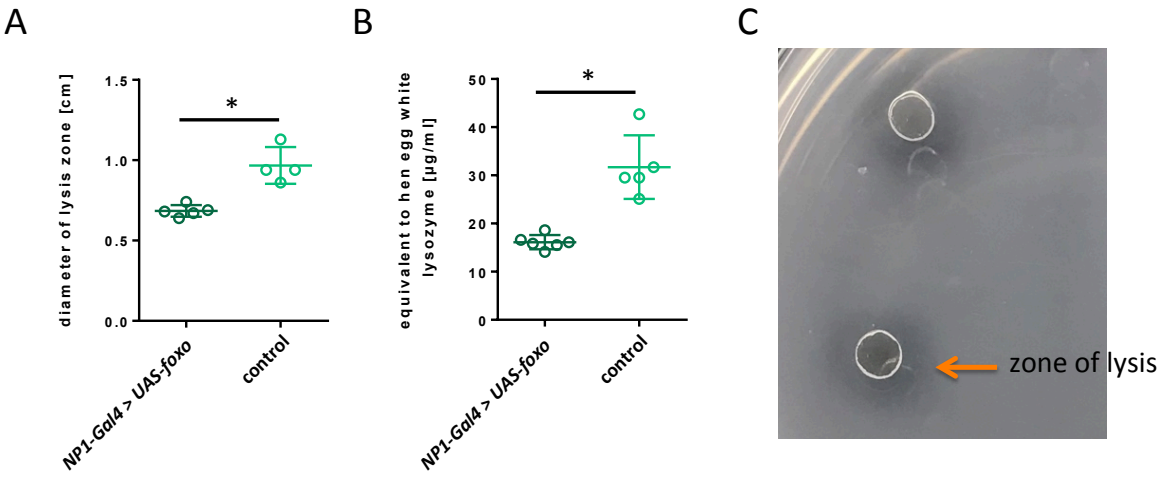

Fig. 3.32: Lysozyme lysis assay. (A) The intestines of flies overexpressing dFoxO in enterocytes cause smaller lysis zones than the control, suggesting less lysozyme activity. (B) Image of lysis plate of controls with zone of inhibition (orange arrow). *NP1-Gal4 = NP1-Gal4;tubPGal80ts*, control = *NP1-Gal4 > UAS-foxo* (not induced, kept at 18°), *p < 0.05, n = 5. Represented are means ± SD.

3.2.9. Survival under starvation condition

The resilience to starvation stress was also tested in flies overexpressing dFoxO in enterocytes. Populations of 10 female flies each were transferred to vials filled with 5 ml

agar-agar for moisture (n = 12-13) and monitored every 2 hours in the daytime until all individuals had died. Surprisingly, under starvation conditions, the overexpression of dFoxO prolonged the life span (Fig. 3.33), although under normal conditions on NM, the survival was strongly reduced (Fig. 3.18). The median life span during starvation increased to 62 hours compared to 48 hours in control flies.

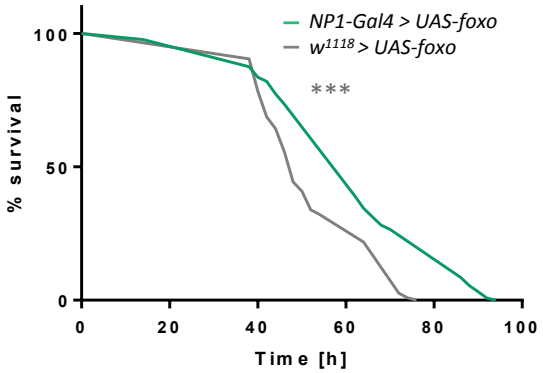

Fig. 3.33: Survival under starvation condition of flies overexpressing dFoxO in enterocytes. Flies were monitored every 2 hours during the days until all individuals had died (n = 12-13; 10 flies each). *NP1-Gal4 = NP1-Gal4;tubPGal80ts*; ***p < 0.001.

3.2.10. Changes of the microbial composition

The analysis of the microbial composition of dFoxo-deficient flies showed a tendency to dysbiosis that increases over time (3.1.10). Fecal samples of flies overexpressing dFoxO in enterocytes were also tested for their microbial profile.

Drosophila embryos were sterilized by dechorionation and recolonized with a defined mix of five *Drosophila* gut bacteria (Santos et al. 2017). Four to five replicates of 70 to 100 female flies each were transferred onto sterile NM in vials. During the experiment, several flies died. Therefore, the number of individuals in the tested populations was decreasing. Fecal samples were collected after 24 h, 5 days, 10 days and 20 days. Genomic DNA was extracted and amplified with specific primers for bacterial variable regions 1 and 2 of 16S rRNA genes. Illumina MiSeq was used to sequence the amplificates. The bacteria mix used for recolonization was analyzed as well (Sarah Frömbling, Master thesis 2019). It contained the desired bacteria *Lactobacillus* (14 %), *Acetobacter* (25 %), *Enterococcus* (24 %) and *Commensalibacter* (35 %). The bacteria mix was contaminated with 2 percent of other, not specifiable bacteria (Fig. 3.34 A). The results at day 5 and 20 were chosen to represent

differences in the microbiota of young and old flies (Fig. 3.34 B+C). The results for all time points are displayed in the appendix (Fig. 9.3).

Samples 1 and 2 of 5-day-old dFoxO-overexpressing flies contained mainly *Acetobacter* (35 and 27 %) and *Lactobacillus* (34 and 66 %). 6 percent of *Enterococcus* were found in both samples, but sample 1 was contaminated with 25 percent while sample 2 showed hardly any contamination. Sample 3 comprised of *Acetobacter* (68 %), *Lactobacillus* (7 %) and *Enterococcus* (11 %) and 14 percent of contamination. The 4th replicate contained only 97 percent of *Acetobacter* and 3 percent contamination (Fig 3.34 B). In the control, four out of five samples were very similar. They comprised of 68 to 88 percent *Acetobacter*, 4 to 24 percent *Lactobacillus* and 1 to 23 percent of contamination. Sample 2 however is composed of primarily of *Acetobacter* (75 %), only 1 percent of *Lactobacillus* and 24 percent of contamination (Fig. 3.25 B). None of the samples had any *Enterococcus* or *Commensalibacter* (Fig. 3.34 C).

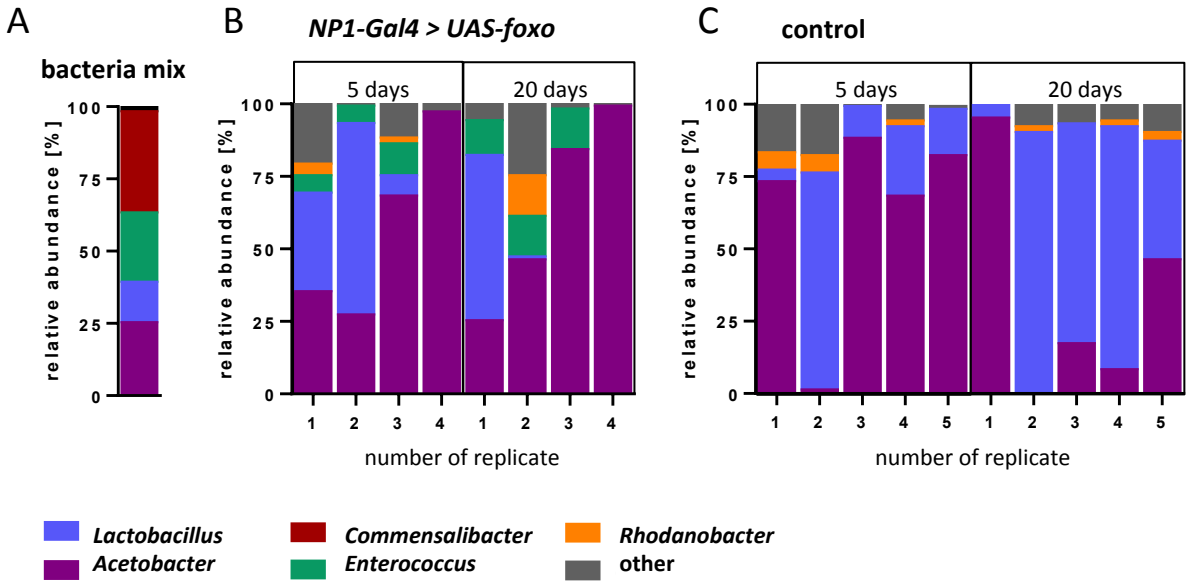

Fig. 3.34: Microbial composition of the bacteria mix used for recolonization and of feces collected from dFoxo-overxpressing and control flies. (A) The bacteria mix consisted of 25 % *Acetobacter*, 14 % *Lactobacilli*, 24 % *Enterococcus*, 35 % *Commensalibacter* and 2 % of not specifiable other bacteria (Sarah Frömbling, Master thesis 2019). (B) Microbial composition of individual replicates of flies overexpressing dFoxO in enterocytes and (C) controls at age 5 and 20 days. *Rhodanobacter* and other bacteria were undesirable contaminations*, NP1-Gal4 = NP1-Gal4;tubPGal80ts.* control = *w^{1118} > UAS-foxo*.

In dFoxO-overexpressing flies at an age of 20 days, three out of four samples were composed of mainly bacteria from the recolonization mix with only minor contaminations (Fig. 3.34 B).

Four out of five control samples at age 20 days comprised predominantly *Lactobacillus* (41 to 90 %) and *Acetobacter* (8 to 46 %) with contaminations of 7 to 13 percent. Replicate 1 was not contaminated and showed 95 percent of *Acetobacter* and 5 percent *Lactobacillus*.

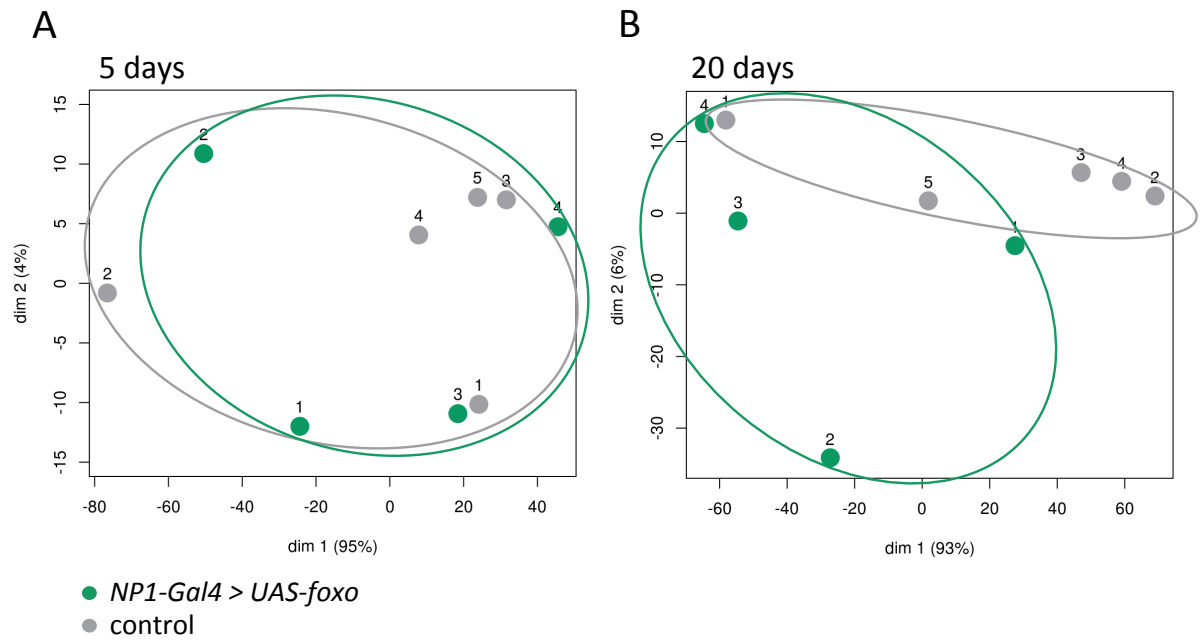

Fig. 3.35: PCoA plots were calculated to identify clusters of microbial compositions. (A) At age 5, the microbial profiles of feces from flies overexpressing dFoxO in enterocytes are almost completely overlapping. (B) At age 20 days, the microbiota of both groups is diverting into two clusters, but not separated significantly. Ellipses were added manually. *NP1-Gal4 = NP1-Gal4;tubPGal80ts.* control = w^{1118} > *UAS-foxo.*

A Principal Coordinates Analysis (PCoA) was used to visualize similarities of the microbial profiles of fecal samples dFoxO-overexpressing flies compared to control flies. In young, 5-day-old flies, the microbiota of flies overexpressing dFoxO in ECs and their controls are mainly overlapping. In older flies at the age of 20 days, samples cluster significantly into two profiles (p = 0.027) (Fig. 3.35). The results for all time points are illustrated in the appendix (Fig. 9.4).

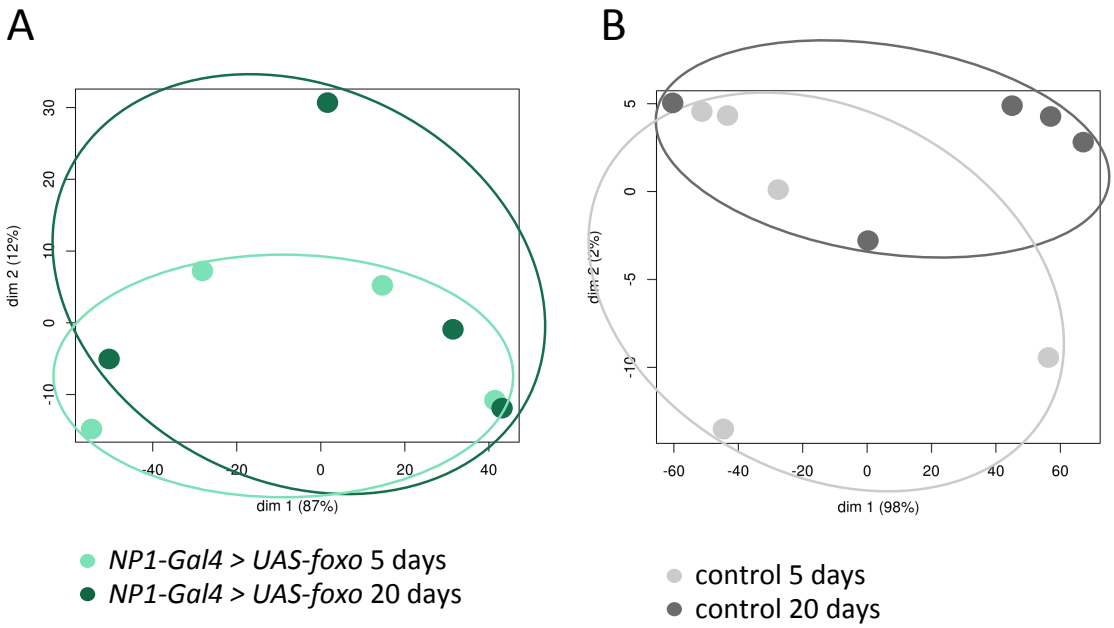

Fig. 3.36: PCoA plots show clusters of microbial compositions of young and old flies. (A) Microbial profiles of feces from 5 and 20 days old flies overexpressing dFoxO in enterocytes and control flies are mainly overlapping. (B) In control flies at age 5 and 20 days, the microbiota of both groups seem to be diverting into two clusters, but not separated significantly. Ellipses were added manually. *NP1-Gal4 = NP1-Gal4;tubPGal80ts.* control = w^{1118} > *UAS-foxo.*

Aging has been associated with changes in the microbiota that led to a dysbiosis of the intestine. Therefore, microbial profiles of young and old flies of both fly genotypes were compared to each other (Fig. 3.36). It revealed significant differences of bacterial composition of feces of neither flies overexpressing dFoxO in ECs ($p = 0.49$) nor controls ($p = 0.082$).

3.3. Effects of an overexpression of a constitutive active form of dFoxo in Enterocytes

The overexpression of dFoxO in enterocytes had drastic effects on the survival (Fig. 3.18) and on digestive functions (Fig. 3.19). When these experiments are conducted with flies overexpressing a constitutive active form of dFoxO, the effects were even more severe compared to the native dFoxO overexpression. The survival was drastically reduced with the median life span being reduced to 9 days compared to 25 and 32 days in both genetic controls (Fig. 3.37 A). The number of fecal spots excreted in 24 hours is strongly reduced (Fig 3.37 B) and the transit time from ingestion of food until excretion is drastically prolonged (Fig 3.37 C). Both effects are stronger than in flies overexpressing the native dFoxO.

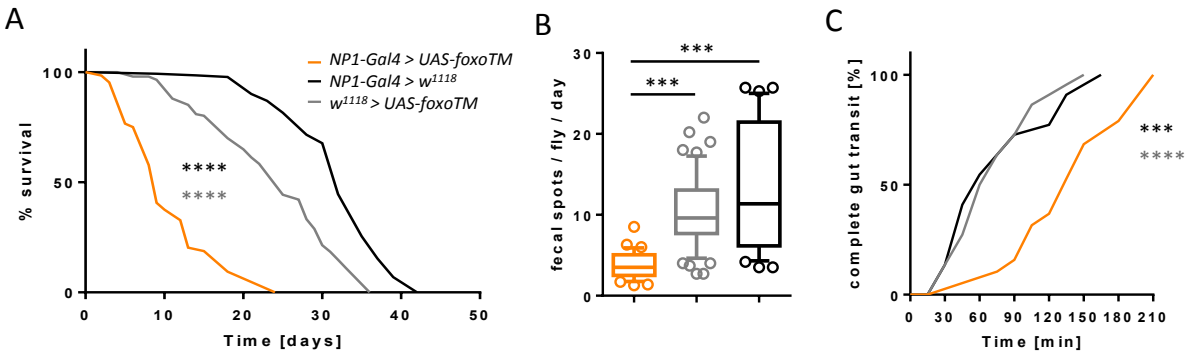

Fig. 3.37: Influence of an overexpression of a constitutive active form of dFoxO in enterocytes on life span and fecal output. (A) The life span of flies overexpressing a constitutive active form of dFoxO in enterocytes is drastically reduced compared to both controls (n = 5). (B) The number of fecal spots in 24 hours is also highly decreased (n = 32-58). (C) The transit time was measured for 210 minutes after food ingestion. Compared to both genetic controls, the transit time is strongly prolonged (n = 19-23). Color of asterisks represents the corresponding control (A + C). *NP1-Gal4 = NP1-Gal4;tubPGal80ts*, ***p < 0.001, ****p < 0.0001. Box and whiskers represent mean and 10 – 90 percentile (B).

3.4. Effects of an overexpression of dFoxO in intestinal stem cells and enteroblasts

The previous experiments revealed that both the overall deficiency and the overexpression of dFoxO in enterocytes have mostly impairing effects on several physiological aspects (3.1-3.3). However, an overexpression in intestinal stem cells (ISCs) and enteroblasts (EBs) might have other effects on the physiology of *Drosophila* due to their different function. ISCs and EBs express the stem cell specific gene *escargot* (*esg*). A heat-inducible driver line for specific expression in *esg*$^{+}$ cells was crossed to the *UAS-foxo* responder line used before. Female flies from the F1-generation were used in experiments. The driver line contained a UAS-*gfp* element resulting in the expression of GFP in all ISCs and EBs after heat-induction. Both, the Gal4- and the UAS-line crossed to w^{1118} wild type flies were used as genetic controls.

3.4.1. Survival

It was shown that a deficiency as well as an overexpression of dFoxO in enterocytes drastically reduces the survival of *Drosophila* (3.1.1 and 3.2.1). The overexpression in ICSs and EBs seems to have not a distinct effect. Compared to the Gal4-control, the survival is significantly prolonged with the median life span being increased to 32 from 27 in the control. The comparison to the UAS-control however, shows no significant differences (Fig. 3.38).

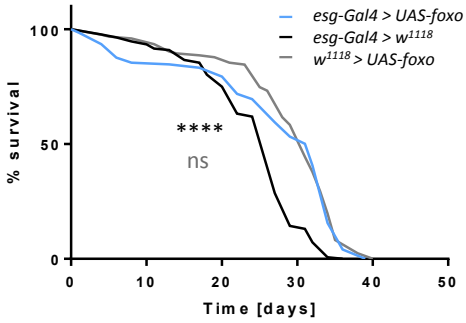

Fig. 3.38: Influence of an overexpression of dFoxO in ISCs and EBs on survival. Flies were monitored until all individuals had died (n = 5; 30-50 flies each). Color of asterisks indicates the comparison to corresponding control. ISCs = intestinal stem cells, EBs = enteroblasts, *esg-Gal4 = esg-Gal4,UAS-GFP;tub-Gal80ts*; ****p < 0.0001, ns = not significant

3.4.2. Influence of an overexpression in ISCs and EBs on digestion

In dFoxO-deficient flies as well as flies overexpressing dFoxO in enterocytes, the amount of ingested food and the number of excreted fecal spots is significantly reduced, while the transit time is increased (3.1.2 and 3.2.2). The amount of ingested food as well as fecal output was quantified for a period of 24 h. The transit time from ingestion of food until defecation was measured for 180 minutes. Flies overexpressing dFoxo in ISCs and EBs showed no differences in food intake compared to their control (Fig 3.39 A). Also, the transit time was similar to genetic controls (Fig 3.39 C). Surprisingly, the number of fecal spots was highly reduced in overexpression flies (Fig 3.39 B), although the amount of ingested food was the same in both groups.

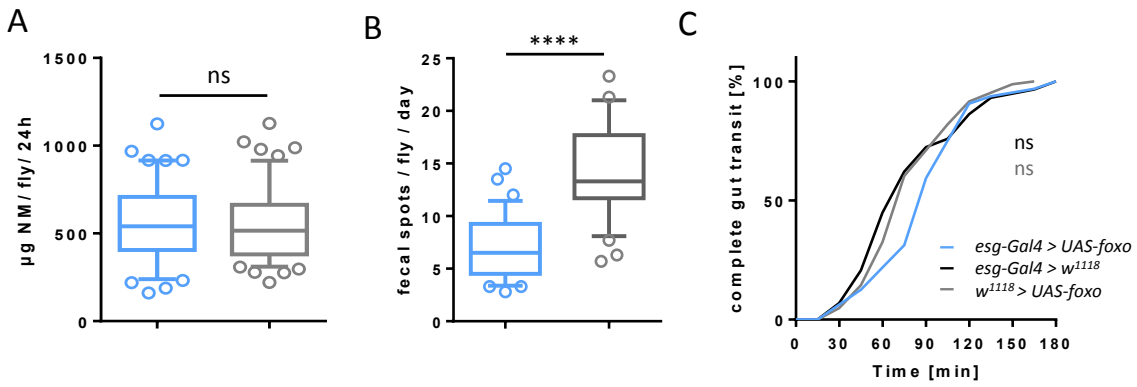

Fig. 3.39: Influence of an overexpression of dFoxO in ISCs and EBs on digestion. (A) The amount of ingested food (n = 49-52) and (B) the fecal output (n = 29-39) was measured for 24 h. (C) The transit time after ingestion of food was monitored for 180 min (n = 29-84). ISCs = intestinal stem cells, EBs = enteroblasts, *esg-Gal4 = esg-Gal4,UAS-GFP;tub-Gal80ts*, ****p < 0.0001, ns = not significant. Box and whiskers represent mean and 10 – 90 percentile (A+B).

3.4.3. Effect of an overexpression of dFoxO in ISCs and EBs on the body composition

The previous experiments showed the overexpression of dFoxO in enterocytes as well as the deficiency of dFoxO drastically reduce the stored fat in *Drosophila* (3.1.3 and 3.2.3). To test this upon overexpression of dFoxO in ISCs and EBs, a mifepristone (RU486) inducible driver line was crossed to the *UAS-foxo* responder line.

Interestingly, in young flies (7 days post induction), the fat content of the overexpression flies was twice as high as in the genetic controls. In older individuals from the same population, flies overexpressing dFoxO in ISCs and EBs still contain twice as much fat as their respective controls, but lost approx. 50 percent compared to their young age (Fig. 3.39 B). However, the weight of the flies showed no significant differences in either the genetic control or the older individuals (Fig 3.39 A). Surprisingly, the protein content of the same individuals was the other way around. Flies overexpressing dFoxO in ISCs and EBs contained significantly less protein than control flies (Fig. 3.39 C).

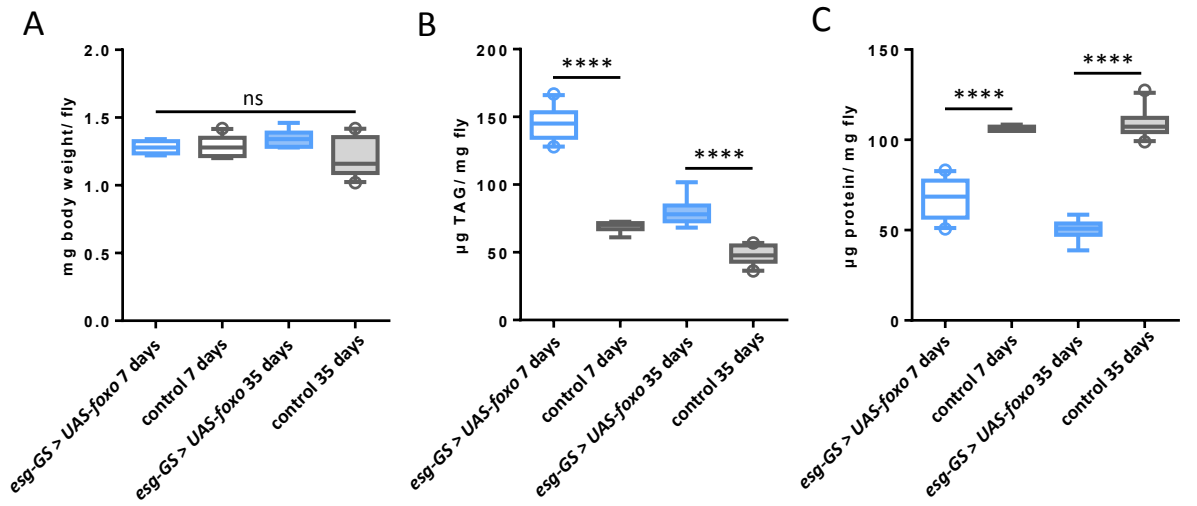

Fig. 3.40: Analysis of the body fat content in young and older flies overexpressing dFoxO in ISCs and EBs. (A) Weight, (B) body fat content, (C) protein content and (C) fat to protein ratio of 7- and 35-day old flies (n = 6-10). ISCs = intestinal stem cells, EBs = enteroblasts, *esg-GS > UAS-foxo* = Mifepristone (RU486)-induced *esg* driver line, control = *esg-GS > UAS-foxo* (-RU486). ****p < 0.0001, ***p < 0.001, ns = not significant. Box and whiskers represent mean and 10 – 90 percentile .

3.4.4. Activity and metabolic rate upon dFoxO overexpression in ISCs and EBs

In dFoxO-deficient flies as well as in those overexpressing dFoxO in enterocytes, the activity was reduced (3.1.4 and 3.2.4). Whether this is also true for flies with an overexpression of dFoxo in *esg*+ cells was measured in the *Drosophila* Activity Monitor system (DAM) with a 12 hour dark/ 12 hour light cycle. After adaptation to the conditions for one day, the activity

was measured for three consecutive days. The circadian rhythm showed lower morning and evening peaks compared to control flies (Fig 3.41 A), but due to a higher activity during the resting phases, the total activity showed no significant differences compared to the UAS-control. However, in comparison to the Gal4-control, the total activity was significantly reduced (Fig 3.41 B). The metabolic rate, which was measured for 2 hours during the resting period, also showed no differences among groups (Fig 3.41 C).

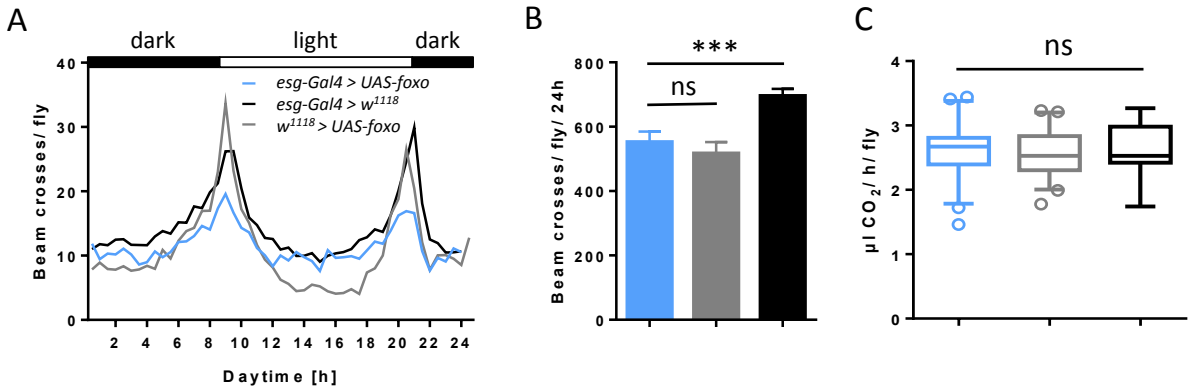

Fig. 3.41: Activity, circadian rhythm and metabolic rate of flies overexpressing dFoxO in ISCs and EBs. (A) Using the *Drosophila* Activity Monitor system (DAM), the circadian rhythm was recorded for three consecutive days. (B) The total activity was calculated (n = 34-145) (C) the metabolic rate was measured for 2 h (n = 7-21). ISCs = intestinal stem cells, EBs = enteroblasts, *esg-Gal4 = esg-Gal4,UAS-GFP;tub-Gal80ts*, ns = not significant. Error bars are represented as means ± SEM. Box and whiskers represent mean and 10 – 90 percentile (C).

3.4.5. Gut integrity

The integrity of both, dFoxO-deficiency and overexpression in enterocytes is strongly impaired in comparison to their respective controls (3.1.5 and 3.2.5). It was tested using a so-called smurf assay in which flies are fed with blue dyed sucrose solution once a week for 24 h. In flies with an intact intestinal epithelium, the blue coloration is restricted to the gut. Upon impairment of the epithelium, food can leak out of the intestine, resulting in blue colored flies called smurfs (Fig 3.6 C).

Table 3-5: Significance of total number of smurf individuals upon overexpression of dFoxO in ISCs and EBs.

Age of flies	p-value (comparison with UAS-control)	p-value (comparison with Gal4-control)	significance
7 days	0.0476	0.4444	no
14 days	>0.9999	0.1667	no
21 days	0.3651	0.3714	no
28 days	0.3095	0.3429	no

Interestingly, flies overexpressing dFoxO in *esg*+ cells showed less smurf phenotypes than both genetic controls but without significance (Table 3-5). Even at age 28 days, only six percent of the flies had an impaired gut epithelium and not a single dead smurf (Fig. 3.42).

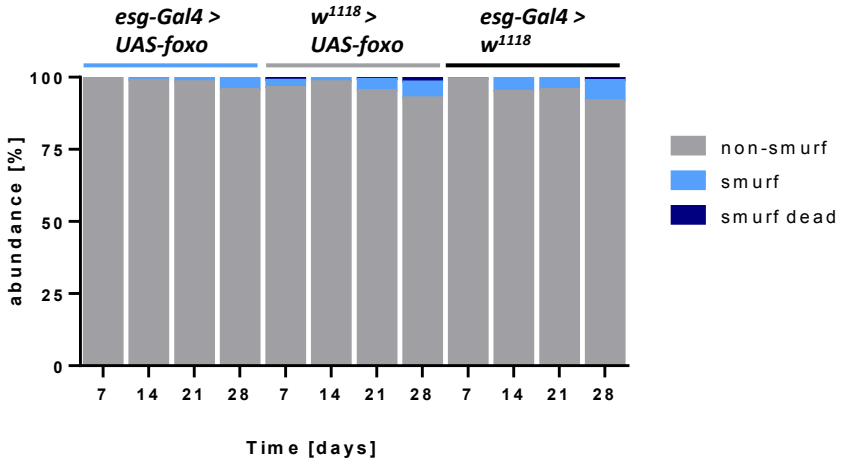

Fig. 3.42: Effects of an overexpression of dFoxO in ISCs and EBs on gut integrity. (A) The overexpression resulted in less smurf individuals at each time point compared to both genetic controls (n = 5). (B) Image of smurf (left) and non-smurf (right) phenotypes of dFoxO-deficient flies. *esg-Gal4 = esg-Gal4,UAS-GFP;tub-Gal80ts*.

3.4.6. Survival during Starvation

The starvation resistance assay was the only experiment so far where the overexpression of dFoxO in enterocytes had a positive effect on *Drosophila* (3.2.9). The deficiency of dFoxO in contrast resulted in a drastically reduced survival under starvation (3.1.9). A mifepristone (RU486) inducible crossing was used to investigate the starvation resistance upon overexpression of dFoxO in ISCs and EBs. Surprisingly, these flies lived up to almost 10 days without food. The median life span was prolonged from 62 h in controls to 160 h in dFoxO overexpressing flies (Fig. 3.43).

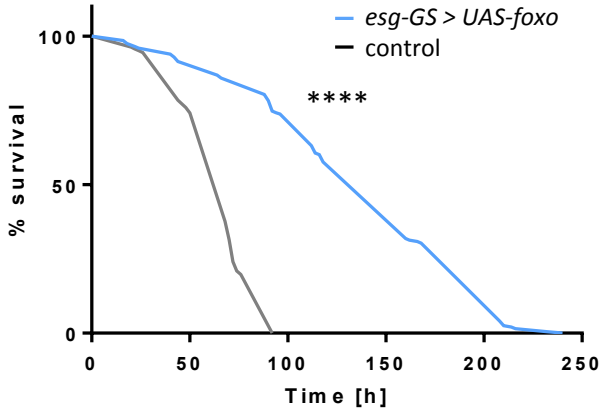

Fig. 3.43: Survival under starvation condition of flies overexpressing dFoxO in *esg*+ cells. Flies were monitored every 2 h during the days until all individuals had died (n = 9-10; 10 flies each). *esg-GS > UAS-foxo* = Mifeprisone (RU486)-induced *esg* driver line, control = *esg-GS > UAS-foxo* (-RU486), ****p < 0.0001.

3.5. The Influence of DSS and Bleomycin on flies upon manipulation of dFoxO expression

The oral application of DSS (Dextran Sulfate Sodium) damages the intestinal tract of mice and causes symptoms of inflammatory bowel disease (IBD) that resemble ulcerative colitis in humans (Okayasu et al. 1990; Kawada et al. 2007). In *Drosophila*, DSS also induced tissue damage, reduction of life span and proliferation (Amcheslavsky et al. 2009). Bleomycin is also used as a tissue-damaging substance in experimental systems. It damages DNA and is used as an anticancer drug (Takada et al. 2003; Morel et al. 2008). Since FoxO is involved in stress responses in *Drosophila*, the influence of DSS and Bleomycin on flies with a manipulated dFoxO expression was tested. Flies were kept in vials containing approx. 5 ml agar-agar for moisture. The substances (5 % DSS or 25 µg/ml Bleomycin) were mixed with a 5 % sucrose solution and applied on filter paper every 1 to 2 days.

3.5.1. Treatment with DSS results in a translocation of dFoxo to the nucleus

The activation and translocation of dFoxO into the nucleus can be induced by various stress stimuli such as oxidative stress, heat shock, UV radiation (Brunet et al. 2004) and metabolic stress (Brunet & Webb 2014). To test whether DSS is also sufficient stress for activating dFoxO, the *NP1-Gal4* fly line that drives expression in ECs was crossed to an *UAS-foxo-gfp* reporter line. As expected, a treatment with DSS resulted in the translocation of dFoxO into the nucleus, while in the sucrose control, dFoxO was restricted to the cytoplasm (Fig. 3.44).

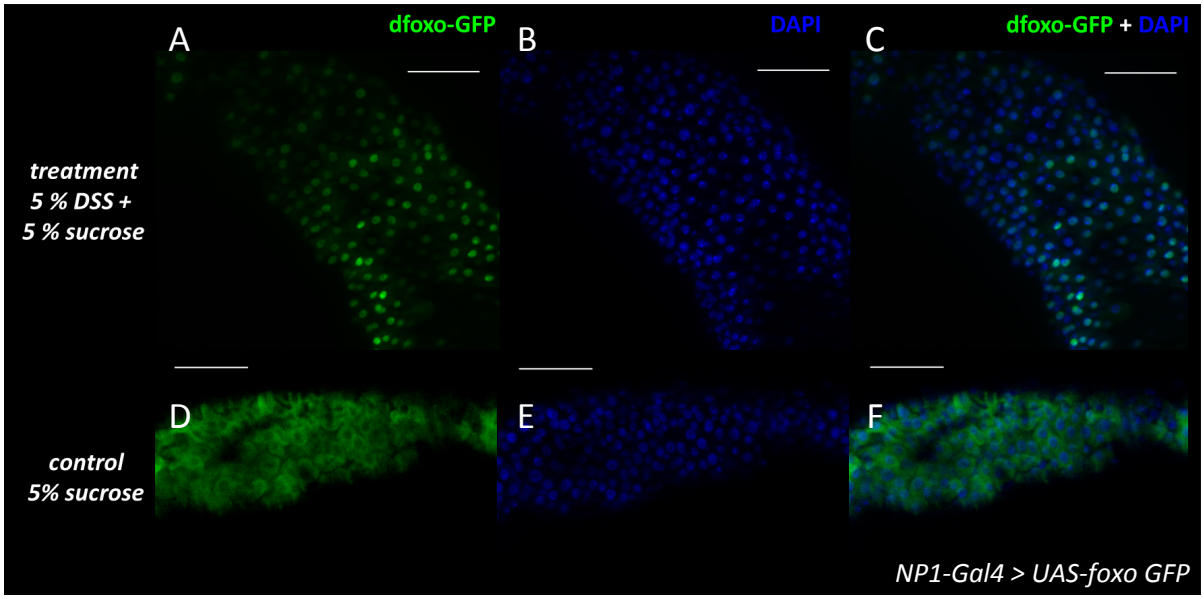

Fig. 3.44: DSS is able to induce stress-dependent translocation of dFoxO. (A-C) Treatment with DSS for 24 h caused the translocation of dFoxO into the nucleus. (D-F) Upon sucrose control treatment, dFoxO remains in the cytoplasm. *NP1-Gal4 = NP1-Gal4;tubPGal80ts*, DSS= Dextran Sulfate Sodium, Scale bar = 50 µm.

3.5.2. Survival upon DSS treatment

Per treatment, the survival rates of 5 to 14 populations with 20 flies each were monitored until all individuals had died. Surprisingly, dFoxO-deficient flies lived significantly longer than control flies when treated with DSS. The median lifespan of 11 days in dFoxO-deficient flies was 37.5 % higher than in the control (median life span = 8 days) (Fig. 3.45 A). In the control treatment group, which did not receive DSS, a dFoxO-deficiency resulted in the expected reduction of life span (Fig 3.45 A'). The medium life span was reduced by almost 50 % from 32 in controls to 18 days.

An overexpression of native dFoxO in enterocytes resulted in a significant reduction of life span in DSS-treated flies with a medium lifespan of 5 days compared to 6 and 7 days in genetic controls (Fig. 3.45 B). In the respective control group, the life span of flies with an overexpression of native dFoxO in enterocytes was also significantly decreased (Fig. 3.45 B'). The medium life span of 14 days was reduced by approx. 20 percent compared to both genetic controls (17 and 18 days).

The overexpression of a constitutive active form of dFoxO resulted in similar effects on the life span of DSS-treated flies (Fig 3.45 D). However, in flies of the control treatment group, the reduction of life span was stronger than in the case of the native dFoxO overexpression.

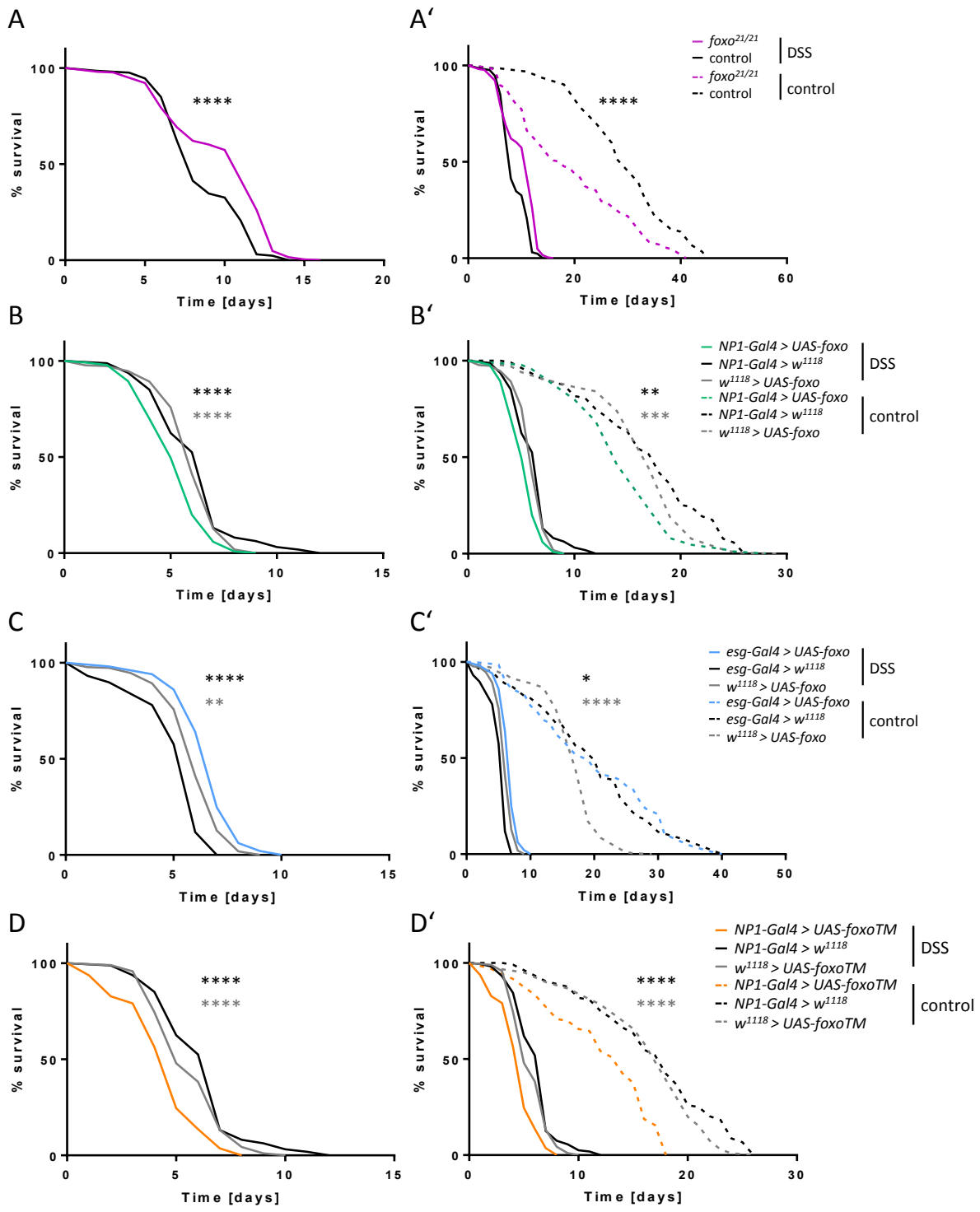

Fig. 3.45: Survival upon manipulation of dFoxO expression levels and DSS treatment. (A-A’) Compared to the control, a dFoxO-deficiency prolonged the life span under treatment with DSS while feeding only sucrose significantly reduced the life span. (B-B’) The overexpression of dFoxO in enterocytes has no specific effect on the response to DSS stress as the DSS treatment as well as the sucrose control reduced the survival. (C-Cs) In flies overexpressing dFoxO in intestinal stem cells and enteroblasts, the treatment with DSS resulted in an increased life span. In the control treatment however, both genetic controls showed opposite effect, making the result inconclusive. (D-D’) The overexpression of a constitutive active form of dFoxO showed similar but stronger effects than the native overexpression. control = w^{1118}, *NP1-Gal4 = NP1-Gal4;tubPGal80ts, esg-Gal4 = esg-Gal4,UAS-GFP;tub-Gal80ts*, DSS= Dextran Sulfate Sodium, n = 5-13, ns = not significant *p < 0.05, **p < 0.01, ***p < 0.001. ****p < 0.0001. Color of asterisks indicate the corresponding control.

Interestingly, flies with an overexpression of native dFoxO in intestinal stem cells (ISCs) and enteroblasts (EBs) lived significantly longer upon ingestion of DSS compared to their genetic controls with the medium life span being prolonged to 7 days compared to 6 days in controls (Fig 3.45 C). The effect of an overexpression of dFoxO in ISCs and EBs in the control treatment group was inconclusive. Compared to the UAS-control, the life span was significantly increased, but compared to the Gal4-control the survival was reduced (Fig 3.45 C').

3.5.3. Survival upon treatment with Bleomycin

Bleomycin reduces the life span of *Drosophila* in a dose-dependent manner (Amcheslavsky et al. 2009). When flies were treated with Bleomycin, the median life span was significantly reduced from 13 days in controls to 11 days in dFoxO-deficient animals (Dustin Hanke, Bachelor thesis 2018). However, the maximum life span showed no differences in both groups (Fig 3.46 A+A'). In flies overexpressing dFoxO in enterocytes, the treatment also resulted in a decrease in life span (Fig 3.46 B+B'). Since the survival is also reduced in the control treatment, Bleomycin had no specific effect. The treatment with Bleomycin of flies with an overexpression of dFoxO in *esg*$^{+}$ cells resulted in a reduced life span compared to the UAS-control, but had no effect in comparison with the Gal4-control.

The sucrose treatment served as control for the survival assay of both, DSS- and Bleomycin-treatment. The results are described in the previous chapter (3.5.1).

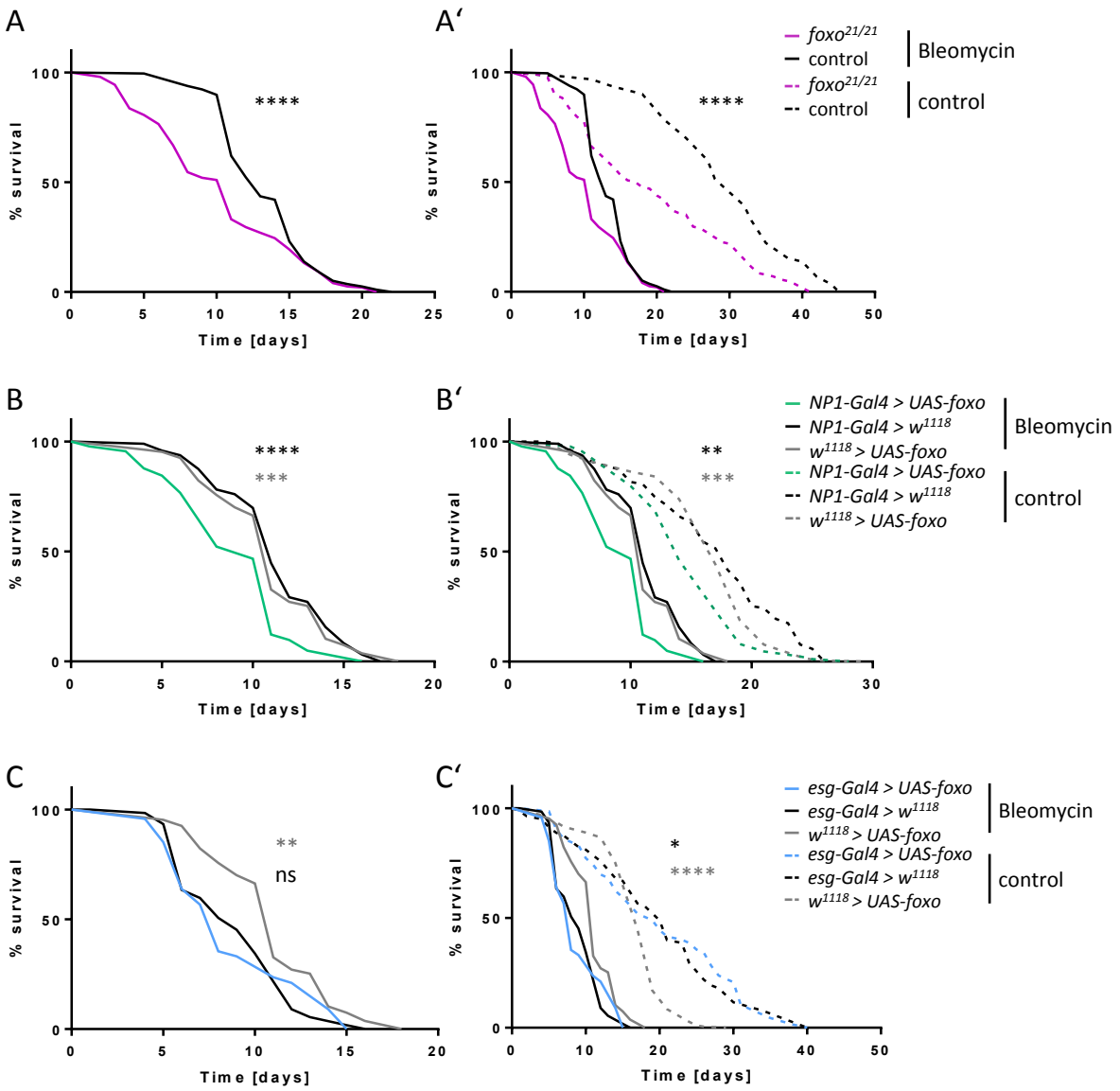

Fig. 3.46: Effect of Bleomycin on the survival upon manipulation of dFoxO expression levels. (A-A') Both, Bleomycin and control treatment reduced the life span of dFoxO-deficient flies. (B-B') The overexpression of dFoxO in enterocytes has no specific effect on the response to Bleomycin stress. The Bleomycin treatment and the sucrose control reduced the survival. (C-C') Compared to the UAS-control, the treatment with Bleomycin in flies overexpressing dFoxO in intestinal stem cells and enteroblasts, reduced the life span, while there is no significant difference to the Gal4-control. In the control treatment, both genetic controls showed opposite effect, making the result inconclusive. control = w^{1118}, *NP1-Gal4 = NP1-Gal4;tubPGal80ts, esg-Gal4 = esg-Gal4,UAS-GFP;tub-Gal80ts*, DSS = Dextran Sulfate Sodium, n = 5-10, ns = not significant *p < 0.05, **p < 0.01, ***p < 0.001. ****p < 0.0001. Color of asterisks indicates the comparison to the corresponding control.

3.5.4. Influence of DSS and Bleomycin on the body fat content

The treatment of dFoxO deficient flies with DSS and Bleomycin had different effects on the survival. In contrast to Bleomycin and the sucrose control, DSS caused an increase in life span. The effect of both substances on the body fat content was also measured to test whether the resilience to these damaging agents is related to the energy status of the fly. The sucrose control showed a lower body fat content in dFoxO deficient flies at all time

points as expected from the experiment on NM (Fig. 3.3). A treatment with DSS of these flies led to a massive loss of body fat of both, overexpressing and control flies in regard to the sucrose-fed flies (Fig 3.47 A). However, dFoxO-deficient flies still possessed significantly more body fat than control flies at day 5. After eight days of treatment, the loss of body fat is even stronger and at the same level in both groups. Interestingly, although the fat content differs drastically, the body weight showed no significant differences Fig. 3.47 A'), neither among DSS samples nor in comparison with the sucrose samples.

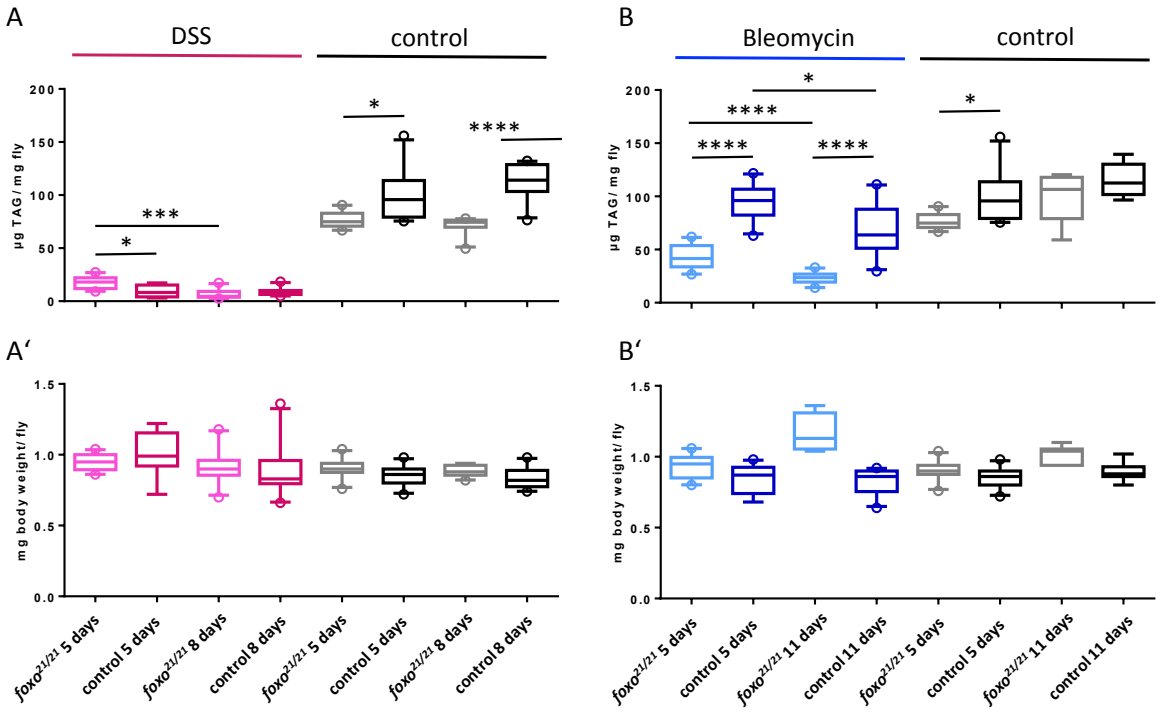

Fig. 3.47 Body fat content of dFoxO-deficient flies upon treatment with DSS and Bleomycin. (A) The treatment with DSS resulted in a massive loss of body fat compared to the control. However, in dFoxO-deficient flies, the body fat content was still higher than in control flies. (A') However, differences in body weight were not detected. (B) The treatment with Bleomycin also significantly reduced the body fat content of dFoxO-deficient flies, but not of control flies. (B') The weight of the flies showed no significant differences, except for dFoxO-deficient flies after 11 days of Bleomycin treatment. n = 6-10, control = w^{1118}, DSS = Dextran Sulfate Sodium, *p < 0.05, ***p < 0.001, ****p < 0.0001. Box and whiskers represent mean and 10 – 90 percentile.

3.5.5. Number of eggs in ovaries of DSS-treated dFoxO-deficient flies

Ovaries of flies were dissected after 5 and 8 days of DSS treatment and eggs were counted manually. After 5 days, DSS treated control flies had significantly less eggs in their ovaries than dFoxO-deficient flies. Compared to the control treatment, ovaries of both groups contained significantly less eggs than their respective control treatment. Between both control treatment groups, no differences were observable (Fig 3.48 A). After 8 days, the difference between DSS treated controls and dFoxO-deficient flies is even stronger. In the

control treatment, dFoxO-deficient flies also had more eggs in their ovaries compared to the genetic control (Fig 3.48 B).

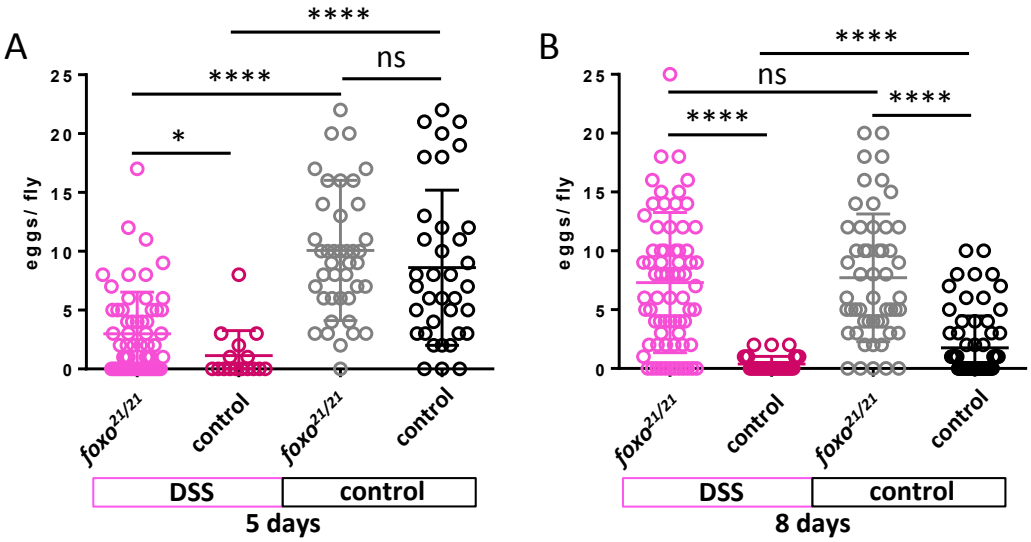

Fig. 3.48: Number of eggs in dissected ovaries of DSS-treated *Drosophila*. (A) After 5 days of treatment, ovaries of dFoxO-deficient and control flies were dissected and the number of eggs was counted. A treatment with DSS resulted in a reduced number of eggs in ovaries of dFoxO-deficient and control flies, but with a stronger effect in control flies. When fed with sucrose only (control), the number of eggs in both groups is not significantly different. (B) After 8 days, the differences between dFoxO-deficient and control flies are even stronger in both DSS and control treatments. DSS = Dextran Sulfate Sodium, n = 16-72, control = w^{1118}, *p < 0.05, ****p < 0.0001. Error bars are represented as mean ± SD.

3.5.6. Changes in gene expression upon treatment with DSS and Bleomycin

3.5.6.1 dFoxo-deficiency

The influence of DSS and Bleomycin on the expression of several genes in the gut of dFoxO-deficient and control flies was tested after 5 days of treatment at 25°C. To reveal an effect of the damaging substances on the cell composition in the gut, the expression of two cell marker genes was measured. *Prospero*, specifically marking enteroendocrine cells and *delta*, a specific intestinal stem cell marker was tested. In control treatment flies (Fig 3.49 A, black and grey bars) and Bleomycin treated flies (blue bars), no significant changes in *prospero* expression were detectable. Only control flies treated with DSS showed an upregulation of *prospero*-expression compared to their untreated control and to DSS-treated dFoxO-deficient flies. *Delta*-expression was down regulated in dFoxO-deficient flies of the control treatment group, but significantly up regulated after treatment with DSS. All other effects were not significant (Fig. 3.49 A).

Upd2 expression was strongly downregulated in untreated dFoxO-deficient flies compared to the control. In DSS- and Bleomycin-treated flies, a deficiency of dFoxO also reduced *upd2* expression, but not significantly (Fig. 3.49 B).

Further, the expression of *dfoxo* and sox2-1a was measured. As expected, dFoxO-deficient flies showed a lower expression than controls when sucrose-fed. Also, under DSS and Bleomycin treatment, the level of *dfoxo* expression was not significantly regulated. In control animals however, dfoxo was upregulated in DSS treated flies. The expression of sox2 1a was not significantly influenced in any group (Fig. 3.49 C).

Because of the damaging effect of DSS and Bleomycin on the gut epithelium, the gene expression of junction proteins *disc large 1* (*dlg1*), *kune* and *e-cadherin* (*de-cad*) was measured (Fig 3.49 D). *Dlg1* expression was strongly downregulated in dFoxO-deficient flies of both untreated and DSS-treated flies in comparison to the respective control. For Bleomycin, no significant regulation could be measured. The expression of *kune* was upregulated in all treatment groups compared to the control. *De-cad* was strongly downregulated in sucrose-fed dFoxO-deficient flies. In DSS- and Bleomycin-fed animals, *de-cad* expression was not significantly regulated. Interestingly in control flies, a treatment with DSS caused an upregulation of *de-cad* whereas Bleomycin led to a downregulation.

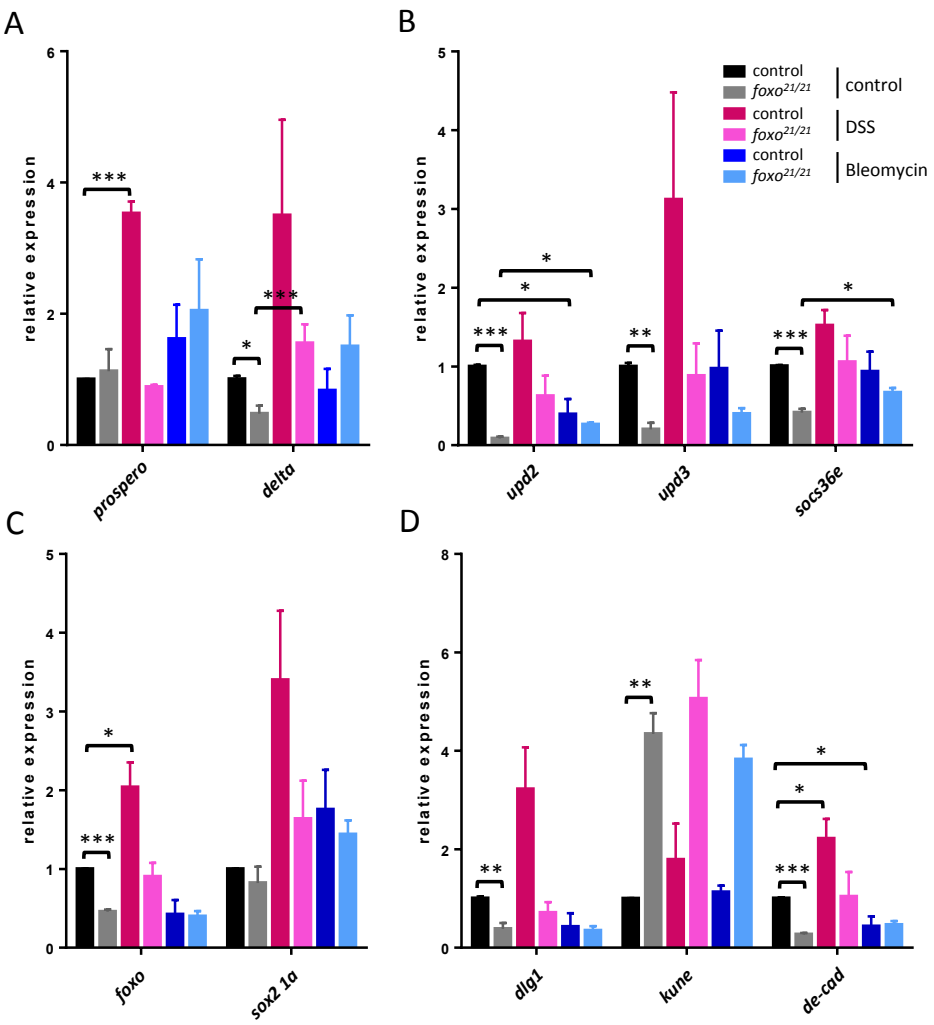

Fig. 3.49: DSS and Bleomycin induced changes in gene expression of dFoxO-deficient flies after 5 days of treatment. (A) The expression of two cell-specific marker genes was measured to reveal differences in the cell composition after treatment. *Prospero*, marking EECs, was significantly upregulated in DSS treated control flies. Expression of the stem cell marker *delta* is downregulated in intestines of dFoxO-deficient flies, but upregulated in DSS-treated dFoxO-deficient flies. (B) *upd2, upd3 and socs36e* are all downregulated in intestines of dFoxO-deficient flies. After treatment with Bleomycin however, *upd2* expression is downregulated in control flies, but upregulated in dFoxO-deficient flies when compared to their sucrose control. In dFoxO-deficient flies, *socs36e* is also downregulated after Bleomycin treatment. (C) *Foxo* expression is downregulated in dFoxO-deficient flies. In intestines of DSS treated control flies, *foxo* is upregulated. *Sox2 1a* is not significantly regulated in any group or treatment. (D) In sucrose fed animals, *dlg1* and *de-cad* expression are downregulated while *kune* is upregulated. Interestingly, in control flies, *e-cadherin* is upregulated after DSS treatment, but downregulated after Bleomycin treatment. DSS = Dextran Sulfate Sodium, n = 3, control = w^{1118}, *p < 0.05, **p < 0.01 ***p < 0.001. Error bars represent means ± SEM.

3.5.6.2 dFoxO-overexpression in enterocytes

In flies overexpressing dFoxO in ECs, the expression of several genes in the gut was also measured after 5 days of treatment with DSS at 29°C. The expression of *prospero*, which marks EECs was significantly downregulated in control flies treated with DSS compared to the sucrose control. Flies with an overexpression of dFoxO in ECs however, showed a significant upregulation of *prospero* expression after treatment with DSS compared to

control flies (Fig. 50 A). The expression of the stem cell marker Delta was upregulated in both fly lines treated with DSS compared to their respective sucrose controls, but these effects were not significant. For the expression of *notch*, the receptor for the ligand Delta of the Notch signaling pathway, the only significant change was detectable in DSS-treated flies overexpressing dFoxO in ECs compared to their sucrose control.

The effect of DSS on the expression of junction proteins *disc large 1* (*dlg1*), *kune* and *e-cadherin* (*de-cad*) was also measured (Fig. 3.50 B). In DSS-treated flies that overexpressed dFoxO in ECs, the expression of *dlg1* and *decad* was significantly upregulated compared to the genetic control treated with DSS as well as their sucrose control. *Kune* expression was only upregulated in DSS-treated overexpression flies compared to control flies.

As expected, the expression of *foxo* was massively upregulated in overexpression flies compared to the genetic control (Fig 3.50 C). The treatment with DSS however, had no effect on *foxo* expression. Interestingly, *upd3* and *socs36e* expression was significantly downregulated in DSS-treated control flies in comparison to the sucrose control, but upregulated in dFoxO overexpression flies that were fed with DSS (Fig 3.50 C).

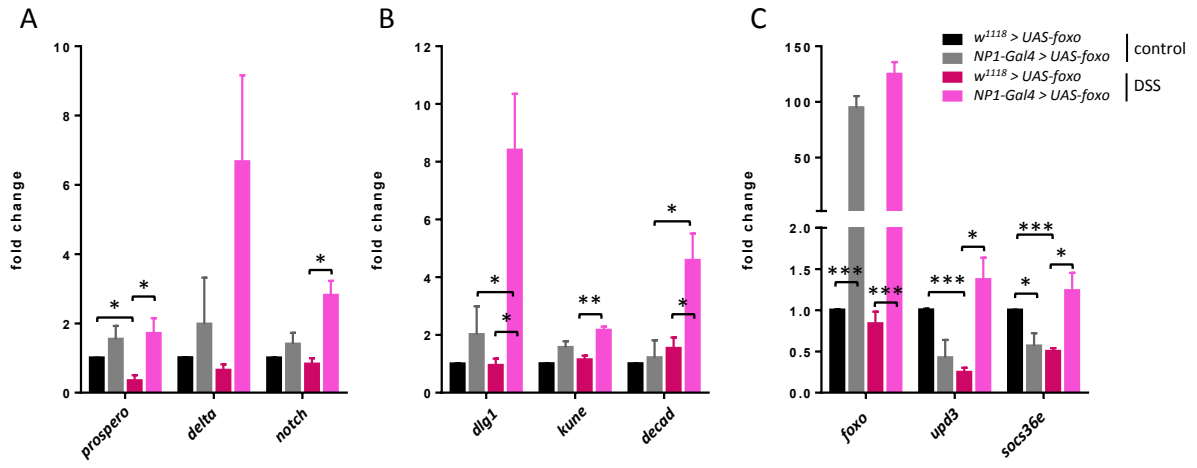

Fig. 3.50: Changes in gene expression of flies overexpressing dFoxO in ECs after 5 days of treatment with DSS and Bleomycin. (A) The expression of three different cell-specific marker genes was measured to show changes in the gut morphology after treatment. *Prospero*, marking EECs, was significantly upregulated in both DSS treated groups. Expression of the stem cell marker *delta* seems to be upregulated after treatment with DSS, but changes are not significant. Notch expression is increased in flies overexpressing dFoxO in ECs compared to control flies after application of DSS. (B) *delta and de-cad* expression is upregulated in dFoxO overexpression flies treated with DSS compared to control flies as well as dFoxO flies fed with sucrose. Kune is also upregulated in overexpression flies in response to DSS treatment. (C) the expression of *foxo* was strongly upregulated as expected in flies overexpressing dFoxO in ECs. The expression of *upd3* and *socs36e* was significantly downregulated in DSS-treated control flies compared to the sucrose control, but upregulated in dFoxO overexpression flies upon DSS treatment. DSS = Dextran Sulfate Sodium, n =3, control = w^{1118}, *p < 0.05, **p < 0.01, ***p < 0.001. Error bars represent means ± SEM.

3.5.7. Effects of DSS and Bleomycin on proliferation

Amcheslavsky et al. showed that the treatment with DSS as well as Bleomycin resulted in an increased proliferation in *Drosophila* (Amcheslavsky et al. 2009). Here, the effect of DSS and Bleomycin on proliferation was examined in flies overexpressing dFoxO in intestinal stem cells (ISCs) and enteroblasts (EBs) with co-expressed GFP enabling microscopic visualization of proliferation in dissected intestines. Additionally, a α-Prospero antibody was used to label enteroendocrine cells (EECs).

In the genetic control (*esg-Gal4; UAS-GFP > UAS-foxo*), the treatment with DSS for 5 days resulted in a massive increase in number of ISCs and EBs (Fig 3.51 B and b). Upon treatment with Bleomycin, proliferation is also increased, but not as strong as with DSS (Fig 3.51 C and c). Remarkably, in flies overexpressing dFoxO in ISCs and EBs, neither DSS nor Bleomycin induces proliferation in the intestine (Fig 3.51 E, e, F and f). The number of EECs showed no significant differences in any group or treatment (Fig 3.51 a'-f' + 3.41).

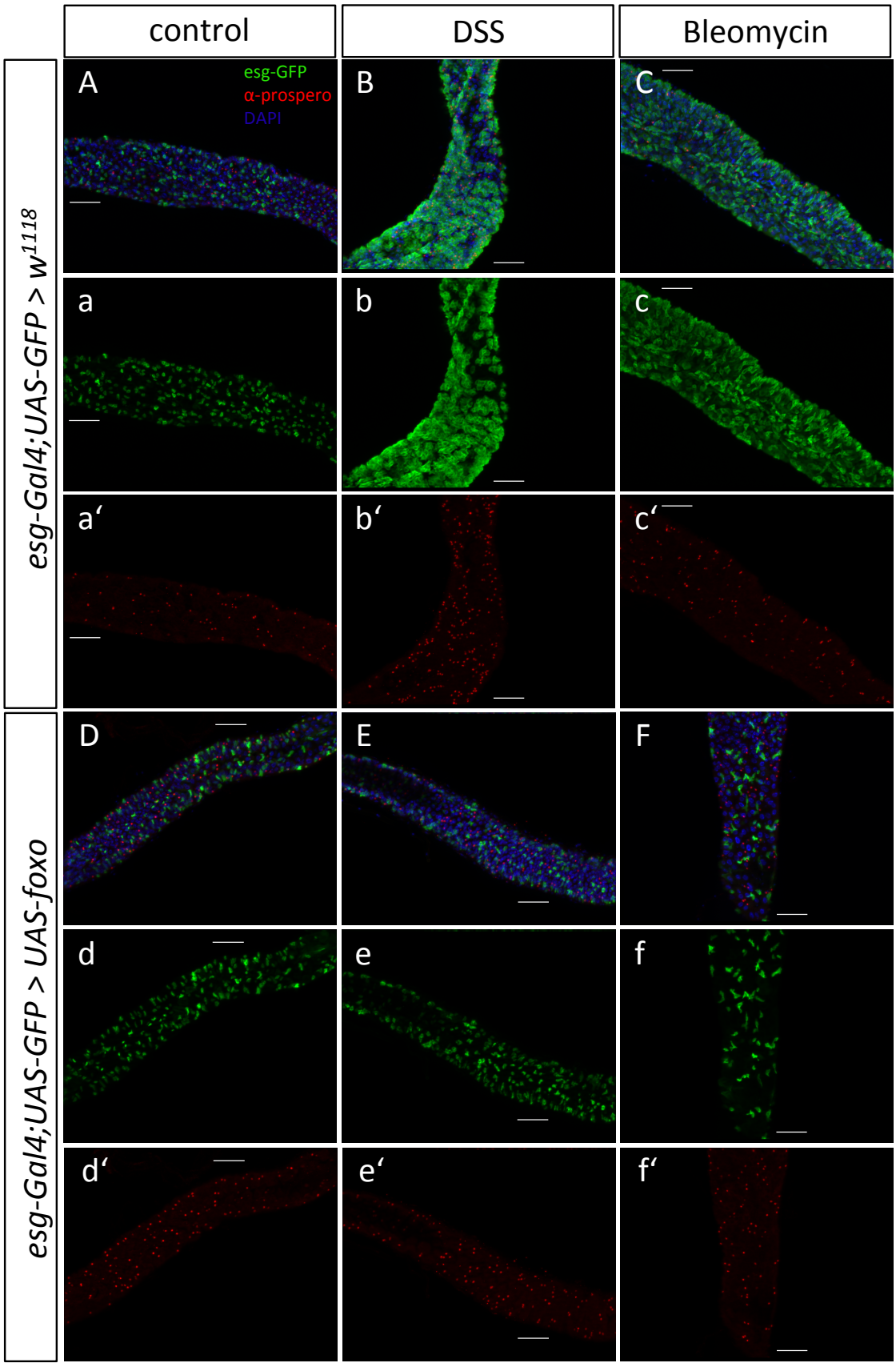

Fig. 3.51 DSS- and Bleomycin induced proliferation in the intestine. (A-c') control, (D-f') dFoxO overexpression in ISCs and EBs. Images show the posterior midgut. (b+c) DSS and Bleomycin massively induced overexpression in control flies. (e-f) Proliferation in guts of dFoxO-overexpressing flies was not influenced. (a'-f') Number of EECs (Prospero^{+} cells) was neither affected by dFoxO expression nor by treatment with DSS or Bleomycin. DSS = Dextran Sulfate Sodium, scale bar = 50 µm.

The number of enteroendocrine cells (EECs) was also measured by counting all prospero^{+} cells in a 100 x 100 µm area in the posterior midgut. Neither the treatment with DSS or Bloemycin nor the level of dFoxO in ISCs and EBs has an effect on the number of EECs (Fig 3.52).

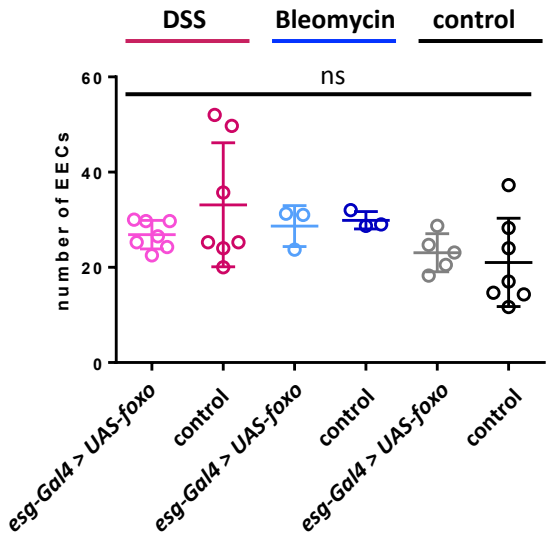

Fig. 3.52 Number of enteroendocrine cells (EECs) upon treatment with DSS and Bleomycin. EECs were labeled using an α-Prospero antibody. Number of prospero^{+} cells was counted in a 100 x 100 µm area in the posterior midgut. Neither the treatment with DSS or Bleomycin nor the expression of dFoxO has a significant effect on the number of EECs (n= 3-7). *esg-Gal4 = esg-Gal4,UAS-GFP;tub-Gal80ts, control = esg-Gal4 = esg-Gal4,UAS-GFP;tub-Gal80ts > w^{1118},* DSS = Dextran Sulfate Sodium, ns = not significant. Represented are means ± SD.

Using a driver line not only inducing the expression of a gene of interest in ISCs and EBs when crossed to a desired UAS-line, but also co-expressing Luciferase (Markstein et al. 2014) the level of proliferation was also quantified with an alternative approach. The luciferase signal was measured after 1, 3, 5 and 7 days of induction and treatment (Fig. 3.53). The genetic control fed with sucrose only showed a relative stabile proliferation rate over time. When treated with Bleomycin, the luciferase signal is increased by approx. 4-fold after just one day of treatment. After 3 days, the signal is increased approx. 8-fold, but decreases slightly after 5 and 7 days of treatment. The treatment with DSS however, drastically increases the proliferation rate. After 3 days, a luciferase signal increased by more than 20-fold could be detected. At day 5 post induction and treatment, the signal reaches a maximum of approx. 40-fold of the basic level. Two days later, the signal is slightly reduced to approx. 30-fold (Fig. 3.53). Flies overexpressing dFoxO in ISCs and EBs show a lower but also stabile basic level of proliferation upon sucrose feeding. The treatment with Bleomycin resulted in a slight increase of the luciferase signal, but is still lower than the untreated genetic control. Feeding with DSS increased the signal by 3-fold after 3 days up to 5-fold

after 7 days. This increased signal however is only slightly higher than the baseline of the control fed only with sucrose (Fig. 3.53).

While in control flies the proliferation rate was drastically affected by DSS and Bleomycin, dFoxo-overexpressing flies showed a much weaker reaction.

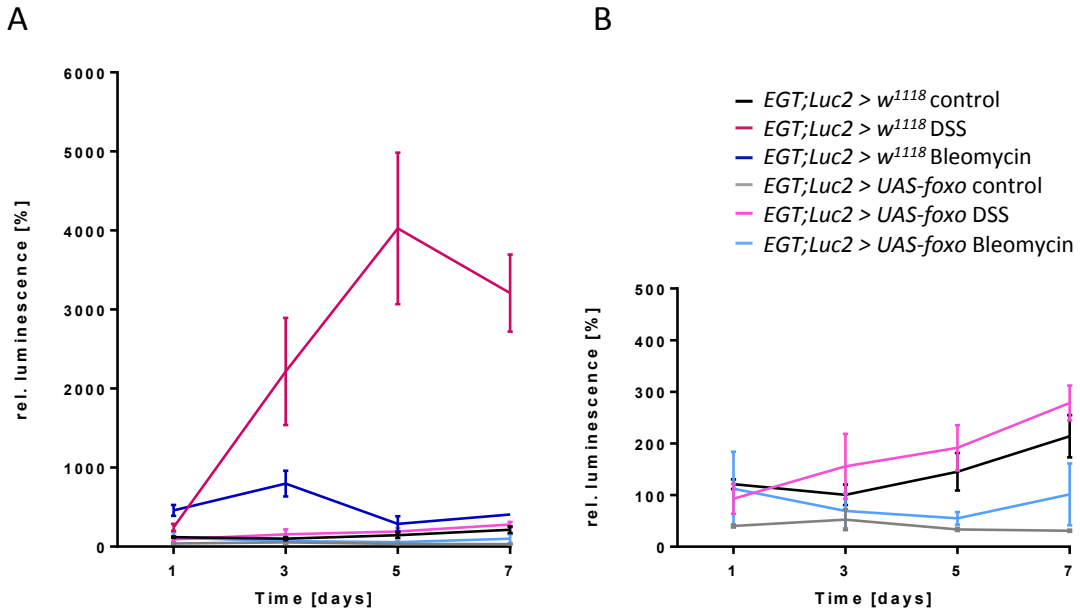

Fig. 3.53: Proliferation upon treatment with DSS and Bleomycin in flies overexpressing dFoxO in ISCs and EBs was measured using co-expressed Luciferase. (A) Treatment with DSS and Bleomycin strongly increased proliferation in control flies (*EGT;Luc2 > w^{1118}*) compared to the sucrose control. (A+B) Treatment with both substances of flies overexpressing dFoxO in ISCs and EBs only had a minor effect on proliferation. Altogether, the level is very similar to the untreated control. n = 5, *EGT;Luc2 = +; p{Esg-Gal4}, p{UAS-GFP}, p{tubulin-Gal80ts}; p{UAS Luciferase at attp2},* DSS = Dextran Sulfate Sodium.

In dFoxO-deficient flies and their controls, proliferation was measured using a phosphorylated-histone 3 (pH3) antibody labeling mitotic active cells. As expected, the treatment with DSS for 7 days caused a significant increase in proliferation in both fly lines, but compared to control flies, dFoxO-deficient flies showed significantly less $pH3^+$ cells. The control treatment with 5 % sucrose was similar in both lines (Fig. 3.54).

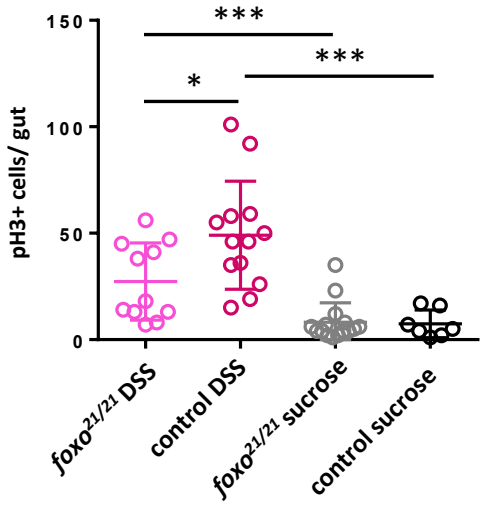

Fig. 3.54: Proliferation of dFoxO-deficient flies after 7 days of treatment with DSS. Treatment with DSS increased number of phosphorylated-histone 3 positive cells (pH3+). Control = yw, n = 7-15, *p < 0.05, ***p < 0.001. Represented are means ± SD.

4. Discussion

The intestine of *Drosophila* consists of an epithelial monolayer made of ISCs that give rise to EBs, which further differentiate into absorptive ECs and secretory EECs. The epithelium is surrounded by visceral muscle, trachea and nerves. It shares functional and structural similarities with the mammalian intestine. Due to its important role in maintaining energy homeostasis, immunity and even influencing the behavior and physiology, the digestive tract and its microbiome recently became of great interest in multiple research fields.

In this study, the effect of the transcription factor dFoxO on the physiology and molecular processes in the digestive tract of *Drosophila* was investigated. Additionally, the role of dFoxO on the response to DSS, which was used as an intestinal stressor, was investigated. For the experiments, a dFoxO-deficient fly line and those overexpressing dFoxO in different cell types of the intestine were used. The native or a constitutive active form of dFoxO was overexpressed in ECs and the native dFoxO was overexpressed in ISCs and EBs.

Surprisingly, in several experiments, the overall deficiency of dFoxO showed the same effect as the overexpression in ECs, whereas the overexpression in ISCs and EBs mainly caused changes into the opposite direction or had no significant effect at all.

4.1. The manipulation of dFoxO expression massively affects physiological functions

A deficiency of dFoxO in the whole fly caused a severe reduction of life span (Fig. 3.1), confirming previous studies with different dFoxO-deficient fly lines (Slack et al. 2011). Interestingly, the overexpression of dFoxO in ECs, both the native and constitutively active form, led to a strong reduction of life span as well (Fig. 3.18, Fig. 3.37 A), although a positive effect of FoxO activity on survival has been described for other organs in *Drosophila*, such as the fat body (Giannakou et al. 2004; Hwangbo et al. 2004) or muscle (Demontis & Perrimon 2010). Additionally, activation of Daf-16, the FoxO homolog in *C. elegans*, has shown to extent the life span (Kenyon et al. 1993; Lin et al. 1997). The survival experiment with flies overexpressing of dFoxO in ISCs and EBs conducted in this study showed an increase in life span compared to the *UAS*-control but no effect compared to the Gal4-control (Fig. 3.38). This contradicts a previous result from Biteau et al. (2010), which indicates a reduced life

span upon overexpression of dFoxO in ISCs and EBs. Apparently, the effect of a manipulation dFoxO on the survival of *Drosophila* is strongly tissue-specific.

The reduction of dFoxO led to a decrease in food intake (Fig. 3.2 A), activity (Fig. 3.4 A+B) and number of excreted fecal spots (Fig. 3.2 B) while the transit time of ingested food through the intestine was prolonged (Fig. 3.2 C). Additionally, the body fat content was reduced in young and even more in older individuals (Fig. 3.3 A), while the body weight was not influenced by either the dFoxO expression or the age of the flies (Fig. 3.3 B). In mice, the deficiency of FoxO1 in specific neurons in the hypothalamus resulted in a reduced food intake and locomotor activity. The body fat was also strongly reduced while the body weight showed no differences to matching controls (Ren et al. 2012). In *C. elegans* however, the food consumption of *daf-16* mutants was increased compared to wild type animals suggesting a role of FoxO on appetite regulation (Wu et al. 2019). Furthermore, dietary restriction, which usually leads to an extension of life span, does not prolong survival of FoxO3- knockout mice (Shimokawa et al. 2015).

Remarkably, the overexpression of dFoxO in enterocytes showed the same effect on the food consumption (Fig. 3.19 A), digestive functions (Fig. 3.19 B+C), body fat content, weight (Fig. 3.20 A+B) and activity (Fig. 3.21 A+B) as the overall deficiency.

The body fat content was massively reduced in young dFoxO overexpressing flies compared to the control (Fig. 3.20 A), possibly due to reduced lipase expression. The transcriptome analysis revealed a downregulation of the lipase *magro* (4.6 fold) and *lipase1* (13.5 fold) (3.2.6). For digestion of nutritional triglycerides, the lipase lipA/magro is expressed in ECs and secreted into the gut lumen (Karpac et al. 2013; Sieber & Thummel 2012). Reduction of dFoxO by RNAi in ECs results in upregulated *lipA/magro* expression and an increased level of triglycerides in the whole fly. An overexpression of dFoxO in ECs on the other hand caused a reduction of *lipA/magro* expression, stored triglycerides and lipid accumulation in the intestine (Karpac et al. 2013). In adipose tissue of mice, FoxO is also known to regulate the transcription of lipases for lipolysis of stored lipids (Chakrabartl & Kandror 2009). The detected reduction of body fat content on flies was even more severe in older flies (Fig. 3.20 A), confirming previous studies in which a decline in lipid metabolism is associated with progressed age (Biteau et al. 2010; Karpac et al. 2013). Studies show that older flies in general express higher levels of dFoxO (Karpac et al. 2013). The genetically induced

overexpression of dFoxO might therefore be further enhanced by the natural increase of dFoxO in aged flies leading to a stronger disruption of lipid metabolism.

Under starvation conditions, the survival of dFoxO-deficient flies is reduced by almost 50 % (Fig. 3.14). FoxO is activated by various stressors and dFoxO-deficient flies are known to be more sensitive to oxidative stress (Jünger et al. 2003). Thus, a deficiency of dFoxO might also be disadvantageous to withstand starvation stress, as it is known in *C. elegans* (Baugh & Sternberg 2006). Interestingly, flies overexpressing dFoxO in ECs are more resistant to starvation stress compared to control flies (Fig. 3.33). This contradicts previous results where the same flies showed a reduced survival compared to control flies (Karpac et al. 2013). However, this might be due to a different experimental set up. Most impressively, flies overexpressing dFoxO in ISCs and EBs lived up to 10 days when starved and with that more than twice as long as controls (Fig. 3.43).

4.2. Changes in dFoxO expression lead to impairment of intestinal integrity

FoxO is involved in the regulation of responses to stress, cell cycle arrest, DNA repair, apoptosis and proliferation and may play an important role in facilitating inflammatory processes (Greer & Brunet 2005). Therefore, dFoxO-deficient flies were examined for changes in gut morphology. The length (Fig. 3.6 A) as well as the brush border structure and the pH-value (Fig. 3.5) of dissected intestines did not show any visible differences in dFoxO-deficient flies compared to controls. Under normal physiological conditions, mice lacking FoxO4 expression also do not display any abnormal structural changes (Zhou et al. 2009). Albeit, the gut integrity was significantly reduced in dFoxO-deficient flies (Fig. 3.6 B, Table 3-1), suggesting an impaired intestinal structure upon dFoxO reduction. Flies overexpressing dFoxO in ECs also displayed a significantly impaired intestinal integrity (Fig. 3.22, Table 3-3). In both cases, the loss of integrity exacerbated with advancing age. In contrast, the overexpression in ISCs and EBs results in less impairment of the intestines (Fig. 3.42, Table 3-5).

In summary, the deficiency of dFoxO as well as the overexpression in ECs has an overall negative effect on the physiology of *Drosophila.* Among others, the survival, the gut functionality, locomotor activity, metabolic functions, starvation resistance and gut integrity are massively impaired. In contrast, the overexpression in ISCs and EBs seems to have a neutral or rather positive effect on these physiological functions.

4.3. An altered dFoxO expression induces transcriptomic changes in the intestine

The transcriptomic analysis of guts dissected from dFoxO-deficient flies showed a downregulation of many genes associated with chorion and egg formation (Fig. 3.10 A and Fig. 3.11). An egg deposition assay confirmed that the fecundity of dFoxO-deficient flies is indeed reduced. The number of laid eggs as well as the proportion that developed further was drastically decreased (Fig. 3.12). In mice, FoxO3-deficient individuals also have a reduced number of progeny. Furthermore, they display abnormal ovarian follicular development (Castrillon et al. 2003). Insulin signaling is also known to affect fecundity in *C. elegans*, where abnormal gonad morphology and smaller brood sizes are observed in *daf2*-mutants (Gems et al. 1998).

In dFoxO-deficient flies as well as those overexpressing dFoxO in ECs, several lysozyme genes were significantly downregulated and a specific lysozyme activity assay confirmed this result in vivo. Interestingly, the lysis assay of dFoxO-deficient flies showed two distinct lysis zones (Fig. 3.13 C), while flies overexpressing dFoxO in ECs only produced one zone of lysis (Fig. 3.32 C). This might be the result the activity of different lysozymes with specific properties. Genes *lys b*, *lys d* and *lys e* are downregulated in both groups, whereas *lys* s is only reduced in dFoxO-deficient flies and *lys x* only in overexpression flies. Originally, lysozymes were studied as part of the defense against pathogens as they are able to break down bacterial cell walls by cleavage of ß-(1,4)-glycosidic bonds in the peptidoglycan layer (Jolles & Jolles 1984). Later, it became evident that several lysozyme genes (*lysb*, *c*, *d*, *e*, *s* and *x*) are expressed mainly in the digestive tract of *Drosophila* adults and larvae, where they most likely play an important role in digesting bacteria as a food source. These lysozymes are not induced by bacteria and therefore not involved in the immune response (Daffre et al. 1994). A downregulation of lysozymes in the intestines of dFoxO-deficient and overexpression flies (Fig. 3.13, Fig. 3.32, Tab. 3-2, Tab 3-4) may therefore be a disadvantage in terms of nutrition sustenance, which results in negative effects on the physiology such as a reduced life span (Fig. 3.1, Fig. 3.18).

The transcriptomic data from intestines of dFoxO-deficient flies were compared to the transcriptome of larval trachea of the same genotype. Additionally, the intestinal transcriptome of flies overexpressing dFoxO in ECs was compared to larvae overexpressing dFoxO in trachea. As a major result of this comparison mainly tissue specific regulation of

gene expression was identified. This means that overlaps in the cohorts of differentially transcribed genes between trachea and intestines subjected to identical genetic manipulations was surprisingly small (Fig. 3.31). This tissue specificity was also found for muscle and fat body of dFoxO-deficient flies in response to starvation (Teleman et al. 2008).

4.4. The manipulation of dFoxO expression affects the response to intestinal stressors

Dextran sulfate sodium (DSS) is commonly used to induce colitis in mice as a model to study inflammatory bowel diseases (IBDs) such as Crohn's disease (CD) or ulcerative colitis (UC). In *Drosophila*, the oral application of DSS causes a reduction of life span, an increase in stem cell proliferation and a disruption of the membrane organization (Amcheslavsky et al. 2009). Stress stimuli such as oxidative stress, heat shock, UV radiation (Brunet et al. 2004) and metabolic stress (Brunet & Webb 2014) are known to regulate FoxO activity. A *UAS-foxo-gfp* reporter expressed in ECs showed that dFoxO is also activated by DSS-induced stress. In flies treated with sucrose, dFoxO remains in the cytoplasm (Fig. 3.44 D-F), while the treatment with DSS caused the translocation into the nucleus (Fig. 3.44 A-C), implying that this treatment induces, at least in part, a dFoxO-dependent response.

As expected, the treatment with DSS massively reduced the survival compared to the sucrose-fed control (Fig. 3.45 A'). Surprisingly, dFoxO-deficient flies lived longer than controls when treated with DSS, although their survival was drastically reduced in the control treatment (Fig. 3.45 A+A'). Interestingly, *FoxO4*-null mice were more sensitive to trinitrobenzene sulfonic acid- (TNBS-) induced colitis and showed a reduced survival compared to wild type mice (Zhou et al. 2009). Furthermore, the number of eggs in dissected ovaries was reduced upon treatment with DSS. Studies in women suffering from IBD indicate that active CD may reduce fertility (Woude et al. 2015). The decrease in number of eggs in the ovaries was significantly stronger in control flies (Fig. 3.48), although on normal medium, the fecundity of control flies is much higher compared to dFoxO-deficient flies. Apparently, despite of the negative impact on most physiological aspects (3.1), under the DSS stress, the deficiency of dFoxO has a beneficial effect on the fitness of *Drosophila.* Currently, no obvious explanation for this phenotype is apparent.

The investigation of the weight and body fat content revealed that the treatment with DSS resulted in a massive reduction of body fat in dFoxO-deficient as well as in control flies (Fig.

3.47 A). Interestingly, the reduction is more severe in control flies, also indicating a beneficial role of reduced dFoxO expression. Astonishingly, the weight was neither influenced by treatment or dFoxO expression (Fig. 3.47 A'), although mice had a reduced body weight upon oral application of DSS (Poritz et al. 2007). The control treatment with sucrose confirms nicely the reduced body fat content of dFoxO-deficient flies on NM (Fig. 3.3 B). Taken together, the lack of dFoxO might be associated with a reduced, presumably detrimental activity seen normally in response to DSS.

To check for changes in proliferation in response to DSS stress, the number of mitotic cells was determined using a phosphorylated-histone 3 (pH3) antibody. The number of pH3-positive cells was significantly increased upon DSS treatment (Fig. 3.54). This confirms previous results were the epithelial damage caused by DSS induced proliferation to ensure tissue repair (Amcheslavsky et al. 2009). However, in dFoxO-deficient flies, the increase of mitotic active stem cells was only half as strong (Fig. 3.54). Flies overexpressing dFoxO in ISCs and EBs lived significantly longer compared to both controls upon treatment with DSS (Fig. 3.45 C). Additionally, the co-expressed GFP and luciferase revealed a massive increase in proliferation after DSS-treatment in the control animals (Fig. 3.51 B+b and Fig. 3.53 A). The flies overexpressing dFoxO in ISCs and EBs in contrast only show a minimal increase in proliferation upon DSS-treatment (Fig. 3.51 E+e and Fig. 3.53 A+B). These findings complement previous studies which revealed that a mild ubiquitous overexpression of a constitutively active form of dFoxO as well as the mutation of the insulin receptor (InR) reduces proliferation while the expression of a constitutively active InR in ISCs and EBs results in ISC proliferation (Amcheslavsky et al. 2009). Although proliferation is necessary to repair damages induced by agents such as DSS, an overproliferation may cause dysplasia and therefore may have a rather negative effect (Biteau et al. 2010). The number of enteroendocrine cells was not affected by either treatment with DSS or the overexpression of dFoxO in ISCs and EBs, suggesting that increased proliferation mainly replaces damaged ECs to ensure tissue repair. However, previous studies showed that EBs indeed accumulate in DSS-stressed intestines, but due to the damaged basement membrane, signaling system required to induce differentiation might be impaired (Amcheslavsky et al. 2009).

In order to investigate the effect of DSS on genes expression, qPCR was performed. Among others, the expression of the stem cell marker *delta* was regulated in response to DSS. It showed an upregulation in DSS-treated flies, which was about twice as high in control flies

compared to dFoxO-deficient flies (Fig. 3.49 A). This corresponds well to the result of the assessment of pH3-positive cells (Fig. 3.54), as it also indicates a more pronouced increase in proliferation in control flies in response to DSS.

Noteworthy, the expression of genes coding for junction proteins *disc large 1* (*dlg1*), *kune* and *e-cadherin* (*de-cad*) was effected by the level of dFoxO expression rather than by the treatment with DSS. While *dlg1* and *decad* expression are significantly decreased in dFoxO-deficient flies, *kune* expression is upregulated (Fig. 3.49 D). Evidently, the tissue-damaging property is not affecting the cell junctions, as in mice (Poritz et al. 2007), but restricted to the disruption of the basement membrane as described by Amcheslavsky et al. (2009).

Flies overexpressing native dFoxO or the constitutive active form in ECs showed a reduced survival compared to controls upon treatment with DSS (Fig. 3.45 B+D). When fed with just sucrose, the survival was decreased as well, suggesting that the overexpression of dFoxO in ECs has not a strong effect on the response to DSS. Nonetheless, the influence on the expression of several genes was investigated in guts dissected from flies overexpressing native dFoxO. Most of the tested genes were not influenced upon control treatment with sucrose, but the experiment confirmed a massive overexpression of *foxo* of approx. 100-fold (Fig. 3.50 C). Interestingly, all investigated genes were upregulated in flies overexpressing dFoxO in ECs after DSS treatment, although some not significantly.

In summary, the treatment with DSS had negative effects on *Drosophila* as expected from previous studies. The deficiency of dFoxO as well as the overexpression in ISCs and EBs had a beneficial impact on the survival, possibly due to inhibition of overproliferation and consequential dysplasia. The overexpression of dFoxO in ECs in contrast seems not to influence the response to DSS.

Bleomycin, an anticancer drug that is often used in experiments due to its DNA-damaging property, was orally applied to induce intestinal impairment. It reduces the survival in a dose-dependent manner and specifically damages enterocytes upon ingestion (Amcheslavsky et al. 2009). The treatment of dFoxO-deficient flies and those overexpressing dFoxO either in ECs or ISCs and EBs also resulted in a strongly reduced life span compared to sucrose fed controls (Fig. 3.46). However, the manipulation of dFoxO had no specific effect in response to Bleomycin. The weight of dFoxO-deficient and control flies upon treatment with Bleomycin showed almost no significant changes. In control flies, the application of Bleomycin had no effect, but dFoxO-deficient flies contained significantly less fat than

controls. So in contrast to DSS, where a reduced dFoxO expression seems to be beneficial for fly fitness, it doesn't provide any advantages in response to Bleomycin.

4.5. Changes in the expression of dFoxO result in intestinal dysbiosis

An intact intestinal microbiome and epithelial integrity are important for maintaining a healthy organism. Thus, a deregulation of the microbiota may result in chronic inflammatory diseases such as IBD (Clemente et al. 2012). In return, bacteria are able to induce proliferation and tissue regeneration (Buchon et al. 2009b; Broderick et al. 2014) and even host behavior. In African turquoise killifish, the transfer of the intestinal microbiota of young individuals to middle aged animals improved the spontaneous exploratory behavior, which usually decreases with age (Smith et al. 2017). Furthermore, extensive research showed a connection of autism to the gut microbiome (Mulle et al. 2013). For example, bacterial diversity is increased in fecal samples of autistic children compared to healthy controls (Finegold et al. 2010). The microbiota also improves the protection from fungal infection (Fraune et al. 2014). In humans, the microbiota is occasionally even described as "the forgotten organ" as it has a major influence on the health (O'Hara & Shanahan 2006). Due to its ability to regulate the expression of antimicrobial peptides (AMPs) (Becker et al. 2010; Boehm et al. 2012; Fink et al. 2016), FoxO is assumed to play an essential role in maintaining a stable microbiota (Mortzfeld et al. 2018).

Fecal analysis at different time points after recolonization of germfree embryos with a defined bacterial mix containing five commensal *Drosophila* gut bacteria revealed that dFoxO expression levels as well as the individual age has an effect on the intestinal microbiota. While microbial compositions of young individuals of both, dFoxO-deficient flies (Fig. 3.16 A) and those overexpressing dFoxO in ECs (Fig. 3.35 A), do not differ significantly from their controls, older flies with manipulated dFoxO expression seem to develop a dysbiosis with age (Fig. 3.16 B, Fig. 3.35 B). In the freshwater polyp *Hydra*, a deficiency in FoxO signaling resulted in an impairment of AMP expression. Additionally, these animals were more vulnerable to foreign non-commensal bacteria as their ability to select for bacteria of their native microbiota is impaired (Mortzfeld et al. 2018). The same seems to be true for dFoxO-deficient *Drosophila*, which also show a higher percentage of contamination than control flies (Fig. 3.15). In response to oral infection with *Serratia marcescens*, the expression of several AMPs increase whereas dFoxO-deficient flies do not show any change

in AMP expression levels (Fink et al. 2016). The transcriptomic analysis of dissected guts from flies overexpressing dFoxO in ECs revealed an upregulation of the genes for AMPs *drosomycin* (3.7-fold), *attacin* (4-fold) and *metchnikowin* (3.8-fold). In dFoxO-deficient flies, *drosomycin* is 29-fold downregulated. Both, the up- and downregulation of AMPs is likely to influence the gut microbiota. Additionally, the expression of several *lysozymes*, that are known to digest bacteria by cleaving ß-(1,4)-glycosidic bonds in the peptidoglycan layer (Jolles and Jolles 1984; Daffre et al. 1994) are downregulated in both groups (Fig. 3.11, Fig. 3.27). Due to the reduced lytic activity (Fig. 3.13, Fig. 3.32, Table 3-2, Table 3-4), the intestinal microbiota might be affected. However, since lysozymes nonspecifically cleave ß-(1,4)-glycosidic bonds of all bacteria, the bacterial load is likely to be reduced, but the microbial composition might not be influenced as much.

Interestingly, in dFoxO-deficient as well as in controls, the percentage of contaminations is high in young populations. Older dFoxO-deficient flies retain a high proportion of contaminations. Control flies seem to stabilize a healthy microbiota with age (Fig. 3.15), possibly by inducing AMP release to dispose of unfavorable bacteria. However, multidimensional scaling revealed no significant differences of either dFoxO-deficient or control flies Fig. 3.17). This seem to contradict the previous findings that associate aging with dysbiosis as a result of a decline in immune functions (Buchon et al. 2009b; Clark et al. 2015; Li et al. 2016). However, the age of 30 days was chosen based on the life span of dFoxO-deficient flies. At the age of 30 days, approx. 70 percent had already died, while control flies have a medium life span of 49 days and are still relatively young. A dysbiosis of the intestinal microbiota often results in a reduction of live span (Buchon et al. 2013a, Guo et al. 2014; Clark et al. 2015). This may account for the reduced life span of dFoxO-deficient flies (Fig. 3.1) as well as those overexpressing dFoxO in ECs (Fig. 3.18). The pH-value also plays an important role in shaping the microbiota (Overend et al. 2016; Li et al. 2016), but at least in dFoxO-deficient flies, the pH-value of the intestine does not differ from that of control flies (Fig. 3.5 C+D).

In summary, after recolonization of germfree embryos, the fecal microbiota in young dFoxO-deficient flies and those overexpressing dFoxO in ECs did not differ significantly from their matching controls. With progressing age, the microbial composition of flies with a manipulated dFoxO expression diverged from their controls resulting in a dysbiosis in older

populations. Indeed, dFoxO expression seems to have an impact on the intestinal microbiota of *Drosophila*.

4.6. Conclusions and future perspectives

The manipulation of dFoxO expression had a strong influence on several molecular and physiological functions in *Drosophila*. Interestingly, the deficiency of dFoxO in the whole fly and the overexpression in ECs had similar effects on various parameters such as survival, digestive functions, metabolism, activity and intestinal integrity. In contrast, the overexpression of dFoxO in ISCs and EBs was mostly beneficial or neutral with regard to the fly's fitness. To elucidate how dFoxO expression in these cells affects the physiology of *Drosophila,* a cell specific analysis using fluorescence-activated cell sorting (FACS) based on the co-expressed GFP should be performed. The analysis of extracted cells on a transcriptional level might reveal genes or gene clusters regulated by dFoxO expression. Because the dFoxO-deficiency affected the whole fly, a knockdown of dFoxO in ECs or ISCs and EBs via RNAi is necessary to investigate tissue specific effects in response to reduced dFoxO expression and to compare results to the overexpression.

Since FoxO is regulated by stress stimuli, flies were treated with DSS, a substance known to induce colitis in mice (Okayasu et al. 1990; Kitajima et al. 2000). In *Drosophila*, DSS causes a reduction of live span, an increase in proliferation and disruption of the basement membrane (Amcheslavsky et al. 2009). Surprisingly, when treated with DSS, dFoxO-deficient flies lived longer than control flies, although the survival under control conditions is massively reduced. Moreover, in dFoxO-deficient flies, the application of DSS resulted in less proliferation, which seems to be beneficial. Flies overexpressing dFoxO in ISCs and EBs showed a similar response to DSS. To assess the effect of dFoxO on the basement membrane structure in response to DSS, a fly line co-expressing a collagenIV-GFP reporter construct and an inducible dFoxO overexpression or knockdown could be useful.

The analysis of the fecal microbial composition revealed a dysbiosis in flies overexpressing dFoxO in ECs. Besides, the microbiota of dFoxO-deficient flies seems to be shifted as well. However, to provide convincing evidence, more samples should be tested. Furthermore, the analysis of microbial compositions of dissected intestines could complement fecal samples.

5. References

Adams, M.D., Celniker, S.E., Holt, R.A., Evans, C.A., Gocayne, J.D., Amanatides, P.G., Scherer, S.E., Li, P.W., et al., 2000. The Genome Sequence of Drosophila melanogaster. *Science*, 287(5461), p.2185 LP-2195.

Amcheslavsky, A., Jiang, J. & Ip, Y.T., 2009. Tissue Damage-Induced Intestinal Stem Cell Division in Drosophila. *Cell Stem Cell*, 4(1), pp.49–61.

Anderson, M.J., Viars, C.S., Czekay, S., Cavenee, W.K. & Arden, K.C., 1998. Cloning and characterization of three human forkhead genes that comprise an FKHR-like gene subfamily. *Genomics*, 47(2), pp.187–199.

Antonello, Z.A., Reiff, T., Ballesta-Illan, E. & Dominguez, M., 2015. Robust intestinal homeostasis relies on cellular plasticity in enteroblasts mediated by miR-8-Escargot switch. *The EMBO Journal*, 34(15), pp.2025–2041.

Apidianakis, Y., Pitsouli, C., Perrimon, N. & Rahme, L., 2009. Synergy between bacterial infection and genetic predisposition in intestinal dysplasia. *Proceedings of the National Academy of Sciences*, 106(49), pp.20883–20888.

Arum, O., Bonkowski, M.S., Rocha, J.S. & Bartke, A., 2009. The growth hormone receptor gene-disrupted mouse fails to respond to an intermittent fasting diet. *Aging cell*, 8(6), pp.756–760.

Asada, S., Daitoku, H., Matsuzaki, H., Saito, T., Sudo, T., Mukai, H., Iwashita, S., Kako, K., Kishi, T., Kasuya, Y. & Fukamizu, A., 2006. Mitogen-activated protein kinases, Erk and p38, phosphorylate and regulate Foxo1. *Cellular Signalling*, 19(3), pp.519–527.

Bakula, M., 1969. The Persistence of a Microbial Flora during Postembryogenesis of Drosophila melanogaster. *Journal of Invertebrate Pathology*, 14, pp.365–374.

Baugh, L.R. & Sternberg, P.W., 2006. Report DAF-16 / FOXO Regulates Transcription of cki-1 / Cip / Kip and Repression of lin-4 during C . elegans L1 Arrest. *Curr Biol.*, 16(8), pp.780–785.

Becker, T., Loch, G., Beyer, M., Zinke, I., Aschenbrenner, A.C., Carrera, P., Inhester, T., Schultze, J.L. & Hoch, M., 2010. FOXO-dependent regulation of innate immune homeostasis. *Nature*, 463(7279), pp.369–73.

Biggs, W.H., Meisenhelder, J., Hunter, T., Cavenee, W.K. & Arden, K.C., 1999. Protein kinase B/Akt-mediated phosphorylation promotes nuclear exclusion of the winged helix transcription factor FKHR1. *Proceedings of the National Academy of Sciences of the United States of America*, 96(13), pp.7421–6.

Biteau, B., Karpac, J., Supoyo, S., DeGennaro, M., Lehmann, R. & Jasper, H., 2010. Lifespan extension by preserving proliferative homeostasis in Drosophila. *PLoS Genetics*, 6(10), pp.1–15.

Biteau, B., Hochmuth, C.E. & Jasper, H., 2008. JNK Activity in Somatic Stem Cells Causes Loss of Tissue Homeostasis in the Aging Drosophila Gut. *Cell Stem Cell*, 3(4), pp.442–455.

Boehm, A.-M., Khalturin, K., Anton-Erxleben, F., Hemmrich, G., Klostermeier, U.C., Lopez-Quintero, J.A., Oberg, H.-H., Puchert, M., Rosenstiel, P., Wittlieb, J. & Bosch, T.C.G., 2012. FoxO is a critical regulator of stem cell maintenance in immortal Hydra. *Proceedings of the National Academy of Sciences of the United States of America*, 109(48), pp.19697–702.

Brand, A.H. & Perrimon, N., 1993. Targeted gene expression as a means of altering cell fates and generating dominant phenotypes. *Development (Cambridge, England)*, 118(2), pp.401–15.

Broderick, N.A., Buchon, N. & Lemaitre, B., 2014. Microbiota-Induced Changes in Drosophila melanogaster Host

Gene Expression and Gut Morphology. *mBio*, 5(3), pp.1–13.

Broderick, N.A. & Lemaitre, B., 2012. Gut-associated microbes of Drosophila melanogaster. *Landes Bioscience*, 3(4), pp.307–321.

Brunet, A., Kanai, F., Stehn, J., Xu, J., Sarbassova, D., Frangioni, J. V., Dalal, S.N., Decaprio, J.A., Greenberg, M.E. & Yaffe, M.B., 2002. 14-3-3 Transits To the Nucleus and Participates in Dynamic Nucleocytoplasmic Transport. *Journal of Cell Biology*, 156(5), pp.817–828.

Brunet, A., Bonni, A., Zigmond, M.J., Lin, M.Z., Juo, P., Hu, L.S., Anderson, M.J., Arden, K.C., Blenis, J. & Greenberg, M.E., 1999. Akt Promotes Cell Survival by Phosphorylating and Inhibiting a Forkhead Transcription Factor. *Cell*, 96, pp.857–868.

Brunet, A., Park, J., Tran, H., Hu, L.S., Hemmings, B.A. & Greenberg, M.E., 2002. Protein Kinase SGK Mediates Survival Signals by Phosphorylating the Forkhead Transcription Factor FKHRL1 (FOXO3a). *Molecular and Cellular Biology*, 21(3), pp.952–965.

Brunet, A., Sweeney, L.B., Sturgill, J.F., Chua, K.F., Greer, P.L., Lin, Y., Tran, H., Ross, S.E., et al., 2004. Stress-Dependent Regulation of FOXO Transcription Factors by the SIRT1 Deacetylase. *Science*, 303(5666), p.2011 LP-2015.

Brunet, A. & Webb, A., 2015. FOXO transcription factors: key regulators of cellular quality control. *Trends in biochemical sciences*, 39(4), pp.159–169.

Buchon, N., Broderick, N.A., Poidevin, M., Pradervand, S. & Lemaitre, B., 2009. Drosophila Intestinal Response to Bacterial Infection: Activation of Host Defense and Stem Cell Proliferation. *Cell Host and Microbe*, 5(2), pp.200–211.

Buchon, N., Broderick, N.A., Chakrabarti, S. & Lemaitre, B., 2009. Invasive and indigenous microbiota impact intestinal stem cell activity through multiple pathways in Drosophila. *Genes & development*, 23(19), pp.2333–2344.

Buchon, N., Osman, D., David, F.P.A., Yu Fang, H., Boquete, J.P., Deplancke, B. & Lemaitre, B., 2013. Morphological and Molecular Characterization of Adult Midgut Compartmentalization in Drosophila. *Cell Reports*, 3(5), pp.1725–1738.

Buchon, N., Broderick, N.A. & Lemaitre, B., 2013. Gut homeostasis in a microbial world: insights from Drosophila melanogaster. *Nature reviews. Microbiology*, 11(9), pp.615–26.

Buchon, N., Silverman, N. & Cherry, S., 2014. Immunity in Drosophila melanogaster — from microbial recognition to whole-organism physiology. *Nature Reviews Immunology*, 14(12), pp.796–810.

Calnan, D.R., Webb, A.E., White, J.L., Stowe, T.R., Goswami, T., Shi, X., Espejo, A., Bedford, M.T., Gozani, O., Gygi, S.P. & Brunet, A., 2012. Methylation by Set9 modulates FoxO3 stability and transcriptional activity. *Aging*, 4(7), pp.462–479.

Calnan, D.R. & Brunet, A., 2008. The FoxO code. *Oncogene*, 27(16), pp.2276–2288.

Caporaso, J.G., Kuczynski, J., Stombaugh, J., William, A.W., González, A. & Knight, R., 2011. Using QIIME to analyze 16S rRNA gene sequences from microbial communities. *Curr Protoc Bioinformatics*, (December), p.10.7.1-10.7.20.

Carter, M.E. & Brunet, A., 2007. Quick guide FOXO transcription factors. *Current Biology*, 17(4), pp.113–114.

Casali, A. & Batlle, E., 2009. Intestinal Stem Cells in Mammals and Drosophila. *Cell Stem Cell*, 4(2), pp.124–127.

Castrillon, D.H., Miao, L., Kollipara, R., Horner, J.W. & DePinho, R.A., 2003. Suppression of Ovarian Follicle Activation in Mice by the Transcription Factor Foxo3a. *Science*, 301(5630), pp.215–219.

Chakrabartl, P. & Kandror, K. V., 2009. FoxO1 Controls Insulin-dependent Adipose Triglyceride Lipase (ATGL) Expression and Lipolysis in Adipocytes. *Journal of Biological Chemistry*, 284(20), pp.13296–13300.

Chandler, J.A., Lang, J., Bhatnagar, S., Eisen, J.A. & Kopp, A., 2011. Bacterial communities of diverse Drosophila species: Ecological context of a host-microbe model system. *PLoS Genetics*, 7(9), p.e1002272.

Chassaing, B., Aitken, J.D., Malleshappa, M. & Vijay-Kumar, M., 2014. Dextran sulfate sodium (DSS)-induced colitis in mice. *Current Protocols in Immunology*, (SUPPL.104), p.15.25.1-15.25.14.

Christensen, K., Johnson, T.E. & Vaupel, J.W., 2006. The quest for genetic determinants of human longevity: challenges and insights. *Nature Reviews Genetics*, 7(6), pp.436–448.

Clark, R.I., Salazar, A., Yamada, R., Fitz-Gibbon, S., Morselli, M., Alcaraz, J., Rana, A., Rera, M., Pellegrini, M., William, J.W. & Walker, D.W., 2015. Distinct Shifts in Microbiota Composition during Drosophila Aging Impair Intestinal Function and Drive Mortality. *Cell Reports*, 12(10), pp.1656–1667.

Clemente, J.C., Ursell, L.K., Parfrey, L.W. & Knight, R., 2012. Review The Impact of the Gut Microbiota on Human Health : An Integrative View. *Cell*, 148(6), pp.1258–1270.

Cox, C.R. & Gilmore, M.S., 2007. Native microbial colonization of Drosophila melanogaster and its use as a model of Enterococcus faecalis pathogenesis. *Infection and Immunity*, 75(4), pp.1565–1576.

Daffre, S., Kylsten, P., Samakovlis, C. & Hultmark, D., 1994. The lysozyme locus in Drosophila melanogaster : an expanded gene family adapted for expression in the digestive tract. *Molecular Genetics and Genomics*, 242(2), pp.152–162.

Dato, S., Rose, G., Crocco, P., Monti, D., Garagnani, P., Franceschi, C. & Passarino, G., 2017. The genetics of human longevity: an intricacy of genes, environment, culture and microbiome. *Mechanisms of Ageing and Development*, 165, pp.147–155.

Davis, M.M. & Engström, Y., 2012. Immune Response in the Barrier Epithelia : Lessons from the Fruit Fly Drosophila melanogaster. *Journal of innate immunity*, 4(3), pp.273–283.

Demerec, M., 1950. *Biology of Drosophila. John Wiley & Sons, Inc, New York.*,

Demontis, F. & Perrimon, N., 2010. FOXO/4E-BP signaling in Drosophila muscles regulates organism-wide proteostasis during aging. *Cell*, 143(5), pp.813–825.

Dijkers, P.F., Medema, R.H., Pals, C., Banerji, L., Thomas, N.S.B., Lam, E.W.-F., Burgering, B.M.T., Raaijmakers, J.A.M., Lammers, J.-W.J., Koenderman, L. & Coffer, P.J., 2002. Forkhead Transcription Factor FKHR-L1 Modulates Cytokine-Dependent Transcriptional Regulation of p27KIP1. *Molecular and Cellular Biology*, 20(24), pp.9138–9148.

Essers, M.A.G., Weijzen, S., De Vries-Smits, A.M.M., Saarloos, I., De Ruiter, N.D., Bos, J.L. & Burgering, B.M.T., 2004. FOXO transcription factor activation by oxidative stress mediated by the small GTPase Ral and JNK. *EMBO Journal*, 23(24), pp.4802–4812.

Finegold, S.M., Dowd, S.E., Gontcharova, V., Liu, C., Henley, K.E., Wolcott, R.D., Youn, E., Summanen, P.H., et al., 2010. Anaerobe Pyrosequencing study of fecal micro flora of autistic and control children. *Anaerobe*, 16, pp.444–453.

Fink, C., Hoffmann, J., Knop, M., Li, Y., Isermann, K. & Roeder, T., 2016. Intestinal FoxO signaling is required to

survive oral infection in Drosophila. *Mucosal Immunology*, 9(4), pp.927–936.

Flachsbart, F., Caliebe, A., Kleindorp, R., Blaché, H., von Eller-Eberstein, H., Nikolaus, S., Schreiber, S. & Nebel, A., 2009. Association of FOXO3A variation with human longevity confirmed in German centenarians. *Proceedings of the National Academy of Sciences*, 106(8), pp.2700–2705.

Fraune, S., Anton-Erxleben, F., Augustin, R., Franzenburg, S., Knop, M., Schröder, K., Willoweit-Ohl, D. & Bosch, T.C., 2014. Bacteria-bacteria interactions within the microbiota of the ancestral metazoan Hydra contribute to fungal resistance. *The ISME journal*, 9(7), pp.1543–1556.

Frescas, D., Valenti, L. & Accili, D., 2005. Nuclear trapping of the forkhead transcription factor FoxO1 via sirt-dependent deacetylation promotes expression of glucogenetic genes. *Journal of Biological Chemistry*, 280(21), pp.20589–20595.

Furuyama, T., Nakazawa, T., Nakano, I. & Mori, N., 2000. Identification of the differntial distribution patters of mRNA and consensus binding sequences for mouse DAF-16 homologues. *Biochemical Journal*, 349, pp.629–634.

Gems, D., Sutton, A.J., Sundermeyer, M.L., Albert, P.S., King, K. V, Edgley, M.L., Larsen, P.L. & Riddle, D.L., 1998. Two Pleiotropic Classes of daf-2 Mutation Affect Larval Arrest , Adult Behavior , Reproduction and Longevity in Caenorhabditis elegans. *Genetics*, 150(1), pp.129–155.

Giannakou, M.E., Goss, M., Jünger, M.A., Hafen, E., Leevers, S.J. & Partridge, L., 2004. Long-lived Drosophila with over-expressed dFOXO in adult fat body. *Science*, 305(5682), p.361.

Greer, E.L., Oskoui, P.R., Banko, M.R., Maniar, J.M., Gygi, M.P., Gygi, S.P. & Brunet, A., 2007. The energy sensor AMP-activated protein kinase directly regulates the mammalian FOXO3 transcription factor. *Journal of Biological Chemistry*, 282(41), pp.30107–30119.

Greer, E.L. & Brunet, A., 2005. FOXO transcription factors at the interface between longevity and tumor suppression. *Oncogene*, 24(50), pp.7410–7425.

Guo, L., Karpac, J., Tran, S.L. & Jasper, H., 2014. PGRP-SC2 promotes gut immune homeostasis to limit commensal dysbiosis and extend lifespan. *Cell*, 156(1–2), pp.109–22.

Guo, Z., Lucchetta, E., Rafel, N. & Ohlstein, B., 2016. Maintenance of the adult Drosophila intestine: all roads lead to homeostasis. *Current Opinion in Genetics and Development*, 40, pp.81–86.

Ha, E., Oh, C., Bae, Y.S. & Lee, W., 2005. A Direct Role for Dual Oxidase in Drosophila Gut Immunity. *Science*, 310(5749), pp.847–851.

Hanauer, S.B., 2006. Inflammatory Bowel Disease: Epidemiology, Pathogenesis, and Therapeutic Opportunities. *Inflammatory Bowel Diseases*, 12(suppl_1), pp.S3–S9.

Hansen, M., Taubert, S., Crawford, D., Libina, N., Lee, S.-J. & Kenyon, C., 2007. Lifespan extension by conditions that inhibit translation in Caenorhabditis elegans. *Aging Cell*, 6(1), pp.95–110.

Hegedus, D., Erlandson, M., Gillott, C. & Toprak, U., 2008. New Insights into Peritrophic Matrix Synthesis, Architecture, and Function. *Annual Review of Entomology*, 54(1), pp.285–302.

Herskind, A.M., McGue, M., Holm, N. V., Sørensen, T.I.A., Harvald, B. & Vaupel, J.W., 1996. The heritability of human longevity: A population-based study of 2872 Danish twin pairs born 1870-1900. *Human Genetics*, 97(3), pp.319–323.

Hildebrandt, A., Bickmeyer, I. & Kühnlein, R.P., 2011. Reliable Drosophila body fat quantification by a coupled

colorimetric assay. *PLoS ONE*, 6(9).

Hjelmborg, J.B., Iachine, I., Skytthe, A., Vaupel, J.W., McGue, M., Koskenvuo, M., Kaprio, J., Pedersen, N.L. & Christensen, K., 2006. Genetic influence on human lifespan and longevity. *Human Genetics*, 119(3), pp.312–321.

Honjoh, S., Yamamoto, T., Uno, M. & Nishida, E., 2008. Signalling through RHEB-1 mediates intermittent fasting-induced longevity in C. elegans. *Nature*, 457, p.726.

Van Der Horst, A., Tertoolen, L.G.J., De Vries-Smits, L.M.M., Frye, R.A., Medema, R.H. & Burgering, B.M.T., 2004. FOXO4 is acetylated upon peroxide stress and deacetylated by the longevity protein hSir2SIRT1. *Journal of Biological Chemistry*, 279(28), pp.28873–28879.

Huang, H., Regan, K.M., Lou, Z., Chen, J. & Tindall, D.J., 2006. CDK2-Dependent Phosphorylation of FOXO1 as an Apoptotic Response to DNA Damage. *Science*, 314(5797), p.294 LP-297.

Hwangbo, D.S., Gersham, B., Tu, M.-P., Palmer, M. & Tatar, M., 2004. Drosophila dFOXO controls lifespan and regulates insulin signalling in brain and fat body. *Nature*, 429(6991), pp.562–566.

Jackson, B.C., Carpenter, C., Nebert, D.W. & Vasiliou, V., 2010. Update of human and mouse forkhead box (FOX) gene families. *Human genomics*, 4(5), pp.345–52.

Jackson, J.G., Kreisberg, J.I., Koterba, A.P., Yee, D. & Brattain, M.G., 2000. Phosphorylation and nuclear exclusion of the forkhead transcription factor FKHR after epidermal growth factor treatment in human breast cancer cells. *Oncogene*, 19(40), pp.4574–4581.

Jiang, H., Patel, P.H., Kohlmaier, A., Grenley, M.O., McEwen, D.G. & Edgar, B.A., 2009. Cytokine/Jak/Stat Signaling Mediates Regeneration and Homeostasis in the Drosophila Midgut. *Cell*, 137(7), pp.1343–1355.

Jiang, H. & Edgar, B.A., 2011. Intestinal stem cells in the adult Drosophila midgut. *Experimental cell research*, 317(19), pp.2780–2788.

Jolles, P. & Jolles, J., 1984. What's new in lysozyme research? *Molecular and Cellular Biochemistry*, 63(2), pp.165–189.

Jünger, M.A., Rintelen, F., Stocker, H., Wasserman, J.D., Végh, M., Radimerski, T., Greenberg, M.E. & Hafen, E., 2003. The Drosophila forkhead transcription factor FOXO mediates the reduction in cell number associated with reduced insulin signaling. *Journal of biology*, 2(3), p.20.

Kaeberlein, M., Powers, R.W., Steffen, K.K., Westman, E.A., Hu, D., Dang, N., Kerr, E.O., Kirkland, K.T., Fields, S. & Kennedy, B.K., 2005. Regulation of Yeast Replicative Life Span by TOR and Sch9 in Response to Nutrients. *Science*, 310(5751), pp.1193–1196.

Kaestner, K.H., Knöchel, W. & Martínez, D.E., 2000. Unified nomenclature for the winged helix/forkhead transcription factors. *Genes and Development*, 14(2), pp.142–146.

Kapahi, P., Zid, B.M., Harper, T., Koslover, D., Sapin, V. & Benzer, S., 2004. Regulation of lifespan in Drosophila by modulation of genes in the TOR signaling pathway. *Current biology : CB*, 14(10), pp.885–890.

Karin, M. & Clevers, H., 2016. Reparative inflammation takes charge of tissue regeneration. *Nature*, 529, p.307.

Karpac, J., Biteau, B. & Jasper, H., 2013. Misregulation of an Adaptive Metabolic Response Contributes to the Age-Related Disruption of Lipid Homeostasis in Drosophila. *Cell Reports*, 4(6), pp.1250–1261.

Kashii, Y., Uchida, M., Kirito, K., Tanaka, M., Nishijima, K., Toshima, M., Ando, T., Koizumi, K., et al., 2000. A member of Forkhead family transcription factor, FKHRL1, is one of the downstream molecules of

phosphatidylinositol 3-kinase-Akt activation pathway in erythropoietin signal transduction. *Blood*, 96(3), pp.941–9.

Kawada, M., Arihiro, A. & Mizoguchi, E., 2007. Insights from advances in research of chemically induced experimental models of human inflammatory bowel disease. *World Journal of Gastroenterology*, 13(42), pp.5581–5593.

Kenyon, C., Chang, J., Gensch, E., Rudner, A. & Tabtiang, R., 1993. A C. elegans mutant that lives twice as long as wild type. *Nature*, 366(6454), pp.461–464.

Kenyon, C., 2005. The plasticity of aging: Insights from long-lived mutants. *Cell*, 120(4), pp.449–460.

Kenyon, C.J., 2010. The genetics of ageing. *Nature*, 464(7288), pp.504–512.

King, D.G., 1988. Cellular organization and peritrophic membrane formation in the cardia (Proventriculus) of Drosophila melanogaster. *Journal of Morphology*, 196(3), pp.253–282.

Kirkwood, T.B.L., 2005. Understanding the odd science of aging. *Cell*, 120(4), pp.437–447.

Kitajima, S., Takuma, S. & Morimoto, M., 2000. Histological Analysis of Murine Colitis Induced by Dextran Sulfate Sodium of Different Molecular Weights. *Experimental Animals*, 49(1), pp.9–15.

Kitamura, Y.I., Kitamura, T., Kruse, J.P., Raum, J.C., Stein, R., Gu, W. & Accili, D., 2005. FoxO1 protects against pancreatic β cell failure through NeuroD and MafA induction. *Cell Metabolism*, 2(3), pp.153–163.

Kops, G.J.P.L., Ruiter, N.D. de, De Vries-Smits, A.M.M., Powell, D.R., Bos, J.L. & Burgering, B.M.T., 1999. Direct control of the Forkhead transcription factor AFX by protein kinase B. *Nature*, 398(6728), pp.630–634.

Kops, G.J.P.L. & Burgering, B.M., 1999. *Forkhead transcription factors: new insights into protein kinase B (c-akt) signaling*,

Kramer, J.M., Davidge, J.T., Lockyer, J.M. & Staveley, B.E., 2003. Expression of Drosophila FOXO regulates growth and can phenocopy starvation. *BMC developmental biology*, 3, p.5.

Kuraishi, T., Binggeli, O., Opota, O., Buchon, N. & Lemaitre, B., 2011. Genetic evidence for a protective role of the peritrophic matrix against intestinal bacterial infection in Drosophila melanogaster. *Proceedings of the National Academy of Sciences of the United States of America*, 108(38), pp.15966–15971.

Lehtinen, M.K., Yuan, Z., Boag, P.R., Yang, Y., Villén, J., Becker, E.B.E., DiBacco, S., de la Iglesia, N., Gygi, S., Blackwell, T.K. & Bonni, A., 2006. A Conserved MST-FOXO Signaling Pathway Mediates Oxidative-Stress Responses and Extends Life Span. *Cell*, 125(5), pp.987–1001.

Lemaitre, B. & Hoffmann, J., 2007. The host defense of Drosophila melanogaster. *Annual review of immunology*, 25, pp.697–743.

Lemaitre, B. & Miguel-Aliaga, I., 2013. The Digestive Tract of *Drosophila melanogaster*. *Annual Review of Genetics*, 47(1), pp.377–404.

Li, H., Qi, Y. & Jasper, H., 2016. Preventing Age-Related Decline of Gut Compartmentalization Limits Microbiota Dysbiosis and Extends Lifespan. *Cell Host Microbe*, 19(2), pp.240–253.

Liang, J., Balachandra, S., Ngo, S. & O'Brien, L.E., 2017. Feedback regulation of steady-state epithelial turnover and organ size. *Nature*, 548(7669), pp.588–591.

Lin, K., Dorman, J.B., Rodan, A. & Kenyon, C., 1997. daf-16: An HNF-3 / forkhead Family Member That Can Function to Double the Life-Span of Caenorhabditis elegans. *Science*, 278(5341), pp.1319–1322.

Liu, X., Hodgson, J.J. & Buchon, N., 2017. Drosophila as a model for homeostatic, antibacterial, and antiviral

mechanisms in the gut A conserved midgut structure from fly to human. *PLoS Pathogens*, 13(5), pp.10–17.

Ljungquist, B., Berg, S., Lanke, J., McClearn, G.E. & Pedersen, N.L., 1998. The effect of genetic factors for longevity: A comparison of identical and fraternal twins in the Swedish Twin Registry. *Journals of Gerontology - Series A Biological Sciences and Medical Sciences*, 53(6), pp.441–446.

Loftus, E. V, 2004. Clinical epidemiology of inflammatory bowel disease: incidence, prevalence, and environmental influences. *Gastroenterology*, 126(6), pp.1504–1517.

López-Otín, C., Blasco, M.A., Partridge, L., Serrano, M. & Kroemer, G., 2013. The hallmarks of aging. *Cell*, 153(6), pp.1194–217.

Luo, X., Puig, O., Hyun, J., Bohmann, D. & Jasper, H., 2007. Foxo and Fos regulate the decision between cell death and survival in response to UV irradiation. *EMBO Journal*, 26(2), pp.380–390.

Marianes, A. & Spradling, A.C., 2013. Physiological and stem cell compartmentalization within the Drosophila midgut. *eLife*, 2013(2), pp.1–19.

Markstein, M., Pitsouli, C., Villalta, C., Celniker, S.E. & Perrimon, N., 2008. Exploiting position effects and the gypsy retrovirus insulator to engineer precisely expressed transgenes. *Nature Genetics*, 40(4), pp.476–483.

Markstein, M., Dettorre, S., Cho, J., Neumuller, R.A., Craig-Muller, S. & Perrimon, N., 2014. Systematic screen of chemotherapeutics in Drosophila stem cell tumors. *Proceedings of the National Academy of Sciences*, 111(12), pp.4530–4535.

McGuire, S.E., Le, P.T., Osborn, A.J., Matsumoto, K. & Davis, R.L., 2003. Spatiotemporal Rescue of Memory Dysfunction in Drosophila. *Science*, 302(5651), p.1765 LP-1768.

Medema, R.H., Kops, G.J.P.L., Bos, J.L. & Burgering, B.M.T., 2000. AFX-like Forkhead transcription factors mediate cell-cycle regulation by Ras and PKB through p27kip1. *Nature*, 404(6779), pp.782–787.

Micchelli, C.A. & Perrimon, N., 2006. Evidence that stem cells reside in the adult Drosophila midgut epithelium. *Nature*, 439(7075), pp.475–479.

Miguel-Aliaga, I., Jasper, H. & Lemaitre, B., 2018. Anatomy and physiology of the digestive tract of Drosophila melanogaster. *Genetics*, 210(2), pp.357–396.

Molodecky, N.A., Soon, I.S., Rabi, D.M., Ghali, W.A., Ferris, M., Chernoff, G., Benchimol, E.I., Panaccione, R., Ghosh, S., Barkema, H.W. & Kaplan, G.G., 2012. Increasing incidence and prevalence of the inflammatory bowel diseases with time, based on systematic review. *Gastroenterology*, 142(1), p.46–54.e42.

Morel, F., Renoux, M., Lachaume, P. & Alziari, S., 2008. Bleomycin-induced double-strand breaks in mitochondrial DNA of Drosophila cells are repaired. *Mutation Research/Fundamental and Molecular Mechanisms of Mutagenesis*, 637(1), pp.111–117.

Mortzfeld, B.M., Taubenheim, J., Fraune, S., Klimovich, A. V. & Bosch, T.C.G., 2018. Stem cell transcription factor FoxO controls microbiome resilience in hydra. *Frontiers in Microbiology*, 9(APR), pp.1–10.

Mulle, J.G., Sharp, W.G. & Cubells, J.F., 2013. The gut microbiome: a new frontier in autism research. *Current psychiatry reports*, 15(2), p.337.

Nakae, J., Park, B. & Accili, D., 1999. Insulin stimulates Phosphorylation of the Forkhead Transcription Factor FKHR on Serine 253 through a Wortmannin-sensitive pathway. *The Journal of Biological Chemistry*,

274(23), pp.15982–15985.

O'Hara, A.M. & Shanahan, F., 2006. The gut flora as a forgotten organ. *EMBO Reports*, 7(7), pp.688–693.

Obsil, T., Ghirlando, R., Anderson, D.E., Hickman, A.B. & Dyda, F., 2003. Two 14-3-3 Binding Motifs Are Required for Stable Association of Forkhead Transcription Factor FOXO4 with 14-3-3 Proteins and Inhibition of DNA Binding. *Biochemistry*, 42(51), pp.15264–15272.

Obsilova, V., Vecer, J., Herman, P., Pabianova, A., Sulc, M., Teisinger, J., Boura, E. & Obsil, T., 2005. 14-3-3 Protein Interacts with Nuclear Localization Sequence of Forkhead Transcription Factor FoxO4. *Biochemistry*, 44(34), pp.11608–11617.

Oh, S.W., Mukhopadhyay, A., Svrzikapa, N., Jiang, F., Davis, R.J. & Tissenbaum, H.A., 2005. JNK regulates lifespan in Caenorhabditis elegans by modulating nuclear translocation of forkhead transcription factor/DAF-16. *Proceedings of the National Academy of Sciences*, 102(12), pp.4494–4499.

Ohlstein, B. & Spradling, A., 2007. Multipotent Drosophila Intestinal Stem Cells Specify Daughter Cell Fates by Differential Notch Signaling. *Science*, 315(5814), p.988 LP-992.

Ohlstein, B. & Spradling, A., 2006. The adult Drosophila posterior midgut is maintained by pluripotent stem cells. *Nature*, 439(7075), pp.470–474.

Okayasu, I., Hatakeyama, S., Yamada, M., Ohkusa, T., Inagaki, Y. & Nakaya, R., 1990. *A novel method in the induction of reliable experimental acute and chronic ulcerative colitis in mice. Gastroenterology 98, 694-702*,

Overend, G., Luo, Y., Henderson, L., Douglas, A.E., Davies, S.A. & Dow, J.A.T., 2016. Molecular mechanism and functional significance of acid generation in the Drosophila midgut. *Scientific Reports*, 6(June), pp.1–11.

Pfeiffenberger, C., Lear, B., Keegan, K. & Allada, R., 2010. Locomotor Activity Level Monitoring Using the Drosophila Activity Monitoring (DAM) System. *Cold Spring Harbor protocols*, 2010, p.pdb.prot5518.

Pitsouli, C., Apidianakis, Y. & Perrimon, N., 2009. Homeostasis in Infected Epithelia: Stem Cells Take the Lead. *Cell Host and Microbe*, 6(4), pp.301–307.

Poritz, L.S., Garver, K.I., Green, C., Fitzpatrick, L., Ruggiero, F. & Koltun, W.A., 2007. Loss of the Tight Junction Protein ZO-1 in Dextran Sulfate Sodium Induced Colitis. *Journal of Surgical Research*, 140(1), pp.12–19.

Rausch, P., Basic, M., Batra, A., Bischoff, S.C., Blaut, M., Clavel, T., Gläsner, J., Gopalakrishnan, S., et al., 2016. Analysis of factors contributing to variation in the C57BL/6J fecal microbiota across German animal facilities. *International Journal of Medical Microbiology*, 306(5), pp.343–355.

Ren, H., Orozco, I.J., Su, Y., Suyama, S., Gutiérrez-Juárez, R., Horvath, T.L., Wardlaw, S.L., Plum, L., Arancio, O. & Accili, D., 2012. FoxO1 target Gpr17 activates AgRP neurons to regulate food intake. *Cell*, 149(6), pp.1314–1326.

Rena, G., Shaodong, G., Cichy, S.C., Unterman, T.G. & Cohen, P., 1999. Phosphorylation of the transcription factor forkhead family member FKHR by protein kinase B. *Journal of Biological Chemistry*, 274(24), pp.17179–17183.

Rera, M., Bahadorani, S., Cho, J., Koehler, C.L., Ulgherait, M., Hur, J.H., Ansari, W.S., Lo, T., Jones, D.L. & Walker, D.W., 2011. Modulation of longevity and tissue homeostasis by the drosophila PGC-1 homolog. *Cell Metabolism*, 14(5), pp.623–634.

Roxström-Lindquist, K., Terenius, O. & Faye, I., 2004. Parasite-specific immune response in adult Drosophila

melanogaster: a genomic study. *EMBO reports*, 5(2), pp.207–212.

Royet, J., 2011. Epithelial homeostasis and the underlying molecular mechanisms in the gut of the insect model Drosophila melanogaster. *Cellular and Molecular Life Sciences*, 68(22), pp.3651–3660.

Ryu, J., Kim, S., Lee, H., Bai, J.Y., Nam, Y., Bae, J., Lee, D.G., Shin, S.C., Ha, E. & Lee, W., 2008. Innate Immune Homeostasis by the Homeobox Gene Caudal and Commensal-Gut Mutualism in Drosophila. *Science*, 319(5864), pp.777–782.

Salminen, A., Huuskonen, J., Ojala, J., Kauppinen, A., Kaarniranta, K. & Suuronen, T., 2008. Activation of innate immunity system during aging: NF-kB signaling is the molecular culprit of inflamm-aging. *Ageing Research Reviews*, 7(2), pp.83–105.

Salminen, A., Kaarniranta, K. & Kauppinen, A., 2012. Inflammaging: disturbed interplay between autophagy and inflammasomes. *Aging*, 4(3), pp.166–175.

Santos, Z., Francisco, P., Leitão-Gonçalves, R., Anjos, M., Baltazar, C., Elias, P.A., Fioreze, G.T., Anjos, M., et al., 2017. Inoculation of Holidic Media (HM) with bacteria to generate gnotobiotic Drosophila. *PLoS Biology*, pp.4–6.

Sharon, G., Segal, D., Ringo, J.M., Hefetz, A., Zilber-Rosenberg, I. & Rosenberg, E., 2010. Commensal bacteria play a role in mating preference of Drosophila melanogaster. *Proceedings of the National Academy of Sciences of the United States of America*, 107(46), pp.20051–20056.

Shell, B.C., Schmitt, R.E., Lee, K.M., Johnson, J.C., Chung, B.Y., Pletcher, S.D. & Grotewiel, M., 2018. Measurement of solid food intake in Drosophila via consumption-excretion of a dye tracer. *Scientific Reports*, 8(1), pp.1–13.

Shimokawa, I., Komatsu, T., Hayashi, N., Kim, S., Kawata, T., Park, S., Hayashi, H., Yamaza, H., Chiba, T. & Mori, R., 2015. The life-extending effect of dietary restriction requires Foxo3 in mice. *Aging Cell*, 14(4), pp.707–709.

Sieber, M.H. & Thummel, C.S., 2012. Coordination of Triacylglycerol and Cholesterol Homeostasis by DHR96 and the Drosophila LipA Homolog magro. *Cell Metabolism*, 15(1), pp.122–127.

Skytthe, A., Pedersen, N.L., Kaprio, J., Stazi, M.A., Hjelmborg, J.V.B., Iachine, I., Vaupel, J.W. & Christensen, K., 2003. Longevity Studies in GenomEUtwin. *Twin Research*, 6(5), pp.448–454.

Slack, C., Giannakou, M.E., Foley, A., Goss, M. & Partridge, L., 2011. dFOXO-independent effects of reduced insulin-like signaling in Drosophila. *Aging Cell*, 10(5), pp.735–748.

Smith, P., Willemsen, D., Popkes, M., Metge, F., Gandiwa, E., Reichard, M. & Valenzano, D.R., 2017. Regulation of life span by the gut microbiota in the short-lived African turquoise killifish. *eLife*, 6, pp.1–26.

St Johnston, D., 2002. The art and design of genetic screens: Drosophila melanogaster. *Nature Reviews Genetics*, 3(3), pp.176–188.

Stoffolano, J.G. & Haselton, A.T., 2013. The Adult Dipteran Crop: A Unique and Overlooked Organ. *Annual Review of Entomology*, 58(1), pp.205–225.

Takada, S., Kelkar, A. & Theurkauf, W.E., 2003. Drosophila checkpoint kinase 2 couples centrosome function and spindle assembly to genomic integrity. *Cell*, 113(1), pp.87–99.

Teleman, A.A., Hietakangas, V., Sayadian, A.C. & Cohen, S.M., 2008. Nutritional Control of Protein Biosynthetic Capacity by Insulin via Myc in Drosophila. *Cell Metabolism*, 7(1), pp.21–32.

Tran, H., Brunet, A., Grenier, J.M., Datta, S.R., Fornace, A.J., DiStefano, P.S., Chiang, L.W. & Greenberg, M.E., 2002. DNA Repair Pathway Stimulated by the Forkhead Transcription Factor FOXO3a Through the Gadd45 Protein. *Science*, 296(5567), pp.530–534.

Tzou, P., Ohresser, S., Ferrandon, D., Capovilla, M., Reichhart, J.M., Lemaitre, B., Hoffmann, J.A. & Imler, J.L., 2000. Tissue-specific inducible expression of antimicrobial peptide genes in Drosophila surface epithelia. *Immunity*, 13(5), pp.737–748.

Umezawa, H., Maeda, K., Takeuchi, T. & Okami, Y., 1966. New antibiotics, Bleomycin A and B. *The Journal of antibiotics*, 19(5), pp.200–209.

Varma, D., Bülow, M.H., Pesch, Y.Y., Loch, G. & Hoch, M., 2014. Forkhead, a new cross regulator of metabolism and innate immunity downstream of TOR in Drosophila. *Journal of Insect Physiology*, 69(C), pp.80–88.

Vijg, J. & Campisi, J., 2008. Puzzles, promises and a cure for ageing. *Nature*, 454, p.1065.

Weigel, D., Jürgens, G., Küttner, F., Seifert, E. & Jäckle, H., 1989. The Homeotic Gene fork head Encodes a Nuclear Protein and Is Expressed in the Terminal Regions of the Drosophila Embryo. *Cell*, 57(4), pp.645–658.

Willcox, B.J., Donlon, T.A., He, Q., Chen, R., Grove, J.S., Yano, K., Masaki, K.H., Willcox, D.C., Rodriguez, B. & Curb, J.D., 2008. FOXO3A genotype is strongly associated with human longevity. *Proceedings of the National Academy of Sciences of the United States of America*, 105(37), pp.13987–13992.

Wong, A.C.N., Chaston, J.M. & Douglas, A.E., 2013. The inconstant gut microbiota of Drosophila species revealed by 16S rRNA gene analysis. *ISME Journal*, 7(10), pp.1922–1932.

Wong, C.N.A., Ng, P. & Douglas, A.E., 2011. Low-diversity bacterial community in the gut of the fruitfly Drosophila melanogaster. *Environmental microbiology*, 13(7), pp.1889–1900.

Woude, C.J. Van Der, Ardizzone, S., Bengtson, M.B., Fiorino, G., Fraser, G., Katsanos, K., Kolacek, S., Mulders, A.G.M.G.J., et al., 2015. ECCO Guidelines / Consensus Paper The Second European Evidenced-Based Consensus on Reproduction and Pregnancy in Inflammatory Bowel Disease. *J Crohns Colitis*, 9(2), pp.107–124.

Wu, Z., Isik, M., Moroz, N., Steinbaugh, M.J., Zhang, P. & Blackwell, T.K., 2019. Dietary Restriction Extends Lifespan through Metabolic Regulation of Innate Immunity. *Cell Metabolism*, 29(5), p.1192–1205.e8.

Yamagata, K., Daitoku, H., Takahashi, Y., Namiki, K., Hisatake, K., Kako, K., Mukai, H., Kasuya, Y. & Fukamizu, A., 2008. Arginine Methylation of FOXO Transcription Factors Inhibits Their Phosphorylation by Akt. *Molecular Cell*, 32(2), pp.221–231.

Yang, J.-Y., Zong, C.S., Xia, W., Yamaguchi, H., Ding, Q., Xie, X., Lang, J.-Y., Lai, C.-C., et al., 2008. ERK promotes tumorigenesis by inhibiting FOXO3a via MDM2-mediated degradation. *Nature Cell Biology*, 10(2), pp.138–148.

Yatsenko, A.S., Marrone, A.K., Kucherenko, M.M. & Shcherbata, H.R., 2014. Measurement of Metabolic Rate in Drosophila using Respirometry. *Journal of Visualized Experiments*, (88), pp.1–5.

Zaidman-Rémy, A., Hervé, M., Poidevin, M., Pili-Floury, S., Kim, M.S., Blanot, D., Oh, B.H., Ueda, R., Mengin-Lecreulx, D. & Lemaitre, B., 2006. The Drosophila Amidase PGRP-LB Modulates the Immune Response to Bacterial Infection. *Immunity*, 24(4), pp.463–473.

Zhang, W., Patil, S., Chauhan, B., Guo, S., Powell, D.R., Le, J., Klotsas, A., Matika, R., et al., 2006. FoxO1

Regulates Multiple Metabolic Pathways in the Liver. *Journal of Biological Chemistry*, 281(15), pp.10105–10117.

Zheng, W.H., Kar, S. & Quirion, R., 2002. FKHRL1 and its homologs are new targets of nerve growth factor Trk receptor signaling. *Journal of Neurochemistry*, 80(6), pp.1049–1061.

Zhou, W., Cao, Q., Peng, Y., Zhang, Q., Castrillon, D., DePinho, R. & Liu, Z., 2009. FoxO4 inhibits NF-kappaB and protects mice against colonic injury and inflammation. *Gastroenterology*, 137(4), pp.1403–1414.

Ziv, E. & Hu, D., 2011. Genetic variation in insulin/IGF-1 signaling pathways and longevity. *Ageing Research Reviews*, 10(2), pp.201–204.

6. Erklärung

Hiermit erkläre ich, Mirjam Knop, dass diese Dissertation mit dem Titel: „The role of FoxO factors in maintaining intestinal homeostasis in *Drosophila melanogaster*“, sowie die darin beschriebenen Arbeiten, abgesehen von der Beratung durch meinen akademischen Lehrer, nach Inhalt und Form meine eigene Arbeit sind. Diese Arbeit wurde weder im Ganzen noch zum Teil an anderer Stelle im Rahmen eines Promotionsvorhabens eingereicht. Sie wurde nach den Regeln guter wissenschaftlicher Praxis der Deutschen Forschungsgemeinschaft angefertigt. Mir wurde kein akademischer Grad entzogen.

Kiel,

_____

Mirjam Knop

7. Danksagung

Als erstes möchte ich mich bei meinem Doktorvater Prof. Dr. Thomas Roeder für die Möglichkeit bedanken an diesem interessanten Thema arbeiten zu können. Ich bin dankbar für seine wissenschaftliche Betreuung und Unterstützung.

Bei Dr. Judith Bossen und Dr. Christine Fink bedanke ich mich für ihre guten Ratschläge, das Korrekturlesen meiner Arbeit, ihre Freundschaft und ihre motivierenden Worte, besonders wenn es mal nicht so gut lief.

Ein großer Dank geht an Britta Laubenstein und Christiane Sandberg für ihre großartige Hilfe im Labor.

Bei Dr. Daniela Esser möchte ich mich für ihre große Hilfe bei der Auswertung meiner Mikrobiota-Daten bedanken.

Der gesamten Arbeitsgruppe danke ich für die schöne Zeit, die gute Arbeitsatmosphäre und die lustigen Gespräche, die mir die Arbeit leichter gemacht haben.

Mein größter Dank geht an meine geliebte Familie für ihren Rückhalt, ihre Aufmunterungen und ihre riesige Unterstützung, ohne die ich mein Studium und diese Arbeit niemals geschafft hätte.

8. Appendix

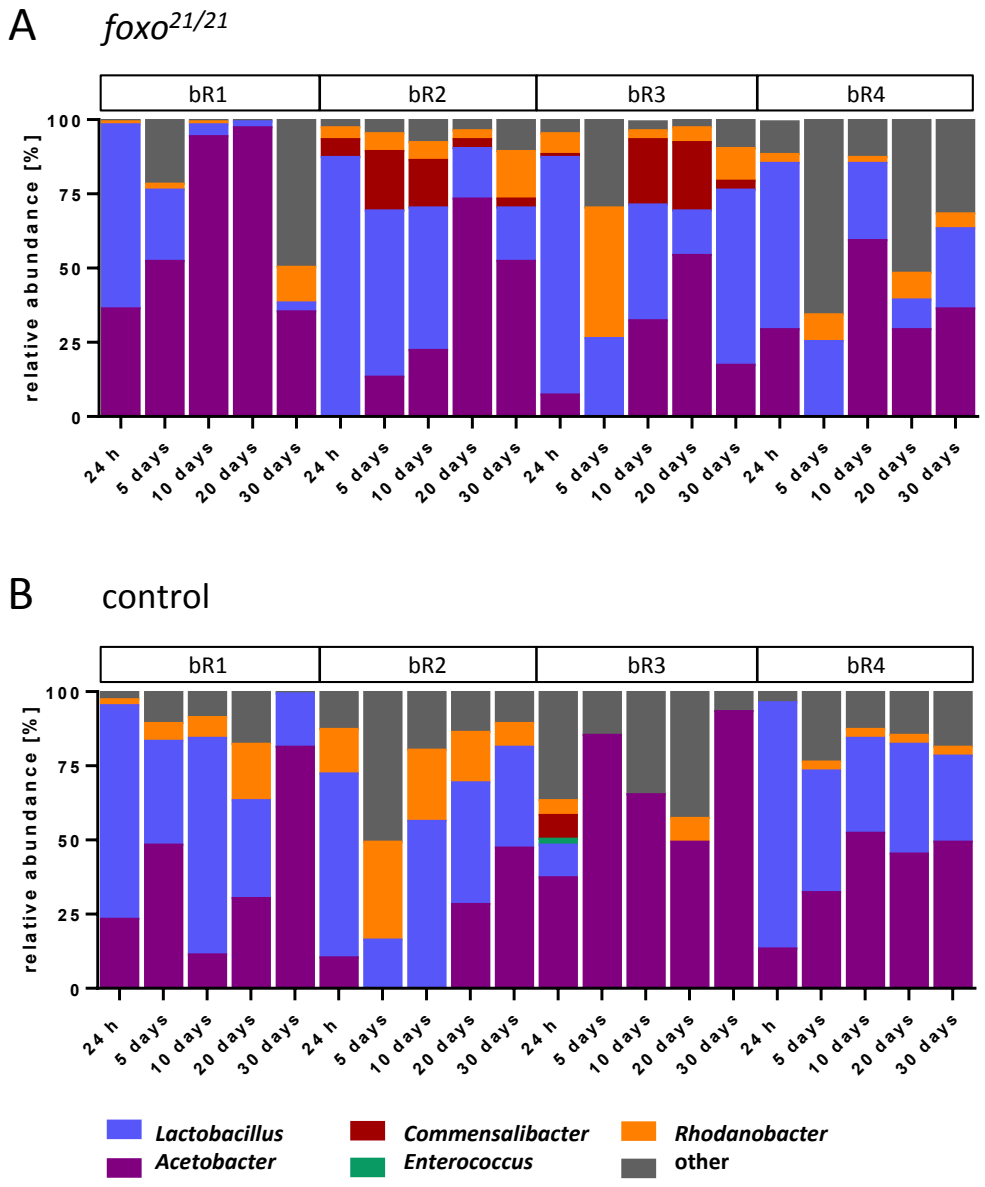

Fig. 9.1: Microbial composition of the bacteria mix used for recolonization and of feces collected from dFoxo-deficient and control flies. (A) Microbial composition of individual replicates of dFoxO-deficient flies and (B) controls at age 24 h, 5 days 10 days, 20 days and 30 days. control = *yw*.

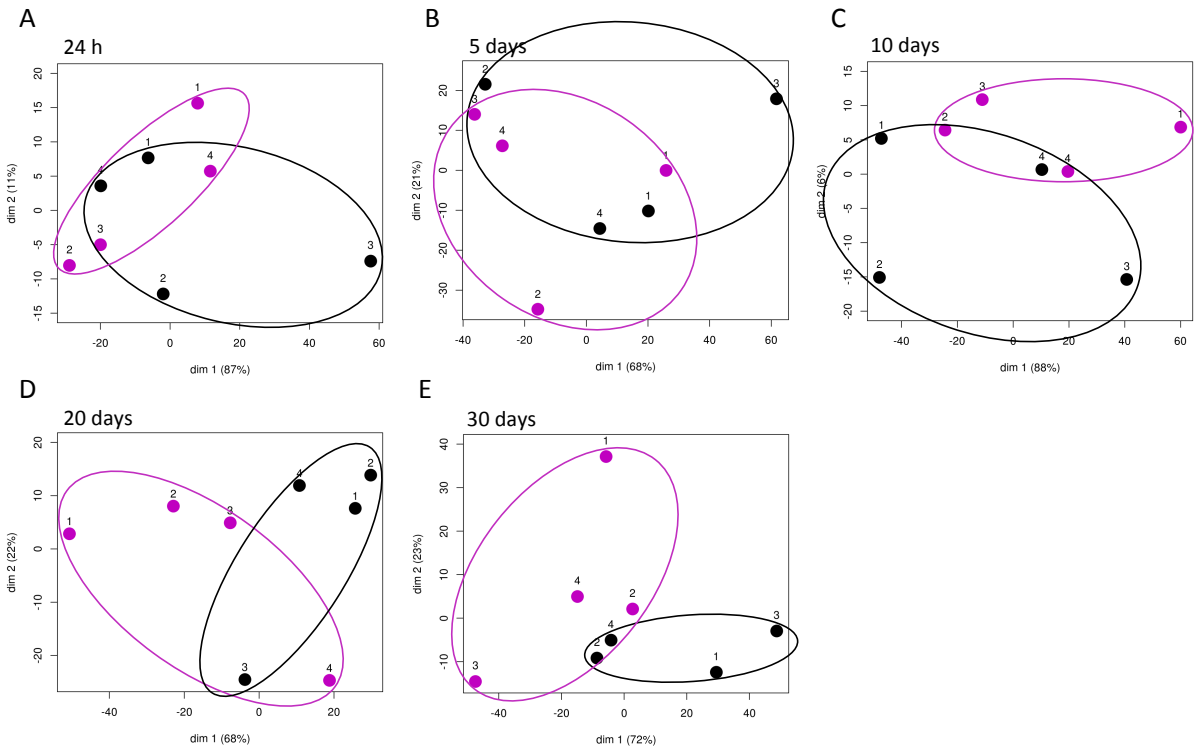

Fig. 9.2: PCoA plots were calculated to identify clusters of microbial compositions. (A) At age 24 h and (B) 5 days, the microbial profiles of feces from dFoxO-deficient flies and controls are mainly overlapping. (C) After 10 days, (D) 20 days and (E) 30 days, the microbiota of both groups seem to diverge into distinct clusters, although not significantly. Ellipses were added manually, pink dots = foxo$^{21/21}$, black dots = control, control = *yw*.

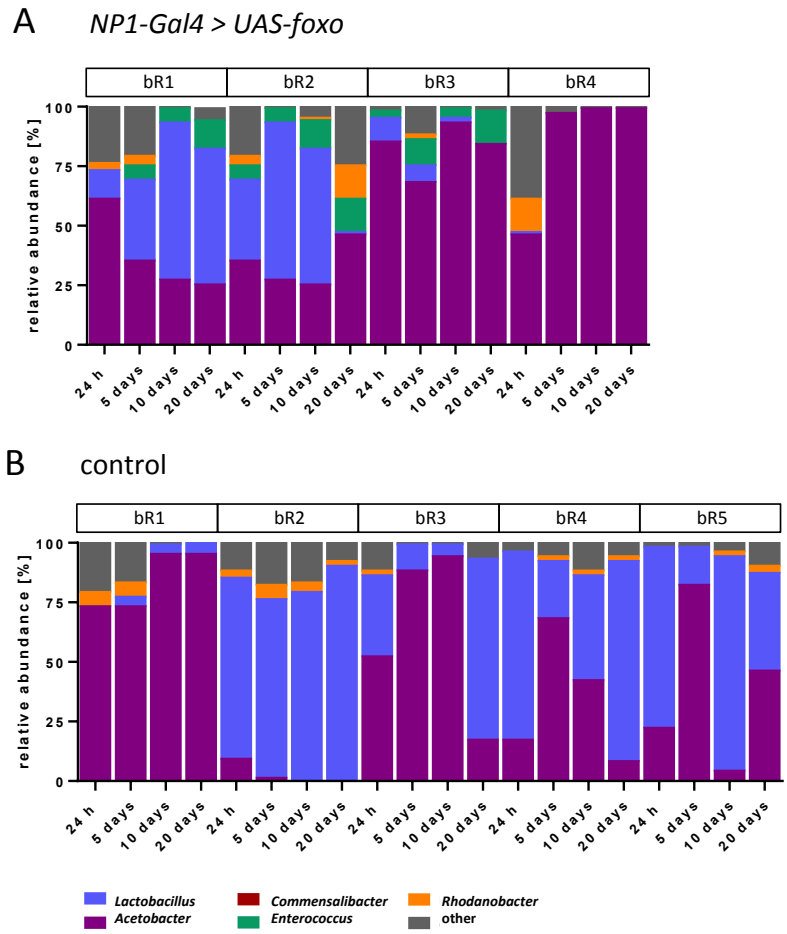

Fig. 9.3: Microbial composition of feces collected from dFoxo-overxpressing and control flies. (A) Microbial composition of individual replicates of flies overexpressing dFoxO in enterocytes and (B) controls at age 24 h, 5 days, 10 days and 20 days. *NP1-Gal4 = NP1-Gal4;tubPGal80ts.* control = w^{1118} > *UAS-foxo*.

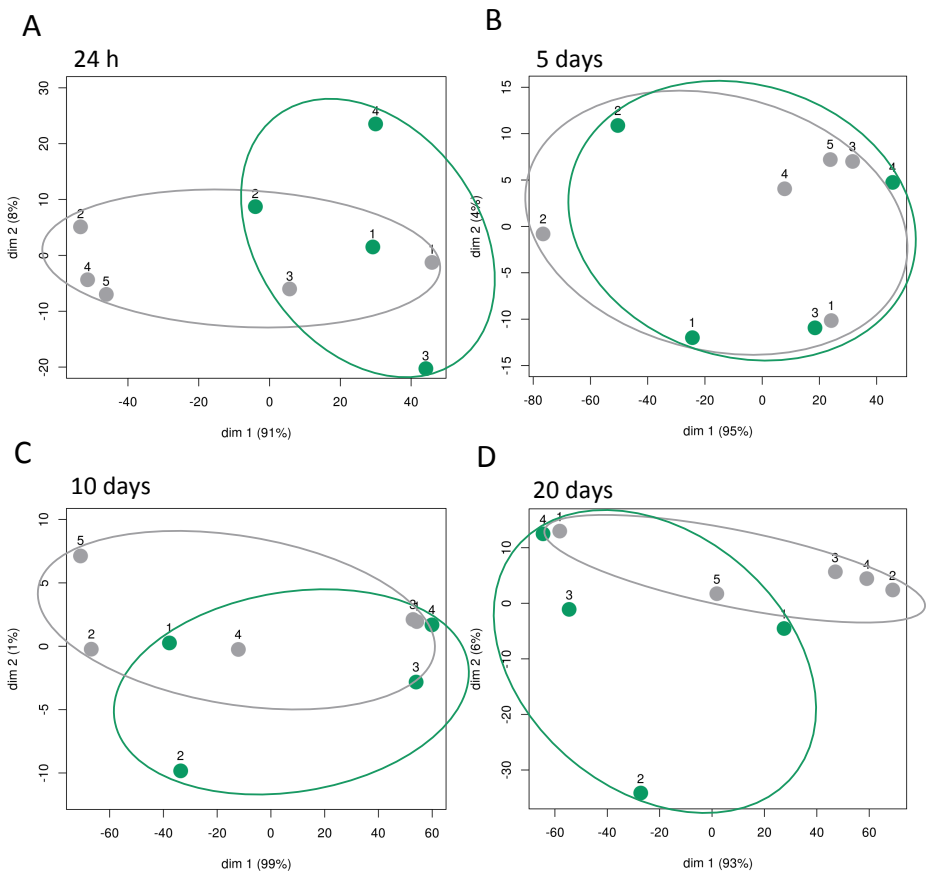

Fig. 9.4: PCoA plots were calculated to identify clusters of microbial compositions. (A-B) At young ages, the microbial copmpositions of feces from dFoxO-deficient flies and controls are mainly overlapping. (C) After 10 days, (D) 20 days both groups are diverting into two clusters, but not separated significantly. Ellipses were added manually. *NP1-Gal4 = NP1-Gal4;tubPGal80ts.* control = w^{1118} > *UAS-foxo.*

Table 8-1: Regulated genes of intestines dissected from dFoxO-deficient flies.

Name	Chromosome	Max group mean	Log_2 fold change	Fold change	P-value	FDR p-value	Bonferroni
CG43049	AE014296	10.2349652	9.9013619	956.328113	1.175E-06	5.8738E-05	0.0207932
CG32204	AE014296	10.1194814	8.7776289	438.863616	0	0	0
Tengl3	AE014134	2.79971968	8.617664	392.803509	2.873E-05	0.00099287	0.5083485
CG14301	AE014297	8.03630594	8.1028807	274.922403	0	0	0
w	AE014298	64.6569594	7.1014774	137.327564	0	0	0
ms(3)76Ba	AE014296	0.40905289	6.867874	116.798182	0.0009855	0.01988619	1
prom	AE013599	0.20911617	6.8640151	116.48619	0.0009695	0.01963062	1
Erk7	AE014298	0.1550286	6.3081494	79.2395824	0.0025274	0.04280216	1
tobi	AE014297	730.801828	6.2371535	75.4345472	0	0	0
Ir76a	AE014296	1.82915962	5.7734476	54.6991913	7.675E-13	1.2127E-10	1.358E-08
CG32302	AE014296	201.676064	5.5377239	46.4537748	0	0	0
CG15263	AE014134	5.15568748	5.0076026	32.1690755	3.331E-16	8.4204E-14	5.894E-12
Lsp2	AE014296	0.46310547	4.9325105	30.5375092	6.795E-05	0.00213967	1
CG31380	AE014297	0.79335933	4.7839083	27.5486221	1.184E-05	0.00045551	0.2095346
Dscam4	AE014296	0.45149489	4.7658341	27.2056436	1.438E-12	2.213E-10	2.545E-08
CG13461	AE014296	1.6375179	4.6749522	25.5447017	0.0005983	0.01308799	1
CG14566	AE014296	3.2152638	4.4901314	22.4731643	5.58E-08	3.7979E-06	0.0009875
CG4250	AE013599	38.9342553	4.4752176	22.242046	0	0	0
Mp	AE014296	1.00183088	4.2896671	19.5577312	0	0	0
CG14572	AE014296	1.09059884	4.1709128	18.0123285	2.054E-05	0.00074033	0.3635041
tut	AE014296	0.85012634	4.0601339	16.6810002	2.122E-05	0.00076321	0.375501
CG6034	AE014296	0.94044259	4.0272479	16.3050611	3.226E-06	0.00014278	0.0570851
CG43795	AE013599	0.7183209	3.9602761	15.5654572	2.028E-13	3.4187E-11	3.59E-09
Drsl2	AE014296	220.217685	3.9127907	15.0614701	5.935E-13	9.6363E-11	1.05E-08
CG17470	AE014134	7.33625765	3.7574812	13.524292	0	0	0
CG34351	AE014134	0.15573225	3.7394902	13.3566863	0.0005085	0.01149381	1
CG42269	AE014296	2.37902793	3.6597612	12.638569	8.771E-15	1.7246E-12	1.552E-10
CG7017	AE014296	18.3154753	3.6533647	12.5826572	6.888E-07	3.6423E-05	0.0121894
CG12035	AE014296	0.82063261	3.6037408	12.1572141	1.99E-05	0.00072148	0.3521142
CG34199	AE013599	0.65892093	3.5384022	11.618905	0.0017235	0.03125049	1
TotA	AE014297	3.95925516	3.5351013	11.5923514	9.108E-07	4.6583E-05	0.0161176
CG5070	AE014298	1.16090725	3.5339807	11.5833508	4.407E-05	0.00144438	0.7799653
CG4465	AE014297	0.22092715	3.5212029	11.4812106	0.001672	0.03063072	1
Ctr1B	AE014297	495.495504	3.4495017	10.9245483	0	0	0
CG8850	AE013599	0.62087445	3.4222632	10.7202242	2.428E-06	0.00011134	0.042976
Cralbp	AE014296	12.6407332	3.4153319	10.6688433	9.797E-13	1.5208E-10	1.734E-08
lectin-24Db	AE014134	0.756049	3.3673848	10.3200984	0.000194	0.0051537	1
CG12520	AE014296	1.30408574	3.3655319	10.3068521	5.566E-07	3.0029E-05	0.0098496
FucTA	AE014296	2.62875263	3.3503008	10.198611	6.106E-15	1.302E-12	1.081E-10
CG13532	AE013599	0.65650128	3.282733	9.73197754	1.162E-05	0.00044799	0.2056292
CG34375	AE014297	10.6030677	3.2795349	9.71042798	0	0	0
GstD2	AE014297	93.9883103	3.171816	9.01180465	0	0	0
CG16995	AE014134	31.9591665	3.0935195	8.53575948	1.354E-14	2.55E-12	2.397E-10

CG11878	AE014297	384.54065	3.0436391	8.24568341	0	0	0
CG30082	AE013599	4.06185362	3.0112338	8.06253669	5.398E-08	3.6882E-06	0.0009552
CG2269	AE013599	0.10025543	2.9768722	7.87277456	0.0028507	0.04732588	1
Act88F	AE014297	1.11439168	2.9348218	7.64661813	1.606E-05	0.00059978	0.2842936
Scp2	AE014297	3.82992461	2.9343515	7.64412564	7.865E-05	0.00243331	1
Cda9	AE013599	4.27050451	2.9175379	7.55555594	1.155E-14	2.1972E-12	2.043E-10
Akh	AE014296	31.271997	2.8809943	7.36657664	1.206E-08	9.9276E-07	0.0002134
CG3984	AE014297	10.0298351	2.8707929	7.31467041	1.052E-11	1.4211E-09	1.862E-07
LManIV	AE014134	4.09049067	2.8450587	7.18535131	4.216E-10	4.3633E-08	7.461E-06
lov	AE013599	0.09240127	2.8140956	7.03278246	0.0024212	0.04131942	1
CG16798	AE014134	0.22072173	2.7652105	6.79847184	0.0011713	0.0231335	1
Mal-A6	AE013599	1027.26144	2.7582033	6.76553175	0	0	0
CG43175	AE014297	2.46092357	2.7559058	6.75476597	0.0001704	0.00466604	1
CG42492	AE014298	0.6644638	2.7444975	6.70156226	1.775E-11	2.2763E-09	3.141E-07
CG14075	AE014296	24.4454516	2.7418783	6.68940669	1.17E-07	7.4474E-06	0.0020704
CG43055	AE014134	569.634881	2.7330394	6.64854864	0	0	0
CG30083	AE013599	0.7489587	2.7003975	6.49980989	0.0014657	0.0276531	1
CG11099	AE013599	0.34800743	2.6476331	6.26638382	0.000415	0.00967729	1
lectin-37Da	AE014134	1779.46247	2.6119925	6.11347433	7.772E-16	1.8338E-13	1.375E-11
CG14515	AE014297	1.27079593	2.5911637	6.02584571	0.0004775	0.01094589	1
CG31028	AE014297	0.22958796	2.5882689	6.01376659	0.0005386	0.01203479	1
CG10345	AE014297	1.6591615	2.5826258	5.99028973	9.756E-07	4.9612E-05	0.0172651
CG31798	AE014134	0.81187024	2.5494749	5.85421157	7.084E-05	0.00221893	1
Burs	AE014297	8.65679729	2.521989	5.74373417	1.312E-11	1.7197E-09	2.322E-07
CG6912	AE014297	24.5395447	2.5183853	5.72940476	3.886E-10	4.0452E-08	6.877E-06
CG3790	AE013599	4.43180828	2.4825122	5.588698	1.762E-11	2.2763E-09	3.119E-07
NimB5	AE014134	0.69843554	2.475285	5.56077136	0.0020179	0.03563959	1
CG13806	AE014296	11.9704884	2.4719609	5.5479735	1.987E-14	3.6257E-12	3.517E-10
dpr7	AE014135	1.40417695	2.4698093	5.5397056	1.31E-05	0.00049868	0.2318878
CG16704	AE014134	9.84983387	2.4549514	5.48294659	0.000648	0.01395165	1
CG9993	AE013599	3.72614946	2.4456561	5.44773324	0.0019045	0.03394118	1
CG4822	AE014134	1.04233129	2.4436249	5.44006866	4.721E-07	2.6188E-05	0.008354
Cyp49a1	AE013599	2.08335206	2.4073539	5.30500434	4.991E-08	3.437E-06	0.0008833
CG6337	AE013599	43.6907868	2.4039882	5.29264229	0	0	0
pre-mod(mdg4)-AE	AE014297	0.85688192	2.3743194	5.18491158	0.0013864	0.02652434	1
CG33958	AE013599	2.75158918	2.3651125	5.15192822	1.109E-06	5.5773E-05	0.019632
TotC	AE014297	4.4130933	2.3488719	5.09425772	0.0002353	0.0060784	1
CG6867	AE014298	3.07902931	2.3434881	5.0752825	8.185E-05	0.00251043	1
Cht4	AE013599	189.634867	2.3383711	5.05731316	2.474E-08	1.8791E-06	0.0004378
CG13285	AE014296	9.61295809	2.3018947	4.93104938	4.393E-11	5.3245E-09	7.774E-07
CNMa	AE014296	3.18723739	2.2999836	4.92452164	0.0001259	0.00359917	1
Ipk2	AE014134	96.4154773	2.2840337	4.87037769	0	0	0
Hml	AE014296	0.10437991	2.2819302	4.8632817	0.0020736	0.0364053	1
Cyp4e1	AE013599	2.19954844	2.2552634	4.77421458	2.277E-07	1.3477E-05	0.0040297
CG5770	AE013599	191.932015	2.2483784	4.75148461	2.554E-15	5.8688E-13	4.519E-11

CG15153	AE014134	8.79068143	2.2315632	4.69642584	1.442E-07	9.0158E-06	0.0025515
CG42255	AE014296	0.16178296	2.2278469	4.68434345	0.0003033	0.00747551	1
CG10353	AE014298	19.2592419	2.2112041	4.63061593	0	0	0
CG14427	AE014298	1.84378335	2.203362	4.60551331	4.788E-05	0.00155488	0.8474112
CG5084	AE013599	1.74210862	2.1855749	4.54908016	5.844E-05	0.00187234	1
GstD6	AE014297	0.84453284	2.1541074	4.45093172	0.002946	0.04856971	1
hdly	AE014297	58.7088902	2.1507182	4.4404879	2.774E-05	0.00096444	0.4908984
GstD8	AE014297	38.9988056	2.1489789	4.43513761	1.11E-16	2.9769E-14	1.965E-12
Try29F	AE014134	6.92508905	2.1447011	4.42200621	7.692E-09	6.6406E-07	0.0001361
nsr	AE013599	0.70119081	2.1204159	4.34819278	0.0006438	0.01391145	1
CG42747	AE014296	3.26484927	2.1192572	4.3447019	3.129E-08	2.2976E-06	0.0005537
CG13488	AE013599	24.962724	2.1135983	4.32769343	6.328E-15	1.3332E-12	1.12E-10
CG15431	AE014134	2.72487585	2.1062971	4.3058471	1.081E-13	1.9137E-11	1.914E-09
CG1909	AE014135	0.41487197	2.090413	4.25869967	0.001601	0.02959459	1
PPO1	AE013599	1.86870022	2.0849517	4.2426089	0.0005355	0.01197975	1
Skeletor	AE014297	0.24993703	2.0797048	4.22720725	0.0007561	0.0159097	1
CG10559	AE014297	19.2369916	2.0648781	4.18398623	0	0	0
Naam	AE014297	6.65961807	2.0608291	4.17226009	2.405E-07	1.4092E-05	0.0042557
Socs36E	AE014134	54.2204566	2.0548909	4.15512226	1.434E-09	1.4026E-07	2.539E-05
kune	AE013599	37.4726624	2.0390806	4.10983526	0	0	0
CG30090	AE013599	36.2824761	2.0344075	4.09654454	1.097E-11	1.4703E-09	1.941E-07
Grip91	AE014298	1.85506066	2.0283281	4.07931833	6.295E-09	5.4876E-07	0.0001114
CG32284	AE014296	74.8402504	2.0156937	4.04374978	5.993E-09	5.25E-07	0.0001061
slbo	AE013599	1.64021935	2.0047804	4.01327617	1.316E-06	6.3918E-05	0.0232976
CG4650	AE014134	1.33115076	1.9837711	3.9552561	0.0010662	0.02129681	1
CG13658	AE014297	47.1835245	1.9788067	3.94166931	0	0	0
Cyp6g2	AE013599	2.50688489	1.9511755	3.86689488	2.99E-06	0.00013362	0.0529152
Fuca	AE014296	1.54475487	1.9488572	3.86068599	3.944E-08	2.7994E-06	0.000698
CG12970	AE013599	8.37079013	1.9476393	3.85742819	1.861E-07	1.117E-05	0.0032928
CG7567	AE014297	184.479225	1.9465422	3.85449588	9.215E-15	1.7726E-12	1.631E-10
CG42238	AE014134	2.00893185	1.9336133	3.82010767	7.731E-10	7.7297E-08	1.368E-05
Pvf2	AE014134	1.6221468	1.921602	3.78843511	0.0002988	0.00739502	1
rho	AE014296	2.74035846	1.9211266	3.78718677	0.0003236	0.00785597	1
HGTX	AE014296	0.53684158	1.9193223	3.7824534	0.00264	0.04436779	1
CG33296	AE014134	0.77563804	1.9154856	3.7724077	0.001651	0.03030894	1
Karl	AE014298	0.66468133	1.9062892	3.748437	0.0007445	0.01571546	1
Ets21C	AE014134	10.5017654	1.903483	3.74115319	1.612E-05	0.00060052	0.2852475
Eo	AE014298	3.09501554	1.8981191	3.72726934	1.722E-07	1.0542E-05	0.0030468
Mal-A3	AE013599	123.445082	1.8925211	3.71283468	1.853E-06	8.7663E-05	0.0327859
Pi3K21B	AE014134	14.7312519	1.8751344	3.66835783	9.104E-15	1.7704E-12	1.611E-10
betaTub60D	AE013599	87.4711122	1.8749795	3.66796406	4.095E-08	2.8756E-06	0.0007247
Gbp1	AE013599	3.31905141	1.8721007	3.66065209	0.0010367	0.02080156	1
sNPF	AE014134	0.9432543	1.8487068	3.60177176	0.0022338	0.03860582	1
CG33346	AE014297	25.4029545	1.8474278	3.59858009	2.512E-11	3.1527E-09	4.445E-07
Cht2	AE014296	6.29653988	1.8303784	3.55630328	1.548E-10	1.7679E-08	2.74E-06
Mal-A7	AE013599	204.767886	1.8198265	3.53038734	4.994E-09	4.4409E-07	8.837E-05

CG32368	AE014296	902.851867	1.8049211	3.49410039	1.81E-07	1.0969E-05	0.0032029
Kaz1-ORFB	AE014296	3.26419994	1.7854699	3.44730728	1.079E-05	0.00042163	0.1909991
CG44013	AE014297	243.922433	1.7838222	3.4433723	1.237E-06	6.0951E-05	0.021893
Cyp6w1	AE013599	20.4395148	1.7832265	3.44195088	1.86E-07	1.117E-05	0.0032913
mtt	AE013599	0.44067645	1.7788869	3.4316132	0.0001745	0.00474479	1
CG17572	AE014134	2.57716927	1.7768973	3.4268839	0.00083	0.01714009	1
CG1090	AE014297	1.05630618	1.764114	3.39665329	3.796E-06	0.00016426	0.0671819
CG43394	AE014134	2.96991253	1.7315001	3.32072929	4.17E-09	3.7464E-07	7.38E-05
upd3	AE014298	2.45574059	1.729779	3.31677015	0.0019579	0.03475311	1
CG14219	AE014298	12.3892739	1.7269417	3.3102535	6.026E-06	0.00024917	0.1066452
Ser	AE014297	0.49207527	1.716834	3.28714255	0.0005644	0.01250071	1
Mal-A1	AE013599	2297.56862	1.7075501	3.26605736	3.331E-16	8.4204E-14	5.894E-12
CG12493	AE014296	2.6522046	1.707376	3.26566317	0.0014581	0.02753813	1
Drep1	AE013599	1.55436559	1.7041834	3.25844435	0.0001848	0.00496659	1
Act42A	AE013599	253.828191	1.7000494	3.24912079	2.525E-10	2.7244E-08	4.468E-06
Eip78C	AE014296	0.32870329	1.6890592	3.22446353	0.0016024	0.02959459	1
Mur29B	AE014134	153.527814	1.6849298	3.2152476	1.006E-07	6.4731E-06	0.0017801
Cyp4s3	AE014298	7.07177622	1.6799911	3.20425966	1.271E-05	0.0004868	0.2249006
Gr94a	AE014297	5.63822274	1.679003	3.202066	0.000442	0.01018493	1
iav	AE014298	1.30733011	1.6745934	3.19229376	1.404E-05	0.00053098	0.248497
Phk-3	AE013599	20.8707011	1.6656044	3.17246532	3.955E-08	2.7994E-06	0.0006999
Cpr51A	AE013599	14.1086151	1.6589238	3.15780875	1.186E-06	5.912E-05	0.0209876
GstD4	AE014297	3.23599183	1.6470979	3.13202971	0.0016835	0.03077707	1
Spn42De	AE013599	5.01401386	1.6428629	3.12284915	4.882E-07	2.6867E-05	0.0086389
PGRP-SD	AE014296	10.9599624	1.6358911	3.10779455	7.548E-05	0.00234746	1
CG14696	AE014297	23.036095	1.6257779	3.08608511	3.643E-11	4.4457E-09	6.446E-07
CG13813	AE014296	13.3888551	1.6190376	3.07170056	3.575E-09	3.2446E-07	6.327E-05
pck	AE014298	13.2245234	1.6180521	3.06960312	3.77E-10	3.9478E-08	6.672E-06
Gba1a	AE014297	106.515845	1.6112146	3.05508931	2.492E-05	0.00088043	0.4410958
pgant3	AE013599	22.3093532	1.6094471	3.05134887	2.653E-08	2.0066E-06	0.0004696
CG5897	AE014296	2.12504206	1.5979089	3.0270425	0.0001596	0.00441908	1
CG14102	AE014296	1.09271734	1.5864671	3.00313045	0.0023389	0.04018661	1
p38c	AE014297	46.5680564	1.574968	2.97928886	2.218E-13	3.6688E-11	3.926E-09
Tsp42Ej	AE013599	4.20145456	1.5710341	2.97117599	6.885E-06	0.00028074	0.1218411
Men-b	AE014297	16.2951574	1.5680172	2.96496939	1.559E-08	1.2482E-06	0.0002759
GstD5	AE014297	52.618652	1.5653268	2.95944538	1.11E-16	2.9769E-14	1.965E-12
Muc55B	AE013599	6.61699691	1.5590572	2.94661211	1.699E-07	1.044E-05	0.0030068
chas	AE014298	3.42881667	1.5455234	2.91909959	7.128E-12	1.0091E-09	1.261E-07
Col4a1	AE014134	3.65967623	1.5358432	2.89957858	0.0020258	0.03570713	1
Mal-A8	AE013599	217.414736	1.5322507	2.89236725	5.206E-07	2.8262E-05	0.0092133
Gfat1	AE014297	13.5141389	1.5284786	2.88481461	1.576E-10	1.7883E-08	2.79E-06
CG32557	AE014298	57.6096661	1.5206447	2.86919242	5.802E-07	3.1114E-05	0.0102677
CG30273	AE013599	7.93302197	1.5199108	2.86773311	7.76E-07	4.0157E-05	0.0137336
CG15199	AE014298	76.8297133	1.5059731	2.84016184	0.0004336	0.01003008	1
CG4377	AE013599	720.919057	1.5033258	2.83495494	8.444E-12	1.1674E-09	1.494E-07
CG46339	AE014297	10.5589992	1.5019914	2.83233401	2.791E-08	2.0928E-06	0.0004939

CG30148	AE013599	2.55681145	1.4951004	2.81883758	0.0020568	0.03614645	1
Pvf1	AE014298	21.9581649	1.4890412	2.8070236	3.025E-06	0.00013485	0.0535372
CG14695	AE014297	12.8969243	1.4882596	2.80550331	0.000102	0.00301827	1
CG4363	AE013599	484.120405	1.4798099	2.78911984	6.79E-11	8.0645E-09	1.202E-06
CG15529	AE014297	8.37516642	1.4695868	2.76942563	2.08E-07	1.2422E-05	0.003681
CG6967	AE013599	8.06133695	1.464071	2.75885764	0.0004893	0.01115095	1
CG14125	AE014296	286.885356	1.4607273	2.75247096	0.0001398	0.00392603	1
drd	AE014298	1.29430986	1.458504	2.74823243	0.000698	0.01481072	1
cher	AE014297	11.6432288	1.4562146	2.74387463	5.848E-12	8.3455E-10	1.035E-07
CG16732	AE014297	16.2748308	1.4415666	2.71615649	4.882E-07	2.6867E-05	0.0086392
CG8620	AE014296	20.2186081	1.435896	2.70550144	7.933E-06	0.00031835	0.140391
CG31104	AE014297	120.465546	1.4331971	2.70044488	1.099E-06	5.5569E-05	0.0194493
Gbp2	AE013599	1.8655119	1.4295445	2.69361664	0.0003307	0.00798332	1
CG2065	AE013599	54.7978331	1.4274466	2.68970249	2.256E-08	1.7286E-06	0.0003993
CG10405	AE014297	18.1274893	1.4248612	2.68488674	1.638E-05	0.000609	0.2898829
firl	AE014134	2.61895652	1.4228643	2.68117301	0.0002317	0.00600249	1
stops	AE014297	3.59511156	1.4220457	2.67965209	5.788E-06	0.00024102	0.102435
CG16898	AE013599	14.5545394	1.4212343	2.67814545	0.0005579	0.012404	1
CG11289	AE014134	4.13223736	1.4164713	2.66931824	9.611E-05	0.00286835	1
CG13531	AE013599	2.97616913	1.408405	2.6544354	1.391E-07	8.7616E-06	0.002462
CG14273	AE014134	3.67025759	1.4077402	2.65321248	0.0017231	0.03125049	1
CG44098	AE014297	1.42757179	1.3948748	2.62965736	0.0001087	0.00318495	1
CG34324	AE014298	749.24436	1.3936653	2.62745368	4.855E-06	0.00020603	0.0859136
unc-104	AE013599	3.29199301	1.3930477	2.62632917	1.736E-08	1.3714E-06	0.0003072
M6	AE014296	41.4920472	1.3817578	2.60585686	6.994E-15	1.4393E-12	1.238E-10
CG43780	AE014296	2.74123327	1.3626276	2.57153116	0.0003659	0.00869177	1
RhoGAP54D	AE013599	0.9541981	1.3618479	2.57014177	0.0011463	0.02269183	1
Sox21a	AE014296	11.1268306	1.3587448	2.5646195	6.145E-06	0.00025291	0.1087519
CG17816	AE014297	0.58008596	1.3578254	2.56298559	0.0001296	0.00368139	1
CG30025	AE013599	376.074766	1.3510155	2.55091612	2.666E-10	2.8512E-08	4.719E-06
CG5550	AE013599	125.821962	1.3500362	2.5491852	1.759E-08	1.3837E-06	0.0003113
CG13482	AE014296	405.595157	1.348179	2.54590567	3.228E-06	0.00014278	0.0571205
CG5773	AE013599	52.9828204	1.3472486	2.5442644	2.232E-09	2.1096E-07	3.95E-05
tacc	AE014297	7.48097458	1.3468515	2.54356414	1.275E-07	8.0869E-06	0.0022562
Mmp2	AE013599	4.68284043	1.3399248	2.53138132	0.0001636	0.00452515	1
CG33469	AE013599	7.08842653	1.3364371	2.52526905	8.002E-05	0.00247083	1
Usp1	AE014297	15.8339565	1.3327627	2.51884565	1.648E-08	1.3076E-06	0.0002916
CG15044	AE014298	171.058599	1.3305105	2.51491641	2.004E-09	1.917E-07	3.546E-05
nolo	AE014134	0.7134646	1.3245236	2.50450175	0.0009515	0.0192875	1
cnn	AE013599	1.03156213	1.3208195	2.49807965	0.0003194	0.00780208	1
CG5065	AE013599	6.83591771	1.3198541	2.49640854	1.389E-06	6.715E-05	0.0245768
Takl1	AE014297	38.8403394	1.3185612	2.49417241	2.278E-05	0.00081442	0.403137
rau	AE014134	2.56600781	1.3173751	2.49212263	0.0003553	0.00848437	1
CG14439	AE014298	6.13587975	1.303492	2.46825588	0.000127	0.00361458	1
ImpL2	AE014296	10.1073889	1.3023136	2.46624076	0.0001573	0.00436271	1
CG8353	AE014134	90.4887857	1.2995477	2.46151707	7.275E-07	3.7977E-05	0.0128743

CG33301	AE014134	167.373526	1.298627	2.45994664	5.851E-05	0.00187234	1
Lip4	AE014134	24.2360956	1.2977804	2.45850353	3.195E-08	2.3368E-06	0.0005655
Sans	AE013599	3.80400215	1.2907457	2.44654476	0.0001203	0.0034785	1
CG42788	AE014297	1.23691295	1.2895313	2.44448628	0.0006862	0.01461234	1
Dhap-at	AE014297	9.77338392	1.2894899	2.44441618	2.7E-08	2.0336E-06	0.0004779
sev	AE014298	0.52419395	1.2811141	2.43026582	0.0015479	0.02883544	1
fuss	AE014135	1.01499282	1.279949	2.42830401	0.0009411	0.01916628	1
CG32982	AE014134	8.25224439	1.2778027	2.42469407	1.001E-08	8.3588E-07	0.0001772
CG3739	AE014297	256.155776	1.2771234	2.42355268	7.445E-07	3.875E-05	0.0131749
CG31997	AE014135	13.9453349	1.2702887	2.41209828	5.222E-05	0.00168343	0.9242014
Jon66Cii	AE014296	10.0329022	1.2689682	2.40989146	0.0001185	0.00343111	1
Tsp42El	AE013599	29.6951086	1.2684162	2.40896961	3.114E-08	2.2963E-06	0.0005511
CG15210	AE014298	172.379585	1.2631906	2.40025989	7.235E-13	1.164E-10	1.28E-08
CG15043	AE014298	2272.03572	1.2539342	2.38490893	1.118E-10	1.293E-08	1.978E-06
Cyp309a1	AE014134	38.6683419	1.2486489	2.37618785	3.037E-08	2.2579E-06	0.0005374
Tsp42Ee	AE013599	58.0592409	1.2442705	2.36898728	9.603E-06	0.00037767	0.1699531
Ddc	AE014134	6.36246276	1.2391821	2.3606467	8.275E-05	0.0025336	1
CG9988	AE014297	1.68721081	1.2386627	2.35979685	0.0007699	0.01612347	1
CG10126	AE014297	21.7300402	1.2321989	2.34924781	7.729E-06	0.00031085	0.136776
Cyp4ad1	AE013599	39.320291	1.2311154	2.34748413	6.089E-06	0.00025119	0.1077602
CG11899	AE014297	58.6501673	1.2281432	2.34265294	9.78E-09	8.2029E-07	0.0001731
pre-lola-G	AE013599	2.29884007	1.2107135	2.31452069	0.0001755	0.00476205	1
CG3906	AE013599	1257.04886	1.2021959	2.30089621	3.344E-06	0.00014683	0.059171
CG15784	AE014298	754.781347	1.1997574	2.29701042	1.087E-06	5.5115E-05	0.0192353
CG13510	AE013599	96.2153509	1.1977573	2.29382809	8.383E-05	0.00255791	1
Cyp4p1	AE013599	34.6232726	1.1931988	2.28659181	3.869E-06	0.00016701	0.0684737
msn	AE014296	12.7539097	1.1916208	2.28409205	6.178E-08	4.1729E-06	0.0010933
Swim	AE013599	141.37897	1.1904775	2.28228266	0.0003191	0.00780208	1
Akap200	AE014134	17.5993595	1.1892532	2.28034676	7.979E-08	5.2887E-06	0.0014121
HP1D3csd	AE014298	5.18223003	1.1860609	2.27530649	0.0006334	0.01373763	1
CG10911	AE013599	2650.27997	1.1829816	2.27045532	0.0001384	0.00389978	1
CG14985	AE014296	12.5624808	1.1829538	2.27041146	3.287E-09	3.0144E-07	5.818E-05
scb	AE013599	77.2010496	1.1819572	2.26884373	2.045E-05	0.00073873	0.3619771
CG10910	AE013599	354.85715	1.1815918	2.26826906	1.518E-05	0.00056921	0.2686676
CG13117	AE014134	25.9895496	1.1811799	2.26762161	0.00014	0.00392603	1
pasi1	AE014297	7.71409766	1.1804238	2.2664335	0.0005871	0.0128744	1
ect	AE014296	1.01117048	1.176471	2.26023227	0.0017939	0.03213255	1
CG4393	AE014297	1.0958671	1.1681523	2.24723701	0.0013393	0.02587589	1
cv-2	AE013599	7.67204244	1.1632618	2.23963221	0.0005485	0.01222421	1
GstD1	AE014297	1421.43013	1.1605683	2.23545463	2.77E-06	0.00012473	0.0490192
CG2121	AE013599	2.56844138	1.1591318	2.23322993	0.0030345	0.04962346	1
CG2310	AE014297	29.5887148	1.157782	2.23114153	9.4E-09	7.959E-07	0.0001663
Gal	AE014134	188.096298	1.1531167	2.22393818	2.468E-06	0.00011256	0.0436748
CG43781	AE014296	2.76618622	1.1489503	2.21752495	0.0028675	0.04755953	1
vsg	AE014296	117.566914	1.1473975	2.21513948	3.74E-07	2.1006E-05	0.0066185
CG1208	AE014297	19.1843186	1.1446775	2.21096695	4.204E-05	0.00138682	0.7440067

CG10352	AE014298	5.20556994	1.1357706	2.19735905	0.0009434	0.0191873	1
Fst	AE014297	446.899459	1.1291255	2.18726125	0.0009454	0.0191873	1
sinu	AE014296	2.56129107	1.1225793	2.17735897	0.0007883	0.01645038	1
CG16791	AE014297	10.4850205	1.1212756	2.17539235	4.397E-08	3.0757E-06	0.0007781
CG7298	AE014296	149.646487	1.1212461	2.17534786	0.0016954	0.03094703	1
pod1	AE014298	5.01780474	1.1207639	2.17462091	5.192E-06	0.00021983	0.091887
ImpL3	AE014296	63.4989975	1.1138954	2.16429238	8.752E-10	8.7012E-08	1.549E-05
Irk2	AE014297	30.4259166	1.1131178	2.16312613	4.578E-09	4.0921E-07	8.102E-05
CG13324	AE013599	573.645686	1.1110748	2.16006506	1.157E-08	9.5686E-07	0.0002048
blot	AE014296	3.59609297	1.1104563	2.1591392	0.0015988	0.02959459	1
CenB1A	AE014297	11.2699674	1.1006611	2.14452947	4.082E-08	2.8756E-06	0.0007224
bond	AE014297	13.0362061	1.098456	2.14125402	0.0001686	0.00464042	1
CG16965	AE014134	15.1433751	1.0968427	2.13886092	7.08E-05	0.00221893	1
Clic	AE014298	86.5281036	1.0943692	2.13519706	0.0002051	0.00540829	1
pgant4	AE014134	46.555517	1.093833	2.13440364	9.062E-05	0.00273668	1
CG13506	AE013599	47.711968	1.090925	2.13010561	0.000231	0.0059947	1
cold	AE014134	11.3398948	1.0883586	2.12631984	2.23E-05	0.00080032	0.3945555
Gli	AE014134	67.9787903	1.0844756	2.12060458	8.565E-07	4.3933E-05	0.015157
MP1	AE014297	3.15313063	1.0836076	2.11932902	0.0017214	0.03125049	1
CG13325	AE013599	56.5300755	1.0795121	2.11332132	0.0005396	0.01204284	1
mys	AE014298	38.8926378	1.0744438	2.10591007	0.0001684	0.00464042	1
Pmm45A	AE013599	25.8339414	1.0744367	2.10589969	3.681E-08	2.6483E-06	0.0006515
CG7806	AE014134	20.38184	1.073013	2.10382245	7.183E-07	3.7609E-05	0.0127119
CG31195	AE014297	4.75719991	1.0709863	2.1008691	1.84E-05	0.00067695	0.3256121
CG42397	AE014296	1343.89466	1.0700635	2.09952578	2.671E-05	0.00093059	0.472742
CG11400	AE013599	40.9850671	1.0695609	2.09879449	0.0001871	0.00501791	1
Nost	AE014298	5.77730908	1.0638824	2.09054985	8.186E-07	4.2111E-05	0.0144863
Tspo	AE014134	711.386278	1.0626091	2.08870548	1.102E-05	0.00042939	0.194941
cib	AE014298	42.5863731	1.0617586	2.0874746	8.29E-06	0.00033041	0.1467023
whd	AE013599	173.429957	1.0514881	2.07266663	0.0002303	0.00598581	1
Phae2	AE014134	246.486143	1.0493188	2.06955247	1.085E-07	6.9307E-06	0.0019198
CG1890	AE014297	77.7381369	1.0475565	2.06702598	1.318E-06	6.3918E-05	0.0233301
Npc2a	AE014134	142.188633	1.0440274	2.06197585	1.911E-08	1.4766E-06	0.0003381
AnxB11	AE014298	8.75678142	1.0438741	2.06175667	2.02E-06	9.3808E-05	0.035741
CG31955	AE014134	14.1284769	1.0391779	2.05505629	4.126E-05	0.00137006	0.7302414
PGRP-SA	AE014298	4.64523176	1.0381555	2.05360037	0.0023934	0.04092441	1
CG10650	AE014134	701.875075	1.0353951	2.04967497	1.883E-08	1.4614E-06	0.0003332
Syx4	AE014298	31.1940593	1.0337888	2.04739399	6.64E-05	0.0020946	1
sdk	AE014298	1.57440781	1.033761	2.04735463	9.711E-05	0.00289315	1
CG8066	AE014297	58.4277975	1.0311597	2.04366635	3.735E-08	2.6764E-06	0.0006611
spict	AE014134	72.1245552	1.0239582	2.03349049	3.135E-10	3.3221E-08	5.548E-06
Atg18b	AE014134	20.0546804	1.0181605	2.02533488	7.452E-06	0.00030249	0.1318849
CG33116	AE014134	26.0650086	1.0108729	2.01513005	7.079E-07	3.7176E-05	0.0125283
CG5162	AE014298	37.7264746	1.0099326	2.01381707	9.26E-06	0.0003666	0.1638684
caup	AE014296	3.47989113	1.0078553	2.01091941	0.0016442	0.03024723	1
rtet	AE014297	39.8927787	1.0058872	2.00817801	1.382E-07	8.7346E-06	0.0024457

Cont	AE014297	2.25743232	1.0057598	2.00800079	0.0005743	0.01264022	1
CG43120	AE014296	42.904	1.005655	2.00785481	0.0001113	0.00325626	1
Rho1	AE013599	129.751689	1.0034977	2.00485468	0.0007284	0.01541821	1
Klp68D	AE014296	4.20310788	1.000402	2.00055739	5.189E-05	0.00167571	0.9182876
CG14879	AE014297	15.4369718	0.9987485	1.99826584	0.0003222	0.00784378	1
drm	AE014134	5.91347935	0.9961653	1.99469105	0.000249	0.00635031	1
CG9701	AE014296	6.98725638	0.9891053	1.98495368	0.0008156	0.01692025	1
CG15093	AE013599	86.2278423	0.9882462	1.98377194	1.366E-08	1.1168E-06	0.0002417
CG10638	AE014296	15.7047989	0.9868193	1.98181087	2.316E-07	1.3618E-05	0.004099
AnxB9	AE014297	142.032467	0.9865836	1.98148713	1.701E-06	8.093E-05	0.0301058
CG11672	AE014297	133.067361	0.9847723	1.97900095	0.0011793	0.02326647	1
CG14907	AE014297	50.1906469	0.9841281	1.97811753	0.0002975	0.00737298	1
CG42240	AE014298	11.3166468	0.9795913	1.97190675	0.0018531	0.03309161	1
CG13631	AE014297	15.8978503	0.9778574	1.9695382	3.378E-06	0.00014798	0.0597852
CG6891	AE014298	122.544737	0.9727406	1.96256523	8.405E-05	0.00255998	1
rols	AE014296	5.50452006	0.9704057	1.9593915	5.655E-05	0.00181643	1
CG9568	AE014134	1314.18184	0.9690915	1.95760745	8.683E-06	0.00034531	0.1536617
CG34198	AE013599	92.8704535	0.9685547	1.95687916	3.682E-05	0.00123172	0.6515787
CG8093	AE013599	244.02824	0.9669289	1.95467516	0.0012447	0.02439368	1
CG18067	AE013599	37.3678576	0.9665214	1.9541231	0.0002146	0.00561791	1
nxf2	AE014296	2.99494101	0.9641297	1.95088634	0.0009012	0.01841535	1
caps	AE014296	30.6391089	0.9636174	1.95019368	1.919E-05	0.00070321	0.3396483
CG14645	AE014297	13976.6662	0.960077	1.94541375	0.0008298	0.01714009	1
CG9676	AE014298	9.97764835	0.9588019	1.94369504	0.000646	0.01393779	1
CG10341	AE014134	18.3342415	0.957216	1.94155963	3.26E-06	0.00014353	0.0577001
axed	AE014296	9.72689475	0.9566734	1.94082951	0.001598	0.02959459	1
Ssadh	AE014297	89.4683521	0.9560268	1.9399599	4.722E-05	0.00153604	0.8356065
MRP	AE014134	39.6369731	0.9557295	1.93956007	0.000188	0.00502695	1
sgl	AE014296	169.851922	0.9555377	1.93930226	0.0001849	0.00496659	1
zip	AE013599	14.5765823	0.9535441	1.93662426	1.981E-05	0.00071989	0.3505857
CG2641	AE014297	4.3939937	0.9519267	1.93445439	0.0017521	0.0316395	1
CG12883	AE014297	27.7334424	0.9518492	1.93435047	5.691E-07	3.0612E-05	0.0100714
Sox100B	AE014297	8.57508946	0.9498871	1.93172149	0.001276	0.02484286	1
CAH2	AE014296	144.421856	0.9493958	1.93106371	1.49E-05	0.00055973	0.2636331
Atg4b	AE014297	16.361035	0.9486225	1.93002901	1.614E-06	7.701E-05	0.0285708
Rhp	AE014298	9.23959352	0.9454368	1.9257719	0.0004277	0.00994549	1
wat	AE014297	48.5089786	0.9449859	1.92517003	0.0008426	0.01733914	1
Damm	AE013599	232.818478	0.9422027	1.92145962	1.234E-05	0.00047365	0.2183505
spartin	AE014297	4.99085809	0.9411884	1.92010921	0.0002482	0.00633946	1
Mctp	AE013599	2.94223696	0.9409695	1.91981793	0.0002715	0.00682392	1
CG11671	AE014297	302.544917	0.9392836	1.91757582	0.0010969	0.02183554	1
Charon	AE014134	34.1630594	0.9264143	1.90054648	0.000257	0.00651611	1
Idgf3	AE014134	11.0572242	0.922853	1.8958607	1.45E-05	0.00054696	0.2565231
Tsf2	AE014296	4.06523174	0.9217443	1.8944043	0.0029305	0.0484224	1
Baldspot	AE014296	66.3992468	0.9215512	1.89415075	0.0014324	0.02719792	1
CG15083	AE013599	22.8392972	0.9207324	1.89307612	0.000805	0.01675216	1

CG5004	AE014298	10.3769774	0.9160209	1.88690384	0.0001012	0.00299907	1
Cpr67B	AE014296	39.4556394	0.9114895	1.88098657	0.0030368	0.04962346	1
CG18635	AE013599	33.0190401	0.9106815	1.87993333	1.556E-06	7.4422E-05	0.027536
CG31469	AE014297	70.5292478	0.9083883	1.87694756	3.736E-06	0.00016204	0.0661118
CG34417	AE014298	2.30424782	0.9043236	1.87166674	1.4E-05	0.00053048	0.2477319
LamC	AE013599	47.9061663	0.9008195	1.86712623	3.597E-07	2.0336E-05	0.0063651
CG31087	AE014297	197.180276	0.8980916	1.86359917	1.312E-06	6.3918E-05	0.0232251
pdm2	AE014134	2.65981571	0.8964488	1.86147834	0.0007685	0.01611342	1
dsd	AE014297	12.7173184	0.8948208	1.85937892	2.977E-07	1.716E-05	0.0052681
Treh	AE013599	123.613116	0.8946684	1.85918257	0.0004951	0.011263	1
cpa	AE013599	90.3243203	0.8926788	1.8566203	0.000325	0.00787866	1
Alh	AE014297	3.97141167	0.8925283	1.85642666	5.661E-06	0.00023796	0.1001819
fu12	AE014134	24.7739942	0.891774	1.85545624	2.67E-05	0.00093059	0.4724901
CG30269	AE013599	87.4700488	0.884778	1.84648051	1.734E-07	1.0579E-05	0.0030678
Ccm3	AE014297	71.0087196	0.8810109	1.84166525	3.751E-07	2.1006E-05	0.0066378
Orct2	AE014297	4.96218305	0.8806675	1.84122693	0.0002419	0.00621957	1
babos	AE013599	16.5757149	0.8789886	1.8390855	6.626E-05	0.0020939	1
CG11318	AE014297	24.4177614	0.878529	1.83849979	3.538E-05	0.00118823	0.6261961
pirk	AE013599	25.2135469	0.8776696	1.83740489	0.0020849	0.03656722	1
Sgt1	AE014297	54.251131	0.8722449	1.83050909	3.608E-06	0.00015689	0.0638525
CG16775	AE014296	570.390306	0.8716818	1.82979473	0.0025461	0.04303485	1
CG33120	AE014134	12.9536572	0.8670307	1.82390517	0.0001044	0.00307853	1
B4	AE014134	3.04334774	0.8644356	1.82062733	0.0015265	0.02858586	1
CG13994	AE014134	18.8690103	0.8639602	1.82002747	0.0002581	0.00653341	1
Ptp4E	AE014298	2.01979191	0.862566	1.81826949	0.000486	0.01109744	1
Ntf-2	AE014298	9.84036563	0.8615324	1.81696717	0.0010155	0.02042153	1
Fas3	AE014134	5.46551057	0.8606081	1.81580347	0.0002118	0.00557048	1
CG10055	AE014297	7.26204001	0.8551666	1.80896759	0.0005742	0.01264022	1
dome	AE014298	23.9007784	0.8545344	1.80817513	3.889E-06	0.00016743	0.0688157
CG18744	AE014297	40.8205832	0.8544193	1.80803082	9.51E-05	0.00284277	1
Pde1c	AE014134	13.0684724	0.8543605	1.80795721	5.04E-07	2.7527E-05	0.0089186
Pax	AE014134	22.2647832	0.8508769	1.80359682	4.901E-07	2.6867E-05	0.0086725
Socs44A	AE013599	32.4741062	0.8411408	1.79146612	1.112E-05	0.00043243	0.1967577
Jra	AE013599	50.7182297	0.8392861	1.78916457	1.107E-06	5.5773E-05	0.019599
CG3719	AE014298	175.924057	0.8372859	1.78668575	3.063E-05	0.00105456	0.542044
Akt1	AE014297	8.96158723	0.8295187	1.77709243	0.0007434	0.01571546	1
Cyp6a9	AE013599	77.8575168	0.8257813	1.77249471	0.0009008	0.01841535	1
shep	AE014296	3.85003689	0.8252164	1.77180078	0.0003633	0.00866589	1
CG32170	AE014296	5.4699125	0.8207028	1.76626622	0.0005347	0.01197975	1
CG13321	AE013599	881.882193	0.8177339	1.76263519	6.487E-06	0.00026574	0.1148005
Kat60	AE014297	17.6851072	0.8175402	1.76239854	0.000351	0.00842842	1
sut2	AE013599	14.2948988	0.8173079	1.76211479	0.0015289	0.02860203	1
CalpC	AE014298	8.82450149	0.8118708	1.75548639	0.0003098	0.00760641	1
CG11241	AE014296	10.5682771	0.8117278	1.75531242	3.187E-05	0.00108674	0.5640164
CG13323	AE013599	744.965355	0.8089801	1.75197251	7.638E-06	0.00030791	0.1351734
mthl15	AE014134	13.5441683	0.8088532	1.75181837	0.0001026	0.00303171	1

CG5613	AE014298	6.90701459	0.8088475	1.75181148	0.000762	0.0159974	1
c11.1	AE014298	15.187801	0.8080095	1.75079415	1.481E-06	7.1411E-05	0.0262079
CG9147	AE014134	9.82021349	0.8062967	1.74871688	0.0013173	0.02550532	1
CG2004	AE014298	57.523273	0.8044716	1.74650599	1.65E-05	0.00061203	0.2919363
Efa6	AE014297	1.31461141	0.8023129	1.74389471	0.0020284	0.03571802	1
Eaat1	AE014134	12.6501674	0.7999325	1.74101963	0.0009052	0.01845506	1
CG18659	AE013599	15.0600754	0.7997053	1.74074546	0.0004854	0.01109744	1
Arpc3B	AE014298	185.495363	0.7950199	1.73510126	5.932E-05	0.00189499	1
lute	AE014297	5.31523997	0.7929965	1.73266945	0.0006627	0.01423371	1
kay	AE014297	12.7035546	0.7900496	1.72913394	0.0005796	0.0127426	1
mesh	AE014297	303.573891	0.7894071	1.72836407	8.133E-05	0.00249865	1
PGRP-LA	AE014296	19.965895	0.7860201	1.72431107	3.817E-05	0.00127197	0.6754158
CG4607	AE014298	102.135094	0.784301	1.72225763	0.0002589	0.00653541	1
CG12926	AE013599	50.1815243	0.7806919	1.71795456	1.296E-06	6.338E-05	0.0229435
CG33111	AE014297	7.38274823	0.7798158	1.71691165	0.0009447	0.0191873	1
alphaTub84B	AE014297	763.328589	0.7794761	1.71650747	3.101E-05	0.00106157	0.5488305
Lfg	AE013599	372.867891	0.7769108	1.71345799	0.0002072	0.00545766	1
ringer	AE014296	67.1599626	0.7749064	1.71107905	4.259E-05	0.00140102	0.7537462
CG44014	AE014297	1162.5226	0.7727467	1.7085195	3.149E-05	0.00107599	0.5573631
Dronc	AE014296	14.0447384	0.7719035	1.70752122	5.97E-05	0.00190357	1
SH3PX1	AE014296	124.370097	0.7708886	1.70632045	0.0001128	0.00328874	1
Sema5c	AE014296	17.7146992	0.768122	1.70305145	2.468E-06	0.00011256	0.0436695
lama	AE014296	17.9149249	0.7678591	1.70274114	2.453E-05	0.00086814	0.4340688
CG16985	AE014296	139.133945	0.766258	1.70085248	8.981E-05	0.00272142	1
CalpB	AE014296	9.17442523	0.7637904	1.69794574	2.562E-05	0.00090125	0.4533295
CG17264	AE014134	25.2914374	0.7632966	1.69736473	0.0020031	0.0354489	1
CG42565	AE013599	6.2396992	0.7590883	1.69242078	0.0008172	0.01693418	1
aPKC	AE013599	14.2712556	0.7571931	1.69019904	1.707E-05	0.00063133	0.3020232
CG3987	AE014297	608.122871	0.7565272	1.68941905	0.000105	0.00309043	1
Tsp42Ef	AE013599	70.5607161	0.7564694	1.68935135	6.748E-06	0.00027579	0.1194186
CG32681	AE014298	3.60656727	0.7537751	1.68619929	0.0029138	0.04823667	1
CG5506	AE014296	4744.073	0.7535285	1.68591111	0.0002177	0.00568965	1
Past1	AE014297	109.308855	0.7534099	1.68577257	0.0003943	0.00926685	1
lpp	AE014297	44.8401171	0.752831	1.68509622	2.649E-05	0.00093001	0.468724
CG1146	AE014296	10.2523161	0.7483063	1.67981959	0.0016129	0.02973265	1
CG10103	AE014296	84.7639444	0.7478443	1.67928173	0.0002893	0.00718986	1
Vps2	AE014297	83.8637156	0.7467264	1.67798103	9.51E-06	0.00037484	0.168305
Arc2	AE013599	33.9450409	0.7455502	1.67661355	0.0013772	0.02646237	1
Est-Q	AE014296	85.9846816	0.7451018	1.67609259	0.0013814	0.02648607	1
Got1	AE013599	252.847302	0.7448947	1.6758519	0.0013435	0.02592735	1
CG3394	AE013599	30.7675597	0.7444448	1.67532943	6.621E-05	0.0020939	1
CG6484	AE013599	440.385521	0.7436926	1.67445613	0.0017835	0.03210851	1
CG10916	AE013599	15.1679737	0.7414438	1.67184817	0.0001502	0.00417823	1
GstE13	AE013599	13.1867608	0.7408488	1.6711588	0.0027858	0.04642239	1
Strica	AE013599	11.2677431	0.7375156	1.66730213	0.0010746	0.02143946	1
sli	AE013599	2.08546202	0.7363354	1.66593881	0.0021692	0.03782067	1

MME1	AE014134	31.2752048	0.7336	1.66278313	3.071E-05	0.00105543	0.5435455
CG18858	AE014134	46.2941753	0.7264599	1.65457407	4.442E-05	0.00145314	0.7861499
rho-4	AE014298	53.9271665	0.7259239	1.65395946	0.0001249	0.00358845	1
Synd	AE014297	41.4661473	0.7242458	1.65203681	7.374E-05	0.00230571	1
CG14495	AE013599	76.8490544	0.7175724	1.64441268	8.316E-05	0.0025417	1
CG8485	AE013599	5.87682686	0.7157768	1.64236723	0.0017906	0.03213255	1
scrib	AE014297	8.05100178	0.7150971	1.64159375	0.0006155	0.0134142	1
cert	AE014296	34.5210719	0.7150083	1.64149269	7.416E-05	0.00231043	1
bark	AE014134	3.04919982	0.7140906	1.64044887	0.002311	0.03978445	1
CG11897	AE014297	8.60814398	0.7132109	1.63944881	0.0003921	0.00922682	1
Dlic	AE014298	20.6128117	0.7128185	1.63900299	0.000693	0.01474078	1
betaTub56D	AE013599	383.265266	0.7122815	1.63839301	0.0017185	0.03125049	1
fbp	AE014134	51.5734536	0.7119499	1.63801653	0.0004111	0.00959873	1
tsr	AE013599	842.764814	0.7109514	1.63688323	0.0027628	0.0460829	1
bif	AE014298	25.1914245	0.7075751	1.63305699	0.0022058	0.038271	1
CG11658	AE014296	45.340353	0.7051586	1.63032385	0.0006216	0.01351371	1
CG5910	AE014296	70.7176127	0.7040253	1.6290437	0.0004373	0.01008991	1
gammaSnap1	AE013599	29.4356347	0.7037406	1.62872222	0.0017521	0.0316395	1
ALiX	AE014297	102.010713	0.7009711	1.62559861	0.0017856	0.03211297	1
Klp10A	AE014298	7.94215593	0.6984004	1.62270461	0.0003196	0.00780208	1
Tep4	AE014134	21.2892749	0.685526	1.60828825	0.0004896	0.01115095	1
Sh3beta	AE014296	33.6294676	0.6844231	1.60705922	0.0012619	0.0246756	1
Mvb12	AE014298	8.93887233	0.6734438	1.59487552	0.0023676	0.04063889	1
CG9119	AE014296	79.6128674	0.6691354	1.59011969	0.0017909	0.03213255	1
ry	AE014297	12.9325384	0.663371	1.58377891	0.0018417	0.03295568	1
CG1213	AE014297	394.43309	0.6564455	1.57619446	0.0003542	0.00848437	1
CG7332	AE014298	13.0322972	0.6499187	1.56907978	0.001771	0.03194797	1
PIG-V	AE013599	19.1635543	0.6468851	1.56578385	0.000234	0.00605501	1
Mmp1	AE013599	24.9762065	0.6467542	1.56564183	0.0023747	0.04068332	1
Drice	AE014297	30.5429097	0.6452236	1.56398167	0.000675	0.01442685	1
rhea	AE014296	11.7865097	0.6436088	1.56223209	0.0005906	0.01293643	1
CG15126	AE013599	149.155413	0.6407555	1.55914546	0.0002785	0.00697087	1
key	AE013599	57.6334511	0.6406074	1.55898543	0.0030064	0.04935467	1
Ugt86Dc	AE014297	41.1373312	0.6401403	1.55848067	0.0030304	0.04961056	1
pnut	AE013599	29.4575024	0.6381597	1.55634262	0.0002367	0.0061066	1
Vta1	AE014296	72.9226703	0.6379705	1.55613849	9.085E-05	0.00273883	1
CG5335	AE013599	104.936313	0.6370774	1.55517546	0.0003768	0.00891559	1
PIG-L	AE014297	50.631572	0.6348543	1.55278095	0.0002481	0.00633946	1
MESR3	AE014134	34.0436625	0.6343466	1.5522346	0.0001927	0.00512902	1
rost	AE014134	41.7452968	0.6330972	1.55089093	0.0001723	0.00470155	1
RtGEF	AE014134	4.37611727	0.6315063	1.54918164	0.0006083	0.0132728	1
I-2	AE014296	21.4865454	0.6234229	1.54052591	0.0004348	0.01004505	1
CG7705	AE014297	11.1756886	0.6213979	1.53836507	0.0009038	0.01844897	1
AOX1	AE014297	446.51278	0.6208509	1.53778187	0.0028428	0.04723895	1
CG43143	AE014297	2.28811789	0.6201257	1.53700907	0.0025171	0.04270807	1
Sep2	AE014297	46.7479391	0.6175781	1.53429735	0.0001814	0.00490754	1

RabX1	AE013599	22.1787284	0.6160078	1.53262821	0.0015585	0.02900187	1
Srp54	AE014134	16.7272803	0.6117948	1.5281592	0.0005336	0.01197975	1
Sk1	AE014298	34.4777552	0.6103518	1.52663143	0.0002476	0.00633946	1
dia	AE014134	13.5953204	0.6049797	1.52095733	0.0011439	0.02266836	1
sdt	AE014298	2.79679961	0.600187	1.515913	0.0017789	0.03205763	1
Flo1	AE013599	24.3267287	0.5976858	1.51328718	0.0024738	0.04205519	1
Patronin	AE013599	7.60319584	0.5974173	1.5130056	0.0019939	0.03532086	1
CG10413	AE014134	22.4781134	0.5948123	1.51027611	0.0025635	0.04320613	1
drpr	AE014296	25.0291022	0.5923627	1.50771387	0.0015976	0.02959459	1
CG8209	AE014296	30.9320886	0.5916775	1.50699796	0.0010624	0.02124438	1
stv	AE014296	10.3515236	0.591345	1.50665076	0.0014232	0.02711083	1
Ssk	AE014296	963.134726	0.5853085	1.50035983	0.0012426	0.02437931	1
CG10472	AE014296	8512.36782	-0.585805	-1.5008759	0.0016418	0.03023486	1
CG17734	AE014297	45.86009	-0.589385	-1.5046048	0.0022303	0.03858472	1
dj-1beta	AE014297	33.0173856	-0.594583	-1.5100357	0.0027344	0.04565206	1
CG15255	AE014134	626.996822	-0.597261	-1.5128419	0.002426	0.04136069	1
SelG	AE014298	79.7335073	-0.602725	-1.5185824	0.0004654	0.01069618	1
Hmgcr	AE014297	13.7873887	-0.610231	-1.5265036	0.0001248	0.00358845	1
Eglp4	AE013599	50.8540177	-0.611541	-1.5278898	0.000508	0.01149381	1
CG2930	AE014298	343.507796	-0.618573	-1.5353561	0.0009789	0.01977532	1
Mpc1	AE014297	69.2994846	-0.631889	-1.5495931	0.0006697	0.01436661	1
CG9005	AE013599	11.648878	-0.637946	-1.556112	0.0002858	0.00712469	1
Ance	AE014134	810.207572	-0.644043	-1.5627028	0.0007912	0.01649264	1
PPP1R15	AE013599	18.9310217	-0.647057	-1.56597	0.001206	0.02371408	1
CG4053	AE014297	113.327756	-0.647472	-1.5664207	0.0022936	0.03952318	1
CG15773	AE014298	28.0113041	-0.650856	-1.5700992	0.0012962	0.02517917	1
CG5110	AE014134	34.5382093	-0.657843	-1.5777216	0.0008225	0.01702341	1
Dh31-R	AE013599	9.70788619	-0.659927	-1.5800022	0.0019435	0.03453221	1
CG40228	AE014296	12.2485801	-0.663093	-1.5834736	0.0006424	0.01389791	1
Rab32	AE013599	19.8343849	-0.66976	-1.5908081	9.769E-05	0.00290548	1
Drip	AE013599	22.7028394	-0.66993	-1.5909955	0.0007176	0.01520982	1
Gs1	AE014134	27.187116	-0.674055	-1.5955516	4.814E-05	0.00156034	0.8519439
RpS15Ab	AE013599	22.0156051	-0.675239	-1.5968609	0.0014322	0.02719792	1
GlyP	AE014134	25.0371835	-0.679872	-1.6019972	0.0001412	0.00394005	1
CG3332	AE014134	71.426874	-0.680432	-1.6026198	0.0006819	0.01455763	1
Ag5r2	AE014298	988.150282	-0.685149	-1.607868	0.0001817	0.00490798	1
CG17292	AE014134	33.0397337	-0.686867	-1.609784	9.435E-05	0.00282526	1
CG45078	AE014297	33.9648237	-0.688815	-1.6119594	0.0003226	0.00784378	1
CG17556	AE014297	23.2764553	-0.690216	-1.6135252	0.0005667	0.01252842	1
CG31705	AE014134	9.6808593	-0.691524	-1.6149881	0.0008422	0.01733914	1
CG17029	AE014296	88.5735064	-0.69266	-1.6162611	0.000221	0.00576854	1
iotaTry	AE013599	284.551653	-0.69301	-1.6166534	0.002579	0.04342509	1
CG9664	AE014134	5.84327416	-0.693399	-1.6170884	0.0013951	0.0266618	1
Phae1	AE014134	166.749324	-0.694389	-1.618199	0.0004444	0.0102269	1
CG6321	AE014296	10.024752	-0.695219	-1.6191302	0.0007775	0.01626442	1
CG6067	AE014298	183.934169	-0.695965	-1.6199672	0.0027333	0.04565206	1

Fer1HCH	AE014297	1237.77179	-0.697676	-1.6218899	0.0001391	0.00391417	1
gb	AE014297	7.75110136	-0.698426	-1.6227335	0.0029043	0.04812472	1
ade3	AE014134	4.46670507	-0.698581	-1.6229073	0.0003645	0.00868103	1
lambdaTry	AE013599	1030.76246	-0.699165	-1.6235649	0.0001257	0.00359917	1
CG8888	AE013599	15.5126685	-0.700964	-1.6255901	0.0001757	0.00476205	1
Ugt37b1	AE014134	19.7621798	-0.701373	-1.6260517	0.0015811	0.02936113	1
CG3534	AE014297	7.75677126	-0.702649	-1.6274907	0.0029702	0.04880552	1
CG7322	AE014298	19.162765	-0.704407	-1.6294745	0.0021358	0.03738624	1
pug	AE014297	20.3334889	-0.707813	-1.633326	4.208E-05	0.00138682	0.7447245
Pmp70	AE014298	161.205041	-0.708272	-1.6338464	0.0014256	0.02712829	1
Peritrophin-15a	AE014134	1535.96852	-0.708293	-1.6338699	0.0011492	0.02272296	1
CG10924	AE013599	12.4510559	-0.708639	-1.6342611	0.0029581	0.04865259	1
CG9981	AE014298	6.41234927	-0.7114	-1.6373925	0.0002746	0.0068921	1
CG1648	AE013599	31.0659178	-0.715364	-1.6418979	0.0015218	0.02852927	1
CG10877	AE014297	27.0482813	-0.717274	-1.6440723	0.0008619	0.01769472	1
CG8468	AE013599	7.26803646	-0.72231	-1.6498217	0.0004969	0.01128768	1
CG5883	AE014296	18.1382098	-0.723568	-1.6512607	0.0026266	0.04418605	1
CG8664	AE014298	12.2345117	-0.72358	-1.651275	0.0017037	0.03105093	1
CG42372	AE013599	11.9680688	-0.723697	-1.651409	0.002922	0.04832782	1
CG43346	AE014134	8.13370058	-0.724485	-1.6523103	0.0005151	0.01161191	1
CG8270	AE014296	4.82798172	-0.729617	-1.658199	0.0017285	0.03127813	1
CG30100	AE013599	11.4452524	-0.733738	-1.662942	0.0022304	0.03858472	1
CG5080	AE014134	15.8376059	-0.734126	-1.6633899	0.0004098	0.00957991	1
CG10505	AE013599	20.5185864	-0.735909	-1.6654468	0.003029	0.04961056	1
RluA-1	AE014134	16.9404418	-0.736431	-1.6660494	1.331E-05	0.00050549	0.2355587
CG17841	AE014298	42.5385733	-0.73723	-1.6669717	4.517E-05	0.00147485	0.7993692
alpha-Man-IIa	AE014297	2.25210002	-0.73912	-1.6691577	0.0011863	0.02337953	1
CG31233	AE014297	798.102628	-0.739327	-1.6693973	0.0004289	0.00995213	1
Gs2	AE014298	142.387782	-0.744698	-1.6756232	0.0013833	0.02649377	1
CG17167	AE014298	33.4317006	-0.745721	-1.6768124	0.0002141	0.00561209	1
CG15443	AE014134	6.67813826	-0.755556	-1.6882816	0.0010246	0.02058246	1
AstA-R2	AE014297	7.50940932	-0.758224	-1.6914067	0.0003385	0.00816126	1
dmGlut	AE014134	369.616212	-0.758588	-1.6918334	6.023E-05	0.00191027	1
CG31821	AE014134	56.480173	-0.769083	-1.7041862	3.494E-06	0.0001523	0.0618342
CG32669	AE014298	83.0823908	-0.775347	-1.7116011	0.0002123	0.00557398	1
mira	AE014297	11.680817	-0.778508	-1.7153563	0.0002937	0.00729074	1
Kaz-m1	AE014297	176.728481	-0.781495	-1.7189116	0.0004291	0.00995213	1
CycG	AE014297	17.5658421	-0.785996	-1.7242821	0.0016751	0.0306558	1
CG5482	AE013599	22.6827696	-0.786563	-1.7249597	4.187E-05	0.00138544	0.741028
CCHa2	AE014297	36.4390329	-0.790893	-1.7301455	0.0002002	0.00529101	1
CG34330	AE014298	1436.63131	-0.796119	-1.7364232	1.709E-05	0.00063133	0.3024077
Nep1	AE014298	10.414999	-0.797582	-1.7381849	3.626E-05	0.00121533	0.6416928
CG5167	AE014297	238.077651	-0.802114	-1.7436545	0.0023235	0.03996017	1
CG30495	AE013599	24.771706	-0.807291	-1.749923	0.0004814	0.01102002	1
CG13601	AE014297	18.1880317	-0.807698	-1.7504167	6.85E-05	0.00215314	1
IA-2	AE014134	6.53481521	-0.813525	-1.7574998	1.493E-06	7.178E-05	0.026415

CG30382	AE013599	118.991988	-0.816223	-1.7607903	3.311E-05	0.00112354	0.5860203
CG3036	AE014134	80.2232042	-0.816331	-1.7609214	0.0003545	0.00848437	1
CG11151	AE014298	422.898764	-0.817584	-1.7624526	0.0008823	0.01809329	1
CG10592	AE014296	752.765644	-0.819739	-1.7650865	0.0001228	0.0035464	1
CG8562	AE014296	705.960711	-0.820701	-1.7662641	1.039E-05	0.00040661	0.1837866
CG17633	AE014134	4966.04922	-0.820913	-1.7665237	0.0001921	0.00512024	1
CG13950	AE014134	12.9631305	-0.828904	-1.7763352	0.0013726	0.02640269	1
CG14516	AE014297	4.3092383	-0.833895	-1.7824914	0.000116	0.0033712	1
ClC-a	AE014297	8.59096122	-0.83407	-1.7827081	1.595E-05	0.00059691	0.2823401
CG9485	AE013599	4.66382363	-0.835489	-1.7844616	0.0002829	0.00706079	1
AstA	AE014297	19.696567	-0.837384	-1.786807	1.484E-05	0.00055893	0.2626986
CG45085	AE013599	18.8899593	-0.837921	-1.7874729	6.341E-06	0.00026035	0.1122092
CG4615	AE014298	9.44989325	-0.840321	-1.7904488	0.000182	0.00490989	1
Fer2LCH	AE014297	712.112301	-0.841313	-1.7916805	0.0002245	0.00585178	1
CG14820	AE014296	174.850565	-0.843851	-1.7948342	0.000141	0.00394005	1
Gabat	AE014296	18.4960769	-0.844147	-1.7952025	0.0016463	0.03025465	1
CG4991	AE014298	31.8718067	-0.84766	-1.7995802	7.058E-06	0.00028712	0.1248986
CG3940	AE014297	45.2911643	-0.856833	-1.8110587	4.746E-06	0.00020189	0.0839847
CG31267	AE014297	122.629267	-0.857187	-1.8115026	0.0001234	0.00355675	1
rgr	AE013599	3.393262	-0.862445	-1.8181173	0.0001724	0.00470155	1
CG9394	AE013599	187.935152	-0.864067	-1.8201625	0.0007584	0.01593913	1
LManVI	AE014134	260.689671	-0.86529	-1.8217055	0.0007453	0.01571546	1
sls	AE014296	0.5329756	-0.868163	-1.8253368	1.947E-05	0.00071195	0.3445859
CG3609	AE014134	174.037377	-0.869406	-1.8269103	0.0012671	0.02473029	1
SmydA-9	AE014298	5.87798587	-0.869716	-1.827303	0.0002398	0.00617657	1
CG3706	AE014298	138.490433	-0.870919	-1.8288278	0.0002458	0.00630504	1
CG31463	AE014297	64.934241	-0.872918	-1.8313634	5.739E-06	0.00024007	0.1015676
CG30043	AE013599	14.4361275	-0.873923	-1.8326391	0.0006847	0.01459845	1
Jon99Fi	AE014297	5150.07379	-0.874635	-1.8335447	0.0001489	0.00415091	1
CG8299	AE013599	599.868653	-0.887372	-1.849804	0.0003304	0.00798332	1
CG31266	AE014297	255.429633	-0.888432	-1.8511626	0.0006466	0.01393779	1
tn	AE013599	5.15374204	-0.891023	-1.8544909	6.603E-07	3.5195E-05	0.0116849
Pdxk	AE014296	178.641745	-0.891705	-1.8553676	4.656E-05	0.00151743	0.8239621
CG8785	AE013599	204.639714	-0.893428	-1.8575846	0.0004321	0.01000855	1
zetaTry	AE013599	367.990941	-0.894848	-1.8594139	0.0002002	0.00529101	1
CG3348	AE014297	137.525201	-0.896082	-1.8610045	2.452E-05	0.00086814	0.4339156
Toll-9	AE014296	4.98158269	-0.898189	-1.8637254	0.0005678	0.01252842	1
Ugt86Dh	AE014297	31.7860819	-0.901522	-1.8680352	2.085E-07	1.2422E-05	0.0036893
Bace	AE014134	12397.0024	-0.904337	-1.8716847	2.949E-05	0.00101736	0.5219076
CG9903	AE014298	73.1233261	-0.908335	-1.8768784	0.0001261	0.00359917	1
LManII	AE014134	135.358586	-0.91055	-1.8797616	0.0008532	0.01753644	1
CG7953	AE014134	2798.18772	-0.911841	-1.8814454	0.0009725	0.01966838	1
CG11852	AE014297	23.7674383	-0.915129	-1.8857383	4.006E-06	0.00017164	0.0708885
CG9609	AE014298	3.79599921	-0.9229	-1.8959224	0.0017257	0.03125944	1
Ppat-Dpck	AE014296	95.0257475	-0.925506	-1.8993506	0.0002534	0.00644338	1
CG31975	AE014134	15.199634	-0.930105	-1.9054145	3.972E-06	0.00017059	0.0702847

Cyp4d1	AE014298	25.7046227	-0.934218	-1.9108548	1.305E-05	0.00049868	0.2310141
CG15534	AE014297	309.002222	-0.937352	-1.9150106	0.000365	0.00868132	1
CG14615	AE014298	26.1611972	-0.937379	-1.9150462	1.174E-06	5.8738E-05	0.0207708
SCAP	AE013599	5.27225982	-0.939426	-1.9177654	5.315E-06	0.00022448	0.0940565
CG8997	AE014134	2988.62034	-0.939616	-1.9180175	0.0005035	0.01141023	1
CG11158	AE014298	15.1869203	-0.943809	-1.9236005	5.112E-07	2.7836E-05	0.0090466
CG13607	AE014297	5.08083029	-0.945218	-1.9254795	0.0021798	0.03789423	1
Oatp74D	AE014296	1.93686966	-0.946242	-1.9268472	0.0015026	0.02822861	1
CG7542	AE014296	1522.6717	-0.948654	-1.9300708	2.627E-07	1.5291E-05	0.0046484
GstE3	AE013599	506.998799	-0.950104	-1.932012	0.0013104	0.02542711	1
CG17475	AE014297	270.834448	-0.957504	-1.9419472	8.946E-05	0.00271553	1
CG6295	AE014297	4011.83147	-0.958599	-1.9434211	1.825E-05	0.00067278	0.3229367
CG1946	AE013599	77.4231245	-0.96485	-1.95186	3.235E-06	0.00014278	0.0572543
PGRP-SC1b	AE013599	71.4462634	-0.966941	-1.9546919	0.0001693	0.00465232	1
lili	AE014297	10.19977	-0.972477	-1.9622073	6.895E-07	3.6423E-05	0.0122016
NPF	AE014297	52.3484481	-0.985127	-1.9794877	2.825E-07	1.6394E-05	0.0050002
CG9629	AE014296	10.1409645	-0.985656	-1.9802136	2.238E-05	0.00080191	0.3961457
CG10365	AE014297	26.764432	-0.989851	-1.9859799	8.154E-06	0.00032574	0.1443036
CG4839	AE014134	14.9963653	-0.990125	-1.9863569	6.046E-07	3.2324E-05	0.0106994
AhcyL2	AE014297	21.1044172	-0.991162	-1.9877855	2.216E-06	0.00010211	0.0392084
CG3552	AE014296	5.48103742	-0.994086	-1.9918188	0.0002003	0.00529101	1
Cyp4d8	AE014296	23.8163318	-0.999052	-1.9986865	7.986E-06	0.00031976	0.1413343
Jon65Aiii	AE014296	24649.4424	-1.007564	-2.0105137	3.081E-07	1.759E-05	0.005453
CG12374	AE013599	44828.1779	-1.009047	-2.0125806	1.981E-06	9.249E-05	0.0350539
Nha1	AE014134	91.0069471	-1.009114	-2.0126745	2.882E-06	0.00012913	0.0510078
CG11912	AE014134	1590.90121	-1.019442	-2.0271346	1.573E-07	9.7436E-06	0.0027839
CG11741	AE014297	24.9173609	-1.021483	-2.030005	5.576E-06	0.00023495	0.0986796
GC1	AE014297	44.8368545	-1.023697	-2.0331225	1.029E-09	1.0175E-07	1.821E-05
Cyp6d5	AE014297	455.91053	-1.026503	-2.0370802	8.014E-05	0.00247083	1
CG17249	AE014296	4.95960022	-1.028099	-2.039336	0.0002877	0.00716034	1
CG13937	AE014296	2.92862601	-1.029812	-2.0417578	0.0014716	0.02773384	1
Pepck	AE013599	15.6422316	-1.032865	-2.046083	3.748E-07	2.1006E-05	0.0066322
mip40	AE013599	7.95763647	-1.035025	-2.0491485	0.0001301	0.00369071	1
Pif1B	AE014297	7.3451517	-1.037281	-2.0523566	7.305E-08	4.8971E-06	0.0012928
CG11162	AE014298	48.1934449	-1.039805	-2.0559495	3.39E-06	0.00014813	0.0599943
CG2493	AE014134	2.82149382	-1.041968	-2.0590347	0.0019109	0.03402086	1
CG34386	AE013599	6.25641833	-1.045535	-2.0641319	3.379E-05	0.00114334	0.5979691
CG14989	AE014296	19.738404	-1.058516	-2.0827881	5.612E-08	3.8052E-06	0.0009931
Cyp311a1	AE014298	25.1726065	-1.059689	-2.0844819	1.862E-07	1.117E-05	0.0032951
AstC	AE014134	32.8191832	-1.06573	-2.0932282	8.119E-05	0.00249865	1
tgy	AE014298	17.4190957	-1.069837	-2.0991955	3.273E-07	1.8623E-05	0.0057919
CG5157	AE014296	8.2795633	-1.07075	-2.100525	0.0003777	0.00892441	1
CG6296	AE014297	172.657532	-1.071822	-2.102086	0.000135	0.00381703	1
yin	AE014298	2.28529575	-1.073737	-2.1048789	0.0014147	0.02697772	1
Tmhs	AE014296	2.01561178	-1.074396	-2.1058397	0.0013337	0.02579518	1
CG4752	AE013599	37.6475182	-1.074458	-2.1059306	0.0002587	0.00653541	1

CG8026	AE013599	38.2895336	-1.078885	-2.1124023	1.775E-07	1.0793E-05	0.0031407
CG8745	AE014296	124.9909	-1.086659	-2.1238167	7.472E-06	0.00030258	0.1322276
Jon99Ciii	AE014297	21240.5119	-1.087505	-2.1250615	3.079E-05	0.0010561	0.5449486
CG32165	AE014296	2.16575378	-1.09405	-2.1347248	0.0005619	0.01246792	1
CG9641	AE014134	2.24028488	-1.095366	-2.1366729	0.0008392	0.01730959	1
CG15706	AE013599	22.0594584	-1.096609	-2.1385145	3.073E-08	2.2751E-06	0.0005438
CG5150	AE014296	692.613267	-1.099918	-2.1434248	2.055E-06	9.5224E-05	0.0363754
CG13313	AE014296	8.87840912	-1.10188	-2.1463421	2.432E-05	0.0008642	0.4303727
CG14629	AE014298	214.88858	-1.102827	-2.1477519	8.295E-08	5.4773E-06	0.0014679
CG3746	AE013599	6.68631623	-1.10481	-2.1507059	0.0006602	0.0141964	1
CG14120	AE014296	157.050121	-1.105762	-2.1521251	0.000154	0.00427753	1
Ctr1A	AE014298	18.2850269	-1.108751	-2.1565889	3.553E-08	2.5661E-06	0.0006287
CG7720	AE014297	15.9469424	-1.111976	-2.1614152	1.161E-05	0.00044799	0.2053972
CG33306	AE014134	761.161528	-1.112735	-2.1625518	9.687E-06	0.00038013	0.1714364
CG18585	AE014134	357.040996	-1.119569	-2.1728212	2.782E-06	0.00012498	0.0492407
CG8661	AE014298	1500.81018	-1.121115	-2.1751495	4.242E-07	2.3679E-05	0.0075064
Jon74E	AE014296	4760.20772	-1.127116	-2.1842163	1.398E-08	1.1347E-06	0.0002474
CG32695	AE014298	9.50463085	-1.129281	-2.1874964	1.31E-05	0.00049868	0.2318382
Jon65Aii	AE014296	1086.76591	-1.129969	-2.1885404	0.0001359	0.00383592	1
CG45087	AE013599	16.3202323	-1.133851	-2.1944367	1.369E-08	1.1168E-06	0.0002423
CG42488	AE014297	2.21673572	-1.13589	-2.1975411	0.0012779	0.02485228	1
CG11594	AE014296	20.7008914	-1.148655	-2.2170709	1.535E-09	1.4846E-07	2.717E-05
Jon65Aiv	AE014296	37523.1024	-1.148719	-2.2171689	9.653E-09	8.1345E-07	0.0001708
7B2	AE014297	17.4425862	-1.152454	-2.222917	2.152E-07	1.2781E-05	0.0038087
CG34423	AE013599	5.93595219	-1.155445	-2.2275297	0.0021726	0.03784342	1
CG6834	AE014297	3.79326157	-1.159222	-2.2333701	0.0001706	0.00466604	1
H2.0	AE014134	2.07451926	-1.163088	-2.2393631	0.0008056	0.01675216	1
CG32407	AE014296	19.6930162	-1.166894	-2.2452772	1.129E-05	0.0004383	0.1998643
l(2)k05911	AE014134	2.0702935	-1.167125	-2.2456375	0.0001875	0.00502009	1
CG17294	AE014134	6.34492163	-1.168412	-2.247642	0.0001257	0.00359917	1
CG1358	AE013599	18.4245615	-1.181561	-2.2682213	1.151E-10	1.3222E-08	2.036E-06
CG9360	AE014298	14.9432685	-1.187073	-2.2769036	0.0023793	0.04072266	1
t	AE014298	6.47400361	-1.188018	-2.2783948	5.976E-06	0.00024767	0.1057537
CG10621	AE014134	57.7684688	-1.188265	-2.2787856	3.303E-08	2.4058E-06	0.0005846
PH4alphaPV	AE014297	9.06574165	-1.18998	-2.2814951	3.485E-05	0.00117491	0.6168262
CG6293	AE014297	3.20997603	-1.191851	-2.2844561	0.0006006	0.01312201	1
CG15661	AE013599	11.2708449	-1.19545	-2.2901618	8.643E-08	5.6439E-06	0.0015295
Nrt	AE014296	0.99456008	-1.199642	-2.296827	0.0013514	0.02605242	1
wit	AE014296	7.57905799	-1.200848	-2.2987474	2.158E-08	1.6606E-06	0.0003819
CG14606	AE014297	22.3535207	-1.202013	-2.3006046	4.319E-05	0.00141813	0.7643701
srp	AE014297	1.97349231	-1.214806	-2.321095	2.911E-07	1.6834E-05	0.0051511
Ugt36Bc	AE014134	155.329726	-1.215837	-2.3227545	1.135E-05	0.00043935	0.2007808
Pal2	AE013599	8.5703033	-1.224124	-2.3361358	5.683E-09	5.0284E-07	0.0001006
hoe1	AE014134	1.40110551	-1.225135	-2.3377733	0.0030302	0.04961056	1
Jon99Ci	AE014297	1869.61672	-1.22517	-2.3378301	5.519E-07	2.9871E-05	0.0097678
LpR1	AE014297	34.6555864	-1.228579	-2.3433611	1.04E-07	6.6713E-06	0.0018413

CG7231	AE014134	239.17184	-1.234402	-2.3528388	4.412E-07	2.4552E-05	0.0078075
Jafrac1	AE014298	370.91659	-1.238535	-2.3595886	5.353E-08	3.672E-06	0.0009474
CG6733	AE014297	3.09413031	-1.239635	-2.361388	0.0029489	0.04856971	1
aay	AE014296	32.6478295	-1.248309	-2.375628	5.675E-06	0.00023799	0.1004324
robo2	AE014134	1.21594982	-1.256671	-2.3894372	2.315E-05	0.00082615	0.409769
CG6656	AE014297	6.33680001	-1.25756	-2.3909102	3.805E-05	0.00127068	0.6734585
Ugt36Ba	AE014134	12.4711207	-1.26974	-2.4111803	9.455E-08	6.1065E-06	0.0016732
CG5107	AE014297	2731.56458	-1.270087	-2.4117605	6.561E-11	7.8448E-09	1.161E-06
Mpcp1	AE013599	7.5978789	-1.283675	-2.4345836	1.994E-05	0.00072148	0.352803
MFS1	AE013599	120.501453	-1.295165	-2.4540503	5.987E-05	0.00190421	1
CG14205	AE014298	82.6464401	-1.311173	-2.4814315	0.0012484	0.02443932	1
CG5160	AE014134	13.0283465	-1.313887	-2.4861042	8.464E-09	7.2713E-07	0.0001498
CG43797	AE014134	4.62803639	-1.315831	-2.4894561	0.0001068	0.00314093	1
Chrac-16	AE014298	4.67366198	-1.334091	-2.521165	0.0005036	0.01141023	1
epsilonTry	AE013599	8419.37014	-1.336783	-2.5258739	1.271E-11	1.6781E-09	2.249E-07
CG4239	AE014298	8.67421327	-1.338927	-2.5296317	3.352E-11	4.148E-09	5.932E-07
CG32212	AE014296	62.8522247	-1.343292	-2.537296	1.732E-09	1.6657E-07	3.065E-05
CG7916	AE014134	2085.73852	-1.351526	-2.5518198	1.409E-07	8.8402E-06	0.0024929
CG30031	AE013599	272.110878	-1.354674	-2.5573927	5.003E-05	0.00161869	0.8854228
CG30338	AE013599	4.64773126	-1.356418	-2.5604866	9.399E-05	0.00281918	1
CG7025	AE014134	111.77336	-1.357069	-2.5616419	3.122E-06	0.00013883	0.0552544
CG1942	AE013599	39.0253164	-1.358761	-2.5646476	3.048E-07	1.7512E-05	0.0053937
CG8319	AE014297	2.4494957	-1.360937	-2.5685197	0.000554	0.01233253	1
CG7881	AE013599	48.7853938	-1.363626	-2.5733113	1.697E-10	1.9134E-08	3.004E-06
CG31343	AE014297	1037.60142	-1.366117	-2.5777575	4.566E-11	5.4973E-09	8.081E-07
CG11560	AE014296	8.62356082	-1.368583	-2.5821684	3.439E-07	1.9507E-05	0.0060862
CG34445	AE013599	6.01278469	-1.371093	-2.5866654	0.0003227	0.00784378	1
Npc2f	AE014297	199.938182	-1.372759	-2.5896537	2.311E-07	1.3618E-05	0.0040903
Pldn	AE014296	29.1117846	-1.388096	-2.6173303	5.351E-12	7.6985E-10	9.469E-08
CG17192	AE014297	636.135191	-1.389628	-2.6201105	6.81E-07	3.6191E-05	0.0120517
CG18404	AE014297	1883.78669	-1.392176	-2.6247426	1.749E-13	3.0338E-11	3.094E-09
CG17906	AE014134	6.75123454	-1.394251	-2.6285201	1.883E-05	0.00069139	0.3332489
CG17119	AE014297	182.321254	-1.405801	-2.6496481	8.46E-08	5.5654E-06	0.0014971
CG7860	AE014298	5.43211124	-1.408401	-2.6544284	2.657E-05	0.00093059	0.4701785
Zip42C.2	AE013599	20.8556926	-1.408924	-2.6553912	3.067E-07	1.7565E-05	0.0054275
CG30047	AE013599	17.7519056	-1.423106	-2.6816223	4.767E-08	3.308E-06	0.0008435
CG7120	AE014296	1.71129636	-1.442471	-2.717859	3.431E-05	0.00115876	0.6071889
Jon99Cii	AE014297	42824.5131	-1.452497	-2.7368134	3.19E-09	2.9405E-07	5.646E-05
Jon65Ai	AE014296	2565.5192	-1.46847	-2.7672832	1.779E-08	1.3927E-06	0.0003148
CG13284	AE014134	35.5033463	-1.475843	-2.781461	0	0	0
Kua	AE014134	9.03560095	-1.481423	-2.7922398	8.827E-11	1.0346E-08	1.562E-06
MFS9	AE014297	6.55917089	-1.494078	-2.81684	4.543E-08	3.1654E-06	0.000804
Tk	AE014297	66.1232349	-1.496442	-2.8214598	5.551E-16	1.3644E-13	9.824E-12
NAAT1	AE014298	133.39107	-1.500257	-2.8289319	1.714E-10	1.9194E-08	3.033E-06
CG12519	AE014296	9.04554351	-1.516688	-2.8613344	1.936E-06	9.0649E-05	0.0342654
thetaTry	AE013599	1531.42595	-1.517846	-2.863632	6.891E-10	6.9689E-08	1.22E-05

CG6462	AE014296	19.964132	-1.518801	-2.8655285	7.967E-11	9.3989E-09	1.41E-06
Ptp10D	AE014298	0.68317946	-1.524157	-2.8761863	9.297E-06	0.00036724	0.1645251
JhI-26	AE013599	86.0971077	-1.526346	-2.880554	2.746E-09	2.5576E-07	4.859E-05
CG8560	AE014296	2252.61403	-1.526591	-2.881042	2.358E-09	2.2074E-07	4.172E-05
LysE	AE014296	68.9602733	-1.527899	-2.8836566	1.033E-10	1.2024E-08	1.828E-06
Oat	AE014296	2.49388167	-1.544917	-2.9178723	0.0001127	0.00328874	1
CG9509	AE014298	92.3874785	-1.552693	-2.9336416	1.588E-11	2.0664E-09	2.81E-07
CG10623	AE014134	66.4031249	-1.585185	-3.0004626	2.489E-12	3.7017E-10	4.405E-08
Gbs-70E	AE014296	4.67270019	-1.595997	-3.0230326	6.9E-08	4.6433E-06	0.0012212
CG12057	AE014298	6308.91817	-1.598093	-3.0274294	2.674E-10	2.8512E-08	4.733E-06
boi	AE014298	0.86957495	-1.600503	-3.0324903	4.131E-06	0.00017617	0.0731122
CG6726	AE014297	9.41259063	-1.607793	-3.0478515	3.143E-11	3.9172E-09	5.562E-07
CG10550	AE014297	162.53335	-1.609135	-3.0506898	1.164E-09	1.1445E-07	2.06E-05
Cadps	AE014135	0.44717142	-1.622216	-3.0784747	0.0003256	0.00788169	1
CG8908	AE013599	0.88899598	-1.626708	-3.0880761	1.999E-06	9.3091E-05	0.0353746
CG9413	AE014298	15.9889553	-1.629784	-3.0946673	1.987E-14	3.6257E-12	3.517E-10
CG1532	AE014298	297.062085	-1.648799	-3.1357249	5.103E-10	5.2507E-08	9.031E-06
CG17571	AE014134	3875.58695	-1.649946	-3.138218	1.571E-13	2.7526E-11	2.78E-09
l(2)03659	AE013599	0.34235311	-1.661072	-3.1625148	0.0025036	0.04252119	1
CG14456	AE014296	5.79445852	-1.664543	-3.170132	2.598E-06	0.0001179	0.0459822
CG30265	AE013599	2.59459922	-1.666892	-3.1752973	7.61E-07	3.9493E-05	0.0134673
CG31454	AE014297	11.5462139	-1.671248	-3.1849007	1.898E-14	3.5366E-12	3.36E-10
vanin-like	AE014298	582.721719	-1.680475	-3.2053348	2.84E-08	2.121E-06	0.0005027
Sod3	AE013599	62.2176838	-1.684278	-3.2137943	1.11E-16	2.9769E-14	1.965E-12
yip7	AE014296	43417.142	-1.707765	-3.2665444	0	0	0
deltaTry	AE013599	1603.00845	-1.712421	-3.2771033	2.87E-12	4.2329E-10	5.079E-08
CG8129	AE014297	18.0290646	-1.728703	-3.3142976	1.192E-11	1.5855E-09	2.109E-07
sug	AE013599	73.2530955	-1.736171	-3.3314981	0	0	0
CG7781	AE014134	0.56316604	-1.769388	-3.4090934	0.0027289	0.04564603	1
CG43074	AE014296	22.1037291	-1.770139	-3.4108692	0.0001136	0.00330699	1
CG6908	AE014297	166.158753	-1.771583	-3.414284	1.263E-06	6.1931E-05	0.0223571
CG18607	AE013599	14.9051183	-1.785412	-3.447168	3.784E-08	2.6999E-06	0.0006696
Wnt5	AE014298	0.23810467	-1.788045	-3.4534669	0.0023746	0.04068332	1
CG14694	AE014297	24.4633647	-1.804687	-3.4935327	3.331E-16	8.4204E-14	5.894E-12
Lsp1gamma	AE014296	1.35013982	-1.811541	-3.5101705	5.273E-05	0.0016968	0.9332411
CG4594	AE014134	7.14402674	-1.817751	-3.5253116	6.592E-10	6.7044E-08	1.167E-05
CG13160	AE013599	2.0716027	-1.822329	-3.536517	1.58E-07	9.7436E-06	0.0027964
Slc45-1	AE014296	0.70390573	-1.825738	-3.5448837	0.0016666	0.03056358	1
Jon25Biii	AE014134	18992.4854	-1.835181	-3.5681608	7.883E-15	1.5852E-12	1.395E-10
CG9246	AE014134	20.9886871	-1.854299	-3.6157614	0	0	0
CG11893	AE014297	18.9290563	-1.85804	-3.6251473	9.166E-12	1.2575E-09	1.622E-07
CG13077	AE014134	28.5475707	-1.859568	-3.6289891	7.655E-13	1.2127E-10	1.355E-08
salt	AE014297	2.77505353	-1.863579	-3.6390926	7.593E-05	0.00235535	1
CG2678	AE014297	0.57976478	-1.890606	-3.7079084	0.0011235	0.02233902	1
CG3635	AE014134	18.726149	-1.890648	-3.7080168	0	0	0
Hayan	AE014298	0.94211949	-1.893694	-3.7158551	0.000423	0.00984885	1

CG12115	AE014298	0.99185446	-1.923274	-3.7928277	0.0022228	0.03852751	1
Zip71B	AE014296	5.52183293	-1.926574	-3.8015144	1.794E-10	1.9965E-08	3.174E-06
pre-mod(mdg4)-Y	AE014297	0.89249892	-1.932285	-3.8165924	0.0016963	0.03094703	1
GstO1	AE014296	3.86438259	-1.940713	-3.838953	7.8E-07	4.0243E-05	0.0138035
CG13012	AE014298	22.6677027	-1.947436	-3.8568848	8.988E-08	5.8265E-06	0.0015906
Smvt	AE014297	2.83693881	-1.960859	-3.8929373	2.624E-06	0.00011876	0.0464347
CG9497	AE014134	0.66784352	-1.968718	-3.9142025	0.0015333	0.02863604	1
CG4830	AE014297	67.9119812	-1.973544	-3.9273182	0	0	0
Ser6	AE014298	383.117567	-1.979836	-3.9444818	0	0	0
CG11889	AE014297	0.39752546	-1.987885	-3.9665513	0.0014924	0.02808964	1
CG9682	AE014297	823.77648	-1.995942	-3.9887654	0	0	0
mthl9	AE014296	8.51008978	-2.003135	-4.0087019	1.825E-13	3.136E-11	3.23E-09
Oatp33Ea	AE014134	90.3551277	-2.014945	-4.0416525	0	0	0
CG5246	AE014297	513.901174	-2.022723	-4.0635015	5.44E-15	1.1886E-12	9.627E-11
CG11911	AE014134	7641.00414	-2.02736	-4.0765818	0	0	0
hig	AE013599	0.17353222	-2.034185	-4.0959127	0.0020096	0.03552825	1
Gen	AE014296	0.26500383	-2.034914	-4.097982	0.0019174	0.03410221	1
Jon25Bi	AE014134	9139.46423	-2.039138	-4.1099998	9.512E-12	1.2948E-09	1.683E-07
GILT2	AE014297	5.20881112	-2.046723	-4.1316631	9.653E-07	4.9228E-05	0.0170821
Fer3	AE014297	8.0246609	-2.079858	-4.2276574	1.444E-08	1.1669E-06	0.0002555
CG12490	AE013599	3.11754602	-2.080094	-4.2283479	1.227E-06	6.0646E-05	0.0217111
st	AE014296	0.64530731	-2.104441	-4.3003124	0.0003461	0.00832208	1
CG13078	AE014134	56.4175728	-2.111882	-4.3225479	3.345E-09	3.0513E-07	5.92E-05
Oatp58Db	AE013599	0.28666103	-2.112054	-4.3230633	0.0024366	0.0415026	1
shd	AE014296	3.85592541	-2.117363	-4.3390005	1.916E-11	2.4223E-09	3.391E-07
Prx2540-2	AE013599	31.7028134	-2.121215	-4.3506031	0	0	0
MtnC	AE014297	2014.0583	-2.138612	-4.4033808	2.998E-15	6.8011E-13	5.305E-11
NaPi-T	AE013599	1.81349354	-2.145066	-4.4231246	6.982E-07	3.6776E-05	0.0123567
CG18180	AE014296	9165.57624	-2.160289	-4.4700425	4.108E-15	9.087E-13	7.27E-11
Hsp27	AE014296	5.9671201	-2.171273	-4.5042061	3.514E-05	0.00118228	0.6218813
Or45b	AE013599	0.62990486	-2.183893	-4.5437812	0.0005672	0.01252842	1
CG7091	AE014297	1.59396428	-2.195043	-4.579034	8.556E-05	0.00260159	1
Cyp6a20	AE013599	9.30180234	-2.207585	-4.6190141	1.11E-16	2.9769E-14	1.965E-12
CG33012	AE013599	1.23809836	-2.242675	-4.7327362	1.891E-06	8.924E-05	0.033465
MtnA	AE014297	2111.50453	-2.249302	-4.754529	0	0	0
CG10560	AE014297	1.59505207	-2.249616	-4.7555619	0.0001168	0.00338866	1
Oatp58Dc	AE013599	1.67735379	-2.270856	-4.8260933	0.00027	0.00679713	1
CG43134	AE014298	117.886051	-2.272539	-4.8317285	2.736E-06	0.00012353	0.0484219
Ggt-1	AE014298	243.006436	-2.275746	-4.8424783	0	0	0
Jon44E	AE013599	855.716644	-2.291142	-4.8944328	0	0	0
CG14292	AE014297	35.7967315	-2.319851	-4.9928073	3.2E-05	0.00108915	0.5663576
CG15820	AE014296	0.59295577	-2.326406	-5.0155418	0.000253	0.00644313	1
CG17191	AE014297	4.04062439	-2.326542	-5.0160152	5.909E-10	6.0444E-08	1.046E-05
GstO3	AE014296	1314.59882	-2.327245	-5.018461	0	0	0
vas	AE014134	0.46041051	-2.331249	-5.0324101	0.0028193	0.04693661	1

Cyp6t1	AE014298	69.5323776	-2.33549	-5.0472248	0	0	0
Mur18B	AE014298	56.0538014	-2.352612	-5.1074803	0.0014382	0.02725081	1
CG4586	AE014298	0.65253918	-2.354532	-5.1142827	0.0014344	0.02720654	1
CG8358	AE014297	4.08070226	-2.358359	-5.1278692	1.847E-13	3.1436E-11	3.269E-09
CG31436	AE014297	31.4537958	-2.361622	-5.1394784	0	0	0
LysD	AE014296	17230.3239	-2.364341	-5.1491727	7.772E-16	1.8338E-13	1.375E-11
Eip71CD	AE014296	814.550039	-2.391306	-5.2463221	3.331E-16	8.4204E-14	5.894E-12
CG10151	AE013599	0.16206576	-2.438719	-5.4215999	0.0026826	0.04499857	1
bru1	AE014134	0.24984348	-2.442604	-5.4362211	0.0014049	0.02682007	1
LysS	AE014296	721.199128	-2.468152	-5.5333452	7.883E-15	1.5852E-12	1.395E-10
Cyp9c1	AE013599	19.8885397	-2.475784	-5.5626957	0	0	0
MtnD	AE014297	507.624695	-2.479233	-5.5760093	0	0	0
CG14743	AE013599	0.29286017	-2.516687	-5.7226644	0.0003792	0.00893546	1
gammaTry	AE013599	788.910522	-2.546927	-5.8438823	0	0	0
Duox	AE014134	0.45228962	-2.569963	-5.9379436	0.0014936	0.02808964	1
kek1	AE014134	0.13970586	-2.582408	-5.9893854	0.0003003	0.0074233	1
fs(1)M3	AE014298	0.14489648	-2.603995	-6.0796774	0.0006718	0.01439427	1
CycB	AE013599	6.98622722	-2.611489	-6.1113397	2.364E-05	0.00084185	0.4183979
CG7366	AE014296	0.35578105	-2.624959	-6.16867	0.0008132	0.01689176	1
mael	AE014296	0.8302619	-2.649758	-6.2756211	1.193E-06	5.9125E-05	0.0211077
brv3	AE014298	2.14679096	-2.657471	-6.3092624	2.348E-13	3.8477E-11	4.155E-09
LysB	AE014296	6225.94781	-2.666354	-6.3482276	0	0	0
CG17570	AE014134	26.010701	-2.68351	-6.4241699	0	0	0
ap	AE013599	0.24241239	-2.707701	-6.5327972	0.0006207	0.01351174	1
CG3285	AE014134	0.53796152	-2.708959	-6.5384962	0.0003099	0.00760641	1
CG13114	AE014134	0.49756518	-2.712164	-6.553037	0.0021918	0.03806583	1
CG42540	AE014296	0.08517086	-2.712401	-6.5541156	0.0013803	0.02648607	1
nAChRalpha5	AE014134	0.04498617	-2.725416	-6.613508	0.0010876	0.02167458	1
Jon25Bii	AE014134	7730.84274	-2.764425	-6.7947723	0	0	0
MtnB	AE014297	289.924312	-2.775259	-6.8459882	0	0	0
MtnE	AE014297	404.884663	-2.796237	-6.9462606	4.441E-16	1.1069E-13	7.859E-12
Ugt36Bb	AE014134	3.93680727	-2.799071	-6.9599222	4.825E-08	3.3358E-06	0.000854
swa	AE014298	1.43740239	-2.801964	-6.9738895	0.0001823	0.00490989	1
CG18853	AE013599	0.75646907	-2.821842	-7.0706438	0.0018497	0.03306533	1
png	AE014298	0.78120615	-2.91124	-7.5226464	0.0016037	0.02959459	1
CG42235	AE014297	0.85792899	-2.927406	-7.6074111	2.153E-10	2.3815E-08	3.81E-06
CG5435	AE014134	0.40994167	-2.946831	-7.7105371	0.0007459	0.01571546	1
otu	AE014298	0.27331127	-2.982543	-7.9037794	0.0001654	0.00456617	1
CG32023	AE014296	4.54718486	-2.983013	-7.9063579	0.0013121	0.02543357	1
trp	AE014297	0.51828869	-2.986028	-7.922899	1.58E-07	9.7436E-06	0.0027955
RpS5b	AE014297	11.9693507	-3.010517	-8.0585307	5.752E-06	0.00024007	0.1017878
Npc2d	AE014297	592.100264	-3.016043	-8.0894568	0	0	0
CG14244	AE014297	0.52053598	-3.029532	-8.1654454	0.0022575	0.03893808	1
CG18179	AE014296	169.820254	-3.04982	-8.2810888	0	0	0
CG7882	AE013599	2.59446068	-3.090917	-8.5203769	3.175E-14	5.7339E-12	5.619E-10
yellow-g2	AE014296	0.62406771	-3.15354	-8.8983645	0.001057	0.02116102	1

CG7227	AE014134	4.95706406	-3.153616	-8.8988296	0	0	0
CG5282	AE014296	0.22840287	-3.16727	-8.9834549	0.0007801	0.01629945	1
stnB	AE014298	0.51712983	-3.175105	-9.0323748	8.579E-13	1.3435E-10	1.518E-08
CG7208	AE014297	0.40579365	-3.177568	-9.0478043	0.0011254	0.02235266	1
Cpr65Au	AE014296	1.61159522	-3.17868	-9.0547823	0.002093	0.03667381	1
rec	AE014297	1.08424339	-3.18638	-9.1032369	1.887E-15	4.3949E-13	3.34E-11
GNBP-like3	AE013599	3.87845489	-3.217505	-9.3017695	4.904E-07	2.6867E-05	0.0086782
CG15408	AE014134	1.30012119	-3.217868	-9.3041097	2.663E-05	0.00093059	0.471247
Listericin	AE013599	5.07972122	-3.231276	-9.3909849	0.0005287	0.01190356	1
wisp	AE014298	0.39091575	-3.23342	-9.4049469	1.951E-05	0.00071195	0.3452941
Cp18	AE014296	3.67531087	-3.300512	-9.8526483	2.427E-06	0.00011134	0.0429463
antr	AE013599	3.55437262	-3.304471	-9.8797257	1.898E-11	2.4169E-09	3.359E-07
stnA	AE014298	0.51508192	-3.328798	-10.047731	2.196E-13	3.6663E-11	3.886E-09
CG11659	AE014297	1.4286396	-3.442479	-10.871496	0.0010078	0.02029092	1
CG9825	AE013599	119.731166	-3.45692	-10.980867	0	0	0
lectin-28C	AE014134	0.18352683	-3.476108	-11.12789	5.993E-05	0.00190421	1
plu	AE013599	0.55686969	-3.485585	-11.201226	0.0030396	0.04962366	1
CG8028	AE014298	0.5541278	-3.550296	-11.715088	0.0002296	0.00597541	1
CG34215	AE013599	16.5856225	-3.720925	-13.185904	0	0	0
Gr64b	AE014296	0.09825027	-3.735271	-13.317677	0.0014401	0.02725747	1
Cp7Fc	AE014298	0.73667105	-3.771457	-13.655946	0.0002421	0.00621957	1
Ama	AE014297	1.02322958	-3.784573	-13.780655	0.0001908	0.00509224	1
CG14545	AE014297	0.80082034	-3.795105	-13.881632	0.000535	0.01197975	1
rpk	AE014297	0.64476273	-3.835499	-14.275796	0.0001087	0.00318495	1
CG34426	AE014296	1.19413129	-3.84396	-14.359762	0.0001737	0.00472995	1
Cp36	AE014298	7.00907083	-3.883423	-14.75798	1.545E-08	1.2428E-06	0.0002734
CG33655	AE013599	0.83724266	-3.890696	-14.83256	2.493E-06	0.0001134	0.0441129
CG7300	AE014134	0.99079463	-3.912149	-15.054767	0.0003144	0.00770674	1
CG5361	AE014297	4.092824	-3.943115	-15.381402	0	0	0
Obp83a	AE014297	0.8870613	-3.960865	-15.571811	9.804E-05	0.00291114	1
Obp56a	AE013599	5.8821034	-4.006753	-16.075064	0.0001403	0.00392989	1
Obp19c	AE014298	0.36494576	-4.012916	-16.143891	0.0009912	0.01997883	1
Trf4-2	AE014297	0.34276879	-4.013507	-16.150503	0.0003052	0.00751284	1
Cpr49Ab	AE013599	1.426425	-4.042129	-16.474115	0.0001706	0.00466604	1
mab-21	AE014298	0.2445114	-4.050956	-16.575214	0.0008996	0.01841535	1
fan	AE014296	0.23842888	-4.056515	-16.639215	0.0028244	0.04697663	1
Cyp6a8	AE013599	100.435777	-4.060108	-16.680698	5.995E-15	1.2939E-12	1.061E-10
zld	AE014298	0.05329707	-4.109827	-17.26558	0.0003548	0.00848437	1
Cnx14D	AE014298	0.73247337	-4.117886	-17.362297	3.688E-10	3.8848E-08	6.526E-06
CG34382	AE014296	0.07344573	-4.128602	-17.491737	0.002177	0.03788184	1
osk	AE014297	0.93568786	-4.133029	-17.545498	5.874E-06	0.00024402	0.1039538
CG9926	AE014297	0.32059409	-4.173059	-18.039148	0.0004025	0.00943647	1
phr	AE013599	10.663915	-4.205892	-18.454383	0	0	0
CG3457	AE014298	0.50155342	-4.214058	-18.559146	0.0003721	0.00882756	1
Spn43Aa	AE013599	1.35229845	-4.233799	-18.814843	2.534E-05	0.00089337	0.4484706
Cp38	AE014298	6.61466318	-4.248239	-19.004106	1.572E-08	1.2533E-06	0.0002782

Obp83b	AE014297	3.26989805	-4.274128	-19.348204	2.85E-09	2.6408E-07	5.044E-05
CG3649	AE013599	0.38073575	-4.279251	-19.417033	0.0005622	0.01246792	1
Cyp6a2	AE013599	463.51923	-4.297138	-19.659269	0	0	0
CG4563	AE013599	29.3619319	-4.311359	-19.854017	0	0	0
CG13299	AE014296	1.22126849	-4.331597	-20.134483	0.0003014	0.00743916	1
gammaTub37C	AE014134	1.03586151	-4.350463	-20.39952	1.974E-05	0.00071887	0.3493704
CG6927	AE014298	0.93885835	-4.361438	-20.555291	1.547E-06	7.4172E-05	0.0273693
Gr64c	AE014296	0.15610684	-4.397809	-21.080086	9.039E-05	0.00273437	1
CG14309	AE014297	0.08375667	-4.409081	-21.245442	0.0018601	0.03318444	1
CG11674	AE014298	1.99228332	-4.418353	-21.38241	8.838E-06	0.00035069	0.1564071
sisA	AE014298	0.36470878	-4.443277	-21.755031	0.001234	0.02423838	1
mtrm	AE014296	2.10121269	-4.447751	-21.822597	4.114E-06	0.00017587	0.0728091
rib	AE013599	0.18329019	-4.456384	-21.953572	9.248E-05	0.00277862	1
CG10154	AE014296	0.2479359	-4.505177	-22.708755	0.0021521	0.03759701	1
gnu	AE014296	3.26218687	-4.553319	-23.47932	1.881E-08	1.4614E-06	0.0003328
fs(1)Ya	AE014298	1.73783296	-4.592709	-24.129222	7.219E-10	7.2587E-08	1.278E-05
fs(1)N	AE014298	0.15057116	-4.599565	-24.244148	7.524E-06	0.00030401	0.1331551
CG3397	AE014297	0.64472746	-4.613647	-24.481952	1.192E-06	5.9125E-05	0.0210931
AANATL2	AE014134	31.2683311	-4.630108	-24.762891	0	0	0
Send1	AE014134	3.76730907	-4.635152	-24.849623	1.546E-07	9.6319E-06	0.0027354
Uro	AE014134	7.16813804	-4.65357	-25.168904	9.648E-14	1.7246E-11	1.707E-09
CG13311	AE014296	1.51698279	-4.671872	-25.490214	7.412E-05	0.00231043	1
Cp7Fb	AE014298	0.16738236	-4.693484	-25.874947	0.0012708	0.02476855	1
Vml	AE014298	0.16890373	-4.720125	-26.3572	0.0014538	0.02748658	1
Pxt	AE014297	1.84192023	-4.737567	-26.677785	2.019E-09	1.9211E-07	3.573E-05
CG33483	AE014297	0.45152281	-4.747781	-26.867326	0.0003728	0.00883269	1
CG1304	AE014298	387.541676	-4.792918	-27.721196	0	0	0
NimC4	AE014134	0.66470133	-4.812139	-28.092999	9.189E-05	0.00276549	1
Drs	AE014296	112.846097	-4.874481	-29.333583	8.438E-15	1.6778E-12	1.493E-10
CG17018	AE014134	0.12168463	-4.879438	-29.434532	2.85E-05	0.00098691	0.5043093
CG15570	AE014298	0.09058678	-4.905841	-29.978181	0.0005319	0.01195968	1
CG17752	AE014297	3.46917628	-4.94792	-30.86544	3.553E-15	7.9585E-13	6.287E-11
BicC	AE014134	0.84161101	-4.951487	-30.941833	4.034E-09	3.6424E-07	7.139E-05
CG30486	AE013599	2.83750767	-4.997217	-31.938339	1.5E-12	2.2883E-10	2.654E-08
CG8329	AE014296	2.67919235	-4.997874	-31.952885	2.984E-12	4.3639E-10	5.28E-08
zpg	AE014296	0.64530936	-5.017038	-32.380146	3.859E-05	0.00128355	0.682848
PVRAP	AE014296	0.79314705	-5.1028	-34.36339	1.765E-12	2.6704E-10	3.124E-08
CG42780	AE014298	0.58160885	-5.123201	-34.852766	0.0002641	0.00665705	1
CG15047	AE014298	0.50041167	-5.156028	-35.654899	0.0005829	0.01279823	1
alphaTub67C	AE014296	4.90191704	-5.190081	-36.506477	3.444E-11	4.2327E-09	6.095E-07
CG4302	AE013599	206.183125	-5.190811	-36.524954	0	0	0
BigH1	AE014297	2.68815497	-5.210072	-37.015867	7.36E-09	6.3851E-07	0.0001303
CadN2	AE014134	0.06738882	-5.295531	-39.27477	7.6E-05	0.00235535	1
CG5568	AE014296	0.26948377	-5.311761	-39.719099	0.0002775	0.00695605	1
CG16727	AE014297	0.69698761	-5.34393	-40.614711	1.722E-06	8.1683E-05	0.0304676
CG31813	AE014134	0.95150801	-5.358333	-41.022207	0.0002542	0.00645474	1

CG32751	AE014298	61.4668749	-5.414447	-42.649213	0	0	0
CG43090	AE014298	25.7885056	-5.42328	-42.911137	0	0	0
yl	AE014298	3.96526564	-5.462432	-44.091612	1.847E-12	2.7703E-10	3.269E-08
dhd	AE014298	34.8979754	-5.470995	-44.354078	4.075E-12	5.9106E-10	7.211E-08
Vm26Ab	AE014134	2.04608242	-5.484166	-44.760868	2.163E-06	9.9931E-05	0.0382734
yellow-e3	AE014297	0.47687356	-5.569395	-47.484835	0.000515	0.01161191	1
CG8420	AE014297	0.26771946	-5.601068	-48.538845	0.0001269	0.00361458	1
CG32277	AE014296	2.55025267	-5.720046	-52.711523	2.241E-09	2.1096E-07	3.966E-05
Sdic2	AE014298	2.86227313	-5.768708	-54.519803	0	0	0
Cp16	AE014296	2.2482854	-5.786543	-55.197943	1.905E-06	8.9644E-05	0.0337061
pgc	AE013599	2.12301825	-5.808242	-56.034449	2.37E-08	1.8078E-06	0.0004194
Cp19	AE014296	4.59087587	-5.823854	-56.644105	9.363E-09	7.959E-07	0.0001657
nos	AE014297	1.16613753	-5.849992	-57.679724	1.077E-08	8.9479E-07	0.0001906
Hsp70Aa	AE014297	0.56978876	-5.858128	-58.005903	2.433E-07	1.4212E-05	0.0043061
CG17751	AE014297	1.48102202	-5.880342	-58.90596	2.367E-10	2.5699E-08	4.189E-06
CG9897	AE013599	6.7983781	-6.013761	-64.613367	1.11E-16	2.9769E-14	1.965E-12
Vm26Aa	AE014134	5.41483217	-6.054055	-66.443454	2.243E-10	2.4659E-08	3.97E-06
CG6300	AE014297	0.96245629	-6.129699	-70.020204	3.314E-05	0.00112354	0.5864875
CG18628	AE014296	37.1246855	-6.246876	-75.944641	2.27E-10	2.48E-08	4.018E-06
CG17239	AE014134	4.9158699	-6.35763	-82.004434	7.781E-12	1.0843E-09	1.377E-07
Vm34Ca	AE014134	3.66437825	-6.37451	-82.969557	8.855E-08	5.7611E-06	0.001567
CG6788	AE014298	0.35498794	-6.536411	-92.82302	0.0025605	0.04319645	1
CG42705	AE014298	2.89672578	-6.569107	-94.950723	8.843E-09	7.5603E-07	0.0001565
CG43255	AE014298	4.24988311	-6.57472	-95.320826	7.434E-08	4.9572E-06	0.0013156
CG4476	AE014296	0.90262752	-6.621071	-98.433088	8.583E-08	5.626E-06	0.001519
Obp57a	AE013599	8.03684698	-6.916649	-120.81444	7.451E-08	4.9572E-06	0.0013186
CG31789	AE014134	29.9498413	-6.972732	-125.60343	0	0	0
CG31274	AE014297	0.43832037	-6.992282	-127.31704	0.0029383	0.04850677	1
CG12011	AE014296	1.68341685	-7.022748	-130.03429	1.919E-06	9.0101E-05	0.0339682
a10	AE014296	0.93646224	-7.188709	-145.88711	0.0017069	0.03107638	1
CG42521	AE014296	13.1254019	-7.218599	-148.9412	6.661E-16	1.6149E-13	1.179E-11
CG31681	AE014134	8.59942376	-7.317894	-159.55327	0	0	0
CG14957	AE014296	9.99489176	-7.365644	-164.92249	3.334E-08	2.4179E-06	0.00059
CG32834	AE013599	2.45116648	-7.57755	-191.01608	7.556E-12	1.0613E-09	1.337E-07
CG14036	AE014134	1.9981884	-7.692299	-206.8296	0.0006345	0.01374484	1
Vm26Ac	AE014134	1.40009599	-7.730365	-212.35949	0.000695	0.01476525	1
CG3588	AE014298	0.27002935	-7.778735	-219.60019	0.0006728	0.01439808	1
nw	AE013599	0.90981002	-7.945361	-246.48577	1.24E-06	6.0951E-05	0.0219423
CG7443	AE014297	9.60052706	-7.9597	-248.94791	1.517E-09	1.4746E-07	2.684E-05
CG34109	AE014134	0.47418751	-8.143657	-282.80358	0.0003783	0.00892665	1
Tom	AE014296	1.37508055	-8.284292	-311.75999	0.0004665	0.01070722	1
dec-1	AE014298	0.6788043	-8.295473	-314.18561	5.952E-09	5.2402E-07	0.0001053
pre-mod(mdg4)-K	AE014297	0.3996934	-8.305482	-316.37285	0.000279	0.00697466	1
CG30289	AE013599	1.25759515	-8.379908	-333.12238	0.0001348	0.00381703	1
sala	AE014134	0.8388437	-8.388177	-335.03719	0.0004026	0.00943647	1

CG42704	AE014298	16.3210412	-8.493627	-360.44291	6.439E-15	1.3407E-12	1.14E-10
CG43112	AE013599	4.95890654	-8.622926	-394.23887	0.0001947	0.00516544	1
CG45084	AE014134	0.55591227	-9.151887	-568.84306	4.188E-05	0.00138544	0.7412119
Vm32E	AE014134	5.74080612	-9.418933	-684.51244	2.84E-05	0.00098551	0.5026095

Table 8-2: Regulated genes of intestines dissected fro flies overexpressing dFoxO in ECs.

Name	Chromosome	Max group mean	Log_2 fold change	Fold change	P-value	FDR p-value	Bonferroni
Osi20	AE014297	0.723471049	7.070749073	134.4335176	0.0007008	0.02074664	1
CG46312	AE014298	0.334259161	6.877264794	117.5609241	0.0020731	0.04535041	1
Cda9	AE013599	44.26296984	6.871919891	117.1261896	0	0	0
Ipod	AE014298	0.333812256	6.580961303	95.73412068	0.0015835	0.03761539	1
CG42815	AE014296	85.84951761	6.317946148	79.77949841	2.568E-10	6.5865E-08	4.545E-06
blanks	AE014296	5.742483177	6.191480169	73.08382152	0	0	0
CG13428	AE013599	4.671645783	6.027735091	65.24227078	2.375E-05	0.00136462	0.4203032
CG16762	AE014296	23.6681119	5.904001882	59.87998198	4.122E-10	1.0132E-07	7.295E-06
CG15263	AE014134	21.48530213	5.845208106	57.48876391	0	0	0
Muc11A	AE014298	7.827927631	5.521551782	45.93595071	7.834E-10	1.8719E-07	1.386E-05
Rcd-1r	AE014134	0.606298725	5.450541736	43.72970576	0.000876	0.02452808	1
CG13228	AE013599	1.622093731	5.247796289	37.99654377	0.000645	0.01957754	1
CG34211	AE013599	9.064863093	5.023994673	32.53666942	1.98E-06	0.00016768	0.0350442
CG16825	AE014134	0.629917368	4.965193184	31.23719887	1.822E-08	3.1935E-06	0.0003225
IM23	AE013599	4.404512577	4.833357668	28.50923985	6.214E-06	0.00046204	0.1099661
CG14963	AE014296	9.563984627	4.760651815	27.10809477	1.823E-08	3.1935E-06	0.0003225
Mal-B1	AE014134	22.07737589	4.666318038	25.39228002	2.331E-15	1.4228E-12	4.126E-11
CG4586	AE014298	14.96957891	4.656903101	25.22711113	0	0	0
Muc14A	AE014298	0.0323335	4.630951261	24.77737182	1.395E-06	0.00012791	0.0246859
CG3604	AE014134	28.423576	4.574271912	23.82281366	2.637E-07	3.0498E-05	0.0046661
Scp2	AE014297	6.728771649	4.448392795	21.83230871	2.153E-08	3.6999E-06	0.0003811
Osi19	AE014297	30.91005632	4.399554046	21.10560157	0	0	0
CG18598	AE014297	1.102443939	4.327926849	20.08333352	0.0008942	0.02492123	1
RpL37b	AE013599	2.734982444	4.276379143	19.37842136	1.109E-06	0.00010612	0.019633
CG14244	AE014297	13.68197543	4.219863639	18.63397604	1.31E-14	6.8189E-12	2.318E-10
CG33258	AE014296	185.228815	4.154445661	17.8079021	4.441E-16	3.2746E-13	7.859E-12
CG42821	AE014297	9.162247936	4.104038847	17.1964498	1.493E-06	0.00013482	0.0264247
CG42729	AE014296	26.60654503	4.086116756	16.98414579	0	0	0
Cp7Fa	AE014298	4.38222415	4.061600782	16.69796959	0.0003274	0.01142661	1
CheA75a	AE014296	1.376636227	3.978272883	15.76084393	0.0010893	0.02877333	1
CG31089	AE014297	10.84421554	3.952256287	15.47917082	8.676E-13	3.5708E-10	1.535E-08
CBP	AE014298	8.905905916	3.870838873	14.62980742	0	0	0
CG5070	AE014298	58.63336843	3.851586872	14.43587721	1.001E-05	0.00068367	0.1770712
CG15213	AE014296	3.297993105	3.816278366	14.08686199	3.1E-06	0.00024826	0.0548661

CG3009	AE014298	0.188116229	3.813328413	14.05808729	0.0004886	0.01577852	1
CG14300	AE014297	3.340983638	3.793227303	13.8635738	1.952E-06	0.00016689	0.0345471
CG6441	AE014134	0.222139033	3.785726081	13.7916779	0.0012523	0.03170397	1
CG43778	AE014134	0.335323047	3.650459756	12.55734669	2.054E-07	2.4724E-05	0.0036344
Cyt-c1L	AE014297	0.783111024	3.568654382	11.86511667	7.722E-06	0.00055327	0.1366588
LManIV	AE014134	9.762921092	3.558668659	11.78327493	1.099E-11	3.474E-09	1.945E-07
DIP-beta	AE014298	0.157019747	3.517001866	11.44782696	1.415E-05	0.00089783	0.2504938
CG13177	AE013599	5.91912361	3.434340943	10.81034712	1.8E-09	4.033E-07	3.186E-05
tut	AE014296	0.460514546	3.374549566	10.37147778	0.000501	0.01606311	1
Cyp4g1	AE014298	21.88643836	3.3711861	10.34732612	3.95E-06	0.00031071	0.0699098
CG34040	AE013599	392.3079337	3.331241605	10.06476516	1.11E-16	8.9307E-14	1.965E-12
CG1889	AE014298	0.305414567	3.318749511	9.977991986	0.0005758	0.01800381	1
Cpr49Ae	AE013599	2.227720829	3.316952699	9.965572585	8.022E-05	0.00370686	1
Lcp1	AE013599	0.731133788	3.315428025	9.955046297	0.0004207	0.01399398	1
CG15021	AE014296	0.949290296	3.299612698	9.846511584	0.0005379	0.0170297	1
CG34043	AE014134	7.236763781	3.24379144	9.472803383	5.994E-05	0.00297974	1
Pdf	AE014297	0.810713551	3.238844932	9.440379994	0.0011615	0.02996472	1
LManIII	AE014134	141.3139625	3.204276486	9.216867339	9.215E-15	4.9417E-12	1.631E-10
5-HT7	AE014297	0.145313418	3.162848247	8.955961009	0.0006247	0.01912742	1
CG34136	AE014134	2.148117975	3.152023424	8.889014154	0.0001363	0.00567067	1
CG30278	AE013599	1.531499093	3.126109317	8.730772547	2.776E-06	0.0002264	0.0491279
CG42728	AE014296	23.60714029	3.103582185	8.595503704	8.349E-14	3.6938E-11	1.478E-09
CG32379	AE014296	0.586436601	3.070587161	8.401151952	0.0006107	0.01889457	1
CG31077	AE014297	71.95624482	3.037271803	8.20937166	1.376E-06	0.00012683	0.0243519
Obp19d	AE014298	1.278435986	3.000029412	8.000163095	0.0004185	0.01394764	1
Obp56d	AE013599	4.901810198	2.897780056	7.452787145	4.022E-05	0.00211223	0.7118216
Act79B	AE014296	5.04593031	2.867041004	7.29567268	7.82E-10	1.8719E-07	1.384E-05
CG31091	AE014297	9.452308072	2.866596316	7.293424247	4.963E-11	1.4398E-08	8.783E-07
Cht7	AE014296	0.666855786	2.85266285	7.223323834	7.194E-07	7.1931E-05	0.0127317
OS9	AE014134	0.730232456	2.834698681	7.133938016	0.0010656	0.02827339	1
CG18095	AE014134	0.920145308	2.831523604	7.118254943	0.0003047	0.01076421	1
CG5791	AE014297	1.649103425	2.830707187	7.114227879	0.0004915	0.0158436	1
IM4	AE013599	7.114239647	2.829803754	7.109774261	9.725E-06	0.00066704	0.1720973
CG42740	AE014297	0.098083634	2.794023259	6.93561232	0.0024174	0.04980321	1
sNPF-R	AE014296	0.179368718	2.768754311	6.815192046	0.0001393	0.00574512	1
CG13202	AE013599	10.41866651	2.767697361	6.810200911	3.498E-07	3.893E-05	0.0061898
CG13068	AE014296	1.495802453	2.76238493	6.785169849	0.0001911	0.00741427	1
GstD11	AE014297	1.232273189	2.749880479	6.726614029	0.0003644	0.01256955	1
CG34220	AE013599	1048.384585	2.732284009	6.645068214	1.395E-07	1.8152E-05	0.0024687
CG5909	AE014297	0.446973517	2.730954518	6.638947384	0.0009921	0.02676389	1
CG42364	AE013599	10.77419495	2.730088031	6.634961207	8.473E-06	0.00059505	0.1499524
IM18	AE013599	3.068634922	2.722164244	6.598619567	0.000109	0.00470279	1
CG9777	AE014298	1.31919944	2.715322296	6.567399856	1.293E-05	0.00083308	0.2287731
CkIIalpha-i3	AE014296	11.65258481	2.687580613	6.442321292	1.887E-15	1.1929E-12	3.34E-11
CG9029	AE014134	1.865567014	2.670163566	6.365013464	0.0001729	0.00686183	1
CG32639	AE014298	0.719503783	2.669294409	6.361179991	0.0015387	0.03679689	1

Peritrophin-A	AE014298	1.504626489	2.65670606	6.305916471	2.495E-06	0.00020728	0.0441503
LManV	AE014134	331.8686462	2.655750078	6.301739328	1.482E-11	4.6002E-09	2.622E-07
Scp1	AE013599	1.596414026	2.636894588	6.219913804	0.0014799	0.03582664	1
CG12717	AE014298	3.941250483	2.63173807	6.19772211	1.118E-05	0.00074674	0.1978869
CG17278	AE014297	5.090528885	2.625277302	6.170029135	3.081E-10	7.789E-08	5.452E-06
pxb	AE014297	0.593482739	2.625041628	6.169021301	0.0001296	0.00547231	1
CG30427	AE013599	1.510499014	2.623618828	6.162940352	2.768E-08	4.5787E-06	0.0004899
CG15353	AE014134	13.16524073	2.597337136	6.051686009	7.024E-06	0.00051158	0.1243043
unc-13-4A	AE014296	0.375845129	2.577600933	5.969462077	0.0003915	0.01324822	1
CG5810	AE014297	0.691417061	2.562909756	5.908982623	0.0006398	0.01948941	1
CG10553	AE014297	6.002886331	2.549468507	5.854185688	0.0005421	0.01710188	1
CG14125	AE014296	1257.683763	2.542370714	5.825454907	8.232E-08	1.1293E-05	0.0014569
CG6403	AE014297	449.8677674	2.521649434	5.74238251	0	0	0
CG7884	AE014298	0.615000933	2.477292896	5.568515971	2.913E-05	0.00162614	0.5154879
CG12402	AE014297	0.60487598	2.463755824	5.51650994	0.0001494	0.00609323	1
CG42784	AE014134	0.45331943	2.462492329	5.511680762	1.049E-05	0.00070883	0.1857127
CG43117	AE014297	18.78818097	2.456925927	5.490455819	2.256E-05	0.0013221	0.3992754
CG9021	AE014134	14.21392805	2.438252919	5.419849981	2.875E-14	1.4135E-11	5.089E-10
CG16789	AE014297	0.765516011	2.427333512	5.378983309	3.635E-05	0.00196702	0.6432149
Sox102F	AE014135	0.218025058	2.406283872	5.301071033	0.0012264	0.03122936	1
cysu	AE014297	0.207473556	2.405513809	5.298242249	0.0012884	0.0322754	1
CG32037	AE014296	0.707880939	2.405375739	5.297735216	0.0001617	0.00654094	1
CG9328	AE014134	2.969529066	2.404945766	5.296156543	4.223E-05	0.0022047	0.7473932
CG17191	AE014297	348.6285478	2.390981762	5.245141748	0	0	0
CG16713	AE014134	34.98092305	2.352421619	5.106807292	0.0018381	0.0417989	1
AstC	AE014134	148.4399572	2.34845519	5.092786331	1.727E-09	3.9609E-07	3.056E-05
CG42494	AE014296	2.803369391	2.344412276	5.078534619	3.365E-05	0.00184954	0.5955534
Ugt35b	AE014297	2.639078675	2.327295893	5.018638022	0.0022271	0.04737075	1
l(2)41Ab	AE013599	0.34473998	2.324986178	5.010609751	0.0013355	0.03312127	1
Prat2	AE014296	4.042772057	2.313072345	4.969402314	3.617E-05	0.00196344	0.6400799
CG7560	AE014296	2.804638816	2.302913859	4.934534037	3.826E-05	0.0020273	0.6771168
CG14642	AE014297	3.335790877	2.299937293	4.924363609	1.772E-06	0.00015368	0.0313507
Ziz	AE014134	1.42045172	2.288676015	4.886075023	8.753E-06	0.00060276	0.1549083
CG41520	AE013599	1.182337524	2.285800509	4.876346045	0.0023372	0.04877518	1
IM1	AE013599	10.82930838	2.280450629	4.858296799	0.0024237	0.04987456	1
smal	AE014134	0.509101347	2.263952581	4.803055838	0.0018254	0.0416225	1
HEATR2	AE014297	0.599098572	2.263891892	4.802853797	0.0001915	0.00741427	1
shams	AE014297	19.82593083	2.259368141	4.787817434	5.929E-09	1.1529E-06	0.0001049
foxo	AE014297	563.8391693	2.243852795	4.736603124	0	0	0
CG17108	AE014134	7.199820364	2.234928611	4.707394007	0.0003872	0.01315437	1
knk	AE014297	0.777052759	2.225480386	4.676665962	0.0004505	0.01493095	1
CG13075	AE014296	58.42651298	2.222117587	4.665777747	6.786E-12	2.2659E-09	1.201E-07
CG12826	AE013599	30.60588336	2.20584485	4.613446256	7.114E-11	2.0306E-08	1.259E-06
Muc68D	AE014296	276.5533435	2.201507168	4.599596058	8.761E-05	0.00393508	1
yuri	AE014134	5.777749577	2.198437062	4.589818364	1.495E-07	1.9166E-05	0.0026449
CG4730	AE014297	1.474196334	2.193224197	4.573263978	0.0002293	0.00857883	1

CG34458	AE013599	0.741880181	2.192451177	4.570814204	0.0017353	0.04014293	1
CG43980	AE014296	0.167024196	2.189046976	4.56004157	0.0005775	0.01802361	1
CG42764	AE014296	0.77292126	2.186613434	4.552356163	0.0014452	0.03513114	1
CG40498	AE013599	0.571972524	2.182201304	4.538455162	0.0001885	0.00736495	1
CG42255	AE014296	0.159618474	2.179808476	4.530934002	0.0006908	0.02051206	1
ppk13	AE014134	0.409634977	2.167317566	4.491874332	0.0015079	0.03625828	1
CG14245	AE014297	124.4626849	2.165341046	4.485724588	3.707E-12	1.3274E-09	6.56E-08
Hml	AE014296	0.135588014	2.157245915	4.460625147	0.0003117	0.01094382	1
IM3	AE013599	6.878340933	2.139351854	4.405640738	0.0008008	0.02300589	1
tow	AE014296	0.982359711	2.132589232	4.385037656	0.0003513	0.01221352	1
Notum	AE014296	0.368347349	2.125338233	4.363053707	0.001285	0.03225622	1
CG32115	AE014296	18.42350714	2.114705591	4.331016266	0.0002795	0.01013732	1
CG12493	AE014296	7.976088206	2.114374706	4.330023053	0.0004145	0.01383904	1
CG14762	AE013599	0.638836608	2.104371681	4.300104384	0.0016852	0.03940026	1
CG11839	AE014297	13.89053557	2.103786641	4.298360963	1.563E-07	1.9621E-05	0.0027666
CG16710	AE014297	0.954429964	2.102922044	4.295785756	0.0013583	0.03347835	1
Ubc84D	AE014297	1.356304786	2.100070811	4.287304276	0.0015021	0.03616701	1
CG32647	AE014298	0.430170121	2.099676449	4.286132499	0.0020334	0.0446456	1
CG13748	AE013599	8.052826209	2.097843837	4.280691411	1.58E-05	0.00097739	0.279533
nompC	AE014134	0.59121314	2.096888569	4.277857925	7.425E-05	0.0035229	1
Nnf1a	AE013599	2.912693655	2.076783134	4.218655071	0.000249	0.00914326	1
Ir21a	AE014134	0.561824484	2.076772307	4.218623412	0.0010714	0.02834217	1
CG7294	AE014134	1.588466606	2.067475167	4.191524803	0.0015722	0.03749751	1
ple	AE014296	7.283010833	2.055132508	4.155818097	0.0001656	0.00661419	1
Mal-A8	AE013599	1111.760505	2.047861268	4.134925305	5.018E-14	2.4002E-11	8.881E-10
DNaseII	AE014297	21.3517816	2.041747763	4.117440388	4.415E-08	6.7361E-06	0.0007814
emc	AE014296	14.72667016	2.01675723	4.046731781	0.0008602	0.02424113	1
CG12985	AE014298	1.981512609	2.010677282	4.02971353	0.0002156	0.00815295	1
sstn	AE014296	2.827790864	2.00624564	4.017354129	0.0007156	0.02110731	1
AttC	AE013599	9.197881364	2.000809894	4.002246132	0.0011943	0.03056312	1
Tep2	AE014134	5.758852935	1.998716023	3.996441644	7.207E-09	1.3864E-06	0.0001276
CG2865	AE014298	3.604371093	1.997981745	3.994408121	0.0013765	0.03378737	1
CG33521	AE014135	4.224112744	1.983184384	3.95364787	0.0021183	0.04582732	1
Hsp23	AE014296	26.8788238	1.976395322	3.935086427	3.046E-07	3.4782E-05	0.0053911
CG2678	AE014297	3.628537997	1.97210603	3.923404354	0.0002408	0.00889614	1
CG13285	AE014296	23.8403818	1.963135364	3.899084346	6.183E-05	0.0030308	1
CG31176	AE014297	0.956453877	1.959396276	3.888992024	0.0015149	0.03637695	1
MtnB	AE014297	163.4296453	1.955267054	3.877877027	1.731E-06	0.00015095	0.0306419
plx	AE014297	1.240192557	1.93507367	3.823976533	4.774E-06	0.00036571	0.0844781
Hsp70Bb	AE014297	77.80538182	1.931124123	3.813522266	0	0	0
CG31999	AE014135	2.675048386	1.929724128	3.809823407	0.0013508	0.03338713	1
Mal-A7	AE013599	1924.844933	1.929301242	3.808706828	7.627E-14	3.461E-11	1.35E-09
CG1124	AE014297	96.84030405	1.927476769	3.803893274	3.545E-08	5.6524E-06	0.0006274
CG42323	AE014298	0.881338339	1.925864035	3.799643423	0.0016876	0.03940026	1
Mtk	AE013599	14.29098781	1.92504806	3.797494987	0.0016905	0.03941646	1
CG1139	AE014296	158.0957955	1.915979453	3.773699258	7.772E-16	5.5013E-13	1.375E-11

Mco1	AE014134	44.66593519	1.91141745	3.761785142	1.571E-08	2.8088E-06	0.0002781
Rbp9	AE014134	2.329626195	1.90458371	3.744008499	6.913E-08	9.6331E-06	0.0012234
Drs	AE014296	622.0895335	1.900492399	3.733405978	1.407E-07	1.8175E-05	0.0024899
Hf	AE014134	6.555430014	1.885421005	3.694607239	1.717E-05	0.00104421	0.3038637
CG14626	AE014298	5.591204532	1.879627741	3.679800979	4.29E-05	0.00223274	0.759131
Thor	AE014134	1426.143301	1.876466383	3.671746311	9.761E-08	1.2988E-05	0.0017275
CG13375	AE014298	0.373310915	1.875182611	3.668480485	0.0018487	0.04194362	1
hbs	AE013599	1.112689621	1.870166679	3.655748135	0.0002818	0.01017887	1
beat-IIa	AE014297	0.543487297	1.865310734	3.643463996	0.0010525	0.02805729	1
CG3812	AE014298	8.969036774	1.857822904	3.624602793	1.445E-05	0.00091028	0.2557878
CG4984	AE013599	0.402966497	1.851708704	3.609274085	0.0021055	0.04566258	1
CG42369	AE014134	2.917165545	1.850713405	3.606784946	0.0007011	0.02074664	1
kek1	AE014134	0.143646553	1.849947974	3.604871851	0.0023848	0.0494184	1
CG33958	AE013599	2.091802745	1.846604538	3.596527256	7.677E-05	0.00358344	1
Su(z)2	AE013599	0.861113557	1.844668452	3.591703982	0.0018811	0.0423542	1
Clect27	AE014134	5.2996102	1.841851971	3.584698967	0.0001776	0.00698576	1
mus201	AE014134	0.90579838	1.835714935	3.569482514	0.0021621	0.04643473	1
mAChR-C	AE014298	1.286421506	1.833346305	3.563626913	0.0022372	0.04752941	1
myo	AE014135	6.137430948	1.83024076	3.555964101	0.0019529	0.04352631	1
Myc	AE014298	3.012887587	1.825740732	3.544889685	0.0018399	0.0417989	1
wtrw	AE014297	1.63680921	1.814444781	3.517242438	0.0001989	0.00765357	1
CG7341	AE014296	1.950314978	1.812990821	3.513699517	0.0009717	0.02633545	1
htl	AE014297	2.466405907	1.810699605	3.508123664	0.0003618	0.01252855	1
CG13618	AE014297	8.949066203	1.79406535	3.467907337	6.322E-05	0.00308218	1
Nipped-A	AE013599	1.338328816	1.793765323	3.467186217	0.001996	0.04409875	1
CG18135	AE014296	320.7628597	1.792969006	3.465272979	5.454E-09	1.0845E-06	9.652E-05
CG1208	AE014297	122.7434251	1.789873925	3.457846736	2.983E-12	1.1232E-09	5.279E-08
Sid	AE014297	3.184412773	1.779731911	3.433623632	0.0010066	0.02711407	1
CG10283	AE014134	10.10204411	1.779421728	3.432885474	4.548E-07	4.8775E-05	0.0080478
Pdp1	AE014296	8.979720951	1.773354601	3.41847909	0.0001972	0.00760349	1
nkd	AE014296	1.181514771	1.772007478	3.415288561	0.001134	0.02959916	1
Spn53F	AE013599	1.747811566	1.770871217	3.412599751	0.0015255	0.03658054	1
CG4650	AE014134	8.182990708	1.770195955	3.411002837	7.567E-05	0.00356146	1
CG4461	AE014296	2.52207168	1.767291235	3.404142038	0.0020205	0.04441738	1
Tsp66E	AE014296	5.48962816	1.749620556	3.362701118	0.0001869	0.00731836	1
spag	AE013599	3.536497283	1.747551177	3.357881172	0.0016731	0.03922821	1
Pdk	AE013599	18.81280477	1.740679608	3.341925583	2.163E-06	0.00018224	0.0382713
CG15153	AE014134	3.16179098	1.737563646	3.334715413	0.0009681	0.02630152	1
CG8908	AE013599	2.997291153	1.734847381	3.328442812	3.22E-06	0.0002567	0.0569879
CG6785	AE014134	0.678897907	1.727017771	3.310428042	0.001494	0.03604233	1
hdc	AE014297	1.035548941	1.725728954	3.307472024	0.0008372	0.02370565	1
norpA	AE014298	1.778080491	1.719432091	3.293067517	0.0004556	0.01501519	1
Jon66Cii	AE014296	60.8464695	1.71710672	3.287763945	3.913E-05	0.00206078	0.6924221
CG30026	AE013599	11.26546519	1.711430742	3.274854347	0.0001251	0.00532322	1
RapGAP1	AE014134	1.707883555	1.710034592	3.271686679	0.0024082	0.04972866	1
PGRP-LF	AE014296	10.34762049	1.709174852	3.269737575	2.332E-05	0.00134888	0.4127581

nbs	AE014296	3.646544276	1.700575127	3.250305054	0.0005421	0.01710188	1
Ama	AE014297	1.377853564	1.696931325	3.242106145	0.0020034	0.04415308	1
apolpp	AE014135	1.563969578	1.692790063	3.232813012	0.0018598	0.0420884	1
Dh31	AE014134	15.37645509	1.690889886	3.228557867	1.93E-08	3.349E-06	0.0003416
CG34166	AE014134	24.00170585	1.690111001	3.226815299	0.0013363	0.03312127	1
CG34324	AE014298	1647.518369	1.679371224	3.202883279	1.241E-06	0.00011683	0.0219637
CG42272	AE014296	3.350327711	1.679368522	3.20287728	0.000453	0.01495713	1
CG13937	AE014296	5.752919645	1.677472966	3.198671787	1.499E-05	0.00093766	0.2653574
CG6175	AE014296	7.967242039	1.676423519	3.196345851	5.685E-05	0.00286625	1
Drat	AE013599	302.6321321	1.661561362	3.163587199	1.794E-07	2.2044E-05	0.0031744
MtnD	AE014297	1105.21322	1.655615044	3.15057476	1.326E-08	2.4708E-06	0.0002347
Snoo	AE014134	1.5038654	1.654118461	3.1473082	0.001805	0.04128584	1
tna	AE014296	6.839691134	1.651844231	3.142350765	1.664E-05	0.00101524	0.2944201
Mal-A3	AE013599	557.0150975	1.648403068	3.134864461	1.398E-08	2.5773E-06	0.0002474
lectin-28C	AE014134	2.52248248	1.646605808	3.130961585	0.0014949	0.03604233	1
scyl	AE014296	22.15899098	1.644986941	3.127450263	0.0014713	0.03566807	1
CG31108	AE014297	3.549152135	1.644218175	3.12578419	0.00043	0.01427561	1
ZnT77C	AE014296	12.7265095	1.64320454	3.123588791	8.821E-07	8.5768E-05	0.0156099
Ect3	AE014297	6.685035867	1.638445716	3.113302402	2.911E-06	0.0002363	0.0515126
CG5065	AE013599	15.36278069	1.634460348	3.104713939	2.753E-05	0.00155678	0.4872735
sty	AE014296	14.35179224	1.63284767	3.101245356	0.0002359	0.00877216	1
CG44085	AE014134	2.754844991	1.630099509	3.095343479	0.0004675	0.01531965	1
CG13896	AE014296	5.652453098	1.625747227	3.086019605	0.0001365	0.00567067	1
CG7296	AE014134	12.16805086	1.615511577	3.064202363	0.0001105	0.00475607	1
mus304	AE014296	1.407355114	1.614651162	3.062375435	0.0015355	0.03677136	1
UbcE2H	AE014298	19.05844495	1.608880466	3.050150576	0.0023509	0.04894653	1
Sulf1	AE014297	4.621587875	1.606232036	3.044556394	0.0001302	0.00547259	1
mtt	AE013599	1.613173921	1.600749061	3.03300749	1.142E-05	0.00075614	0.2020493
Msr-110	AE014296	30.9202923	1.585877132	3.001902524	8.3E-07	8.1154E-05	0.014689
Yp1	AE014298	121.2810283	1.582466725	2.994814668	7.561E-05	0.00356146	1
tobi	AE014297	1215.164999	1.577316557	2.984142763	2.308E-08	3.9273E-06	0.0004084
CG14995	AE014296	3.718910082	1.570634288	2.970352785	0.0002028	0.00774971	1
CG5550	AE013599	225.9825298	1.570167518	2.969391911	6.583E-06	0.00048539	0.1164936
sas	AE014297	0.806759831	1.554862498	2.93805723	0.0021478	0.04624024	1
CG17778	AE014298	10.69696732	1.552113475	2.932464157	8.577E-05	0.00388198	1
CG10140	AE014296	19.31562606	1.55162836	2.931478266	7.673E-07	7.5445E-05	0.0135784
CG1607	AE014297	4.156586818	1.545034343	2.918110153	0.0013209	0.03287676	1
Men-b	AE014297	93.10697916	1.543702162	2.915416821	2.604E-06	0.00021332	0.046078
CG30497	AE013599	6.746535552	1.534963102	2.897810194	0.0018057	0.04128584	1
CG45093	AE013599	6.860244368	1.523096824	2.874073235	0.0011409	0.02964745	1
RIC-3	AE013599	1.431793587	1.520438577	2.868782468	0.0019895	0.04404369	1
CG42390	AE014297	4.154949819	1.516892994	2.861740774	3.809E-05	0.002024	0.6739915
CG10912	AE013599	3513.850697	1.514203562	2.856410966	3.073E-06	0.00024723	0.0543901
tws	AE014297	5.848297585	1.513141671	2.854309287	0.0017267	0.04004963	1
Cyp12d1-p	AE013599	24.23842832	1.512633526	2.853304123	6.176E-05	0.0030308	1
CG16700	AE014298	11.22055406	1.507013766	2.842211206	0.0005024	0.01607928	1

CG31704	AE014134	173.7424303	1.506678587	2.841550957	2.069E-07	2.4744E-05	0.0036621
Rgl	AE014296	1.256736916	1.504642448	2.837543379	0.001127	0.0294607	1
osp	AE014134	2.404787303	1.49552325	2.819663987	0.0003846	0.01311258	1
Pi3K92E	AE014297	8.368347358	1.492116855	2.813014238	5.888E-05	0.00294467	1
Nmdmc	AE014297	81.46626339	1.488306503	2.805594491	7.492E-06	0.00054341	0.132593
ade5	AE014298	48.80098226	1.487164421	2.803374374	2.996E-08	4.9094E-06	0.0005302
AsnRS-m	AE013599	3.40775085	1.481960223	2.79328005	0.0006035	0.01870497	1
CG14989	AE014296	28.15707427	1.476253688	2.78225314	9.342E-08	1.2542E-05	0.0016532
bves	AE014298	3.570940724	1.474117538	2.778136601	0.0023422	0.04882279	1
olf186-M	AE013599	11.18875437	1.465610971	2.761804063	4.006E-06	0.00031234	0.0709018
Tsf1	AE014298	13.79857735	1.449060105	2.730301182	0.0002531	0.00923761	1
aay	AE014296	818.3333267	1.447405137	2.727170949	7.308E-07	7.2656E-05	0.0129328
CG9626	AE014297	2.06232681	1.446463368	2.725391277	0.0001621	0.00654094	1
Slob	AE014134	0.62300163	1.436580259	2.706784926	0.0021763	0.04652568	1
CG3838	AE014134	16.5948393	1.434874713	2.703586871	6.857E-07	6.9346E-05	0.0121355
Cys	AE014297	527.9635684	1.430239854	2.694915158	8.06E-08	1.1144E-05	0.0014264
Orcokinin	AE013599	48.98778875	1.421463291	2.678570542	2.005E-07	2.4308E-05	0.0035489
CG10376	AE014134	11.84652229	1.416946485	2.670197557	5.163E-05	0.00263317	0.9137109
Cep135	AE014296	1.6913797	1.416760512	2.669853374	0.0021542	0.04632292	1
CG15715	AE014296	30.43956735	1.415163874	2.666900267	0.0011046	0.02904621	1
NFAT	AE014298	1.52434126	1.408404571	2.654434553	0.0006686	0.02004966	1
Ndg	AE013599	2.090761501	1.407053498	2.651949859	0.0008471	0.02394734	1
Dab	AE014296	1.142739557	1.406438847	2.650820252	0.0006483	0.01964492	1
bab2	AE014296	7.201246498	1.401571837	2.641892635	0.0017164	0.03986217	1
CG33510	AE014134	22.9509663	1.396504127	2.632628819	0.0006505	0.01967808	1
CG6283	AE014297	5435.964867	1.389326291	2.61956324	3.367E-07	3.7913E-05	0.0059579
FucTC	AE014298	27.94008328	1.385122525	2.611941392	5.11E-08	7.5996E-06	0.0009044
CCHa2	AE014297	106.5311269	1.380944785	2.604388702	4.886E-08	7.3911E-06	0.0008648
CG13067	AE014296	39.69249452	1.379738858	2.602212643	5.016E-06	0.00038265	0.0887743
CG34423	AE013599	12.2840639	1.372947835	2.589992346	0.0016394	0.03876851	1
CG15365	AE014298	7.408838519	1.370421508	2.585460937	1.184E-05	0.00077877	0.2094887
Ptp99A	AE014297	2.336584833	1.370088656	2.584864501	0.0001011	0.00444052	1
Kua	AE014134	17.6926245	1.359581277	2.566106908	1.23E-05	0.00080332	0.2177005
CG8852	AE014134	17.81321109	1.354177734	2.556513659	1.605E-05	0.0009898	0.2840719
CG10383	AE014134	36.90622567	1.352676807	2.553855339	2.176E-05	0.00129199	0.3850133
Kr-h1	AE014134	11.11752991	1.346781095	2.543440059	0.0002099	0.00795464	1
Adgf-A2	AE014296	4.023103107	1.346216306	2.542444543	0.0024165	0.04980321	1
CG4577	AE014134	18.98333536	1.345743223	2.541610971	3.008E-07	3.457E-05	0.0053238
NPF	AE014297	84.80661407	1.34573311	2.541593156	4.099E-07	4.4782E-05	0.0072547
h	AE014296	23.69288434	1.337569909	2.527252669	0.0014079	0.03445942	1
CG43055	AE014134	427.6313856	1.334571045	2.522004841	5.882E-06	0.00043923	0.1040973
egr	AE013599	13.10691579	1.334133936	2.521240838	0.0005126	0.01631607	1
Try29F	AE014134	12.95301129	1.331478916	2.516605215	1.795E-05	0.00108033	0.3176171
Gfat1	AE014297	36.06129467	1.329891021	2.513836851	3.307E-07	3.7512E-05	0.0058519
Dif	AE014134	6.001162749	1.329784697	2.513651593	8.177E-05	0.00376867	1
CG15073	AE013599	2.404917369	1.326618246	2.508140637	0.0020965	0.04552381	1

Lk6	AE014297	30.10219151	1.318815494	2.494612087	0.0003044	0.01076421	1
pirk	AE013599	95.52625673	1.318761434	2.494518613	2.858E-05	0.00160751	0.5057419
Mal-A4	AE013599	1252.067708	1.310828357	2.480839422	2.569E-06	0.00021146	0.0454646
CG5107	AE014297	776.1525651	1.307602982	2.475299306	0.000719	0.02113791	1
Mrtf	AE014296	3.463684774	1.302754448	2.466994412	0.0022722	0.04791168	1
CG7530	AE014297	13.87800751	1.301992685	2.465692149	3.863E-05	0.00204075	0.6836499
mthl10	AE014296	22.4100045	1.301620685	2.46505645	0.0009455	0.02613074	1
CG6928	AE014296	11.5727535	1.29897195	2.46053485	4.535E-05	0.00233369	0.8024939
CG5953	AE014134	20.63221203	1.296578235	2.456455722	0.0003873	0.01315437	1
LManI	AE014134	27.97875793	1.293719973	2.45159382	0.0002181	0.00823099	1
CG10939	AE013599	22.31299412	1.292478662	2.449485348	0.0002805	0.01015062	1
neur	AE014297	5.770204231	1.291981072	2.448640659	0.0020782	0.04538832	1
LManVI	AE014134	974.6261931	1.290556994	2.446224808	1.642E-05	0.00100897	0.2905822
odd	AE014134	10.51929938	1.286409402	2.439202277	0.0008779	0.02454357	1
CG7744	AE013599	4.098313726	1.286273494	2.438972504	0.0018873	0.04243834	1
CG11384	AE014298	10.65125881	1.285001099	2.436822383	8.576E-06	0.00059648	0.1517672
CG3714	AE014134	18.94991382	1.283326048	2.433994736	5.534E-05	0.002806	0.9792937
CG11807	AE013599	4.878614089	1.279395434	2.427372357	0.0019304	0.04313342	1
Cyp6g1	AE013599	272.9751114	1.275432559	2.420713865	0.0001411	0.00580513	1
CG3906	AE013599	2385.512493	1.274571867	2.419270131	2.471E-05	0.0014109	0.4373779
CG6277	AE014297	2819.273511	1.270569536	2.412567882	3.385E-07	3.7913E-05	0.0059903
Dic1	AE014297	64.67766536	1.267684485	2.407748134	6.283E-08	8.8946E-06	0.0011118
Nep1	AE014298	12.8684477	1.266940257	2.406506396	2.038E-05	0.00121423	0.3606253
Adar	AE014298	2.313566235	1.264848057	2.403019003	0.0022432	0.04759852	1
SclB	AE014134	7.306649692	1.264445717	2.402348939	0.0016725	0.03922821	1
Su(Tpl)	AE014296	14.37367661	1.263618318	2.400971565	0.0004109	0.01377106	1
CG10979	AE014297	3.706005418	1.262809157	2.399625316	0.0006824	0.02036627	1
Pdcd4	AE014298	18.97636334	1.259869396	2.394740609	0.0001141	0.00488961	1
dnc	AE014298	1.410266947	1.251740834	2.381285885	0.0023688	0.04924977	1
UK114	AE014134	183.5823044	1.249170929	2.377047823	1.327E-05	0.00085077	0.2348119
CG7220	AE013599	70.81207097	1.248335588	2.375671878	0.0011514	0.02978562	1
CG15556	AE014297	7.208814623	1.247852722	2.374876879	0.000466	0.01529999	1
Mbs	AE014296	5.956318883	1.247225462	2.373844547	0.0015711	0.03749751	1
tim	AE014134	50.40017081	1.242583338	2.366218562	4.428E-06	0.00034358	0.0783606
PRAS40	AE013599	61.19517236	1.2412209	2.363985031	3.923E-07	4.312E-05	0.0069423
gce	AE014298	11.18986461	1.241018114	2.363652772	0.0007684	0.02236495	1
CG4363	AE013599	2204.741873	1.239392425	2.360990809	1.622E-06	0.00014356	0.0287126
CG43120	AE014296	84.47195386	1.238248012	2.359118703	9.55E-05	0.00423915	1
Ugt37b1	AE014134	24.3677214	1.237997408	2.358708947	0.0001774	0.00698576	1
CG32369	AE014296	7.10898994	1.233650973	2.351613513	0.0009079	0.02526348	1
CG12934	AE013599	12.66665034	1.226699671	2.340310044	0.0011191	0.02929701	1
CG14219	AE014298	89.23545167	1.224504223	2.336751343	0.0007844	0.02271938	1
AdamTS-A	AE014297	3.50430595	1.215216775	2.321756663	0.0003011	0.01069919	1
CG5080	AE014134	34.81421787	1.201641965	2.30001292	6.659E-06	0.00048901	0.1178504
ADPS	AE013599	21.58079316	1.192142903	2.284918811	0.0003753	0.01287316	1
grnd	AE014134	6.398025242	1.190145176	2.28175703	0.0020697	0.04533142	1

CG2841	AE014298	15.42335489	1.188571512	2.27926949	0.0006161	0.01896145	1
Mip	AE014296	8.58414095	1.181419115	2.267997602	0.0009509	0.02613074	1
CG10911	AE013599	9740.863108	1.181085844	2.267473742	2.251E-05	0.0013221	0.3982728
CG6271	AE014297	568.2842741	1.178224171	2.262980529	9.087E-05	0.00406108	1
CycG	AE014297	55.90343021	1.178106435	2.262795857	0.001789	0.04117124	1
zormin	AE014296	1.982761116	1.178040651	2.26269268	0.0006696	0.02004966	1
CG31823	AE014134	9.286004998	1.177538571	2.261905367	0.0006185	0.01900336	1
CG44098	AE014297	2.5404659	1.174058298	2.256455454	0.0014482	0.03515643	1
CG5059	AE014296	116.7414387	1.171133955	2.251886251	2.368E-05	0.00136462	0.4189994
Dad	AE014297	5.837499167	1.166555178	2.24475062	0.0006837	0.02036948	1
puf	AE014297	1.500701755	1.159404895	2.233652714	0.0012314	0.03131083	1
Stat92E	AE014297	36.00433884	1.156103495	2.228547165	3.673E-05	0.00198149	0.6499279
Ugt86Dd	AE014297	86.02465634	1.15602641	2.228428095	0.0008055	0.02310262	1
CG8620	AE014296	34.81317785	1.15377557	2.224954093	0.0009621	0.02627526	1
CG7328	AE014296	9.353149153	1.152184454	2.222501594	0.0007997	0.02300589	1
CG3726	AE014298	16.8652119	1.150202373	2.219450254	1.097E-05	0.00073541	0.1941471
SMC1	AE014297	4.387378811	1.150054181	2.219222286	0.0010971	0.02889272	1
CG2991	AE014134	24.98783637	1.14466591	2.21094925	0.0012458	0.03158515	1
Pepck	AE013599	64.93844596	1.142557732	2.207720799	1.006E-05	0.00068468	0.1780178
Gprk2	AE014297	6.954944585	1.142335356	2.207380528	0.0007901	0.02280878	1
Rel	AE014297	61.97026281	1.136075617	2.197823628	9.928E-07	9.6004E-05	0.0175687
CG45087	AE013599	64.20722682	1.131842152	2.191383756	2.183E-05	0.00129225	0.3863818
CG6845	AE014296	9.203387049	1.127885465	2.185381974	4.426E-05	0.00229081	0.7832525
CG43394	AE014134	6.093028752	1.125894265	2.182367802	0.0022576	0.04767706	1
Glut4EF	AE014297	3.50422114	1.125667928	2.182025448	0.0009388	0.02603984	1
CG14645	AE014297	21852.68743	1.118518577	2.171239056	0.0005046	0.01611787	1
Cbp53E	AE013599	17.27164805	1.114200224	2.164749702	0.0011715	0.03008908	1
CG43348	AE014134	739.0104921	1.113981912	2.164422152	0.0004567	0.01502165	1
wgn	AE014298	8.746817533	1.110559689	2.159294002	6.825E-05	0.00330896	1
lqf	AE014296	14.18292617	1.106235521	2.152831672	0.000969	0.02630152	1
ced-6	AE013599	6.142391941	1.09940089	2.142656956	0.0004875	0.0157715	1
CG11836	AE014297	12.92686049	1.096093544	2.137750589	0.0006122	0.01890639	1
Sur-8	AE014297	12.26234586	1.0922225	2.132022259	0.0024078	0.04972866	1
Xrp1	AE014297	111.6183323	1.092039744	2.131752198	0.0018673	0.04220495	1
sno	AE014298	4.444346718	1.09194983	2.131619343	0.0011529	0.02978562	1
CG43349	AE014134	2559.524029	1.090999211	2.130215242	4.427E-05	0.00229081	0.7834576
pio	AE013599	5.363500148	1.089561602	2.128093593	0.0004868	0.0157715	1
wcy	AE014298	6.53329365	1.08916367	2.127506692	0.0008862	0.02473708	1
CG7966	AE014297	52.75985517	1.088397347	2.126376914	0.0001374	0.0056825	1
CG13868	AE013599	166.6099307	1.08831792	2.126259851	8.453E-05	0.00384536	1
Amy-p	AE013599	10611.69022	1.086774119	2.123985797	0.0001374	0.0056825	1
Mal-A1	AE013599	6246.975001	1.08507635	2.121487753	3.076E-05	0.00171163	0.5442985
CG31368	AE014297	2.499900305	1.07677568	2.109316637	0.0021161	0.04582732	1
CG30394	AE013599	6.139036447	1.075649433	2.107670631	0.0017315	0.04010813	1
CG15431	AE014134	2.98245599	1.075393321	2.107296505	0.0011128	0.02917411	1
oys	AE013599	22.65228502	1.06808004	2.096641268	0.0013534	0.03340374	1

CG43897	AE014296	14.89546894	1.066012419	2.093638586	0.0007152	0.02110731	1
LanB2	AE014296	3.153623455	1.061520811	2.087130502	0.0004517	0.0149421	1
barc	AE014296	7.974604816	1.058840075	2.083255912	0.0003979	0.01338773	1
CG17681	AE014134	15.65020371	1.056308064	2.079602888	0.0003187	0.0111673	1
Oscillin	AE014134	29.49554774	1.048959905	2.06903766	9.584E-05	0.00424026	1
CG34386	AE013599	27.16985089	1.045266702	2.063747835	0.0006144	0.01894251	1
puc	AE014297	26.07209358	1.043529275	2.061263975	0.0016408	0.03876851	1
Vps13B	AE014297	1.454059263	1.033811223	2.047425877	0.0010587	0.0281306	1
Ugt86Dj	AE014297	40.29422688	1.027779928	2.038884326	0.0007417	0.02173149	1
CG17919	AE014297	26.81089293	1.025288471	2.035366321	0.0012186	0.03107404	1
Usp1	AE014297	18.15252919	1.023147601	2.032348203	0.0002949	0.01050083	1
CG10477	AE014296	640.6708954	1.020071348	2.028019253	0.0001623	0.00654094	1
Cyp4p2	AE013599	43.17448439	1.015779751	2.02199545	0.001397	0.03424118	1
Eip75B	AE014296	3.435929547	1.007709642	2.010716441	0.0010248	0.02752144	1
Gadd45	AE013599	31.51284478	1.003437661	2.004771292	0.000108	0.00467227	1
CG6839	AE014296	546.8523608	0.999171877	1.998852308	0.0023999	0.049674	1
CG17931	AE014297	18.85232507	0.995318715	1.993520879	0.0012894	0.0322754	1
Ssrp	AE013599	20.96588213	0.993898081	1.991558808	7.266E-05	0.00345653	1
mth	AE014296	7.757895888	0.993780831	1.991396957	0.0006543	0.01975876	1
NUCB1	AE014296	59.72724435	0.986053927	1.980759783	0.0009569	0.02617465	1
CG32103	AE014296	27.81030962	0.985192919	1.979578007	0.0017779	0.04096914	1
pyd3	AE014297	11.47835229	0.978920051	1.970989446	0.0023711	0.04924977	1
CG9801	AE014297	9.073874563	0.9786628	1.970638025	0.0015835	0.03761539	1
vir-1	AE014134	30.67646066	0.978313653	1.970161167	0.0020959	0.04552381	1
Capr	AE014296	18.47568849	0.963343285	1.949823162	0.0023167	0.04857761	1
Mal-A6	AE013599	2751.787595	0.948907062	1.930409689	0.0003675	0.0126534	1
Amy-d	AE013599	4446.724053	0.948552574	1.929935422	0.0011384	0.02964745	1
Pect	AE014134	39.28212512	0.944537887	1.924572323	0.0008328	0.02361805	1
Jon99Ci	AE014297	1444.37575	0.940458383	1.919137903	0.0017559	0.0405136	1
CCHa1	AE014297	40.97870334	0.939108718	1.917343358	0.0022742	0.04791168	1
ade2	AE014134	80.16934756	0.931082018	1.906705485	0.0020906	0.04550729	1
CG5355	AE014134	71.36725308	0.922279591	1.895107373	5.607E-05	0.00283491	0.9922184
Myo95E	AE014297	3.295479667	0.9182713	1.889849436	0.0011712	0.03008908	1
Acox57D-p	AE013599	105.2642353	0.900971337	1.86732279	0.0007711	0.02240879	1
CG8788	AE013599	24.54174952	0.892523978	1.856421071	0.0002922	0.01042467	1
crq	AE014134	42.50207473	0.891188078	1.854702866	0.0023333	0.04875236	1
Myo28B1	AE014134	20.96869895	0.88982583	1.852952412	0.0001294	0.00547231	1
Nhe3	AE014134	25.09393319	0.889434917	1.852450403	0.0003081	0.01084141	1
rut	AE014298	1.914035216	0.885032328	1.846806005	0.0018793	0.0423542	1
CG11897	AE014297	12.93464148	0.883415828	1.844737868	0.0021412	0.04621111	1
egh	AE014298	31.07592771	0.879200671	1.839355919	0.0006781	0.02027198	1
CG11334	AE014297	64.97492535	0.877025369	1.836584619	0.0003928	0.01326491	1
CG13324	AE013599	2743.157213	0.869908823	1.827547398	0.00208	0.04538832	1
Mdr49	AE013599	140.9369752	0.864646545	1.8208935	0.0018275	0.0416225	1
IA-2	AE014134	14.69844022	0.863478657	1.81942005	0.0002619	0.00953717	1
CG14764	AE013599	15.42140436	0.849002245	1.801254763	0.0011448	0.02970688	1

Tpr2	AE014134	50.0947529	0.845460772	1.796838534	8.528E-05	0.00386989	1
CG10924	AE013599	43.62417693	0.842911615	1.793666428	0.0006638	0.01994327	1
IP3K1	AE014134	58.35067189	0.838247085	1.787876502	0.0004873	0.0157715	1
CG31689	AE014134	38.329741	0.837497715	1.786948077	0.000968	0.02630152	1
CG14495	AE013599	147.8101045	0.826713941	1.773640896	6.774E-05	0.00329333	1
CG34198	AE013599	217.8526658	0.809289781	1.752348573	0.0013029	0.03247403	1
Smg5	AE014134	32.01704683	0.795699504	1.735918847	0.0021763	0.04652568	1
Mal-A2	AE013599	546.1347367	0.794346382	1.73429147	0.0013421	0.03321837	1
CG14499	AE013599	2568.530775	0.79174516	1.731167307	0.0022265	0.04737075	1
Mocs1	AE014296	53.83491432	0.750103536	1.681913529	0.0019682	0.043758	1
CG10353	AE014298	22.12657613	0.746356421	1.677550761	0.0017945	0.04124357	1
Fmo-2	AE013599	102.9331932	0.696878063	1.620993227	0.0013727	0.03373901	1
Syx13	AE014296	140.7446092	0.691916846	1.615428443	0.0014365	0.03501539	1
CAP	AE013599	9.580645195	0.691691961	1.615176651	0.0012798	0.03225622	1
roh	AE013599	169.6173552	-0.643020796	-1.561595494	0.0020027	0.04415308	1
Roc1a	AE014298	109.8712632	-0.685518231	-1.608279588	0.0021407	0.04621111	1
CG33523	AE014296	49.831629	-0.694249509	-1.618042507	0.0008286	0.02357652	1
sowah	AE014296	43.21669938	-0.700708316	-1.625302568	0.00087	0.0244399	1
CG11050	AE014134	64.83738512	-0.731840128	-1.660756001	0.0003074	0.01083685	1
cher	AE014297	10.32791794	-0.733494556	-1.662661587	0.0018937	0.04247513	1
Nha1	AE014134	66.2983059	-0.735900771	-1.665436989	0.001485	0.03590153	1
Arp1	AE014297	122.3382728	-0.745671464	-1.676754489	0.0009858	0.02666359	1
Sec61beta	AE013599	250.640163	-0.760872698	-1.69451534	0.0019763	0.04386427	1
CG17109	AE014297	139.2013283	-0.765302667	-1.699726551	0.0007536	0.02204445	1
GckIII	AE014297	39.44821106	-0.772910135	-1.708713043	0.0015791	0.03761216	1
ClC-a	AE014297	7.000415933	-0.774471661	-1.710563499	0.0018932	0.04247513	1
CG12171	AE014297	152.2181594	-0.775024752	-1.71121941	0.0009677	0.02630152	1
Inx7	AE014298	151.0708187	-0.781643942	-1.719088648	0.0010531	0.02805729	1
CG3987	AE014297	707.6205268	-0.786281559	-1.724623638	0.0018517	0.04195856	1
Psa	AE014296	55.55430241	-0.790905903	-1.730160531	0.0004032	0.01353848	1
pgant6	AE014296	74.44342883	-0.79614399	-1.736453756	0.0008146	0.02328809	1
CG33170	AE014296	36.28266935	-0.797029014	-1.737519313	0.0018719	0.04225394	1
CG12384	AE013599	241.7356563	-0.800665859	-1.741904897	0.0008314	0.02361741	1
CG4729	AE014296	70.83081718	-0.806724592	-1.749235572	0.0006876	0.02045154	1
CG15347	AE014298	1492.563867	-0.808772706	-1.751720628	0.0009561	0.02617465	1
Cyp28a5	AE014134	56.26402494	-0.815165696	-1.759500222	0.0010674	0.02827744	1
CG13220	AE013599	50.76823803	-0.818530083	-1.763608191	0.0017541	0.0405136	1
CG31233	AE014297	791.4762194	-0.827784846	-1.77495795	0.0023275	0.04874582	1
PrBP	AE014134	15.8837439	-0.827809775	-1.774988619	0.0020662	0.04531	1
ND-30	AE014296	106.4729966	-0.832490835	-1.780757215	0.0012817	0.03225622	1
CG10863	AE014296	101.0857039	-0.83988164	-1.789903291	0.0005741	0.01798182	1
CG14777	AE014298	24.39430344	-0.841479144	-1.791886357	0.0014232	0.03473983	1
BI-1	AE014296	178.9139047	-0.842993031	-1.793767655	0.0002002	0.00767171	1
dnk	AE014297	12.85934159	-0.844386705	-1.795501309	0.0021687	0.04652096	1
CG12825	AE013599	434.1340604	-0.844432058	-1.795557755	0.000242	0.00892271	1
CG7630	AE014296	580.4630054	-0.845638603	-1.797060031	0.0007301	0.0214282	1

Arv1	AE014296	17.79495104	-0.847641173	-1.799556218	0.0022528	0.04767706	1
VhaM8.9	AE014297	538.7165537	-0.854589079	-1.808243642	0.0019276	0.04312718	1
Timp	AE014297	26.03458175	-0.856489933	-1.810627703	0.0017096	0.03975654	1
CG11030	AE014134	4.473275857	-0.861160085	-1.816498387	0.001991	0.04404369	1
CG18493	AE014297	958.642029	-0.86504176	-1.821392389	0.0018227	0.04162047	1
Vha13	AE014297	944.4310299	-0.866616297	-1.823381316	0.0012988	0.03246522	1
CG15117	AE013599	34.42218294	-0.869819431	-1.827434163	0.0003632	0.01255505	1
CG6891	AE014298	125.0212693	-0.874452378	-1.83331206	0.0002303	0.00859971	1
CG9646	AE013599	15.32966635	-0.874638446	-1.833548522	0.0019348	0.04317836	1
AnxB9	AE014297	181.0831822	-0.880548954	-1.841075709	0.0014098	0.03445942	1
CG3332	AE014134	55.83591888	-0.882250089	-1.843247869	0.000104	0.00453385	1
mRpS18A	AE014297	31.61693607	-0.88289811	-1.844075994	0.002331	0.04875236	1
CG43340	AE013599	8.017896732	-0.886855916	-1.849141871	0.0001903	0.00740073	1
CG9663	AE014134	65.71326408	-0.888259351	-1.850941567	0.0002854	0.01024385	1
axo	AE014296	4.684348437	-0.888849922	-1.85169941	0.0005901	0.01835348	1
CG31975	AE014134	18.54033916	-0.891965792	-1.855702951	0.0009472	0.02613074	1
CG5885	AE014134	205.6363253	-0.896311323	-1.861300927	0.0001765	0.00698576	1
CG13630	AE014297	42.40782265	-0.896371963	-1.861379164	0.0022461	0.04760465	1
Fdx2	AE014296	91.69475645	-0.897382304	-1.862683172	0.0010458	0.02799816	1
CG33080	AE014298	29.01184883	-0.898799397	-1.864513699	0.0004744	0.0154894	1
Tango2	AE014298	19.69249984	-0.900622946	-1.866871912	0.0016157	0.03832823	1
sni	AE014298	45.92796207	-0.9037978	-1.87098475	0.001147	0.0297203	1
Pen	AE014134	5.980934297	-0.912283846	-1.882022461	0.0019779	0.04386427	1
CG7968	AE014134	803.661094	-0.915430542	-1.886131864	0.0020161	0.04437618	1
CG33966	AE014296	66.84905721	-0.918061481	-1.889574605	0.0016607	0.03917949	1
CG8031	AE014297	59.56768781	-0.920486423	-1.892753352	0.0010097	0.0271555	1
CG4781	AE013599	188.4197961	-0.931975898	-1.907887227	0.0010926	0.02881635	1
Rab18	AE014298	88.51796859	-0.93202033	-1.907945987	0.0009532	0.02615396	1
Pmp70	AE014298	149.5353278	-0.932246995	-1.908245773	0.0009869	0.02666359	1
CG34159	AE014134	41.9171953	-0.932899383	-1.909108878	0.001638	0.03876851	1
His3.3A	AE014134	206.8901363	-0.936680028	-1.914118342	0.0001776	0.00698576	1
CG10467	AE014296	94.96756525	-0.937412271	-1.915090103	6.86E-05	0.00331707	1
CG9914	AE014298	76.58692656	-0.937978568	-1.915841975	0.0007891	0.02280878	1
CG1840	AE014298	27.77073119	-0.941935959	-1.921104448	0.0021869	0.04667606	1
Sec61gamma	AE014298	112.457739	-0.942992359	-1.922511675	0.0003783	0.0129476	1
Ttc19	AE014134	10.03764015	-0.944241725	-1.92417728	0.0011951	0.03056312	1
CG14696	AE014297	18.16883314	-0.960183224	-1.945556968	0.0011119	0.02917411	1
CAH1	AE014134	252.7325874	-0.961907901	-1.947884184	0.0011406	0.02964745	1
CG13086	AE014134	53.00071259	-0.962194931	-1.948271762	0.0022555	0.04767706	1
rtet	AE014297	47.96818828	-0.965507952	-1.952750936	0.0014445	0.03513114	1
CG15083	AE013599	42.97405494	-0.968052133	-1.956197635	0.0008655	0.02435063	1
CG10337	AE014134	46.30155638	-0.968715051	-1.957096714	0.0005559	0.01750525	1
ImpL3	AE014296	67.72123763	-0.969656568	-1.95837435	0.0001629	0.00655025	1
SpdS	AE014297	11.09771281	-0.973671723	-1.963832281	0.0003819	0.01304889	1
Abp1	AE014296	53.74268665	-0.975406502	-1.966195125	7.557E-05	0.00356146	1
CG3702	AE014134	117.8804483	-0.977132876	-1.968549345	0.0004776	0.015565	1

Jon99Ciii	AE014297	9535.781419	-0.977137152	-1.968555179	0.0016649	0.03917949	1
CG32485	AE014296	96.29581086	-0.977387513	-1.968896826	3.472E-05	0.00190232	0.6144493
CG9498	AE014134	122.3207951	-0.979907267	-1.972338627	6.025E-05	0.00298676	1
CG8134	AE014298	24.13627244	-0.980363747	-1.972962789	0.0018033	0.04128584	1
thetaTry	AE013599	941.4725614	-0.98156971	-1.974612698	0.0005362	0.01700587	1
CG9674	AE014296	44.97883618	-0.982021516	-1.975231181	0.0005066	0.01615487	1
LpR1	AE014297	16.28446978	-0.987344995	-1.982533158	5.029E-05	0.00257205	0.8899291
GstE13	AE013599	14.32001959	-0.987962645	-1.983382106	0.001663	0.03917949	1
CG5969	AE014296	22.3280925	-0.992592353	-1.989757139	0.0007788	0.02259517	1
SsRbeta	AE014296	336.8182467	-0.992789339	-1.99002884	0.0005918	0.01837319	1
CG31810	AE014134	48.9210626	-1.006047332	-2.008400978	0.0020882	0.04550729	1
Cyp6a17	AE013599	16.5031482	-1.007096879	-2.009862602	0.0004868	0.0157715	1
CG31267	AE014297	136.8101899	-1.008355085	-2.011616211	0.000245	0.00901476	1
CG10472	AE014296	7947.084517	-1.0161895	-2.022569811	0.0012836	0.03225622	1
CG9896	AE013599	129.4932134	-1.019507644	-2.027227	5.194E-06	0.00039279	0.091912
CG8834	AE013599	2274.197346	-1.022234133	-2.031061793	0.0001695	0.00675705	1
CG4741	AE013599	26.12364252	-1.022321987	-2.03118548	5.941E-05	0.00296152	1
CG10799	AE013599	28.99395425	-1.024587369	-2.03437744	0.0007594	0.02217655	1
CG8051	AE014298	60.14086716	-1.029254735	-2.040969659	1.775E-05	0.0010721	0.3141266
pch2	AE014297	4.917834479	-1.03128074	-2.043837846	0.0023138	0.04857424	1
Mgstl	AE014298	151.9881556	-1.032761123	-2.045936151	5.42E-05	0.00275636	0.9592117
CG2061	AE014298	11.09292557	-1.033204465	-2.046564967	0.0009325	0.02590588	1
CG16892	AE014298	7.486860623	-1.036061226	-2.0506215	0.0005572	0.01751476	1
CG11576	AE014297	57.04366728	-1.04138736	-2.058205965	6.165E-05	0.0030308	1
Toll-9	AE014296	4.583452155	-1.050552847	-2.071323436	0.0006415	0.0195073	1
TyrR	AE014297	3.308506431	-1.051865664	-2.073209147	0.0002229	0.00837693	1
CG8498	AE014134	65.12012075	-1.054110013	-2.076436875	0.000792	0.02282597	1
CG2930	AE014298	466.8332874	-1.058792749	-2.083187575	0.0001271	0.00539486	1
Jon99Cii	AE014297	17940.77977	-1.063150034	-2.089488812	0.000625	0.01912742	1
CG42336	AE013599	134.7226512	-1.06370148	-2.090287637	5.321E-07	5.5724E-05	0.0094173
CG9527	AE014134	511.809385	-1.065839107	-2.09338709	0.0001033	0.00452648	1
Cyp6a23	AE013599	231.461973	-1.075560179	-2.107540243	0.0002396	0.00886973	1
CG11671	AE014297	407.1840559	-1.090459975	-2.12941918	1.937E-05	0.00116197	0.3427798
Cyp9f2	AE014297	499.890733	-1.093115238	-2.13334196	3.781E-05	0.00202159	0.669147
alphaTub84D	AE014297	45.48339595	-1.094958544	-2.136069435	7.785E-05	0.00360642	1
CG15534	AE014297	229.6178875	-1.095699609	-2.137166946	0.0008597	0.02424113	1
Jon25Bii	AE014134	8223.257953	-1.098502349	-2.14132288	7.771E-05	0.00360642	1
Acox57D-d	AE013599	51.15345572	-1.10166861	-2.146027569	0.0002385	0.00884819	1
MFS1	AE013599	64.90811276	-1.101831067	-2.14626924	0.0010344	0.02773553	1
CG10962	AE014298	62.19853633	-1.105799043	-2.152180445	0.0005242	0.01665345	1
etaTry	AE013599	312.9100513	-1.108296303	-2.155909029	8.442E-05	0.00384536	1
CG12057	AE014298	3127.164046	-1.111269115	-2.160356067	0.0007184	0.02113791	1
CG5767	AE013599	269.9274752	-1.113258269	-2.163336769	5.68E-06	0.00042592	0.1005164
Rbp1-like	AE014298	5.909329078	-1.113527862	-2.163741064	0.0005866	0.01827604	1
CG1358	AE013599	18.00473428	-1.113567666	-2.163800763	0.0002708	0.00983898	1
Pgcl	AE014298	97.76150451	-1.114065429	-2.164547453	1.332E-05	0.00085082	0.2356784

CG33306	AE014134	898.2569211	-1.114213673	-2.164769882	0.0001569	0.0063742	1
CG4630	AE013599	13.21405378	-1.114876121	-2.165764117	0.0002904	0.01038058	1
Jafrac2	AE014296	60.97442295	-1.117541035	-2.169768365	7.648E-05	0.00358344	1
CG11686	AE014297	403.3401992	-1.119672176	-2.172975903	7.025E-06	0.00051158	0.1243148
Sec61alpha	AE014134	354.4058721	-1.119973827	-2.173430295	3.483E-05	0.00190245	0.6163944
CG8860	AE013599	160.727022	-1.120709681	-2.174539147	8.356E-05	0.00382116	1
CG13360	AE014298	107.833441	-1.123475346	-2.178711764	2.507E-06	0.00020733	0.0443684
CG31087	AE014297	156.4912844	-1.123862987	-2.179297246	7.813E-06	0.00055752	0.1382647
Sodh-1	AE014297	28.83375701	-1.124345609	-2.180026405	0.0004137	0.01383904	1
Qtzl	AE014134	13.1135772	-1.127117273	-2.184218634	0.0016736	0.03922821	1
CG7881	AE013599	56.40339809	-1.128804248	-2.186774182	4.536E-05	0.00233369	0.8027894
CG7639	AE013599	16.21590492	-1.133182192	-2.193420157	0.0001841	0.00722361	1
CG7631	AE014134	124.0252699	-1.138923042	-2.202165722	7.684E-05	0.00358344	1
Ugt36Bc	AE014134	106.1907543	-1.140448879	-2.204496031	3.632E-06	0.0002882	0.0642697
CG7054	AE014297	169.94764	-1.150239952	-2.219508066	1.547E-07	1.9553E-05	0.0027375
CG30339	AE013599	58.54441614	-1.151683586	-2.221730131	8.787E-05	0.00393669	1
CG1532	AE014298	199.4404169	-1.153247435	-2.224139743	1.116E-06	0.00010615	0.0197434
CG10182	AE014297	85.2801072	-1.15495433	-2.226772744	0.0002047	0.00779212	1
Neb-cGP	AE014298	134.5790645	-1.154972723	-2.226801134	5.358E-06	0.0004035	0.0948222
fabp	AE014297	479.3959839	-1.157343558	-2.230463528	3.245E-05	0.00179475	0.5743192
CG5618	AE014296	73.0363064	-1.158336226	-2.23199876	4.487E-06	0.00034522	0.0794008
Pxn	AE014296	71.8783541	-1.160965729	-2.236070584	6.257E-05	0.00305879	1
CG8661	AE014298	688.5119254	-1.161814476	-2.237386466	0.0002895	0.01036992	1
CG15674	AE013599	98.62517578	-1.163031147	-2.239274122	7.592E-06	0.00054838	0.134354
CG8112	AE014297	17.0596695	-1.170380445	-2.250710413	0.0017989	0.04128584	1
GstE3	AE013599	1026.449021	-1.170444411	-2.250810207	7.206E-05	0.00343716	1
Orct	AE014297	17.11685198	-1.172541549	-2.254084421	0.0002212	0.00832929	1
CG6084	AE014296	441.9204235	-1.179784041	-2.26542863	7.004E-05	0.00335931	1
CG31265	AE014297	151.4054872	-1.185376505	-2.274227382	0.0001725	0.00685925	1
CG9826	AE013599	6.258805593	-1.191415508	-2.283767063	0.000823	0.02345246	1
prtp	AE014298	112.8830218	-1.193447711	-2.28698628	1.56E-06	0.00014014	0.0276067
CG32483	AE014296	216.912624	-1.196013046	-2.291056513	0.0001635	0.006562	1
Jheh3	AE013599	319.9308276	-1.19628871	-2.291494321	0.000108	0.00467227	1
Sod3	AE013599	45.62908695	-1.197429208	-2.293306539	0.0001341	0.00559546	1
MFS3	AE014134	5.075214138	-1.218753951	-2.327456091	0.0016874	0.03940026	1
regucalcin	AE014298	65.79024756	-1.220504804	-2.330282405	1.581E-06	0.00014062	0.0279825
CG40472	AE014296	57.51729179	-1.221825219	-2.332416153	0.0011647	0.03000219	1
CG31259	AE014297	23.07464671	-1.22659391	-2.340138488	9.558E-05	0.00423915	1
CG10550	AE014297	123.5285035	-1.227489751	-2.341592047	3.701E-05	0.00199081	0.6549762
CG17036	AE014134	16.65955458	-1.236083521	-2.355581945	0.000157	0.0063742	1
Gpo-1	AE013599	51.44848403	-1.236625292	-2.356466695	4.613E-07	4.9179E-05	0.0081637
CG7497	AE014296	28.40518116	-1.239676727	-2.361456118	1.145E-05	0.00075614	0.2026466
dUTPase	AE014134	30.69302688	-1.240847061	-2.363372542	0.0002046	0.00779212	1
CG11236	AE014134	18.54310532	-1.243914941	-2.368403582	0.0001928	0.00745088	1
RpL41	AE013599	4973.958052	-1.244046426	-2.368619445	1.67E-06	0.00014635	0.0295619
CG17337	AE013599	141.7112897	-1.244831445	-2.369908642	2.299E-07	2.6945E-05	0.0040686

PIG-L	AE014297	28.57545701	-1.248924866	-2.376642433	3.838E-06	0.00030324	0.0679265
CG3344	AE014296	1284.581725	-1.251378307	-2.38068758	3.804E-05	0.002024	0.6731795
lambdaTry	AE013599	1231.103907	-1.257822282	-2.391344997	7.849E-06	0.00055785	0.1389053
Jon44E	AE013599	727.9400966	-1.263239936	-2.400341934	7.679E-06	0.00055239	0.1358877
CG11911	AE014134	3215.953465	-1.269102821	-2.410116394	1.657E-05	0.00101472	0.2932549
Fkbp14	AE013599	152.3823978	-1.271882015	-2.414763694	1.155E-07	1.5256E-05	0.0020444
CG5577	AE014296	16.85702752	-1.272926887	-2.416513219	4.709E-05	0.00241576	0.8334369
CG14695	AE014297	14.18803324	-1.279787551	-2.428032194	2.468E-05	0.0014109	0.4366916
CG3597	AE014134	6.361239841	-1.279921115	-2.42825699	0.0016949	0.03946663	1
agt	AE014297	10.64544584	-1.280756774	-2.429663929	0.0001074	0.00466859	1
CG17477	AE014297	12.94954991	-1.283735275	-2.434685248	0.0009495	0.02613074	1
Eglp4	AE013599	29.74285048	-1.284317676	-2.435668303	8.629E-06	0.00059648	0.152699
CG9119	AE014296	56.34216749	-1.285195811	-2.437151289	8.716E-05	0.00392481	1
CG4267	AE014134	17.16922373	-1.290052092	-2.44536885	3.159E-05	0.00175274	0.5591243
DNApol-alpha73	AE014297	2.288080127	-1.292440198	-2.449420043	0.0023824	0.0494184	1
CAH2	AE014296	80.40403694	-1.294533224	-2.45297618	9.355E-08	1.2542E-05	0.0016556
CG13325	AE013599	87.97131312	-1.301854422	-2.465455856	6.169E-05	0.0030308	1
Ugt37a1	AE014134	34.18179729	-1.30265364	-2.466822038	0.0001234	0.00526231	1
CG30479	AE013599	9.394642299	-1.303984222	-2.469098211	2.555E-05	0.00145367	0.4520926
CG13488	AE013599	34.06489051	-1.304027998	-2.469173132	2.863E-05	0.00160751	0.5067255
CG34236	AE013599	120.3373156	-1.309860786	-2.479176159	6.723E-07	6.8373E-05	0.0118969
CG11034	AE014134	142.7121051	-1.311005818	-2.481144602	1.295E-05	0.00083308	0.2290966
CG4562	AE014297	141.2095471	-1.311047367	-2.481216058	2.285E-06	0.00019071	0.0404313
CG6048	AE014298	233.8947409	-1.317942534	-2.49310308	1.136E-05	0.00075568	0.2010102
Adk3	AE014297	41.72624454	-1.318757713	-2.494512179	3.968E-06	0.00031075	0.07023
dmGlut	AE014134	228.3466496	-1.322381776	-2.500786293	1.948E-05	0.00116446	0.3446798
CG6295	AE014297	3107.439054	-1.323475815	-2.502683434	1.364E-05	0.00086833	0.2413952
Tsp42Ei	AE013599	37.51025237	-1.324135189	-2.503827529	1.273E-06	0.00011924	0.0225357
CG31086	AE014297	1384.834427	-1.327849811	-2.510282641	1.283E-05	0.0008318	0.2270828
CG8562	AE014296	425.7612346	-1.332589616	-2.518543442	9.709E-05	0.00428463	1
Grip71	AE014134	2.210327628	-1.335783216	-2.524124753	0.0013643	0.03358093	1
CG42747	AE014296	2.552662247	-1.361229763	-2.569040729	0.0012848	0.03225622	1
PIG-Wb	AE014296	106.0100238	-1.3680218	-2.581163983	1.634E-06	0.00014391	0.0289254
shf	AE014298	7.392023139	-1.371190089	-2.586838683	6.991E-05	0.00335931	1
Gabat	AE014296	31.20242893	-1.378359215	-2.599725347	8.204E-05	0.00377119	1
CG1304	AE014298	20.53658759	-1.382254393	-2.606753911	8.187E-06	0.00057725	0.1448887
CG10469	AE014296	9.799660634	-1.391435463	-2.623395754	0.000945	0.02613074	1
Ser6	AE014298	176.9799418	-1.394806708	-2.629533192	5.8E-08	8.3443E-06	0.0010263
CG30090	AE013599	11.22781241	-1.398401007	-2.636092521	0.0002532	0.00923761	1
Prip	AE013599	66.69469519	-1.401918486	-2.6425275	4.438E-07	4.789E-05	0.007854
CG7953	AE014134	4461.69823	-1.405494463	-2.649085602	0.0001431	0.00586196	1
CG16749	AE014297	1088.982866	-1.411143428	-2.6594786	5.165E-06	0.00039232	0.0914111
Npc2e	AE014297	1824.051873	-1.412677494	-2.662308017	1.969E-06	0.00016756	0.0348525
CG32368	AE014296	1182.366532	-1.412881347	-2.662684228	2.211E-06	0.00018542	0.039124
CG7458	AE014296	20.6961673	-1.413598693	-2.664008513	4.996E-07	5.294E-05	0.008841

CG8774	AE014297	160.7075884	-1.421611574	-2.678845865	2.686E-05	0.00152352	0.4753379
CG10562	AE014297	60.21231023	-1.422901323	-2.681241785	8.467E-08	1.1526E-05	0.0014983
CG17906	AE014134	14.70266068	-1.429528622	-2.693586923	0.000132	0.00553672	1
CG31269	AE014297	34.65632003	-1.430511374	-2.695422397	7.695E-05	0.00358344	1
CG3348	AE014297	95.81639421	-1.439623872	-2.712501381	0.0002272	0.00851791	1
CG16986	AE014296	402.0836329	-1.441082688	-2.715245579	6.238E-08	8.8946E-06	0.001104
CG13078	AE014134	40.79423554	-1.445552433	-2.723670975	0.0001039	0.00453385	1
CG44013	AE014297	216.5506279	-1.449968059	-2.732020027	1.983E-07	2.4197E-05	0.0035086
tok	AE014297	1.481874454	-1.454161424	-2.739972519	0.0002067	0.00785111	1
Npc1b	AE014298	394.9985933	-1.456035156	-2.743533431	4.074E-05	0.00213324	0.7210353
CG31266	AE014297	181.215266	-1.457306832	-2.745952809	6.475E-07	6.6302E-05	0.011458
CG7381	AE014297	412.2145655	-1.461652199	-2.754236029	3.597E-05	0.00195841	0.636482
CG15210	AE014298	206.9750614	-1.474186249	-2.778268917	5.148E-09	1.0353E-06	9.111E-05
Jon65Ai	AE014296	1813.872113	-1.479464343	-2.788451819	3.831E-07	4.2376E-05	0.0067802
pdm2	AE014134	3.71467426	-1.479497006	-2.78851495	1.054E-06	0.00010142	0.018661
CNT2	AE013599	99.82838805	-1.480667399	-2.790778065	2.338E-08	3.9409E-06	0.0004138
Dbi	AE014296	2239.977892	-1.481015075	-2.791450696	2.353E-07	2.7393E-05	0.0041637
CG9903	AE014298	67.28240992	-1.481229835	-2.791866263	4.446E-06	0.00034358	0.0786805
borr	AE014134	3.180286785	-1.481268841	-2.791941748	0.0012154	0.03103802	1
CG15096	AE013599	124.8735178	-1.482904862	-2.795109615	2.959E-11	9.0292E-09	5.237E-07
GstD9	AE014297	288.0459944	-1.486604391	-2.802286364	1.86E-09	4.064E-07	3.292E-05
CG7912	AE014297	12.2329226	-1.491569496	-2.811947182	3.26E-05	0.00179745	0.5769827
CG7272	AE014296	178.0867877	-1.498737116	-2.825952303	5.521E-08	8.0091E-06	0.0009771
CG7231	AE014134	177.1923467	-1.500009484	-2.828445719	1.583E-07	1.9733E-05	0.0028021
LysD	AE014296	581.4713683	-1.514071468	-2.856149443	0.0010502	0.02805729	1
GstD5	AE014297	38.99546705	-1.528171007	-2.884199595	0.0002511	0.00920043	1
CG43207	AE013599	32.29100257	-1.532459339	-2.892785475	2.303E-05	0.00134038	0.4074767
Gba1a	AE014297	212.4943615	-1.542308679	-2.912602213	6.487E-06	0.00048035	0.1148036
Cyp6a13	AE013599	41.39222786	-1.569601648	-2.968227452	3.706E-08	5.8036E-06	0.0006558
CG17929	AE014297	10.8834502	-1.570218197	-2.969496223	1.373E-06	0.00012683	0.0242951
CG13950	AE014134	13.62172257	-1.581972828	-2.993789588	5.215E-07	5.4934E-05	0.0092289
CG42700	AE013599	1.772158623	-1.582932998	-2.995782735	0.0001418	0.00582441	1
Jon99Fi	AE014297	2454.616926	-1.583437289	-2.996830087	5.356E-07	5.5752E-05	0.0094778
Prx2540-2	AE013599	93.62098683	-1.59860504	-3.028503419	1.53E-07	1.9485E-05	0.0027084
CG17028	AE014296	13.98183115	-1.606774488	-3.04570136	1.621E-07	2.0061E-05	0.0028688
Cyp4d2	AE014298	23.41078675	-1.62149788	-3.076943346	1.325E-08	2.4708E-06	0.0002345
CG18179	AE014296	170.9159099	-1.622440184	-3.078953723	3.678E-08	5.8036E-06	0.0006509
CG7860	AE014298	6.471828371	-1.635893131	-3.107798853	2.87E-05	0.00160751	0.5079732
Ctr1B	AE014297	332.2665027	-1.65955646	-3.159193841	1.73E-05	0.00104877	0.3062401
CG43400	AE014134	2.600674097	-1.665566208	-3.172381352	0.0021891	0.04667606	1
Ag5r2	AE014298	1141.097099	-1.674576356	-3.192256009	2.825E-09	5.9517E-07	4.999E-05
CG4615	AE014298	15.97481982	-1.686640296	-3.21906185	2.118E-07	2.5155E-05	0.003748
CG7298	AE014296	156.5433581	-1.69145524	-3.229823302	5.519E-08	8.0091E-06	0.0009768
zetaTry	AE013599	216.0883052	-1.694195739	-3.235964407	3.921E-11	1.1762E-08	6.94E-07
Vha100-4	AE014297	93.1973443	-1.699815832	-3.248594859	3.412E-10	8.5039E-08	6.038E-06
Jon99Fii	AE014297	3858.968607	-1.706287932	-3.263201176	2.581E-08	4.3098E-06	0.0004568

Amyrel	AE013599	62.03305978	-1.716802518	-3.287070771	0.0001334	0.00558232	1
CG4053	AE014297	83.83810723	-1.720665586	-3.295884271	6.904E-07	6.9423E-05	0.0122185
CG15695	AE014297	1.918455845	-1.733374921	-3.325047433	0.0001903	0.00740073	1
CG7384	AE014134	1.777033976	-1.733472309	-3.325271895	0.0008109	0.02322201	1
JhI-26	AE013599	101.3060234	-1.741314793	-3.343397278	2.317E-10	6.0291E-08	4.1E-06
CG15529	AE014297	7.398011499	-1.754403682	-3.373868354	2.228E-05	0.00131438	0.3943148
Ts	AE014134	7.55126453	-1.757810932	-3.381845922	1.422E-05	0.00089881	0.2516668
Prx2540-1	AE013599	44.58988541	-1.762184614	-3.392113901	0.0001451	0.00593082	1
CG17633	AE014134	3039.91319	-1.796463386	-3.473676457	5.194E-08	7.6599E-06	0.0009192
CG12896	AE013599	19.95664261	-1.802552149	-3.488367772	8.297E-05	0.00380397	1
PGRP-SC1b	AE013599	144.1784093	-1.819512182	-3.529618316	4.127E-09	8.4922E-07	7.303E-05
hdly	AE014297	254.2358529	-1.859506434	-3.628834934	8.1E-11	2.2754E-08	1.433E-06
CG3640	AE013599	3.650131581	-1.869401962	-3.653810878	0.000304	0.01076421	1
brv3	AE014298	2.702945288	-1.881660676	-3.684989928	1.058E-05	0.00071187	0.1872227
CG12824	AE013599	115.1150594	-1.902495181	-3.738592377	1.746E-09	3.9609E-07	3.089E-05
Zmynd10	AE014296	0.738218624	-1.907592112	-3.751823895	0.0021768	0.04652568	1
CG13386	AE014134	1.943508055	-1.921741516	-3.788801391	0.0006258	0.01912742	1
CG14688	AE014297	24.78854881	-1.927184346	-3.803122333	3.341E-08	5.424E-06	0.0005912
CG42397	AE014296	768.1494589	-1.947819842	-3.857910946	7.933E-10	1.8719E-07	1.404E-05
CG6901	AE014297	29.34315212	-1.969139078	-3.915344027	3.763E-08	5.8416E-06	0.0006659
Jon65Aii	AE014296	490.4646153	-1.983596306	-3.954776886	9.363E-10	2.1803E-07	1.657E-05
CG33337	AE014297	7.287339255	-1.998562546	-3.996016517	7.156E-05	0.00342287	1
LysB	AE014296	396.246776	-2.001223442	-4.003393542	6.342E-07	6.563E-05	0.0112227
CG14339	AE014134	0.285587478	-2.035452155	-4.099511919	0.0013012	0.03247403	1
CG10163	AE014296	7.548720744	-2.041729457	-4.117388143	0.0001643	0.00657956	1
CG16779	AE014297	0.104069215	-2.045235965	-4.127407734	0.0019643	0.04372527	1
slo	AE014297	2.542139223	-2.055253202	-4.156165781	2.122E-09	4.5798E-07	3.755E-05
shd	AE014296	3.070988164	-2.057335867	-4.162169929	7.674E-07	7.5445E-05	0.0135801
dgt2	AE014134	5.377498115	-2.067809483	-4.192496219	1.344E-06	0.00012522	0.0237912
Fer3	AE014297	3.440544046	-2.071220971	-4.202421793	8.651E-05	0.0039056	1
CG31446	AE014297	113.4998603	-2.082346901	-4.234955766	1.028E-11	3.3068E-09	1.819E-07
CG3106	AE014298	263.6340938	-2.087183179	-4.249176229	1.437E-10	3.913E-08	2.543E-06
CG34251	AE014296	0.773394223	-2.089284147	-4.255368728	0.0009486	0.02613074	1
Peritrophin-15a	AE014134	1067.718153	-2.111383648	-4.321055161	1.728E-10	4.5655E-08	3.059E-06
Drsl2	AE014296	743.7050241	-2.113032457	-4.325996377	2.887E-15	1.7028E-12	5.108E-11
Pebp1	AE014297	6346.840732	-2.148898952	-4.43489194	6.561E-14	3.0557E-11	1.161E-09
Cyp9b2	AE013599	570.0395194	-2.175296598	-4.516786112	5.311E-12	1.8074E-09	9.398E-08
CG34034	AE014297	2.533613235	-2.176186527	-4.519573158	0.0003952	0.0133219	1
mag	AE014296	598.8662947	-2.187603725	-4.555482052	2.436E-12	9.3736E-10	4.312E-08
CG10559	AE014297	9.150991824	-2.191430885	-4.567582809	5.928E-09	1.1529E-06	0.0001049
CG4830	AE014297	16.86834022	-2.191717351	-4.568489854	6.481E-07	6.6302E-05	0.0114702
CG32706	AE014298	2.010887002	-2.220423018	-4.660300611	0.0002003	0.00767171	1
CG6592	AE014296	1.943658621	-2.233839415	-4.703841391	3.713E-05	0.00199131	0.6571316
ninaD	AE014134	74.63418397	-2.236390472	-4.712166354	2.283E-07	2.6931E-05	0.0040396
CG15829	AE014296	144.8389993	-2.257903273	-4.782958499	1.548E-10	4.1506E-08	2.739E-06

CG11741	AE014297	11.82867412	-2.259666486	-4.788807642	1.576E-06	0.00014062	0.027884
Zip42C.1	AE013599	15.41292428	-2.265503302	-4.808221314	1.409E-06	0.00012851	0.0249317
AnxB10	AE014298	146.6873104	-2.280262548	-4.857663477	0	0	0
CG3301	AE014297	112.5280574	-2.281041848	-4.860288149	1.332E-15	8.7323E-13	2.358E-11
CG5724	AE014297	105.4767502	-2.289874107	-4.890134368	1.499E-14	7.5784E-12	2.652E-10
CG4462	AE014297	52.1662546	-2.291993529	-4.897323602	3.944E-13	1.6616E-10	6.979E-09
Npc2d	AE014297	246.1407206	-2.299138039	-4.921636265	4.466E-11	1.3171E-08	7.903E-07
CG7290	AE014296	0.377059757	-2.316521494	-4.981297216	0.0006594	0.01984532	1
Ugt36Bb	AE014134	0.558480747	-2.340211531	-5.063768781	0.000354	0.01228231	1
mab-21	AE014298	0.25816893	-2.389958402	-5.241422483	0.0008187	0.02336939	1
GstD7	AE014297	51.91664131	-2.395397995	-5.26122225	4.156E-12	1.442E-09	7.354E-08
CG13358	AE014298	0.260679397	-2.421460075	-5.357129142	0.0022783	0.04794104	1
CG15199	AE014298	22.81649609	-2.434772962	-5.406792394	1.189E-06	0.00011251	0.0210394
Cyp6a21	AE013599	96.03621194	-2.452284179	-5.472819135	1.11E-16	8.9307E-14	1.965E-12
CG3339	AE014297	0.057557014	-2.474824848	-5.558997944	0.0002831	0.01018708	1
PH4alphaSG2	AE014297	1.745162984	-2.475997405	-5.563517881	1.556E-05	0.00096591	0.2752851
CG5999	AE014297	13.34824569	-2.485751982	-5.60126227	5.995E-15	3.3155E-12	1.061E-10
CG14757	AE013599	14.52353813	-2.487388603	-5.607620058	3.475E-08	5.5914E-06	0.0006151
trp	AE014297	1.738529726	-2.492332955	-5.626871256	2.959E-06	0.0002391	0.0523632
Gba1b	AE014297	1.927738372	-2.499346076	-5.654290772	1.208E-05	0.00079189	0.2138095
Ucp4B	AE014134	1.430888449	-2.521226602	-5.740699753	1.049E-05	0.00070883	0.1856891
CG30082	AE013599	1.953440391	-2.537168159	-5.804485357	2.3E-05	0.00134038	0.4071167
CG17571	AE014134	2160.612627	-2.538702223	-5.810660736	9.046E-11	2.5013E-08	1.601E-06
CG10581	AE014296	11.13938727	-2.544943765	-5.835853897	4.227E-08	6.5054E-06	0.0007481
CG43645	AE014134	0.945769287	-2.548934845	-5.85202059	0.0012384	0.03144209	1
PGRP-SC1a	AE013599	257.7130629	-2.572198897	-5.947151786	3.751E-09	7.8095E-07	6.638E-05
CG12490	AE013599	1.56212848	-2.578185125	-5.97187979	1.542E-05	0.0009608	0.2728673
CG9192	AE014296	1.804181201	-2.597587583	-6.052736655	0.0001117	0.00479722	1
CG17145	AE014296	16.10282647	-2.598491444	-6.056529936	1.83E-09	4.0476E-07	3.238E-05
Obp83b	AE014297	8.687808764	-2.623009743	-6.160338995	4.376E-07	4.7514E-05	0.0077448
CG6996	AE014296	0.923662067	-2.625532646	-6.171121271	7.994E-06	0.00056585	0.1414628
CG14456	AE014296	1.251844302	-2.650138399	-6.277274937	0.0004967	0.01598126	1
CG15773	AE014298	27.92429063	-2.653084169	-6.2901053	2.335E-13	1.0078E-10	4.132E-09
CG17192	AE014297	132.9350446	-2.660492168	-6.322487012	3.423E-12	1.262E-09	6.058E-08
CG10725	AE014296	24.5394817	-2.756658114	-6.758289326	1.772E-12	7.1267E-10	3.136E-08
CG5804	AE014296	4386.600737	-2.767188876	-6.807801048	1.11E-15	7.5568E-13	1.965E-11
CG9682	AE014297	112.9262306	-2.775530676	-6.847278423	3.886E-15	2.2183E-12	6.877E-11
CG32820	AE014298	0.164612105	-2.843940726	-7.179785414	0.0010543	0.02805729	1
GstD10	AE014297	83.09743001	-2.869677507	-7.309017599	1.11E-16	8.9307E-14	1.965E-12
LysE	AE014296	210.6010926	-2.897940607	-7.453616579	9.958E-12	3.2635E-09	1.762E-07
CG14567	AE014296	3.034731568	-2.927420644	-7.607490588	5.769E-05	0.00290021	1
CG11912	AE014134	1978.683745	-2.936484888	-7.655437815	0	0	0
CecA1	AE014297	40.50363515	-2.956509267	-7.762434916	4.465E-09	9.0818E-07	7.901E-05
CG17104	AE014134	0.29243909	-3.052553443	-8.296790993	0.0012804	0.03225622	1
CG11300	AE013599	1.271456418	-3.077794718	-8.443228262	0.0006571	0.01980949	1
CG4998	AE014296	1.754558229	-3.081040214	-8.462243584	1.45E-08	2.6183E-06	0.0002566

CG33109	AE014297	15.10722148	-3.09632975	-8.552402488	0.000388	0.01315437	1
CG43221	AE014134	0.762989168	-3.139146454	-8.810027084	0.0013316	0.03309856	1
Peritrophin-15b	AE014134	184.7038669	-3.184107955	-9.088914202	0	0	0
CG12374	AE013599	11580.53527	-3.235208152	-9.416612429	0	0	0
Vm26Aa	AE014134	0.642901697	-3.237889043	-9.434127138	0.0008755	0.02452808	1
CG18606	AE013599	1.819128914	-3.277467384	-9.69652212	0.0002347	0.00874416	1
LysX	AE014296	717.3683848	-3.346289136	-10.17029157	0	0	0
CG32198	AE014296	6.539850979	-3.46603103	-11.05043326	6.944E-05	0.00334855	1
CG42521	AE014296	5.86150612	-3.525668302	-11.51680236	0.0022883	0.04809518	1
CG43090	AE014298	29.1864183	-3.603279993	-12.15333196	0.0003685	0.01266135	1
CG32277	AE014296	1.923393531	-3.615113544	-12.25342832	0.0003319	0.0115634	1
CG14958	AE014296	0.576358112	-3.616409472	-12.26444014	0.001176	0.03016077	1
CG18607	AE013599	18.85428836	-3.673881906	-12.76287907	3.75E-12	1.3274E-09	6.637E-08
fs(1)Yb	AE014298	0.098014908	-3.713018478	-13.11384168	0.0004983	0.01600488	1
prt	AE014297	6.636388729	-3.73496363	-13.31484409	2.582E-09	5.5061E-07	4.57E-05
Cpr78Ca	AE014296	0.750069591	-3.751463199	-13.46799512	1.478E-05	0.00092766	0.2616012
Lip1	AE014134	0.205662312	-3.759527512	-13.54348873	0.0005645	0.01771174	1
CG6933	AE014296	21.85946423	-3.881739922	-14.74076939	0	0	0
CG15282	AE014134	1.280182731	-3.919190706	-15.12843353	0.0003193	0.01116734	1
Cp7Fc	AE014298	10.87289716	-3.925562454	-15.19539691	0.0018974	0.04250366	1
CG17239	AE014134	5.893079805	-3.944535961	-15.39655803	0.0002832	0.01018708	1
Cp15	AE014296	24.47354594	-4.026734669	-16.29926122	0.0004714	0.01541931	1
Cpr47Eb	AE013599	0.551281557	-4.040402891	-16.4544157	0.0007655	0.02231749	1
CG14309	AE014297	0.167051371	-4.126759234	-17.46941308	0.0021444	0.04622348	1
CG31041	AE014297	532.1641899	-4.142118375	-17.65638851	0	0	0
CG42705	AE014298	2.811078898	-4.222792506	-18.67184398	0.0006315	0.01926786	1
CG32834	AE013599	3.980463744	-4.436403625	-21.65162836	0.0001167	0.00498991	1
CG34459	AE013599	0.957463932	-4.451091302	-21.87318344	1.274E-05	0.00082892	0.2254668
CG42704	AE014298	16.39113506	-4.480086656	-22.31723911	5.89E-05	0.00294467	1
dec-1	AE014298	0.586475989	-4.569116279	-23.73783209	8.612E-06	0.00059648	0.1524079
CG8664	AE014298	7.827360594	-4.652961073	-25.15827452	0	0	0
CG31468	AE014297	2.157275032	-4.672881233	-25.50805927	5.037E-08	7.5545E-06	0.0008914
CG14850	AE014297	2.84268188	-4.865169619	-29.14486106	1.806E-06	0.00015512	0.0319539
CG10918	AE014298	4.376325435	-4.865656292	-29.15469433	6.453E-08	9.0641E-06	0.0011421
CG9897	AE013599	4.181894783	-4.905367358	-29.96834189	2.317E-05	0.00134424	0.4099936
CG17147	AE014296	5.170063322	-5.171923403	-36.04990128	3.331E-16	2.5627E-13	5.894E-12
CG42713	AE014134	1.54205442	-5.40098993	-42.25323598	8.626E-06	0.00059648	0.1526583
CG11289	AE014134	2.01556393	-5.429863646	-43.10740004	1.998E-12	7.8569E-10	3.536E-08
CG32642	AE014298	0.743966715	-5.459962296	-44.01618782	0.0001301	0.00547259	1
Cp19	AE014296	21.45776722	-5.604803935	-48.66470604	1.473E-06	0.00013365	0.0260608
Send1	AE014134	9.654592713	-5.761143597	-54.23467377	1.781E-06	0.00015374	0.0315162
CG43255	AE014298	2.728399039	-6.481667802	-89.36684589	9.811E-05	0.00431891	1
CG31681	AE014134	8.727042628	-6.795577375	-111.0894017	1.188E-07	1.557E-05	0.0021019
Cp18	AE014296	86.69717287	-6.933563393	-122.2392167	1.438E-08	2.6183E-06	0.0002544
Cp16	AE014296	28.8395198	-6.960380376	-124.5326628	1.171E-08	2.2287E-06	0.0002073

CG31789	AE014134	3.006792108	-8.711184513	-419.1098194	9.392E-05	0.00418674	1